

NASA

MSFC

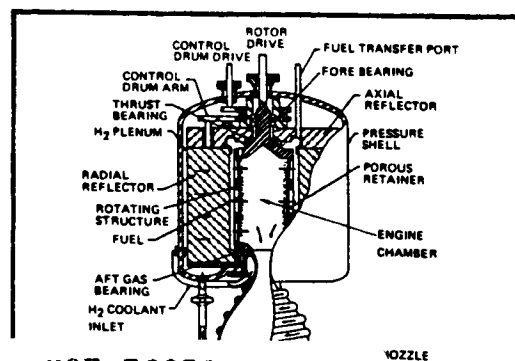
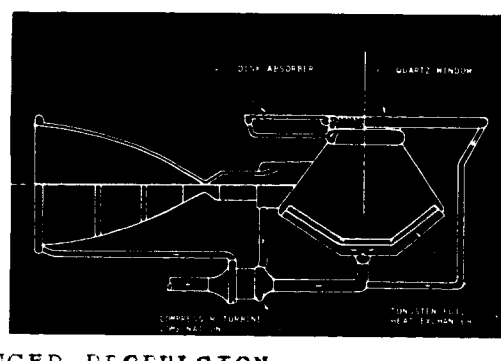
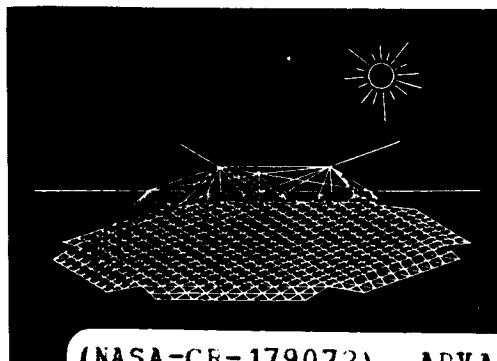
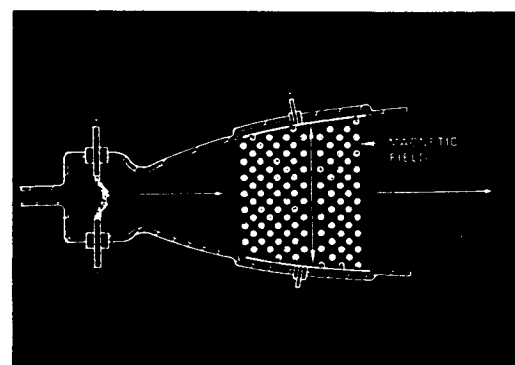
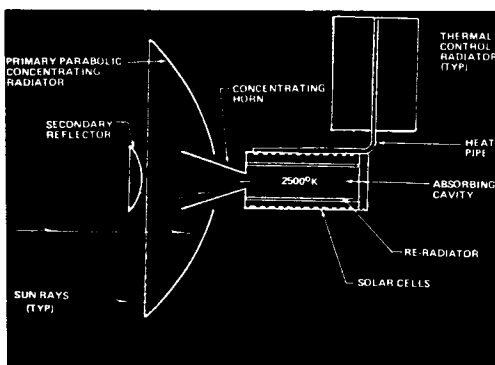
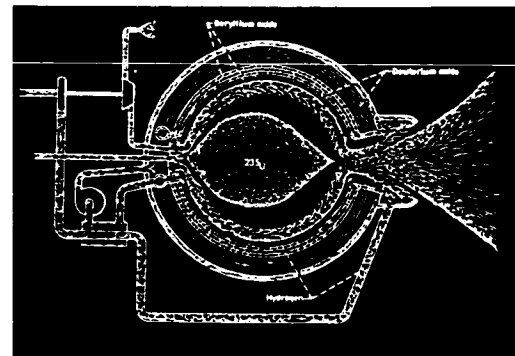
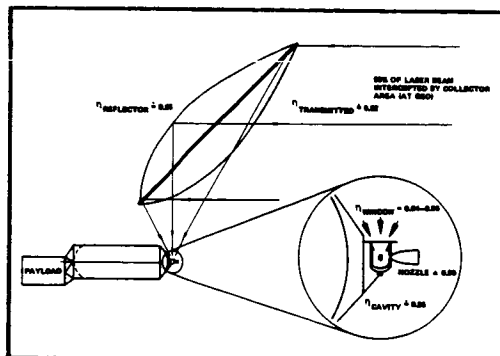
BOEING

FOLDER 2

STUDY TECHNICAL
RESULTS

D180-26680-2

ADVANCED PROPULSION SYSTEMS CONCEPTS FOR ORBITAL TRANSFER



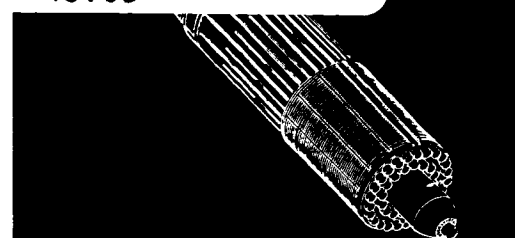
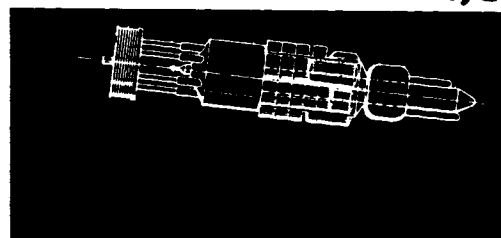
(NASA-CR-179072) ADVANCED PROPULSION
SYSTEMS CONCEPTS FOR ORBITAL TRANSFER STUDY.
VOLUME 2: STUDY TECHNICAL RESULTS Final
Report (Boeing Co., Seattle, Wash.) 185 p

N87-70372

67913

Unclass
43705

00/20



ADVANCED PROPULSION SYSTEMS
CONCEPTS FOR ORBITAL TRANSFER STUDY

Final Report
Volume II

STUDY TECHNICAL RESULTS

D180-26680-2
1981

Submitted to
National Aeronautics and Space Administration
George C. Marshall Space Flight Center
by
Boeing Aerospace Company
Seattle, Washington

CONTENTS

	<u>Page</u>
FOREWORD	xi
1.0 INTRODUCTION	1
1.1 Background	1
1.2 Summary of Key Study Questions	2
2.0 APPROACH AND GUIDELINE	11
2.1 Study Approach	11
2.2 Study Ground Rules	12
2.2.1 Mission Models and Mission Capture	12
2.2.2 Aeroassist Technology	17
2.2.3 Advocate Data Base	18
3.0 TECHNICAL RESULTS	19
3.1 Task 1 - Advanced Propulsion Concept Survey and Characterization	20
3.1.1 Thermodynamic Rocket Concepts	21
3.1.2 Electric Rocket Concepts	27
3.2 Task 2 - Candidate Propulsion System Analysis and Sizing	35
3.2.1 Optimization of Manned Nuclear Rockets	35
3.2.2 Laser Propulsion Trades	42
3.2.2.1 Laser System Trades	42
3.2.2.2 Space-Based Laser System	51
3.2.2.3 Ground-Based Laser System	56
3.2.2.4 Air-Based Laser System	57
3.2.3 Solar Rocket Trades	61
3.2.3.1 Engine Configurations	61
3.2.3.2 Propulsion System Definition	64
3.2.3.3 Solar Vehicle Sizing	67

	<u>Page</u>
3.2.4 Electric Propulsion Vehicle Sizing	72
3.2.4.1 Solar Photovoltaic-Ion Rocket	78
3.2.4.2 Solar Photovoltaic-Arc Jet	98
3.2.4.3 Solar Thermophotovoltaic-Ion Thruster	101
3.2.4.4 Solar Thermoelectric-Ion	107
3.2.4.5 Nuclear (Fission) Power Source-Ion Thruster	108
3.2.4.6 Nuclear Power Source MPD Propulsion Systems	112
3.3 Task 3 - Competitive Transportation System Definition and Cost Evaluation	124
3.3.1 Space Transportation System Scenarios	125
3.3.2 System Acquisition Costs	130
3.3.3 Operation Costs	137
3.3.4 Life Cycle Costs	138
3.3.5 High Mission Model Life Cycle Costs	141
3.4 Task 4 - Definition of Key Technology Development Requirements	150
4.0 REFERENCES	152
APPENDIX A - Summary Weight Statement - Single-Stage Nuclear OTV	A-1
APPENDIX B - Summary Weight Statement - Single-Stage Space-Based Solar-Powered OTV	B-1
APPENDIX C - Basics of Ion Thruster Efficiency	C-1
APPENDIX D - MPD Efficiency Convention	D-1

FIGURES

		<u>Page</u>
1.2-1	Propulsion System Performance	3
1.2-2	Upper-Stage Vehicle and Mission Chronology	4
1.2-3	Life Cycle Cost Summary Chart	6
1.2-4	Life Cycle Cost Summary	7
2.2-1	Mission-Imposed Transportation Requirements	14
2.2-2	Low Mission Model	15
2.2-3	High Mission Model	16
2.2-4	Mission Model Categories	17
3.1-1	Advanced Propulsion Concepts	20
3.1-2	Summary of Advanced Chemical Rocket Characteristics	21
3.1-3	Summary of Nuclear Fission Thermodynamic Rocket Characteristics	22
3.1-4	Summary of Nuclear Fission Pulsed Rocket (Orion) Characteristics	23
3.1-5	Summary of Fusion Rocket Characteristics	24
3.1-6	Typical Laser Heated Rocket Concept	25
3.1-7	Solar Thermal Rocket	26
3.1-8	Summary of Separately Powered Fluid Dynamic Rocket Characteristics	27
3.1-9	Morphology of Possible Electric Rocket Concepts	28
3.1-10	Summary of Electric Rocket Characteristics	29
3.1-11	Nuclear Thermoelectric Rocket	30
3.1-12	25-kW Thermal Arc-Jet Concept	31
3.1-13	Photovoltaic Systems Comparison	32
3.1-14	Thermophotovoltaic (TPV) Power System	32
3.1-15	Mass Driver Features/Risks	33
3.1-16	Solar Electric Rail Gun Rocket	34
3.2.1-1	Nuclear Rocket Configurations Based on NERVA Results	36/37
3.2.1-2	Shuttle-Compatible Manned Sortie Configuration Using Rotating-Bed Reactor Rocket	38

	<u>Page</u>
3.2.1-3 Rotating-Bed Rocket - Basic Module	38
3.2.1-4 Tank Modules for Rotating-Bed Rocket	39
3.2.1-5 First-Order Shielding Requirements (3 rem per Mission Dose)	39
3.2.1-6 Aerobraked Manned Capsule	40
3.2.1-7 Effect of Aerobraked Capsule on Shielding Requirements	41
3.2.1-8 Nuclear Rocket Manned Sortie Using Aerobraking Capsule	42
3.2.2-1 Laser Propulsion Trade Tree	43
3.2.2-2 Nonrigidized Inflatable Off-Axis Collector Configuration	44
3.2.2-3 Laser Collector Characteristics	46
3.2.2-4 Intensity Distribution in Focal Plane	47
3.2.2-5 Effects of Design Parameters on Space-Based Laser Concept	48
3.2.2-6 Conceptual 1.5-MW Laser Engine Design	49
3.2.2-7 Laser Engine Efficiency	50
3.2.2-8 Space-Based Laser Vehicle with 1.5-MW Engine	50
3.2.2-9 Space-Based Laser Vehicle with 5.63-MW (75N) Engine	51
3.2.2-10 Space-Based Laser System Sizing	52
3.2.2-11 Conceptual Space-Based Laser	53
3.2.2-12 Spiral Trajectory with Space-Based Laser	54
3.2.2-13 Space-Based Laser Multiple Impulse Trajectory - 12t Payload, 2000N Thruster	55
3.2.2-14 Effect of Vehicle Orbit Height on Ground-Based Laser Burn Time	58
3.2.2-15 Ground-Based Laser Orbital Mechanics	58
3.2.2-16 Selected Mission for 30-Day GEO Delivery Mission	59
3.2.2-17 Laser-Carrying Aircraft Clustered To Reduce Trip Time	60
3.2.3-1 Tungsten Foil Heat Exchanger Element	62
3.2.3-2 Porous-Wall Solar Rocket Engine	63
3.2.3-3 Rotating-Bed Absorber Solar Rocket	64
3.2.3-4 Solar Thermodynamic Rocket Configuration	65
3.2.3-5 Concentrator Performance (1/8-deg Standard Deviation)	66
3.2.3-6 Aerobraked Laser/Solar Vehicle Concept	68
3.2.3-7 LEO-to-GEO Orbit Transfer Propulsion (One Way)	69

	<u>Page</u>
3.2.3-8 Multiple Impulse Trajectory Characteristics	70
3.2.3-9 Aerobraked Solar Thermal Rocket Sizing	71
3.2.3-10 Aerobraked Solar Thermodynamic Rocket Concept	72
3.2.4-1 Generalized Electric Propulsion System	73
3.2.4-2 Morphology of Possible Electric Rocket Concepts	73
3.2.4-3 NPS-Ion Optimum Specific Impulse	75
3.2.4-4 Electric Propulsion OTV Sizing Procedure	76
3.2.4-5 Solar Electrical Propulsion System Schematic	78
3.2.4-6 Solar Electric Ion Rocket	79
3.2.4-7 Simulation Requirements	81
3.2.4-8 50-cm Ion Thruster	82
3.2.4-9 J-Thruster Characterization Program Block Diagram	83
3.2.4-10 First-Order Discharge Model	84
3.2.4-11 Correlation of J-Thruster Optical Transmissivity Data	84
3.2.4-12 Discharge Control Optimization - 50-cm Argon Ion Thruster	86
3.2.4-13 Discharge Optimization - 50-cm Argon Ion Thruster	86
3.2.4-14 Life Trends for a 50-cm Argon Thruster	87
3.2.4-15 50-cm Argon Ion Thruster Power Requirement	88
3.2.4-16 50-cm Argon Ion Thruster Performance Characterization	88
3.2.4-17 50-cm Argon Ion Thruster Life Trends	89
3.2.4-18 Power Processing Requirements for 50-cm Argon Thruster	90
3.2.4-19 CDVM PPU for 50-cm Argon Ion Thruster	91
3.2.4-20 Solar Array Specific Mass	92
3.2.4-21 EOTV Design Driver - Van Allen Radiation Impact	93
3.2.4-22 Effect of Thruster Voltage on SPV-Ion Powerplant Characteristics	93
3.2.4-23 SPV-Ion Parametric Characterization	94
3.2.4-24 Effect of Specific Impulse and Delivery Time on Solar Array Sizing	95
3.2.4-25 Limit SPV-Ion Performance	96
3.2.4-26 Effect of Accelerated Technology of SPV-Ion Vehicle Configurations	97
3.2.4-27 25-kW Thermal Arc-Jet Concept	99

	<u>Page</u>
3.2.4-28 Effect of Trip Time for SPV-Arc Concept	100
3.2.4-29 Effect of I_{sp} on SPV-Arc OTV Performance	100
3.2.4-30 Key Elements of the Thermophotovoltaic Concentrator	101
3.2.4-31 Optical Response of Lightweight Inflatable Solar Concentrator	103
3.2.4-32 Estimated Cell Performance for TPV System	104
3.2.4-33 Optimization of TPV Cell Temperature	105
3.2.4-34 TPV-Ion OTV Parametric Performance	106
3.2.4-35 TPV-Ion OTV Characteristics - 240-Day Upleg Transits	106
3.2.4-36 Nuclear Thermionic-Ion Thruster OTV (NTI-Ion)	108
3.2.4-37 Predicted Specific Weight for Nuclear Brayton Cycle Power Systems	109
3.2.4-38 Sensitivity of Specific Mass to Energy Conversion Efficiency	110
3.2.4-39 NEP-Ion OTV Sizing Data	111
3.2.4-40 NTI-Ion OTV Nominal Characteristics	111
3.2.4-41 Candidate Nuclear-Electric OTV Configuration	113
3.2.4-42 Princeton Pulsed Self-Field Thruster	116
3.2.4-43 Summary of Princeton MPD Thruster Inferred Efficiency Data	117
3.2.4-44 Efficiency Comparison for Princeton MPD Thruster	118
3.2.4-45 Effect of Thrust Efficiency and I_{sp} Variation on MPS-MPD OTV Performance	121
3.2.4-46 Effect of Thrust Efficiency on Powerplant Size for NPS-MPD OTV	122
3.2.4-47 Effective Efficiencies on MPD Vehicle Characteristics	123
3.3.1-1 Characteristics of Vehicles Selected for Costing - Low Model	125
3.3.1-2 Low Mission Model	126
3.3.1-3 Production Quantities for High-Thrust Concepts	127
3.3.1-4 Production Quantities for Low-Thrust Concepts	127
3.3.1-5 Comparison of SDV Launch Requirements - Low Model, High-Thrust Concepts	128
3.3.1-6 Comparison of SDV Launch Requirements - Low Model, Low-Thrust Concepts	128
3.3.1-7 Propellant Tanker	129
3.3.1-8 Maximum Size LH_2 Tank Compatible With SDV-1 Launch - Ground-Based Tank Module	130

	<u>Page</u>
3.3.2-1 System Acquisition Costing Ground Rules	131
3.3.2-2 H ₂ -O ₂ OTV DDT&E and TFU Cost Estimate	131
3.3.2-3 Rotating-Bed Rocket DDT&E and TFU Cost Estimate	132
3.3.2-4 Space-Based Laser OTV DDT&E and TFU Cost Estimate	132
3.3.2-5 Ground-Based Laser DDT&E and TFU Cost Estimate	133
3.3.2-6 Solar Thermal Rocket DDT&E and TFU Cost Estimate	133
3.3.2-7 SPV-Ion DDT&E and TFU Cost Estimates	134
3.3.2-8 TPV-Ion DDT&E and TFU Cost Estimates	134
3.3.2-9 NPS-Ion DDT&E and TFU Cost Estimates	135
3.3.2-10 High-Thrust System Acquisition Costs	136
3.3.2-11 Low-Thrust System Acquisition Costs	136
3.3.3-1 OTV Operation Costs - Low Model	138
3.3.4-1 Life Cycle Cost Summary by Hardware Element - High-Thrust Concepts	139
3.3.4-2 Life Cycle Cost Summary by Hardware Element - Low-Thrust Concepts	139
3.3.4-3 Life Cycle Cost Summary Chart	140
3.3.5-1 Characteristics of Vehicles Selected for Costing - High Model	141
3.3.5-2 Comparison of SDV Launch Requirements	142
3.3.5-3 Comparison of SDV Launch Requirements - High Mission Model	143
3.3.5-4 Production Quantities for Vehicles Unique to High Model	143
3.3.5-5 Large Solar ABOTV DDT&E and TFU Cost Estimate	144
3.3.5-6 Large Nuclear RBR DDT&E and TFU Cost Estimate	144
3.3.5-7 Large Chemical ABOTV DDT&E and TFU Cost Estimate	145
3.3.5-8 Large SDV-Ion DDT&E and TFU Cost Estimate	145
3.3.5-9 Large TPV-Ion DDT&E and TFU Cost Estimate	146
3.3.5-10 High Model Systems Acquisition Costs	146
3.3.5-11 OTV Operations Costs - High Model	147
3.3.5-12 Interest Costs - High Model	147
3.3.5-13 Life Cycle Costs Summary by Hardware Element for High Model	148
3.3.5-14 High Model LCC by Category	148
3.3.5-15 Life Cycle Cost Summary Chart - High Mission Model	149

ABBREVIATIONS AND ACRONYMS

AB OTV	aerobraked OTV
BAC	Boeing Aerospace Company
BOE	balance of energy
BOL	beginning of life
COTV	chemical OTV
CR	concentration ratio
DDT&E	design, development, test, and evaluation
EDL	electron discharge laser
EIS	Executive Information System
EMC	electromagnetic compatibility
EMI	electromagnetic compatibility interference
EOL	end of life
EOTV	electrical orbital transfer vehicle
F_2-H_2	fluorine-hydrogen (rocket)
FEL	free electron laser
FOTV	future orbital transfer vehicle
GaAs	galium arsenide (solar cell)
GEO	geosynchronous Earth orbit
H_2-O_2	hydrogen-oxygen (rocket)
HLLV	heavy lift launch vehicle
IOC	initial operating capability
IR&D	independant research and development
I_{sp}	specific impulse
LASL	Los Alamos Scientific Laboratory
LCC	life cycle cost
LEO	low Earth orbit
MPD	magnetoplasmadynamic
MPS	main propulsion system
MSFC	Marshall Space Flight Center
NASA	National Aeronautics and Space Administration

NERVA	nuclear engineering reactor vehicle assembly
NPS	nuclear power source
NWD	nuclear waste disposal
OTV	orbital transfer vehicle
PBFA	partical beam fusion apparatus
PCM	Parametric Cost Model
PPU	power processing unit
RBR	rotating-bed reactor
SDV	shuttle-derived vehicle
SEPS	solar electric propulsion system
SI	silicon (solar cells)
SP	special performance (airplane)
SPS	solar power satellite
SPV	solar photovoltaic
STE	solar thermoelectric
STI	solar thermionic
STR	solar thermal rocket
STS	Space Transportation System
TFU	theoretical first unit
TPV	thermophotovoltaic
TVC	thrust vector control
T/W	thrust-to-weight (ratio)

FOREWORD

This final report of the Advanced Propulsion Systems Concepts for Orbital Transfer Study was prepared by the Upper Stages and Launch Vehicles Preliminary Design organization of the Boeing Aerospace Company (BAC) for the National Aeronautics and Space Administration's George C. Marshall Space Flight Center in accordance with Contract NAS8-33935. The study was conducted under the direction of the NASA study manager, Mr. William Galloway, during the period from July 1980 through July 1981. The final report is organized according to the following three documents:

- Volume I: Catalog of Advanced Propulsion Concepts
- Volume II: Study Technical Results
- Volume III: Life Cycle Cost Estimates

Key personnel during the performance of this study were:

Dr. Dana G. Andrews - Study manager, responsible for nonelectric concepts

Mr. Don Grim - Deputy study manager, responsible for electric vehicle concepts

Supporting personnel during this study were:

Structures and Weights	R. T. Conrad
Electrical Power	R. J. Gewin
Systems Analysis	E. E. Davis and R. P. Reinert
Cost and Programmatics	J. C. Jenkins
Constructive Criticism	V. A. Caluori

1.0 INTRODUCTION

NASA has long recognized the potential of advanced propulsion to improve space transportation and has supported several design and development efforts for advanced propulsion concepts (e.g., nuclear and electric rockets). Unfortunately, none of these previously developed concepts has ever been used in primary propulsion, although the technology developed has seen use in other applications. The primary reason for this has been that long development cycles, combined with escalating costs and changing mission requirements, have always succeeded in stopping the program before final development. For instance, development of a nuclear rocket (NERVA) could no longer be justified when this country cancelled any plans for a Mars landing or a permanent lunar habitat, and development of an electric rockets (SEPS) was halted when NASA cancelled future comet or asteroid rendezvous-type missions.

In order to circumvent this problem, the current study sought to determine if there was a new propulsion concept available which could significantly improve orbit-to-orbit transportation relative to first generation chemical vehicles and, in addition, have developmental costs which could be justified by operational cost savings. Such a vehicle concept could be justified by its overall usefulness and would not be dependent upon the survival of a single mission for its development.

1.1 Background

The ability to move payloads from place to place in space is fundamentally dependent on the capability to control and apply energy. The practicality of any propulsion concept is determined by the size, mass, efficiency, and cost of the method of energy conversion from its initial form, such as high-temperature combustion gases or high-energy nuclear reactions, to the production of force or thrust. As mankind continues exploration and utilization of the resources of the solar system, the ability to proceed will depend upon the quality and quantity of space transportation systems available. This relationship is analagous to the situations in many developed

and undeveloped countries today where economies are critically dependent upon the quality and quantity of aeronautical transportation systems.

The historical dependence of aeronautical transportation progress on advancements in propulsion technology has its analog in space also. The hydrogen-oxygen (H_2-O_2) rocket engine is now about 20 years old. Its latest application in the space shuttle orbiter requires that nearly its ultimate theoretical potential be realized in practical application, especially with respect to efficiency and endurance. Although it is reasonable to expect this performance can be achieved, it is also evident that further progress in propulsion technology is highly desirable to more effectively perform currently visualized missions. The key to an excellent space transportation system is the effective use of more advanced energy sources than the simple combustion of fuel and an oxidant. In the foreseeable future, the most likely sources of energy for this purpose are nuclear fission and fusion reactions--either directly from an onboard reactor or indirectly via collection of energy transmitted from a remote reactor (e.g., the Sun). Present concepts for the conversion and application of these alternative energy sources are probably still primitive; but even at this early stage, nuclear energy and beamed power offer large performance benefits.

1.2 Summary of Key Study Questions

Principal results of this study are reported here as responses to questions addressing the key issues developed at the beginning of the study. The sequence of results is a logical progression beginning with the most fundamental program issues.

ARE THERE LEAP-FROG PROPULSION TECHNOLOGIES AVAILABLE WITH REASONABLE DEVELOPMENT RISKS?

Several advanced propulsion options exist which could provide marked improvements in engine specific impulse. Performance levels attainable with these advanced concepts are shown in Figure 1.2-1. All use nuclear energy,

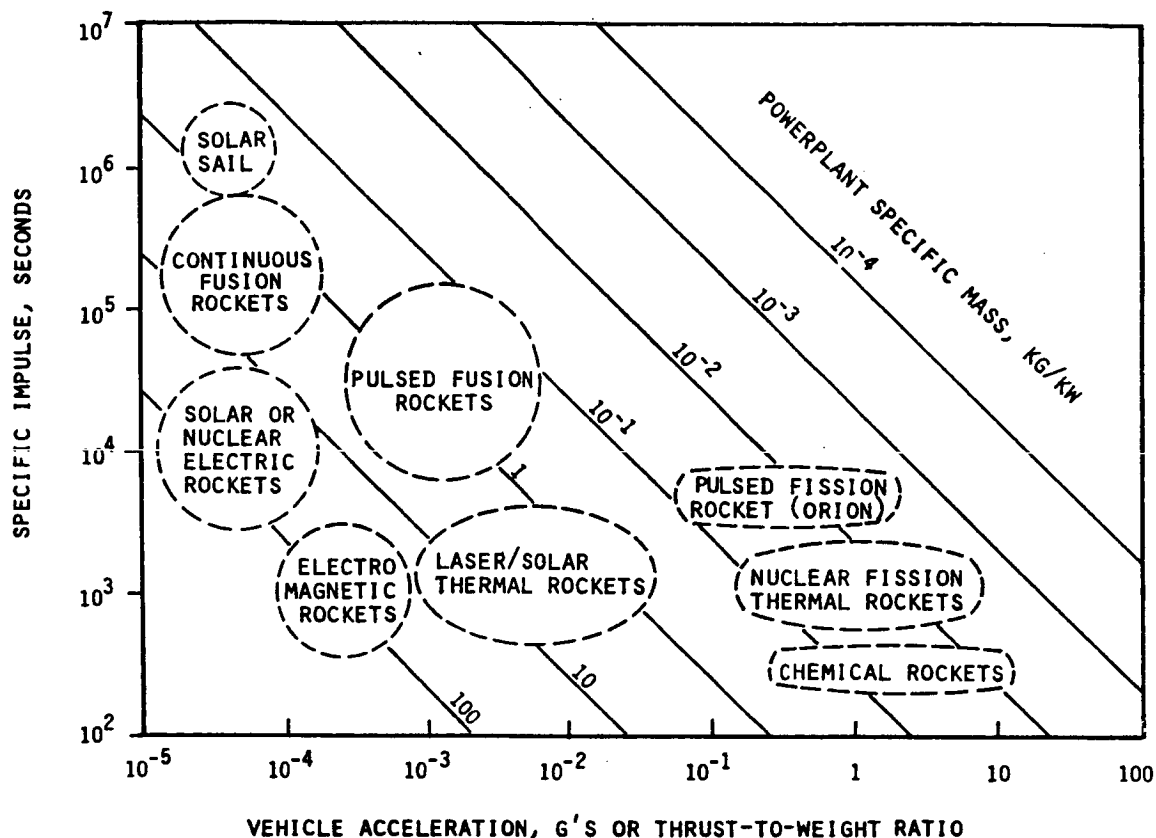


Figure 1.2-1: Propulsion System Performance

solar energy, or beamed power, and all have performance (measured as specific impulse) superior to chemical rockets. The advanced propulsion concepts shown fall into two categories: (1) those which can be developed in the near future using today's design level technology as a basis and (2) those which appear to be physically realizable, extrapolating from today's technology, but for which no detailed design data exists.

The first category includes solar and nuclear electric rockets, laser and solar thermal rockets, and nuclear fission thermal rockets. These concepts were characterized, sized to meet a specific mission model, and costed during the course of this study. The second category includes the pulsed fission rocket (Project Orion), the pulsed fusion rocket, and the continuous fusion rocket. These concepts were surveyed and cataloged, but no attempt was made to size or cost them.

The solar sail concept is a special case in that some design data exist but it appears unlikely that a solar sail could ever operate below 1000 km because of air drag, and operation from low Earth orbit (LEO) was a study prerequisite. Hence this concept was surveyed and cataloged but not pursued

as an alternative for near Earth space transportation vehicles.

HOW DOES ADVANCED PROPULSION FIT INTO FUTURE SPACE TRANSPORTATION REQUIREMENTS?

A chronology of predicted future missions for upper stage vehicles in the shuttle space transportation era with related vehicle requirements is shown in Figure 1.2-2. The first phase in upper stage missions was assumed to start

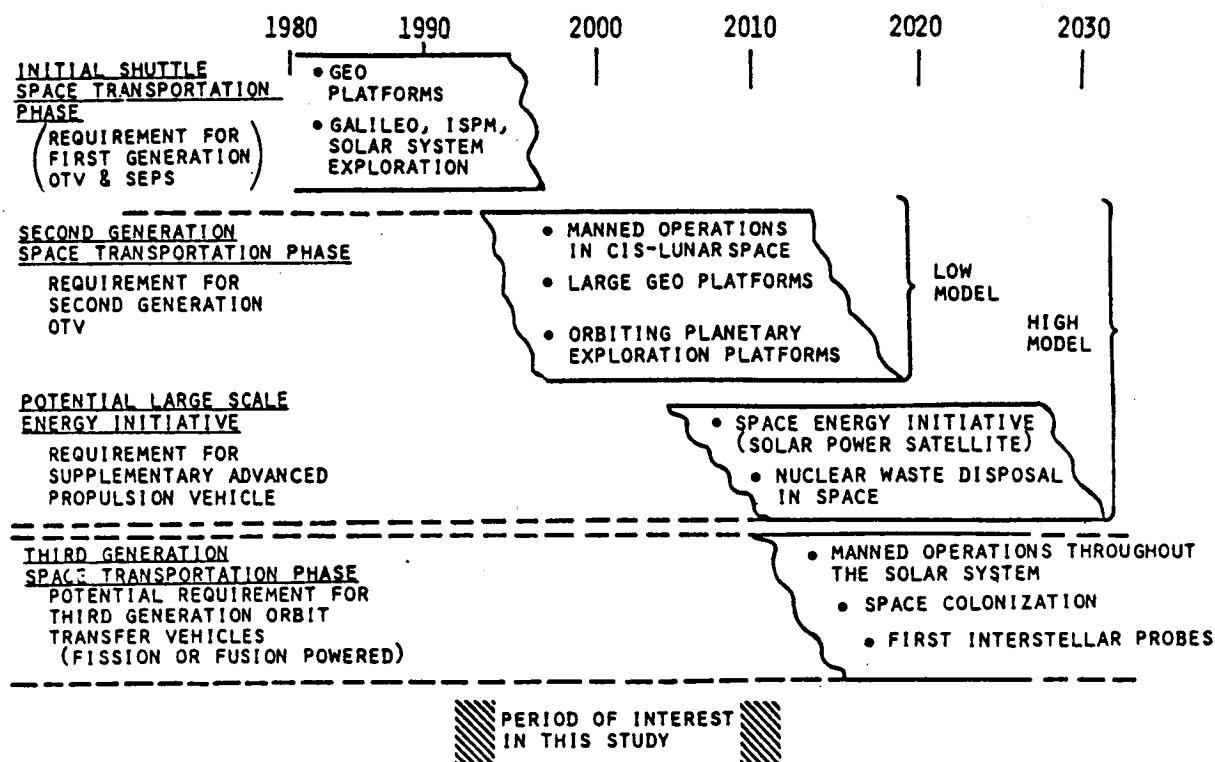


Figure 1.2-2: Upper Stage Vehicle and Mission Chronology

with IUS and end with a first-generation orbital transfer vehicle (OTV) and solar electric propulsion system (SEPS). These vehicles would be used predominately as expendable stages and be capable of performing early geosynchronous Earth orbit (GEO) platform delivery and solar system exploration missions.

Starting in 1992 and through about 1998, there are a series of "new start" missions involving manned presence in GEO and large-scale use of cislunar space for commercial and military applications. These missions will

require new transportation vehicles with larger payloads and reuse capability. The advanced propulsion vehicles in this study were designed and sized to accomplish the missions in this second space transportation era. Late in this era (2005-2010), there is potential for a large-scale space energy initiative, culminating with a go-ahead on a solar power satellite (SPS) program to start about 2010. This energy initiative would increase the annual payload mass to GEO during the 2005-2010 time period by an order of magnitude, in order to construct an SPS demonstrator, and by another order of magnitude when SPS construction actually begins.

Missions proposed for the period 1995-2010, without the space energy initiative, are termed the low mission model; missions proposed for the period 1995-2010, including the energy initiative missions, are termed the high mission model. The low model is heavily influenced by the manned missions which constitute about one-third of the total on-orbit mass requirements. The high model, on the other hand, is dominated by the bulk cargo delivery requirements for the SPS demonstrator. This diversity in mission design requirements will result in different vehicle recommendations, as will be discussed later.

A third space transportation era would begin with manned exploration and operations throughout the solar system. Space transportation in this era would require very high delta-V's and intermediate thrust-to-weight ratios (0.01 to 0.001) to reduce manned mission times to acceptable limits (1 to 2 years). This necessitates the use of high energy fission and/or fusion propulsion to reach the power levels required. Requirements for this type of propulsion system were assumed to occur some time after 2010 when the general level of technology to support these missions might be available. Because of the far-term nature and technical uncertainties involved in advanced fission and fusion propulsion concepts, they were not actively pursued in this study.

CAN DEVELOPMENT OF ADVANCED PROPULSION BE JUSTIFIED BY FUTURE MISSION REQUIREMENTS?

The advanced propulsion concepts comprising the first category from Figure 1.2-1 (solar and nuclear electric rockets, laser and solar thermodynamic rockets, and nuclear fission thermodynamic rockets) were all characterized to the degree where they could be used to define vehicles and sized to capture the low mission model requirements mentioned above. These vehicles, by themselves or in combination with a baseline chemical (H_2/O_2) OTV, were then used to define transportation system scenarios for which life cycle costs (LCC) could be estimated.

A comparison of total life cycle costs for the low mission model is shown in Figure 1.2-3. The surprise result of the LCC study was that all propulsion

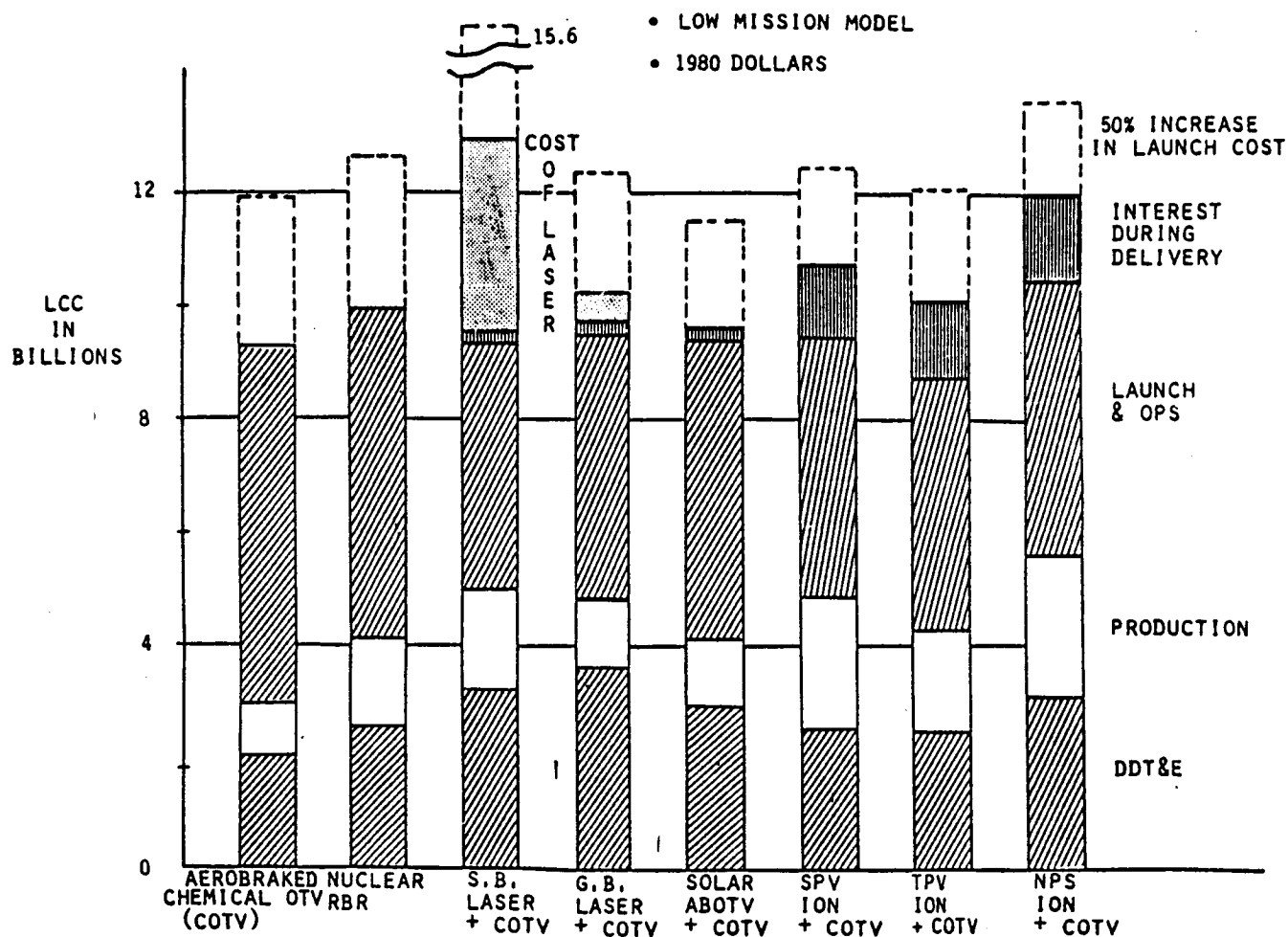


Figure 1.2-3: Life Cycle Cost Summary Chart

concepts had life cycle costs for the low mission model within 5% to 10% of a median value (\$10.0 billion for the low mission model excluding interest charges during delivery). This effectively excluded cost savings as a discriminator for recommending an advanced propulsion concept and left the selection process to more quantitative discriminators such as technical risk or technology availability.

Vehicles were also sized to capture the high mission model (large-scale energy initiative scenario) and the life cycle costs incremented to reflect the large increase in traffic. A summary comparison of high model LCC's is shown in Figure 1.2-4. The high model, with its large number of bulk cargo

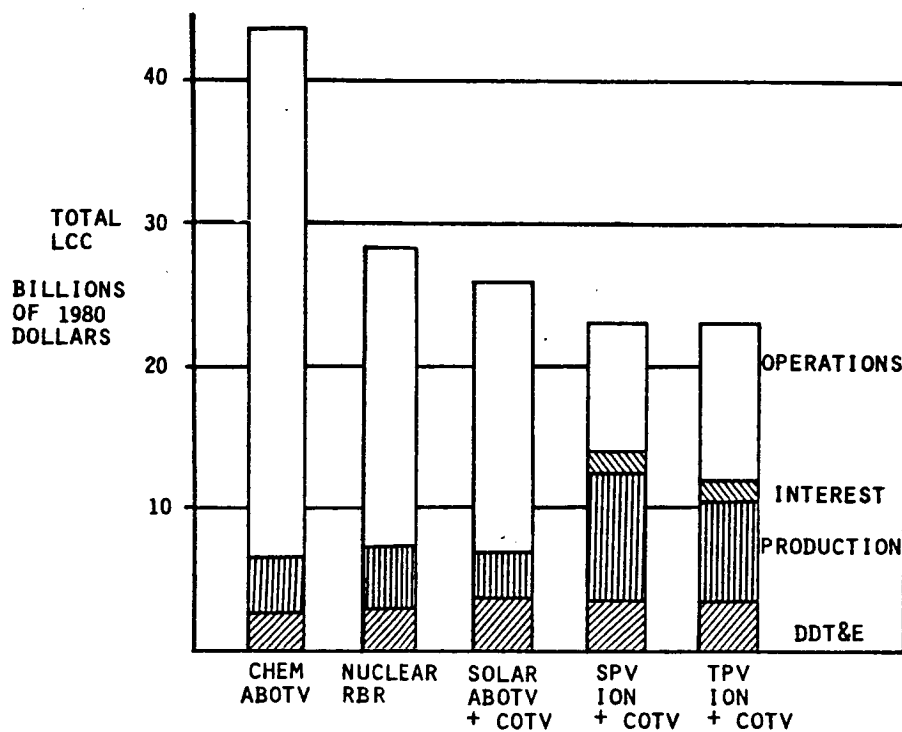


Figure 1.2-4: Life Cycle Cost Summary Chart—High Mission Model

deliveries, produced LCC's dominated by operations costs (propellant launch costs). Therefore, the higher specific impulses characteristic of the advanced propulsion concepts would pay dividends in the form of reduced propellant launch costs and, hence, reduced LCC's as shown in Figure 1.2-4.

In the low mission model, life cycle costs of advanced vehicles are adversely affected by the need to develop a second class of vehicles (chemical OTV's and their support tankers) to perform the manned portion of the model. (The nuclear thermodynamic rocket has enough thrust to perform the manned mission but has an inefficient configuration to meet the manned radiation

dosage requirement.) In the high model, the penalty associated with satisfying the manned portion of the model does not seriously impact the total costs; therefore, the difference.

WILL ADVANCED PROPULSION REPLACE, AUGMENT, OR IMPROVE CURRENTLY ENVISIONED UPPER-STAGE VEHICLES?

Study results indicate that for the time period associated with the low model (1990-2005), the vehicle which would best meet the upper stage transportation requirements, as currently understood, would be the H_2-O_2 aeroassisted OTV. This conclusion follows from the facts that the H_2-O_2 OTV could (1) meet all assumed mission requirements, (2) had LCC's equal to or better than any advanced concept, and (3), if development risk or cash flow discounting were included, would be a runaway winner with respect to costs. In fact, it is doubtful that a mixed fleet could be justified for the low model even if a breakthrough occurred that reduced production costs for one of the advanced concepts: the development cost advantage of the H_2-O_2 rocket is just too great to overcome in a small mission model.

However, if a large-scale space industrialization scenario or space energy initiative should develop, a mixed fleet of upper stage vehicles would be attractive. In this case, an H_2-O_2 aeroassisted OTV would be required for manned missions and priority cargo, with a higher performance advanced propulsion vehicle for bulk cargo delivery. Exactly which concept would be best for bulk cargo delivery is a subject for speculation. One of the solar electric concepts would probably be the best bet, especially if there is a breakthrough in either efficiency or cost; but one cannot dismiss the solar thermal or laser rockets which offer faster LEO-to-GEO transits and less radiation damage. Because we are discussing a vehicle with an IOC of 2004, this decision does not have to be made for 10 to 20 years, if at all.

The most likely driver in selecting the advanced propulsion concept to follow the H_2-O_2 engine will be an additional mission scenario brought on by factors unforeseen at this time. Mission scenarios change rapidly and chances are the mission driver in the year 2000 will be something we cannot even guess

at in 1981. For these reasons, we do not propose the development of any advanced propulsion vehicles at this time. We do propose that low-scale development of all concepts listed here be continued and, as additional mission scenarios appear, that technology development efforts be directed toward those mission requirements where they will result in definite payoffs.

HOW SHOULD WE ALTER OUR CURRENT COURSE OF ACTION TO BE BETTER PREPARED FOR THE FUTURE?

Recommendations from this study are relatively straightforward:

1. Move ahead with the H_2-O_2 aeroassisted OTV. There are no near-term replacements.
2. Direct on going advanced propulsion technology efforts toward mission requirements where they will have definite performance payoffs. For example, direct solar electric technology toward long-duration high delta-V missions, such as multiple asteroid or comet rendezvous, and nuclear electric technology toward long-duration deep-space probes.
3. Stimulate key technology areas for possible breakthroughs which could revolutionize various advanced propulsion concepts. Examples of such key technologies would be: direct coupling of radiant energy with propellant/working fluid; low-cost, lightweight vapor-deposited solar arrays; high efficiency direct nuclear-to-electric power conversion; or a low-cost, high-power, nuclear-pumped laser.
4. Initiate fundamental propulsion research to incorporate more high energy physics. Manned missions to the asteroids or beyond will require specific impulses of several seconds and vehicle thrust-to-weight ratios of 0.01 to 0.001 for reasonable payload

fractions and reasonable trip times (1 to 2 years). Only advanced fusion or fission rockets are capable of meeting these requirements and both appear to have rather long development cycles. Hence, it is important that some effort get underway to at least define the technology requirements and a technology development plan to meet some future manned solar system exploration scenario.

WHY DO THE RESULTS OF THIS STUDY DIFFER FROM RESULTS OF PREVIOUS ADVANCED PROPULSION SURVEY STUDIES?

There are three ways this study differed from earlier advanced propulsion surveys. First, a truly advanced H_2-O_2 vehicle including aeroassist was used for the first time. Previous studies tended to use a "strawman" chemical stage, often sized for an entirely different mission. Second, this study ground ruled the use of shuttle-derived vehicles (SDV) to carry propellant to LEO which reduces fuel transportation costs and improves the economics of lower specific impulse vehicles relative to more efficient advanced propulsion concepts. Third, this study included a mixed mission model containing LEO-to-GEO delivery missions, manned missions, and planetary probes. This tended to stress flexibility that is not available with many advanced concepts, forcing them into an expensive mixed-fleet scenario.

2.0 APPROACH AND GUIDELINES

2.1 Study Approach

This section is an overview of the study technical approach, including a summary of its key features and rationale. This study surveyed and analyzed advanced propulsion system concepts for orbital transfer missions postulated for the post-1990 time period, compared these advanced concepts with each other and with currently planned systems, identified required technology program plans, and recommends action items.

The major challenge was to compare, on an equal basis, propulsion system concepts which had widely disparate data bases, different levels of technical risks, and performance characteristics which differ by one or more orders of magnitude. This large variation between concepts required an innovative study and put a premium on the judgment and analysis capability of the study personnel. Accordingly, the study was time phased to produce exactly the information required for early decisionmaking, and maximum advantage was taken of concurrent studies to supplement the analyses. Key features of the technical approach included the following.

1. Advanced propulsion options were surveyed and characterized at the concept level and those options with unresolved feasibility issues or those not suited to the mission model were eliminated. Thus no effort was wasted developing vehicle configurations and transportation system scenarios for those concepts.
2. The remaining advanced propulsion options were developed into vehicle configurations which were parametrically sized to optimize their usefulness to the overall mission model. Each vehicle concept was tested against the complete mission model so that those concepts requiring significantly more shuttle launches to complete the mission model could be eliminated. Again, no effort was wasted developing transportation system scenarios for those concepts.

3. After the midterm review, a total transportation system scenario was defined for each remaining advanced propulsion concept, including project programmatic, operations analyses, and life cycle costing, which allowed comparison of the advanced systems to each other and to currently planned systems (OTV and SEPS) on the basis of life cycle costs. This provided the final screening of advanced concepts because those systems having estimated life cycle costs significantly higher than the current technology systems could be safely discarded (unless convincing rationale for enhanced performance margin was available).
4. The final task was to address key issues identified with respect to advanced propulsion technology, resolve trades indicated from the life cycle costing, and document the study results.

2.2 Study Ground Rules

A basic ground rule was that first-generation chemical and electrical vehicles already existed and could be used for missions for which the larger, more expensive advanced concepts were not suitable. It was also assumed that all advanced vehicles were space based using a permanent LEO base for maintenance, payload manifesting, and propellant storage/transfer. Most advanced concepts must be space based because of size or radiation risks associated with their powerplants, and space basing brings an additional benefit in allowing the use of shuttle-derivative vehicles which reduce launch costs for propellants and replacement parts.

2.2.1 Mission Models and Mission Capture

The mission model assumed was identical to the model proposed for the Future OTV (FOTV) Technology Study conducted by Langley Research Center and Boeing Aerospace Company (Reference 1). This model, in turn, was an

extrapolation of the mission model constructed by MSFC during the Phase A Orbital Transfer Vehicle Study (Reference 2). The mission-imposed transportation requirements are summarized in Figure 2.2-1. The overall model is composed of 24 separate missions which have been divided between two mission model levels.

The two mission models consisted of 297 missions (low model) and 1137 missions (high model) from 1995 through 2010. The low model, Figure 2.2-2, assumes a straightforward extrapolation of currently planned activities into the future with only one new start, a GEO base, to begin operation in 1999. The high model is much more ambitious. It assumes this country will begin a large-scale space energy initiative in the late 1990's, with space disposal of nuclear wastes commencing in 1995, construction of a solar power satellite demonstration platform commencing in 2004, testing starting in 2007 (see Figure 2.2-3).

Mission Capture Analysis: To select a vehicle size which adequately matches the mission transportation requirements, the mission models were categorized and the high model energy initiative missions repackaged to be more compatible with SDV launch characteristics. Mission model categories and key requirements are summarized in Figure 2.2-4. Mission capture analysis yields the following results: (1) Many of the free-flying satellites under 6 metric tons (6t) go into high inclination orbits which are not readily accessible from the 28.5-deg inclination orbit current planned for our LEO base. Satellites under 6t can be delivered via a Space Transportation System (STS) launch using the initial ground-based aeroassisted OTV in its reusable mode, and this appears to be the best method of operation for this category. (2) Large assembled platforms and GEO base components range in mass from 6.8t to 35.3t with a large break in the number of elements at just under 12t (see Figures 2.2-1 and 2.2-2).

Hence, the advanced propulsion vehicles for the low mission model were sized to deliver 12t of payload to GEO and return empty to LEO. Mission capture analysis showed that vehicles of this size could capture the unmanned deep-space exploration missions shown in Figure 2.2-4. It was assumed that

MISSION TYPE	MAX G LEVEL (DELIVERY)	ORBIT TRANSFER Δ (MVS) DELIVERY RETURN	PAYLOAD MASS (M.T.) EACH DELIVERY RETURN	COMMENTS
1. COMMUN PLATFORM	0.2	4398	6.8	6 PLATFORMS JOINED TO FORM 1 CLUSTER
2. ADV COMMUN PLAT.	0.2	4358	31.8	
3. PERS. COMMUN SAT	0.1	4388	24.5	
4. SPACE BASED RADAR	0.1	4388	11.4	
5. DOD CLASS III	0.1	4388	11.4	
6. DEEP SPACE RELAY	0.1	4388	6.8	
7. SOLAR TERRES OBSER	1.0	4282	11.0	
8. SPS EYTA	0.1	4434	Δ	Δ 32 FOR PWR GEN; 8.6 FOR YNTR; TRANSPORT SEPARATELY
9. SPS DEMO	3.0	4322	6446 Δ	Δ INCL 10s FOR CONTAINERS Δ 2 GEO CONSTRUCTION
10. DOD CLASS IA	3.0	4282	2.7	
10a. DOD CLASS IB	3.0	4282	4.0 (AVG)	
11. DOD CLASS II	1.0	4282	5.5	
12. COMMERCIAL & NASA	3.0	4282	4.5 (AVG)	MULTIPLE PAYLOAD DELIVERY
13. G.P. GEO BASE	3.0	4322	Δ	Δ 35.3 FOR 4 MAN; 20.7 FOR Δ 4 MAN
14. G.P. BASE MISS-EQUIP	3.0	4322	Δ	Δ 9 FOR APPLIC MOD; 7 FOR SERV SHUTTLE
15. SAT. MAINT PROV.	3.0	4322	2	WILL BE INCORP WITH MISSION # 19
16. CONST BASE ELEMENTS	3.0	4322	1420 Δ	Δ INCLUDES 50 FOR REPAIR MODULE
17. DEMO SAT. MAINT PROV	3.0	4322	10	
18. MAINT SORTIE	3.0	4322	5.9	
19. G.P. BASE SUPPORT	3.0	4322	Δ 5.6	Δ 4 MAN ROTATION Δ 8 MAN ROTATION
20. CONST BASE SUPPORT	3.0	4322	Δ 12.4	CREW OF 25 AND SUPPLIES FOR 90 DAYS
21. SCIENCE SORTIE	3.0	4322	32.4	
22. UHMAN. SERVICING	3.0	4471	8.1	VISIT TO 2 SATELLITES
23. PLANETARY	3.0	Δ	4.8	Δ PROVIDE C ₃ = 55 km ² /sec ²
24. HUC WASTE DISPOSAL	3.0	3350	11.4	Δ INCLUDES WASTE PKG PLUS SOLAR INSERTION STG (MSFC REF)
			Δ 11.5	Δ WASTE PKG + SOIS + REENTRY SHIELD
			Δ 19.5	

Figure 2.2-1: Mission Imposed Transportation Requirements

CATEGORY	MISSIONS	MISSIONS PER YEAR																		COMMENTS
		TOTAL	95	96	97	98	99	00	01	02	03	04	05	06	07	08	09	10		
LARGE ASSEMBLED SATELLITES (LAS)	1. COMMUN PLATFORM	7	1	1	2	2	1							1		1		1	2700 XPONDERS (40 MHz) BY YEAR 2000 ADDITIONAL 6000 XPONDERS BY 2010 80 MILLION SUBSCRIBERS; Δ CHANGE TO BLOCK II MODEL	
	2. ADV. COMMUN PLATFORM	4					1													
	3. PERS COMMUN SAT	8	1		1	1		1	Δ	1		1		1		1				
	4. SPACE BASED RADAR	2								1										
	5. DOD CLASS III	9	1	1	1	1	1									1	1			
	6. DEEP SPACE RELAY SAT	1																		
	7. SOLAR TERRES. OBSER	1								1										
FFAS	10. DOD CLASS IA	32	2	2	2	2	2	2	2	2	2	2	2	2	2	2	2	2		
	10a. DOD CLASS IB	10																		
	11. DOD CLASS II	5						1	1	1								1		
	12. COMEP & NASA	16	2		2		2		2					2						
CARGO TO MAN MANNED GEO BASE	13. GEN. PURP. BASE	2					Δ 1										Δ 2		Δ 14 MAN CAPAB; Δ 8 MAN CAPAB. Δ 3 APPLIC MODULE; Δ 1 SAT. SERVICE SHUTTLE ALSO REFLECTS MAINTAINED MAINT. SORTIES PER YR	
	14. G.P. MISSION EQUIP	5					Δ 3	1	Δ 4		Δ 1	Δ 3	1	Δ 4			Δ 3			
	15. SAT. MAINT. PROV.	16						1	2	1	2	1	2	1	2	1	3			
	18. GEO MAINT. SORTIE	11	2	1	3	2	1	2	Δ 6								Δ 5			
MANNED ROUND TRIPS	19. G.P. BASE SUPPORT	54				2	4	4	4	4	4	4	4	4	4	1	8	8	Δ 6 AFTER YR 2000 MAINT. SORTIE STAGED FROM GEO BASE Δ 5 REFLECTS 8 MAN BASE; 4 MEN & SUPPLIES/FLT.	
	21. SCIENCE SORTIES	3				1						1						1		
OTHER	22. UNMANNED SERVICING	103	2	4	4	5	6	7	8	7	8	7	8	7	8	7	10			
	23. PLANETARY	8		1		1		1	1		1		1		1					
	TOTAL MISSIONS	297	11	10	16	14	19	20	19	19	20	20	19	20	18	20	24	27		

Figure 2.2-2: Low Mission Model

CATEGORY	MISSION	TOTAL	MISSIONS PER YEAR																	COMMENTS
			95	96	97	98	99	00	01	02	03	04	05	06	07	08	09	10		
LARGE ASSEMBLED SATELLITES (LAS)	1. COMMUN. PLATFORM	7	1	1	2	2	1											1	◊ CHANGE TO BLOCK II MODEL	
	2. ADV. COMMUN PLAT.	4																		
	3. PERS. COMMUN. SAT	8	1	1	1	1	1	◊				1	1	1		1				
	4. SPACE BASED RADAR	2								1										
	5. DOD CLASS III	9	1	1	1	1	1							1	1	1				
	6. DEEP SPACE RELAY SAT	1																		
	7. SOLAR TERRESTIAL OBSER	1																		
	8. SPS ENGR VERIF TEST ART	1						1	◊		T	T	T							
	9. SPS DEMO SATELLITE	1						1					1	◊	T	T	T			
FFAS	10. DOD CLASS I, IA, IB	32	2	2	2	2	2	2	2	2	2	2	2	2	2	2	2	2	◊ 12 YRS TO CONST & LEO TEST (01, 02); 3 YR GEO TEST ◊ 2 YR TO CONST AT GEO; TEST FOR 3 YRS (T) ◊ REQ 80 FLTS WITH 80 MT OTV	
	10a. DOD CLASS IB	10																		
	11. DOD CLASS II	5						1	1	1							1			
	12. COMMERCIAL & NASA	10						2		2				2		2				
CARGO TO GEO BASE	13. GEN. PURPOSE BASE	2					1	◊											◊ 14 MAN CAPAB; ◊ 18 MAN CAPAB. ◊ 5 APPLIC MODULE ◊ 6 SAT SERV SHUTTLE ALSO REFLECTS MANNED MAINT SORTIES FROM GEO BASE. ◊ 7 YRS TO CONST (04, 05) ◊ 8 REPAIR MODULE (20 FLTS WITH 80 MT OTV)	
	14. G.P. BASE MISSION EQUIP	5					1	◊					1	◊		1	◊			
	15. SATELLITE MAINT PROV.	16					1	2	1	2	1	2	1	2	1	1	3			
	16. CONST BASE	2									1	◊		1	◊					
	17. DEMO SAT MAINT PROV.	16												4	4	4	4			
MANNED ROUND TRIPS	18. MAINT. SORTIE	11	2	1	3	2	1	2											AFTER YR 2000, MAINT SORT. STAGED FROM GEO BASE AFTER YR 2000, REFLECTS 8 MEN AND SUPPLIES/FLT REFLECTS 25 MEN & SUPPLIES PER FLIGHT	
	19. G.P. BASE SUPPORT	46				2	4	◊	4	4	4	4	4	4	4	4	4			
	20. CONST BASE SUPPORT	44								4	8	16	4	4	4	4	4			
	21. SCIENCE SORTIES	3						1				1						1		
OTHER	22. UNMANNED SERVICING	103	2	4	4	5	6	7	8	7	8	7	8	7	8	7	10		REFLECTS 200 GWE GRD OUTPUT & 29 MT STS CAPAB.	
	23. PLANETARY	8		1	1	1	1	1	1			1	1	1	1	1	1			
	24. NUCLEAR WASTE DISPOSAL	790	10	20	20	40	40	60	60	60	60	60	60	60	60	60	60	60		
	TOTAL MISSIONS (EXCLUDING ACTUAL FLTS FOR SPS)	1137	19	30	34	54	56	81	81	79	80	85	87	97	87	88	87	92		

Figure 2.2-3: High Mission Model

	NO. OF MISSIONS	
	LOW MODEL	HIGH MODEL
• FREE FLYING SATELLITES < 6 MT	63	63
• LARGE ASSEMBLED PLATFORMS AND GEO BASE EQUIPMENT < 12 MT	41	41
• GEO STATION COMPONENTS AND LARGE PLATFORMS > 12 MT	6	6
• UNMANNED SERVICING (5 MT UP-1 MT DOWN)	103	103
• MANNED CISLUNAR MISSIONS (8 MT ROUND TRIP)	68	104
• VERY LARGE CARGO (ENERGY INITIATIVE)		
• SPS (60 MT TO GEO)	-	137
• NWD (35 MT TO 0.85 A.U.)	-	240
• UNMANNED DEEP SPACE EXPLORATION		
• 3 MT to $C_3 = 130-140 \text{ km}^2/\text{sec}^2$	8	8
• MANNED EXPLORATION OF SOLAR SYSTEM	-	3

Figure 2.2-4: Mission Model Categories

the few GEO station and platform components larger than 12t would be broken down into 12t modules and launched separately, with assembly in GEO.

The advanced propulsion vehicles for the high mission model were sized to deliver 60t of payload to GEO and return empty to the LEO base. This allowed the SPS demonstrator components to be packaged in 60t modules for the SDV launch (SDV payload to 400 km = 60.5t) and then transferred intact to the advanced OTV for the trip to GEO.

2.2.2 Aeroassist Technology

As this study evolved, it became apparent that GEO delivery performance of several of the lower specific impulse candidate concepts would benefit from the aeroassist/aerobraking technology developed in the previous OTV studies (References 1 and 2). This technology allows the vehicle to use the Earth's upper atmosphere to help circularize the transfer orbit when returning from GEO to LEO, reducing the vehicle delta-V requirements by about 2100 m/sec. At NASA request, aerobraking of all thermodynamic rocket concepts was investigated and incorporated where practical.

One of the more difficult design missions in the proposed mission model was a "fast" outer-planet orbiter mission exemplified by the requirement to place a 1000-kg spacecraft in orbit around Neptune. "Fast" in this case was assumed to mean a trip time of 8 years or less (a Hohmann-type transfer to Neptune requires 30 years). Hyperbolic-type trajectories using Jupiter

swingby maneuvers can provide trip times of 6 to 8 years for C_3 's of 130 to 140 km^2/sec^2 , but the approach velocities at Neptune are 15 to 20 km/sec . Application of aeroassist/aerocapture technology developed by JPL (References 3 and 4) would allow a 3000-kg aerocapture bus to deliver the desired payload into the required orbit reducing the total mission delta-V by 60% to 70%. Use of aerocapture technology reduces the vehicle delta-V requirements to the point where any of the candidate propulsion concepts, including the $\text{H}_2\text{-O}_2$ baseline vehicle, can meet the planetary mission requirement. The high specific impulse (electric) candidate concepts can deliver somewhat larger payloads with slightly reduced trip times, but the improvements are not significant enough to warrant special consideration with respect to mission capture. It appears that aerocapture technology could be a key technology in future deep-space exploration missions.

2.2.3 Advocate Data Base

Another ground rule which evolved as the study progressed was the use of the advocate data base for engine performance and costs. Through a large number of personal contacts (phone calls and face-to-face discussions) during the survey and characterization phase of the study, it became apparent that any effort to decrease the performance (or increase the cost) of estimates was not welcome and, in fact, resented. To maintain a working relationship with the people involved, it was decided to use the data as made available and not to second guess or reengineer the results. This resulted in a certain degree of optimism, which varies between concepts, but the overall impact was not judged sufficient to change the relative results.

3.0 TECHNICAL RESULTS

The study was conducted in four phases. The initial phase (3 months) was dedicated to surveying and characterizing as many advanced propulsion concepts as possible. This phase required sufficiently detailed analysis to note unresolved feasibility issues and to recommend for elimination those propulsion options not suited to the mission model. This phase is covered in Volume I. In the second phase (second 3 months), the remaining advanced propulsion options were developed into vehicle configurations and parametrically sized to optimize their usefulness to the overall mission model. In the third phase (third 3 months), a total transportation system scenario was defined for each remaining concept. This allowed comparison of advanced transportation systems to each other and to the baseline systems outlined in the previous two studies, based on life cycle costs. The fourth phase (final 3 months) was used to address key issues with respect to advanced propulsion technologies and to document the study.

This section presents an indepth review of the study technical results. Detailed documentation of the first task (survey and characterization) is included in Volume I and life cycle cost estimating is in Volume III.

3.1 Task 1 - Advanced Propulsion Technology Survey and Characterization

A variety of advanced propulsion concepts have been proposed for use with the STS. The elements of these concepts (principal components and interfaces) require identification, characterization, and preliminary technology evaluations to establish viable propulsion options for consideration in the vehicle-level evaluations. Accordingly, the objective of this task was to survey the existing data base for advanced propulsion concepts; characterize their performance, technical, and developmental risks; and recommend the options or suboptions having the greatest suitability to the study mission model requirements. This process provided an excellent parametric characterization data base which has been compiled into a separate volume (see Volume I for indepth data). Accordingly, the results of the survey and characterization task will be covered only briefly in this volume.

During the survey, a literature search identified over 600 references. Almost 200 of these were read; and some 80 to 100 are referenced in the final report. From these references, a list of 20 candidate advanced propulsion concepts was compiled. These concepts, listed in Figure 3.1-1, were

<u>THERMODYNAMIC ROCKET CONCEPTS</u>	<u>ELECTRIC ROCKET CONCEPTS</u>		
<ul style="list-style-type: none">● ADVANCED CHEMICAL ROCKETS<ul style="list-style-type: none">HIGH ENERGY CHEMICAL ROCKETSFREE RADICAL ROCKETMETASTABLE MOLECULE ROCKET● NUCLEAR THERMODYNAMIC ROCKETS<ul style="list-style-type: none">SOLID CORE NUCLEAR ROCKETROTATING FLUIDIZED-BED ROCKETLIQUID CORE NUCLEAR ROCKETOPEN-CYCLE GAS-CORE NUCLEAR ROCKETCLOSED-CYCLE GAS-CORE NUCLEAR ROCKET● NUCLEAR FISSION PULSED PROPULSION● FUSION ROCKETS<ul style="list-style-type: none">MAGNETIC MIRROR FUSION ROCKETEXTERNAL PULSE FUSION ROCKET● FLUID DYNAMIC ROCKETS<ul style="list-style-type: none">SOLAR THERMAL ROCKETLASER ROCKET	<ul style="list-style-type: none">● ELECTRIC ROCKETS<ul style="list-style-type: none">SOLAR-ELECTRIC ION ROCKETNUCLEAR THERMIONIC MPDNUCLEAR BRAYTON ARC-JETTHERMOPHOTOVOLTAIC ION ROCKETCOLLOID ROCKETMAGNETIC THRUSTER ROCKET <tr><th><u>OTHER ROCKET CONCEPTS</u></th></tr> <tr><td><ul style="list-style-type: none">● SOLAR SAIL</td></tr>	<u>OTHER ROCKET CONCEPTS</u>	<ul style="list-style-type: none">● SOLAR SAIL
<u>OTHER ROCKET CONCEPTS</u>			
<ul style="list-style-type: none">● SOLAR SAIL			

Figure 3.1-1: Advanced Propulsion Concepts

investigated and their performances characterized to the degree necessary to recommend concepts for vehicle-level assessment. The criteria for concept-level screening were: (1) performance in the form of specific impulse, thrust-to-weight (T/W) ratio, and efficiency; and (2) risk and feasibility issues in the form of the data base available, possible showstoppers, and operational considerations such as engine lifetime, maintainability, and the environmental and/or social impact of engine operation in near Earth orbit. A summary of these characteristics and results from the concept-level screenings for each candidate concept follow.

3.1.1 Thermodynamic Rocket Concepts

Characteristics of advanced chemical rockets are summarized in Figure 3.1-2. High-energy chemical rockets offer theoretical performance increases of 20 to 80 sec over the baseline H_2-O_2 rocket for large increases in system

CHEMICAL REACTION	THEORETICAL PERFORMANCE	RISK/FEASIBILITY ISSUES
HIGH-ENERGY CHEMICAL ROCKETS	SPECIFIC IMPULSE - SECONDS	
$O_2 + H_2$ 3.2 KCAL/GM	500 AT MR 6:1	BASE (1995 IOC)
$F_2 + H_2$ 3.2 KCAL/GM	520 AT MR 12:1	FLUORINE REACTIVITY
$F_2 + Li (+H_2)$ 5.6 KCAL/GM	560 AT MR 1:1	COMPLEX FEED SYSTEM
$O_3 + H_2$ 4.2 KCAL/GM	570 AT MR 5:1	OZONE DETONATION PROBLEM
$O_3 + B_8 (+H_2)$ 6.2 KCAL/GM	600 AT MR 1:1	ALL OF THE ABOVE PLUS BERYLLIUM TOXICITY
FREE RADICAL ROCKET		
$H + H \rightarrow H_2$ 51.7 KCAL/GM	1500 SECONDS	HIGH DENSITY STORAGE VERY UNCERTAIN
METASTABLE HELIUM ROCKET		
$He^* + He^* \rightarrow 2He$ 114 KCAL/GM	2700 SECONDS	HIGH DENSITY STORAGE APPEARS INFEASIBLE
COMMENTS		
<ul style="list-style-type: none"> • A FLUORINE OR FLUORINE-OZONE ENGINE APPEARS TO HAVE REASONABLE REWARD VERSUS RISK FOR ADVANCED OTV APPLICATION • $F_2 + H_2$ ROCKET WAS EXAMINED IN LARC FOTV STUDY & RESULTS INCORPORATED IN TASK 2. 		

Figure 3.1-2: Summary of Advanced Chemical Rocket Characteristics

complexity and development cost. The free radical or atomic hydrogen rocket offers theoretical specific impulses (I_{sp}) of up to 1500 sec, but current quantum mechanics theory indicates that storage densities higher than 10 g/m^3 are doubtful, which effectively cancels any performance advantage available. Metastable helium has never been stored for more than a few milliseconds under any conditions, so its use as a propellant appears infeasible. The only advanced chemical rocket which appeared to have a reasonable performance reward versus development risk was the fluorine-hydrogen ($\text{F}_2\text{-H}_2$) rocket which was examined in a related study (Reference 1) and the results incorporated in this study. Those results showed that development of the $\text{F}_2\text{-H}_2$ rocket reduced propellant requirements and made payload manifesting easier by reducing stage length; however, cost savings did not justify the developmental risks.

The characteristics of five types of nuclear fission thermodynamic rockets are summarized in Figure 3.1-3. Much work was expended on these

<u>REACTOR TYPE</u>	<u>PERFORMANCE</u>	<u>OPERATIONAL CAPABILITY</u>	<u>RISK/FEASIBILITY ISSUES</u>
SOLID CORE REACTOR	800 - 1000 SECS ENGINE T/W ≈ 3	LIMITED LIFETIME POOR MAINTAINABILITY	RADIATION HAZARD FROM USED ENGINE; MUCH DESIGN DATA AVAILABLE.
ROTATING BED REACTOR	1000 - 1200 SECS ENGINE T/W ≈ 8	LIMITED LIFETIME CAN BE SERVICED	RADIATION HAZARD MODERATED BY CORE REMOVAL; DESIGN LEVEL TECHNOLOGY AVAILABLE.
LIQUID CORE REACTOR	1400-1600 SECS ENGINE T/W ≈ 1	VERY SHORT LIFETIME ONE SHOT MISSIONS	NO CONTAINMENT OF FISSION PRODUCTS; VERY LIMITED DATA BASE.
OPEN-CYCLE GAS-CORE REACTOR	1500 - 2000 SECS ENGINE T/W ≈ 1	LONG LIFETIME, BUT MUST BE REFUELED EVERY BURN	NO CONTAINMENT OF FISSION PRODUCTS; GOOD DATA BASE BUT FEASIBILITY NOT PROVEN.
CLOSED-CYCLE GAS CORE REACTOR	1500 - 2000 SECS ENGINE T/W ≈ 1	LIFETIME UNKNOWN CAN BE SERVICED	"LIGHTBULB" EXTREMELY HIGH RISK GOOD DATA BASE BUT FEASIBILITY NOT PROVEN.

RECOMMENDATION

SOLID CORE AND ROTATING BED REACTORS SHOULD BE CARRIED INTO TASK 2.

Figure 3.1-3: Summary of Nuclear Fission Thermodynamic Rocket Characteristics

concepts prior to abandonment of the U.S. nuclear rocket program in 1973 and, for most of these concepts, the data base is quite good. Of the five concepts, the solid-core and rotating-bed rockets were recommended for vehicle-level assessment. The liquid-core reactor was dropped for not being reusable, the open-cycle gas-core reactor was dropped for being too large and too expensive to operate in near-term applications, and the closed-cycle gas-core or "light bulb" reactor was dropped because of feasibility issues concerning the light bulb.

The pulsed fission rocket is best remembered as Project Orion (see Figure 3.1-4) which was studied at the General Atomic Division of General Dynamics, Inc., from 1958 until May 1965. This vehicle has a good data base (still classified) and exceptional performance, but it suffers from political unacceptability. The 1963 nuclear test ban treaty specifically prohibits atmospheric or space nuclear explosions, thereby preventing the testing or use of a pulsed fission rocket. This treaty would have to be changed and the current political opposition to nuclear devices in general would have to be overcome before such a vehicle could be tested or flown.

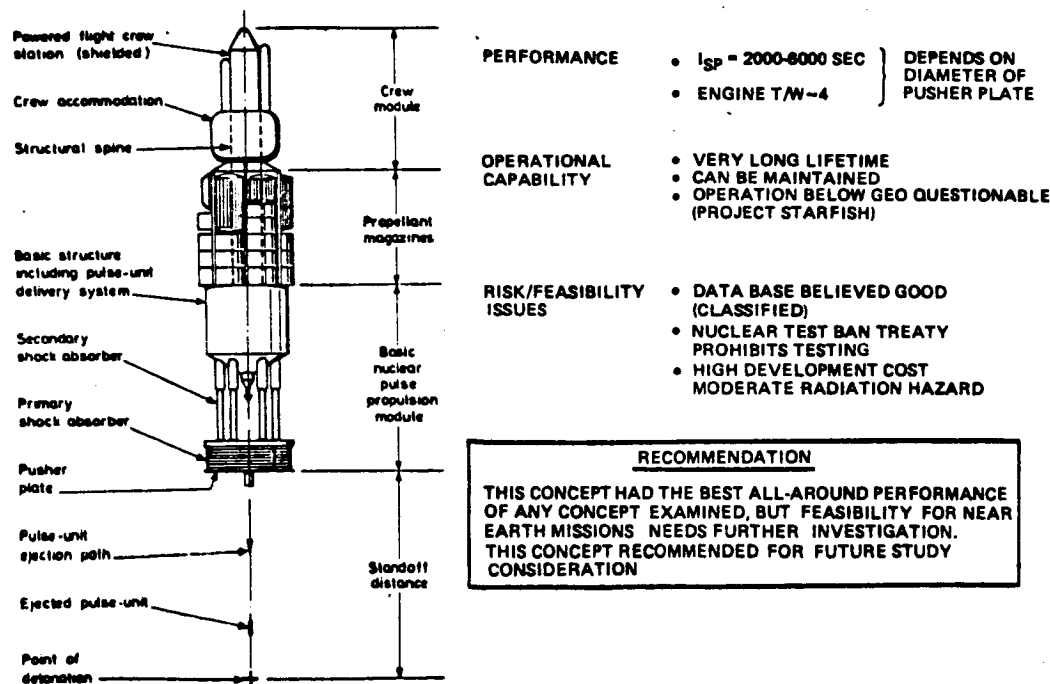


Figure 3.1-4: Summary of Nuclear Fission Pulsed Rocket (Orion) Characteristics

Two fusion reactor concepts were examined (Figure 3.1-5). The first was a magnetically confined, continuous fusion reactor typified by the dual-mirror test reactor (MFTF-B) scheduled for completion in late 1982. This type of engine requires large, heavy, superconducting magnets which raise the specific mass and decrease the T/W. The second type considered was the external-pulse, light-ion heated, inertially confined fusion rocket exemplified by the Project Daedalus vehicle proposed by members of the British Interplanetary Society (Reference 5). The light-ion heated, inertial-confinement reactor will have a proof of principle test when the particle beam fusion apparatus (PBFA) is completed, also in late 1982. The external-pulse fusion rocket has the potential for a much lower specific mass than the continuous fusion rocket because it will not require the large superconducting confinement magnets with their associated shielding and refrigeration. However, neither fusion reactor is sufficiently developed to be characterized at the vehicle level in this study.

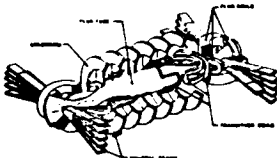
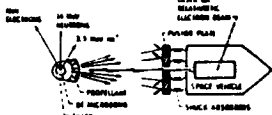
<u>FUSION ROCKET TYPE</u>	<u>PERFORMANCE</u>	<u>OPERATIONAL CAPABILITY</u>	<u>RISK/FEASIBILITY ISSUES</u>
DUAL-MIRROR 	2500 - 10^6 SECS $T/W \approx 10^{-4} - 10^{-5}$	PROOF OF PRINCIPLE TEST REACTOR (MFTF-B) TO BE COMPLETED IN 1982	<ul style="list-style-type: none"> • WEIGHT OF DIRECT CONVERTER & SUBSYSTEMS • FUEL AVAILABILITY FOR D-He₃ REACTION • SUPERCONDUCTING MAGNET WEIGHTS
EXTERNAL PULSE 	5000 - 10^6 SECS $T/W \approx 10^{-3} - 10^{-4}$	PROOF OF PRINCIPLE TEST REACTOR (PBFA) TO BE COMPLETED IN 1982	<ul style="list-style-type: none"> • PARTICLE BEAM FOCUSING • FUEL AVAILABILITY FOR D-He₃ REACTION • RADIATION HAZARD
COMMENTS <ul style="list-style-type: none"> • THERE IS \$20 BILLION TO BE SPENT ON FUSION RESEARCH THROUGH THE YEAR 2000. • PRACTICAL FUSION ROCKETS WILL PROBABLY REQUIRE 2ND GENERATION FUSION FUEL (D-He₃ OR P-B₁₁) TO BRING RADIATION SHIELDING WEIGHT DOWN TO REASONABLE LEVELS 			
RECOMMENDATION EXAMINE FUSION VEHICLE SUBSYSTEM REQUIREMENTS AND FEASIBILITY ISSUES IN A LATER STUDY WHEN MORE DATA IS AVAILABLE.			

Figure 3.1-5: Summary of Fusion Rocket Characteristics

A great deal of money is scheduled to be spent on fusion research over the next 20 years and, once a successful fusion reactor is developed, a successful fusion rocket could follow shortly. It appears to these authors that only fusion (or pulsed-fission) rockets could provide the short mission times necessary for manned exploration of the outer planets.

Laser thermodynamic rockets offer higher acceleration than electric rockets combined with high specific impulse (approx. 1500 sec). The critical issues associated with this concept come primarily from the required combination into one system of many new and untried technology components. Some experimental and theoretical work has been done on laser rockets, but the technology base and the resources spent to date are small. A schematic of a laser rocket concept is shown in Figure 3.1-6. The general concept uses a

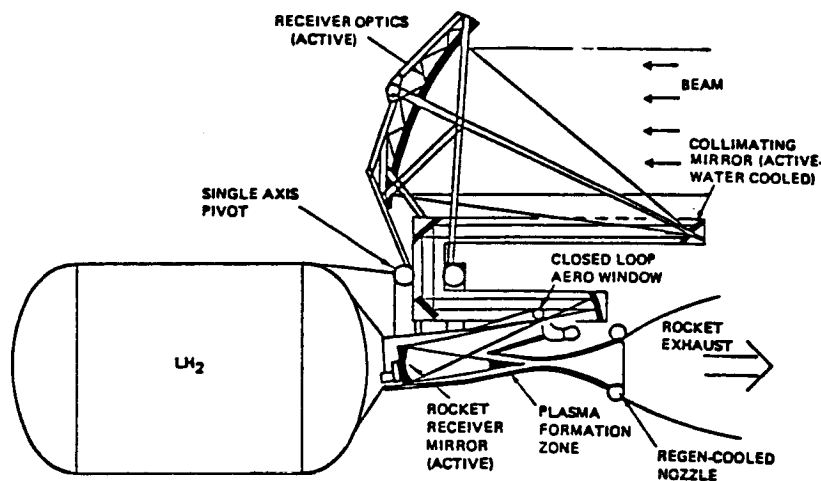


Figure 3.1-6: Typical Laser Heated Rocket Concept

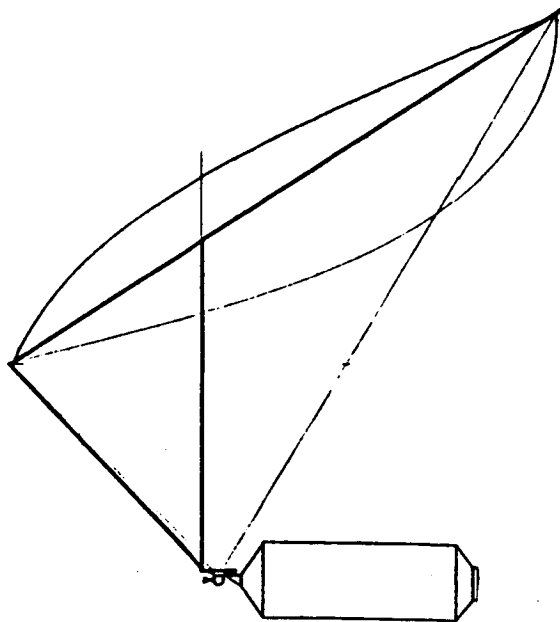
gimbaled concentrator to receive the laser beam and direct it into an optic train containing a set of active mirrors and/or windows (material and/or aerodynamic), where it is recollimated and focused into the combustion chamber of a regeneratively cooled rocket nozzle.

The principal feasibility issue currently is the mechanism by which the energy of the laser beam will be coupled or transferred to the hydrogen propellant/working fluid. Gaseous hydrogen is transparent to light at virtually all laser wavelengths, so a special coupling mechanism must be used. The two current frontrunners for energy coupling are (1) inverse

Bremsstrahlung, where the laser light is absorbed by free electrons in a plasma introduced through a spark discharge, and (2) molecular resonance, where the hydrogen propellant is "seeded" with molecules which undergo a rotational or vibrational transition at the laser wavelength used.

Other key risk and feasibility issues include: transmitter pointing and tracking accuracy to impinge a beam upon a collector 40,000 km away; and window lifetimes which require a window to efficiently transmit tens of kW/cm^2 of laser light for periods of 10 minutes or more, at the same time reflecting back into the combustion chamber infrared radiation of intensity levels approaching tens of kW/cm^2 , and have a lifetime of hundreds of off-on cycles.

The solar thermodynamic rocket consists of a steerable solar concentrator which focuses the Sun's energy into an absorption cavity, where it is used to superheat hydrogen working fluid which is then expanded through a regeneratively cooled nozzle to provide thrust. The specific impulse is determined by the highest achievable gas temperature which, in turn, is determined by the highest material temperature which can be sustained in the absorption cavity. A key issue addressed in Task 1 was the trade between heat-exchanger lifetime and operating temperature. This resulted in the requirement shown in Figure 3.1-7 where a tungsten foil heat exchanger was designed to run 170 hr at 3300°K .



ADVANTAGES

- DESIGN LEVEL TECHNOLOGY
- STRAIGHT FORWARD DEVELOPMENT

REQUIREMENTS

- 170 HOURS RUN TIME AT 3300°K (6000°R)
- MUST ACCEPT OCCULTATION
- POINTING ACCURACY OF 0.1 DEG.

KEY ASSUMPTIONS

- LIGHTWEIGHT CONCENTRATOR WITH $1/8$ DEGREE OPTICS
- TUNGSTEN FOIL HEAT EXCHANGER
- FUSED QUARTZ WINDOW

Figure 3.1-7: Solar Thermal Rocket

Both the laser and solar thermodynamic rockets were recommended for vehicle-level assessment. Their characteristics and risk and feasibility issues are summarized in Figure 3.1-8. An extensive review of the laser and solar powered rockets is found in Sections 2.5 and 2.6 of Volume I.

<u>CONCEPT</u>	<u>PERFORMANCE</u>	<u>MISSION CAPABILITY</u>	<u>RISK/FEASIBILITY ISSUES</u>
LASER ROCKET	800-1500 SECS $T/W \approx 10^{-2}$	<ul style="list-style-type: none"> • UNMANNED ONLY • NEAR EARTH ONLY • 2-DAY GEO DELIVERY 	<ul style="list-style-type: none"> • LASER COUPLING MECHANISM • POINTING & TRACKING ACCURACY • WINDOW LIFETIME
SOLAR THERMAL	800-1200 SECS $T/W \approx 10^{-2} \cdot 10^{-3}$	<ul style="list-style-type: none"> • UNMANNED ONLY • 20-DAY GEO DELIVERY 	<ul style="list-style-type: none"> • CONCENTRATOR WEIGHT & ACCURACY • AIR DRAG AT LEO • WINDOW CONTAMINATION PROBLEM • POINTING AND TRACKING ACCURACY

RECOMMENDATION:

- 1) ASSUME SPECIFIC IMPULSE UP TO 1500 SEC WILL BE AVAILABLE AND CARRY INTO TASK 2
- 2) CARRY SOLID HEAT EXCHANGER SOLAR ROCKET INTO TASK 2.

Figure 3.1-8: Summary of Separately Powered Fluid-Dynamic Rocket Characteristics

3.1.2 Electric Rocket Concepts

The specific impulse of thermodynamic rockets is limited by the energy of combustion (chemical rockets) or the maximum temperature sustainable in the combustion chamber (nuclear, solar, or laser rockets). The highest specific impulse for which a small regeneratively cooled nozzle appears feasible is 1500 sec. This corresponds to a chamber temperature of about 4000°K, near the melting point of the best refractory materials.

These limits can be overcome by using electromagnetic forces to directly accelerate charged molecules, thereby eliminating the nozzle and its cooling problems. However, thruster concepts using electrostatic or electromagnetic forces instead of fluid dynamic forces must operate at extremely low densities to enable the electric forces to predominate, and this implies very low thrust densities and commensurate low thrust levels.

Electric rockets generally consist of a power source, a power processor which converts raw power into the forms required by the thruster, and a

thruster which electrically accelerates the propellant. Contemporary options for combining power source concepts with thruster concepts are shown in Figure 3.1-9. The checkmarks indicate combinations characterized in this study. The approach for evaluation and characterization of these options was to start with a well-defined concept (solar photovoltaic power source with argon electrostatic-ion thrusters) and then systematically evaluate alternative concepts which incorporate either a change of thruster or change of power source. This procedure established the salient features of all possible combinations and maximized the applicability of the existing data base for advanced propulsion concepts.

APCS-280

THRUSTER	POWER SOURCES								
	SOLAR PHOTO-VOLTAIC	ANNEALABLE CELLS	VAPOR DEPOSITED CELLS	NUCLEAR BRAYTON	NUCLEAR THERMONIC	NUCLEAR THERMO-ELECTRIC	THERMO PHOTO-VOLTAIC	SOLAR THERMO-ELECTRIC	LASER/MICROWAVE ELECTRIC
ION	✓	✓	✓		✓		✓	✓	
MPD	✓				✓				
ARC-JET									
INDUCTIVE PLASMA									
RESISTOJET									
COLLOID									
RAIL GUN	✓								
MASS DRIVER	✓								

Figure 3.1-9: Morphology of Possible Electric Rocket Concepts

Characteristics of electric rocket options evaluated are summarized in Figure 3.1-10. The solar electric ion propulsion system (SEPS) represents 20 years of technology development; the only remaining technical risk concerns

<u>CONCEPT</u>	<u>PERFORMANCE</u> I _{SP} - SEC T/W G'S	<u>MISSION CAPABILITY</u>	<u>RISK/FEASIBILITY</u>
SOLAR ELECTRIC ION	1000 - 20000 10 ⁻⁵	UNMANNED ONLY	RADIATION DEGRADATION OF SOLAR ARRAY
NUCLEAR-THERMIONIC MPD	1000 - 3000 10 ⁻⁶	UNMANNED ONLY	MPD TECHNOLOGY TBD SYSTEM WEIGHTS TBD
NUCLEAR-BRAYTON ARC-JET	800 - 1200 10 ⁻⁴	UNMANNED ONLY	ARC-JET TECHNOLOGY TBD SYSTEM WEIGHTS TBD
THERMO-PHOTOVOLTAIC ION	1000 - 20000 10 ⁻⁵	UNMANNED ONLY	SYSTEM DESIGN TBD
COLLOID ROCKET	1000 - 5000 10 ⁻⁷	NONE	VERY LOW VEHICLE THRUST -TO-WEIGHT RATIO
ELECTRO-MAGNETIC (RAIL GUN)	800 - 1500 10 ⁻³ - 10 ⁻⁵	UNMANNED ONLY	DESIGN LEVEL TECHNOLOGY UNDER DEVELOPMENT

<p align="center"><u>RECOMMENDATION</u></p> <p align="center">CARRY ALL ELECTRIC CONCEPTS, EXCEPT COLLOID, INTO TASK 2.</p>

Figure 3.1-10: Summary of Electric Rocket Characteristics

degradation of the solar array (and prospective payloads) caused by high-radiation levels in the Van Allen belts. The solar array, the power processors, and the ion thrusters are well-defined items with detailed performance and cost breakdowns, which makes them an excellent departure point for characterizing the other more exotic electrical propulsion options.

The nuclear thermoelectric magnetoplasmadynamic (MPD) rocket uses a compact nuclear reactor as a heat source, generates DC electricity via thermoelectric (or thermionic) converters, and charges a pulse-forming energy storage system (power processor) which powers an MPD thruster of the type being developed at Princeton and JPL. The overall system has been defined and analyzed in the form of a deep-space probe during design work conducted by Los Alamos, JPL, and Princeton; that configuration (Figure 3.1-11) is the basis for the characterization used in this study.

The nuclear Brayton arc-jet rocket uses a compact nuclear reactor as a heat source, with a helium Brayton-cycle turbine-generator system to generate DC electricity (also functions as power processor), and an electric arc jet to heat hydrogen propellant which is expelled for thrust. Ordinarily, arc jets have low electrical efficiency because of frozen flow losses associated with

PERFORMANCE

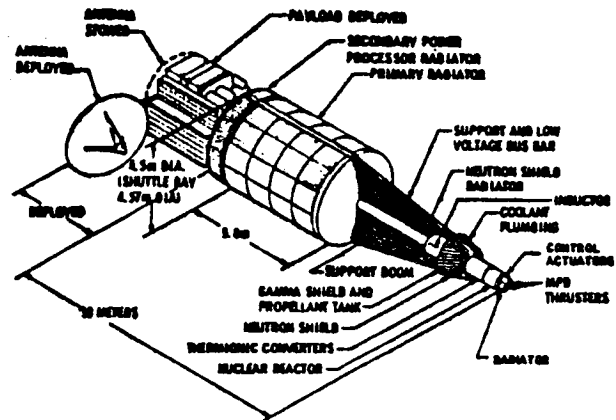
- 2500-10,000 SECONDS (MPD OR ION THRUSTERS)
- $T/W \approx 10^{-4}-10^{-5}$ ($\alpha = 20$ kg/kw)

MISSION CAPABILITY

- NOT SUITABLE FOR MANNED MISSIONS
- DESIGNED PRIMARILY FOR DEEP SPACE PROPULSION AND POWER GENERATION

SUMMARY OF RESULTS

- COST OF DELIVERY TO GEO = \$5385/kg
- NUCLEAR ELECTRIC VEHICLES REQUIRE SPECIAL FACILITIES FOR CHECK-OUT AND MAINTENANCE
- DISPOSAL OF USED REACTOR AN UNSOLVED ISSUE



NUCLEAR ELECTRIC VEHICLES HAVE FEW PERFORMANCE ADVANTAGES AND SERIOUS OPERATIONAL CONSTRAINTS WHEN OPERATING IN NEAR EARTH SPACE

Figure 3.1-11: Nuclear Thermoelectric Rocket

dissociation and ionization originating in the arc heating process. The arc jet characterized in this task (Figure 3.1-12) used a downstream mixing chamber which should allow time for molecular recombination, thereby achieving high efficiency.

The solar thermophotovoltaic (TPV) ion rocket is similar to the baseline solar photovoltaic ion concept except that a highly concentrating optical system is used to focus the Sun's energy into an absorption cavity/reradiator which then illuminates a small area of solar cells. This system provides several advantages over the conventional solar photovoltaic array. First, by carefully sizing the optics and the cavity, the reradiator can be designed to operate at temperatures of 2000°K to 2500°K , which provides a blackbody spectrum matched to the peak absorption wavelength of silicon solar cells (see Figure 3.1-13). In addition, by using edge junction silicon cells over a highly reflective substrate, the cells can be made to reflect back into the reradiator most of those photons with insufficient energy to generate an electron. This concept has about triple the maximum theoretical efficiency relative to a conventional solar cell array and in preliminary testing has achieved efficiencies on the order of 40%.

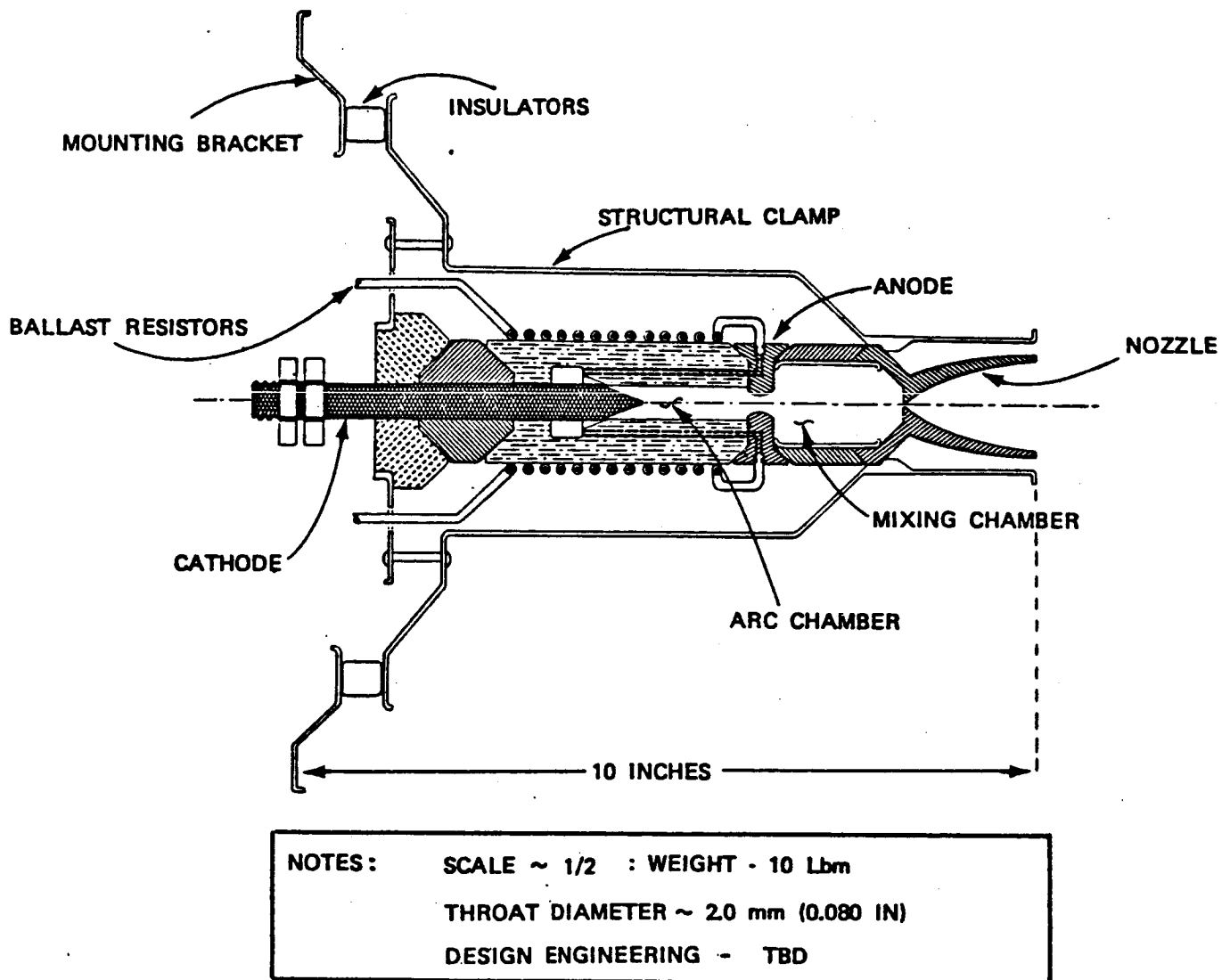
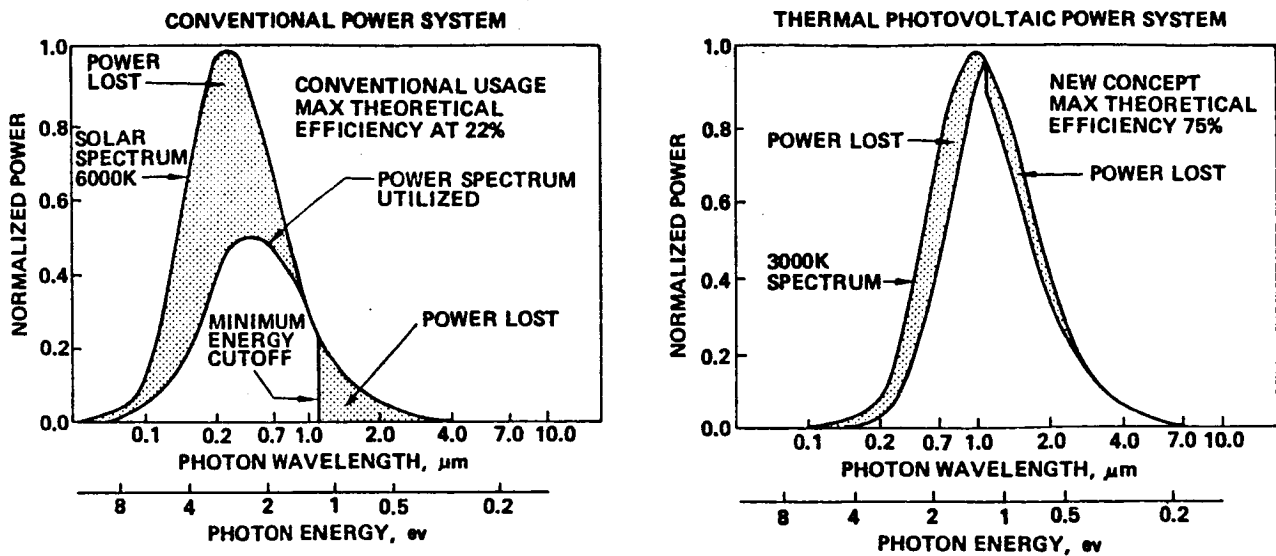


Figure 3.1-12: 25-kW Thermal Arc-Jet Concept

Further advantages of TPV over conventional solar arrays are reduced cost and lack of radiation degradation. TPV operates at very high concentration ratios which reduce the amount of very expensive solar cells to a few square meters. Basically TPV reduces cost by using a large area of cheap radiators instead of a large area of expensive solar cells. Because the solar cells are enclosed within a matrix of heat pipes and radiators, they are protected from



- NEW TPV CONCEPT TRIPLES MAX THEORETICAL EFFICIENCY

Figure 3.1-13: Photovoltaic Systems Comparison

radiation effects and do not degrade during transits of the Van Allen belt like a conventional solar array. A schematic of the TPV power system is shown in Figure 3.1-14.

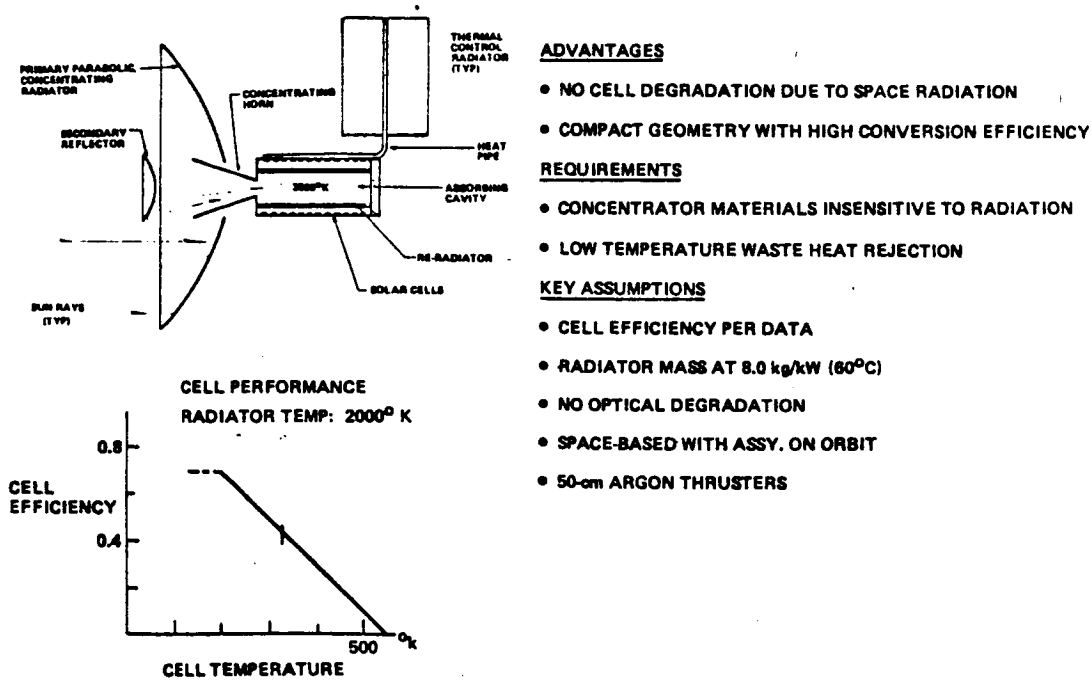
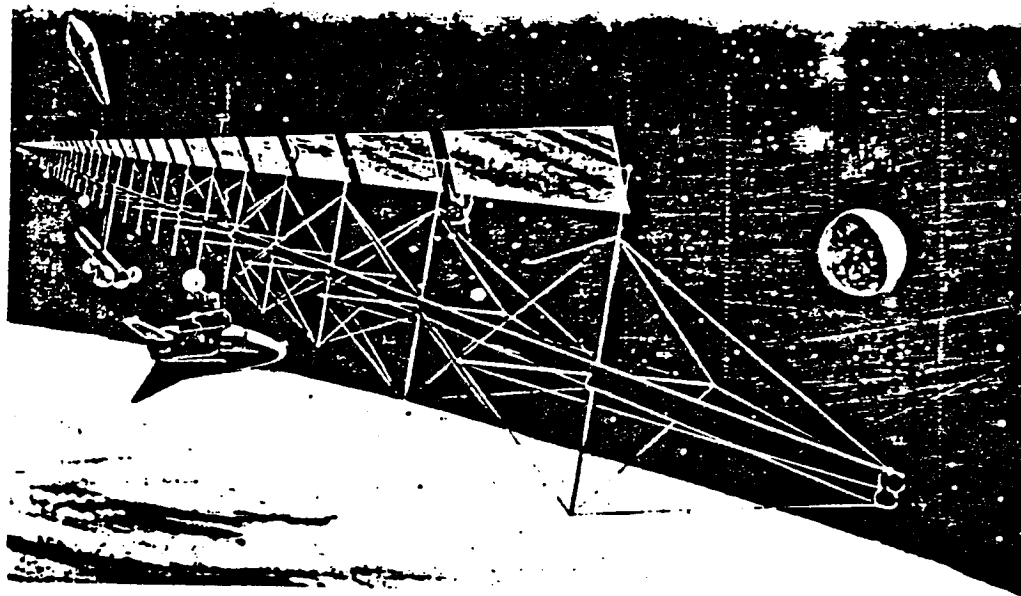


Figure 3.1-14: Thermophotovoltaic: (TPV) Power System

The colloid rocket works by electrostatic acceleration of charged aerosol droplets compared to ionized molecules for a conventional ion thruster. This concept was motivated by the fact that electrical efficiency and thrust to weight increase with increasing mass of the accelerated particles. Mercury, which is the heaviest practical molecule to use, provides poor thrust efficiency below 2500 sec, which is already higher than optimum for some near Earth applications. It has been shown that uniformly sized and charged aerosol droplets can be electrostatically drawn off of a highly charged needle and accelerated in a conventional electrostatic ion thruster providing good thrust efficiencies of specific impulses as low as 1000 sec. Unfortunately, the thrusters had poor lifetime characteristics because of a tendency to strike a high-voltage arc between the needle and the accelerator grid. This problem seems to be inherent in the thruster design; for this reason, colloid thrusters were not recommended for vehicle-level assessment.

Electromagnetic rockets utilize the forces generated when a magnetic field interacts with electrical currents to accelerate solid conductors, or plasmas, to high velocities, thereby generating thrust. One scheme, the mass driver, as shown in Figure 3.1-15, is essentially a synchronous linear motor



FEATURES

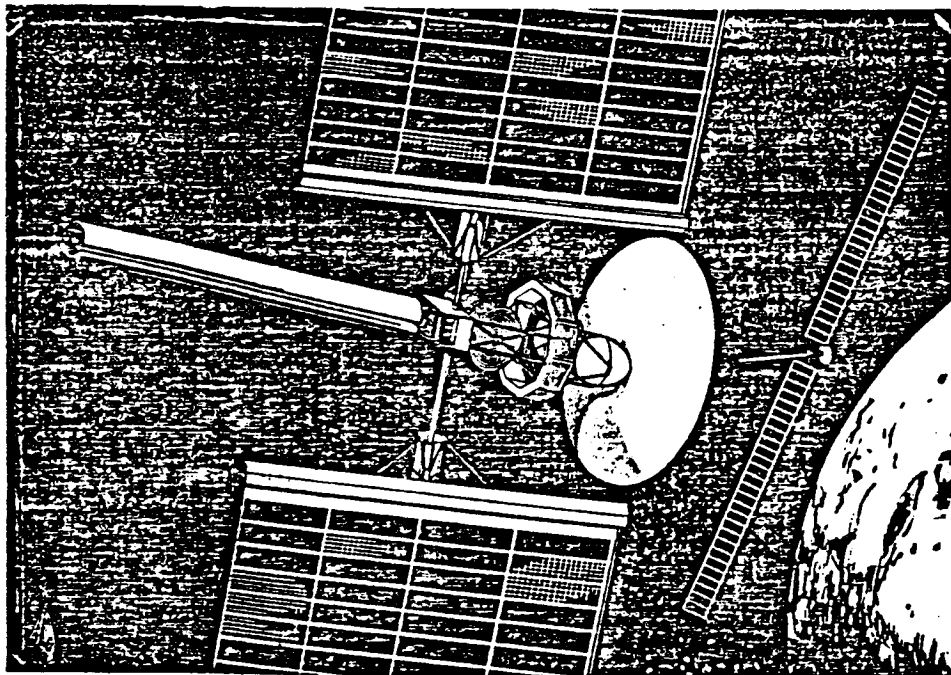
- ISP = 800 - 1500 SECS (OPTIMUM FOR EARTH - MOON SYSTEM)
- INITIAL T/W = 3×10^{-4}
- VERY HIGH ELECTRICAL EFFICIENCY

RISK/FEASIBILITY ISSUES

- LACK OF CHARACTERIZATION/HIGH COMPLEXITY
- REUSABLE BUCKET REQUIRES VERY LARGE SYSTEM (10 KM)

Figure 3.1-15: Mass Driver Features/Risks

where the magnetic field is used to transfer forces between current-carrying wires. Another scheme, the rail gun shown in Figure 3.1-16, uses a single current loop to accelerate a plasma armature with the $J \times B$ magnetic force. The plasma armature and its confining reaction mass are driven from the gun at high velocity to generate thrust. Other less publicized schemes use the repulsion force between eddy currents, generated in a conductor by a time-varying magnetic field, and the magnetic field itself to accelerate the conductor as a reaction mass. Examples of these schemes are the direct current induction accelerator proposed by MIT and the pulsed inductive plasma thruster proposed by TRW.



FEATURES

- $I_{sp} = 800-1500$ SECONDS
- $T/W = 10^{-3}-10^{-4}$

RISK/FEASIBILITY ISSUES

- ARC EROSION OF BARREL SURFACES
- FINAL DEPOSITION OF FIRED PELLETS

Figure 3.1-16: Solar Electric Rail Gun Rocket

All of the electromagnetic thruster concepts just discussed would operate with specific impulses between 800 and 1500 sec and all are in the preliminary design level of development. Concept-level assessment of the electromagnetic thrusters indicated that the mass driver was inherently too big and too complex to be competitive in the current mission model, that the inductive thrusters were not sufficiently defined to be incorporated into this study, and, hence, that the rail gun rocket was the only electromagnetic vehicle recommended for vehicle-level assessment.

3.2 Task 2 - Candidate Propulsion System Analysis and Sizing

The overall purpose of this task was to ensure that each advanced propulsion vehicle and its support systems were defined to the same level of detail, used the same level of technology (1990), and were sized for optimum performance with respect to mission requirements. A major difficulty in many earlier studies, comparing widely different vehicle concepts, has been that the

vehicles were sized for different missions. For instance, a vehicle designed and sized for an interplanetary mission is often not competitive doing geocentric payload deliveries.

Examination of this mission model showed that, as it has been in our previous OTV studies, the planetary missions may be design drivers but not cost drivers. Accordingly, the best approach to sizing the various OTV concepts was to generate basic parametric performance data for the geocentric missions, which were the cost drivers, and then treat the planetary missions as unique missions which may require a special kick stage or derivative of the basic vehicle.

Configuration analyses and sizing of many advanced propulsion concepts required special trade studies to optimize vehicle performance. The results of these trade studies, configuration analyses, and vehicle parametric performance follow.

3.2.1 Optimization of Manned Nuclear Rockets

The nuclear fission rocket was the only advanced propulsion option recommended for vehicle-level assessment which had sufficient thrust to be capable of the manned missions. Preliminary performance analysis indicated that the manned GEO resupply mission (8.8t up and 6.2t down) would require the most propellant of any mission; consequently, it was used as a baseline for optimization of the vehicle configuration and radiation shielding.

There were two extra safety requirements put on the nuclear vehicle. First, there must be sufficient radiation shielding from the reactor to limit the radiation dose inside the manned capsule to 3 rem per mission. The

maximum dose during a nonnuclear GEO sortie would be 30 to 40 rem; 3 rem per mission from the reactor would not seriously impact the design or safety of the manned capsule. The second requirement was that once the nuclear engine had been fired, it must always be in a "safe" trajectory. A safe trajectory was defined as any trajectory not intercepting the Earth's atmosphere with a lifetime of at least 1 year.

The specific impulse performance assumed for the nuclear rockets was:

Solid-core rocket:

975 sec without afterheat cooling

920 sec with afterheat cooling

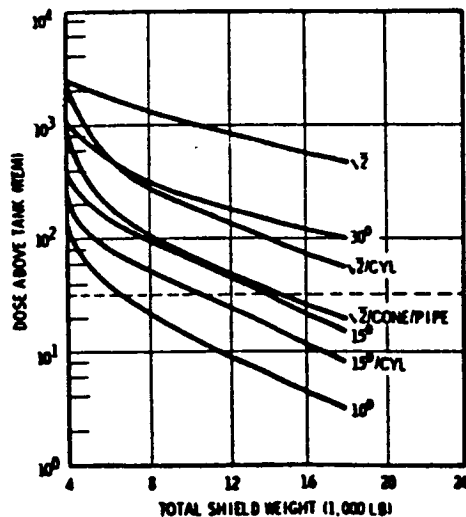
Rotating-bed reactor:

1050 sec without afterheat cooling

1000 sec with afterheat cooling

Configuration selection was based on NERVA results summarized in Figure 3.2.1-1. As can be seen in Figure 3.2.1-1a, the shape of the LH₂ tank aft

A) EFFECT OF LH₂ TANK SHAPE ON TOTAL SHIELD WEIGHT



B) TIME DEPENDENT DOSE RATES

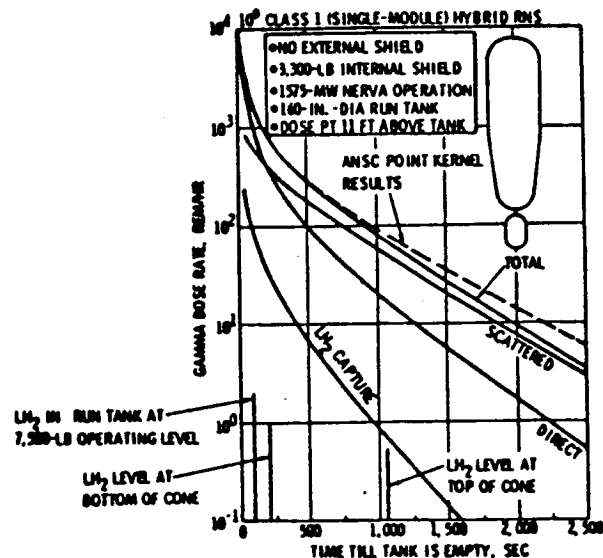
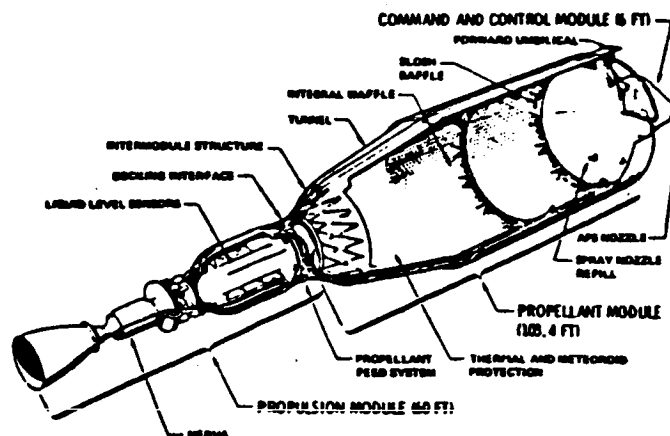


Figure 3.2.1-1: Nuclear Rocket Configurations Based on Nerva Results (A) (B)

CLASS 1 SINGLE-MODULE HYBRID RNS



**C) EXAMPLE OF SINGLE
MODULE NERVA STAGE**

Figure 3.2.1-1: Nuclear Rocket Configurations Based on Nerva Results (C)

bulkhead has a very large effect on the total radiation dose above the tank (i.e., at the manned capsule). In fact, a tank ending in a 10-deg cone will reduce the radiation dose by two orders of magnitude relative to a conventional $\sqrt{2}$ elliptical tank end. There are two reasons for this. First, the 10-deg cone is not very efficient, volumetrically, and hence the manned capsule is much further away from the reactor for the same amount of propellant. Second, as shown in Figure 3.2.1-1b, most of the radiation dose occurs in the last few seconds of the final burn when the depth of LH_2 in the tank is at its minimum. Therefore, a tank with a conical aft section retains a sufficient depth of LH_2 longer into the final burn and reduces the integrated dose.

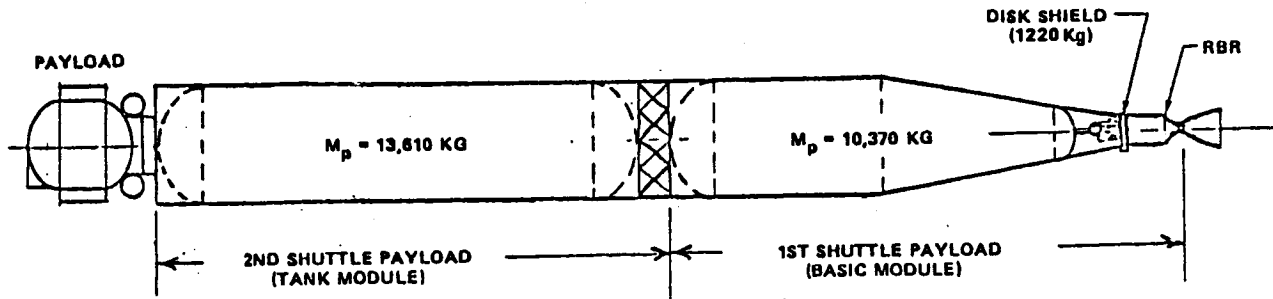
The nuclear rocket configuration selected is shown in Figure 3.2.1-2. This configuration consists of two modules which could be launched in separate shuttle launchers and assembled in orbit. The first launch would be the basic module (see Figure 3.2.1-3) containing a conical tank and the nuclear reactor rocket (rotating-bed reactor in this case). The second launch would contain a tank module to fit in front of the basic module and provide sufficient volume for either the 12t delivery mission or the manned sortie (Figure 3.2.1-4).

The shielding requirements for the configuration shown in Figure 3.2.1-2 were calculated using relative attenuation factors compared to the NERVA configuration shown in Figure 3.2.1-1c. This NERVA configuration has been

SIZED FOR MANNED GEO STATION RESUPPLY (8.8 MT UP-6.2 MT DOWN)

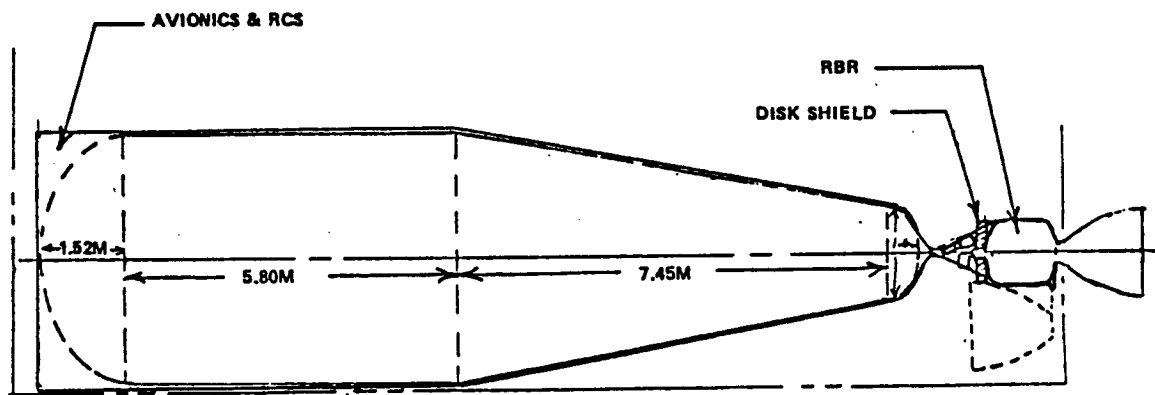
TOTAL STARTBURN MASS = 42.9 MT (94,540 LB)

TOTAL MISSION PROPELLANT MASS = 24.0 MT (52,865 LB)



SCALE 1/200

Figure 3.2.1-2: Shuttle Compatible Manned Sortie Configuration Using Rotating Bed Reactor Rocket



SCALE 1/100

Figure 3.2.1-3: Rotating Bed Rocket-Basic Module

previously analyzed, in depth, to determine the relative effects of changes in geometry, fuel loading, and shielding (Reference 6), and so provided an excellent baseline to scale from. The results of the first-order shielding study are shown in Figure 3.2.1-5. This analysis incorporates only first order effects and assumes equal burn times and equivalent configuration geometries, but it should be sufficiently accurate for this application.

The large amount of shielding required (240 kg internal and 1220 kg in the external disk shield) comes directly out of the round trip payload capability and severely penalizes the performance of a nuclear rocket. Noting

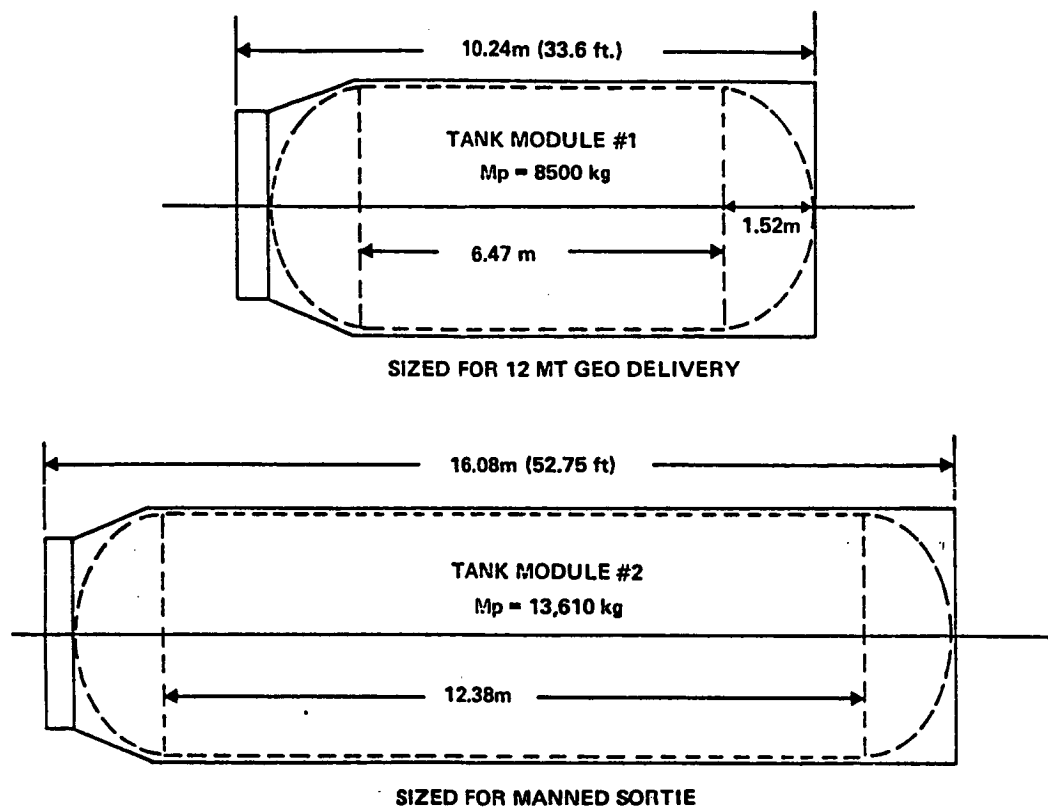


Figure 3.2.1-4: Tank Modules for Rotating Bed Rocket

	<u>NERVA</u>	<u>RBR</u>	<u>LASL α</u>	RELATIVE ATTENUATION FACTOR
POWER LEVEL, MW	1575	420	300	3.75 (5.26)
DOSE POINT SEPARATION DISTANCE, M	47	38	38	0.65
RESIDUAL LH ₂ DEPTH, CM	207	282	282	1.02
RELATIVE ATTENUATION REQUIRED	1.0	0.40	0.29	
SHIELD THICKNESS REDUCTION, CM	-	2.8	3.8	
SHIELD MASS, KG	4535	2920	2350	
THE SHIELD DIAMETER SCALES WITH CORE DIAMETER SO:				
CORE DIAMETER, CM	142	100	100	
TOTAL SHIELD MASS, KG	4535	1460	1175	

Figure 3.2.1-5: First Order Shielding Requirements (3 REM per Mission Dose)

that the shielding could be greatly reduced by removing the manned payload prior to the last burn, an aerobraked manned capsule (Figure 3.2.1-6) was designed which could return to the LEO base separately from the nuclear rocket. The aerobraked manned capsule would have autonomous life support and maneuvering capability. In operation the manned capsule would separate from the nuclear rocket, after it had inserted itself into the GEO-LEO transfer orbit, and would perform a small (75 m/sec) burn to reduce its perigee altitude into the atmosphere. The manned capsule would complete an aerobraking maneuver, using the methods described in Reference 2, and then rendezvous and dock with the LEO base using its on-board propulsion and navigation capability. The nuclear stage meanwhile would circularize in LEO, all propulsively, then rendezvous and dock with the nuclear storage and maintenance facility located in the same orbit a ~~same~~ safe distance from the LEO base.

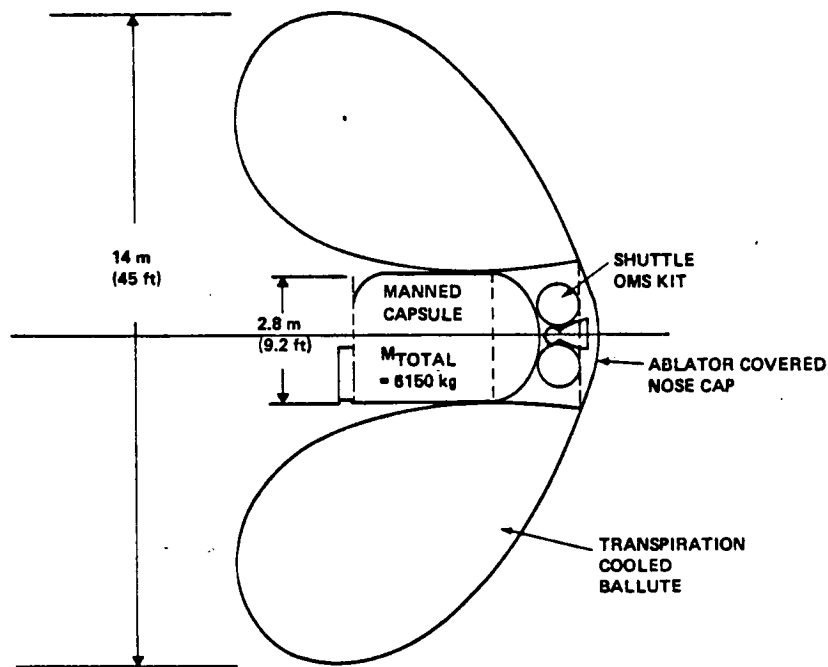


Figure 3.2.1-6: Aerobraked Manned Capsule

Switching to an aerobraked manned capsule had several effects. First, the reactor disk shield could be reduced by 450 kg because of the additional depth of LH_2 during the manned burns and the additional shielding provided by the propulsion, life support, and aerobraking subsystems on the manned capsule

(see Figure 3.2.1-7). Second, the total amount of LH_2 propellant could be reduced by about 4000 kg because of the mass removed (manned capsule and 450 kg of shielding) prior to the circularization burn.

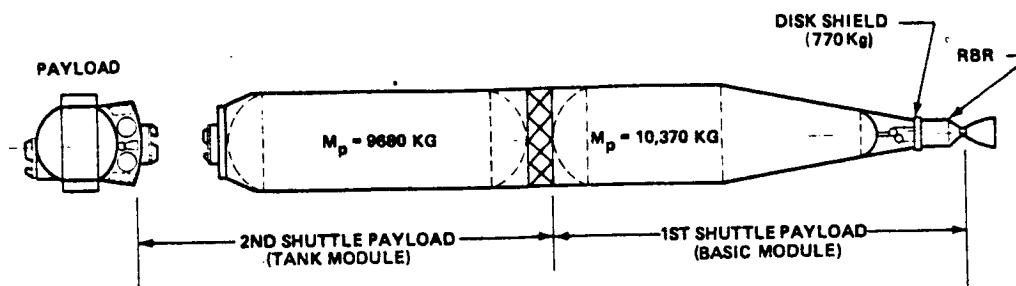
	RBR	RBR + AEROBRAKE CAPSULE	RELATIVE ATTENUATION FACTOR
POWER LEVEL, MW	420	420	1.0
DOSE POINT SEPARATION DISTANCE, M	35	33	0.848
RESIDUAL LH_2 , CM DEPTH	280	620	1.78
ADDITIONAL SHIELDING, GM/CM ² AT CAPSULE	-	~ 40	1.81
EXTERNAL DISK SHIELDING, KG	~ 1220	~ 770	2.43

Figure 3.2.1-7: Effect of Aerobraked Capsule on Shielding Requirements

The addition of autonomous maneuver and life support capability to the manned capsule could have several beneficial effects. First, it is safer because the manned capsule can now rendezvous with manned facilities and can leave the nuclear rocket some kilometers away where it does not present a radiation hazard if it should lose its stability and control functions. Also, the autonomous manned capsule with its 290 m/sec of delta-V capability is capable of rescuing itself from many potentially dangerous situations. It is conceivable that the aerobraked manned capsule could even function as a lifeboat for returning the personnel from the LEO base to the Earth's surface in an emergency. On the negative side, the addition of autonomous maneuver and life support capability added 1150 kg to the capsule mass, including 600 kg of OMS bipropellant.

The revised vehicle configuration is shown in Figure 3.2.1-8. The addition of aerobraking reduced the required LH_2 mass to do the manned sortie design mission by 4000 kg. The difference between the tank module to do the manned sortie versus the tank module sized for the 12t delivery mission is now so small that only one size tank module would be necessary.

TOTAL START BURN MASS = 38.6 MT (84,860 LB)
 TOTAL MISSION PROPELLANT MASS = 20.0 MT (44,100 LB)



Scale 1/200
 Revised 1-6-81

Figure 3.2.1-8: Nuclear Rocket Manned Sortie using Aerobraking Capsule

3.2.2 Laser Propulsion Trades

Of all applications proposed for high-power lasers, none challenges every aspect of laser technology as thoroughly as the concept of using lasers to transmit power to provide thrust to a free-flying rocket thousands of kilometers away. This concept of a laser-powered rocket has the potential to revolutionize space transportation, but it also carries with it many developmental risks and operational concerns. The primary issues to be addressed here are the problems of selecting a laser, selecting a laser location, and optimizing the entire system (laser power source, laser, laser beam transmitter, beam collector, and laser rocket engine), including the vehicle trajectory.

3.2.2.1 Laser System Trades

Defining and sizing the laser propulsion systems and vehicles was greatly complicated by the multiple design options available. These design options have been arranged into a laser propulsion trade tree shown in Figure 3.2.2-1. As can be seen, there are different laser types available with different characteristic wavelengths, three different laser locations to be examined, and different types of transmitters, collectors, and laser-coupling modes which result in different performance levels available. Each

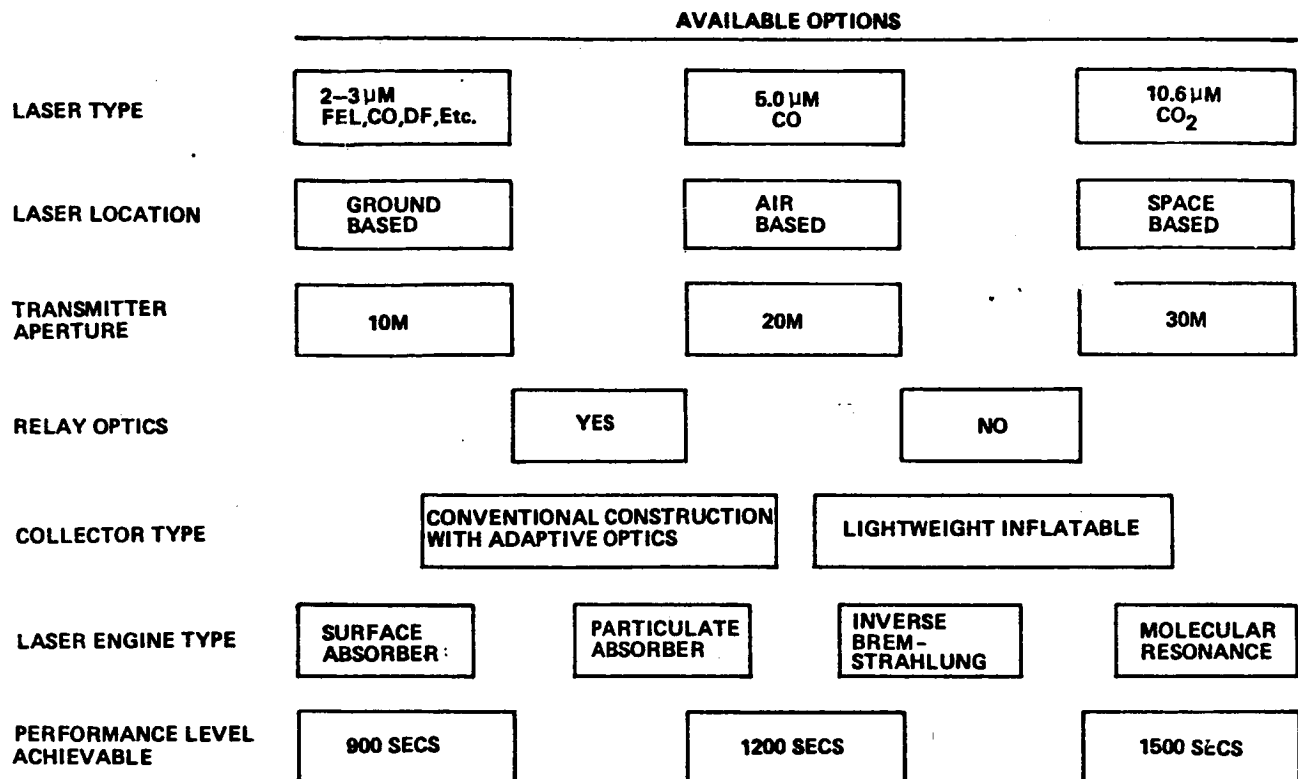


Figure 3.2.2-1: Laser Propulsion Trade Tree

permutation down through the trade tree appears viable, so some basic ground rules must be assumed and the basic problem must be scoped.

Key assumptions to start this process were as follows:

1. A peak power density requirement of at least 25 kW/cm² was assumed to enable direct coupling between the laser beam and hydrogen propellant. This power density was thought to be adequate to maintain coupling for any of the proposed coupling schemes (see Volume I, Section 2.5 for details).
2. Current benchtop optical response ($\lambda/20$) was assumed to be available for 20m- to 30m-diameter space-based or ground-based optics by the 1995 time period.
3. The atmosphere-induced aberrations in a ground-based laser beam were assumed correctable to a beam divergence half-angle of 1 μ rad using interactive-adaptive optics.

4. The vibration-induced beam jitter in an airborne laser, transmitter, and tracking system were assumed correctable to a total beam divergence half-angle of $3 \mu\text{rad}$.

Beam Collector: The first laser system element analyzed was the OTV beam collector. There are several types of collectors available. The highest concentration ratios can be achieved with adaptive optics where the mirror consists of multiple small segments positioned by electric-driven servos. This type of collector also has the best tracking accuracy because fine angle adjustments are made with the individual segments instead of rotating the entire mirror assembly. Unfortunately, this type of collector is also very heavy, weighing about 30 kg/m^2 even when using lightweight structure. The specific mass falls rapidly if the adaptive optics are discarded for a rigid shaped dish, but the optical response also degrades rapidly since the reflecting surface will now vary with thermal and acceleration stresses. The lightest collector investigated and the type eventually selected was a nonrigidized inflatable configuration of the type shown in Figure 3.2.2-2.

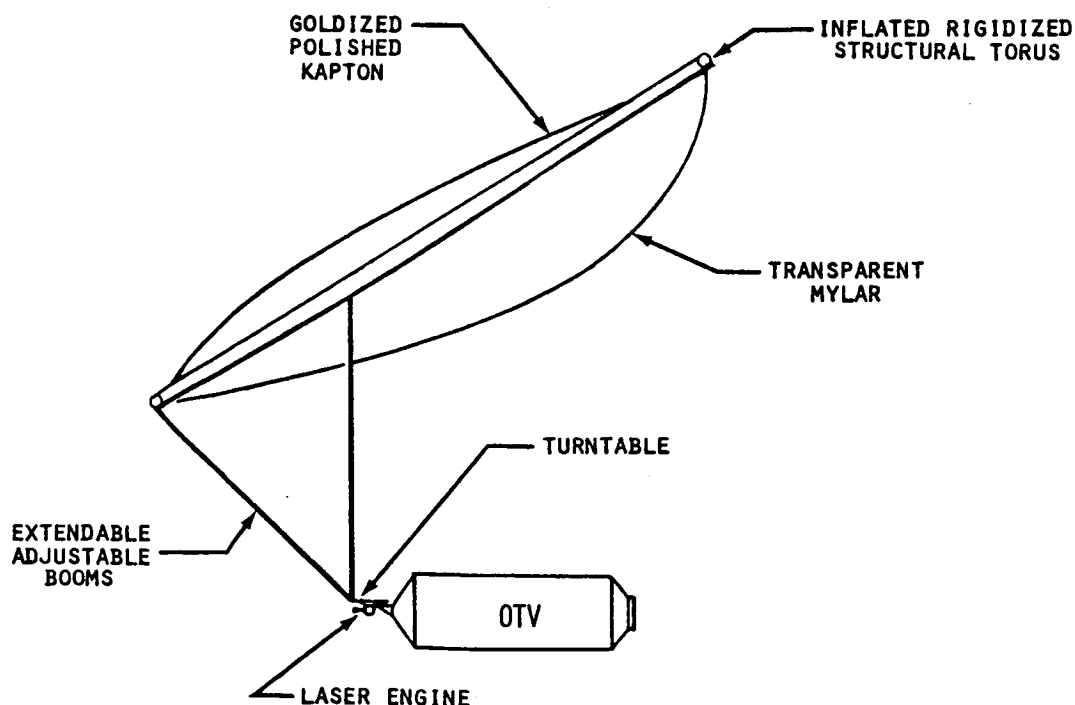


Figure 3.2.2-2: Nonrigidized Inflatable Off-Axis Collector Configuration

This collector consists of several elements; the first is an inflatable torus with rigidizing aluminum wires buried in its surface. As the torus is inflated, the wires are stressed beyond their yield point to follow the toroidal shape. The torus can then be deflated and the wires will hold the toroidal shape and support the inflated parabolic reflector. The reflector working surface would be goldized polished kapton which was been fabricated on a paraboloidal tool using taped butt joints and tear stoppers. The front surface would consist of a specially treated high-transmittance mylar fabricated on a similar tool. The shape is maintained by internal gas at 10^{-5} atm of pressure, so the leakage from micrometeorite punctures is extremely small and is easily made up from the propellant tankage.

The vehicle collector is sized by the requirement to capture a high percentage of the laser beam at its maximum working range. For the space-based laser, the maximum working range is LEO to GEO or 42,000 km. Using the criteria outlined in Reference 7, the divergence half angle of the beam from a nearly perfect ($\lambda/20$) mirror is:

$$1) \quad \sigma_T = \left[(1.3\sigma_0)^2 + \sigma_j^2 + \left(\frac{\lambda_{20}}{D} \right)^2 \right]^{1/2} \mu\text{rad}$$

$$\text{where } \sigma_0 = \frac{1.3\lambda}{\pi D}, \quad \sigma_0 = \text{diffraction-limited half-angle}$$

$$\sigma_j = 0.05 \times 10^{-6}, \quad \sigma_j = \text{beam jitter}$$

$$\text{and} \quad \frac{\lambda_{20}}{D} = \text{wave front error}$$

The spot size at distance R from the transmitter mirror is:

$$2) \quad d_{\text{spot}} = 4 \sigma_T R$$

which for $\lambda = 10.6 \times 10^{-6}\text{m}$ and $D = 30\text{m}$ equates to a theoretical spot size of 33m. A 60m-diameter circular collector inclined at 42 deg was selected to intercept this beam. Reducing the wavelength to $2.8 \mu\text{m}$ reduces the diffraction-limited half-angle by a factor of four but does nothing for beam jitter which now predominates. As a result, reducing the wavelength to $2.8 \mu\text{m}$ only reduces the collector diameter to 20m.

The optical response available with the various collectors varied from diffraction-limited (1/20 wavelength) accuracy for the adaptive optics to nonimaging 1/8-deg accuracy for the inflatable collector. The impact of this dispersion in optical responses on collector characteristics is shown in Figure 3.2.2-3. The concentration ratio for a diffraction-limited mirror is

	<u>SPECIFIC MASS</u>	<u>CONCENTRATION RATIO</u>	<u>MAX FOCAL INTENSITY</u> <u>($D_{\text{COLLECTOR}} = 20 \text{ M}$, $P_{\text{JET}} = 1.5 \text{ MW}$)</u>
CONVENTIONAL DESIGN COLLECTOR WITH ADAPTIVE OPTICS	$\sim 30 \text{ KG/M}^2$	$\sim \frac{D_{\text{COLLECTOR}}}{\lambda_{\text{LASER}}} = 2 \times 10^8$	1000 KW/CM ²
LIGHTWEIGHT INFLATABLE COLLECTOR	$\sim 0.5 \text{ KG/M}^2$	$\frac{1}{4(\Delta \alpha)^2} = 5 \times 10^4$	25 KW/CM ²

Figure 3.2.2-3: Laser Collector Characteristics

approximated by the diameter over the wavelength. The minimum mirror diameter required at GEO to intercept a beam of wavelength 10 μm from a 30m diffraction-limited transmitter located at LEO is approximately 40m. This results in a concentration ratio of about 4 million and a peak intensity of 2000 kW/cm² assuming a thrust power of 1.5 MW and a 50% efficient engine. This amount of thrust is the minimum required to complete the mission in the allotted time. The concentration ratio for the inflatable collector is approximated by 1 over 4 times the standard deviation squared which is equal to about 50,000, assuming a standard deviation of 0.00218 rad (1/8 deg). This results in a peak intensity of 25 kW/cm² assuming the same thruster power as before. Given that the lightweight concentrator can generate adequate power densities at 1/50th of the weight of the adaptive collector, it is not surprising that the inflatable concentrator was selected for vehicle analysis.

Laser Engine: The laser engine cannot be defined in detail without knowledge of the coupling mechanism. Since there is insufficient data at this time to select the best coupling mechanism, a conceptual engine design has been defined which could conceivably operate using any of the three candidate.

coupling mechanisms. The optical response of the collector is the key characteristic used to define the size and shape of the laser rocket engine. For the nonimaging optics of the lightweight inflatable collector defined in the last subsection, the theoretical light intensity distribution at the focal spot can be described by the equations and diagram shown in Figure 3.2.2-4. The radius of the laser spot of the focal plane is a function of the collector focal length (which varies with diameter and f-number) and the standard deviation (accuracy) of the collector surface. The peak intensity of the focal point is proportional to the incident power divided by the square of the standard deviation radius (see Figure 3.2.2-4).

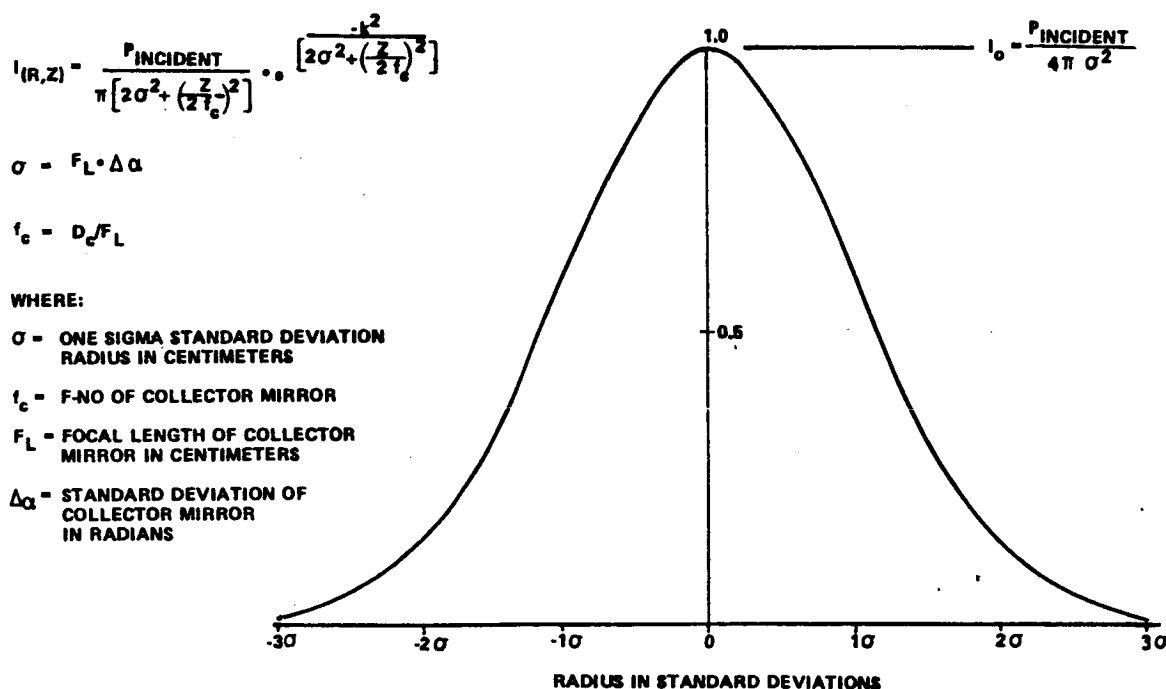


Figure 3.2.2-4: Intensity Distribution in Focal Plane

An example of the combined effect of laser system design parameters is shown in Figure 3.2.2-5. For a space-based laser concept (transmitter diameter = 30m) the minimum collector diameter required at GEO is determined by the beam divergence half-angle which is a function of the laser wavelength, the beam jitter, and the transmitter accuracy as discussed earlier. Assuming a collector f-number of 1 (based on effective diameter), the one-sigma standard deviation radius is shown for best case (1/20 deg) and worst case (1/8 deg) collector surface standard deviation. Then, assuming a combined optical system efficiency of 50% and an engine internal concentration ratio of

LASER TYPE	LASER WAVELENGTH μM	MIN COLLECTOR DIAMETER M	COLLECTOR SURFACE ERROR STD DEV. ~ DEG	ONE-SIGMA RADIUS, CM	MIN BEAM POWER TO REACH 25 kW/cm ² • MW	TOTAL LASER WEIGHT MT
EDL-CO ₂	10.6	60	0.125	10.4	25	1925
EDL-CO ₂	10.6	60	0.05	4.2	4.2	400
FEL	2.8	20	0.125	3.5	3.0	150
FEL	2.8	20	0.05	1.4	0.5	90

*ASSUMES OPTICAL EFFICIENCY OF SYSTEM EQUAL TO 88% AND ENGINE INTERNAL CONCENTRATION RATIO OF 2.0

Figure 3.2.2-5: Effects of Design Parameters on Space Based Laser Concept

2, the total laser beam power required to reach 25 kW/cm² can be calculated using the one-sigma radius. The advantages of the shorter wavelength free-electron laser (FEL) are apparent. The shorter wavelength results in a smaller collector, which results in a smaller focal spot, which requires less power to reach ignition intensities, which in turn results in a lighter laser to be put into orbit. A standard collector surface error of 1/8 deg is thought to be realizable using current technology (Reference 8) and a standard deviation of 1/20 deg is thought to be physically possible someday, but more work is required in either case to prove the inflatable collector concept.

A conceptual 1.5-MW, 200N laser engine design is shown in Figure 3.2.2-6. The engine is double walled and regeneratively cooled using an expander cycle with hydrogen propellant as the working fluid. The converging laser beam from the collector enters the engine through a single crystal zinc-selenide window which has been antireflective coated. This window is convectively cooled by GH₂ flowing radially inward from the edges. The laser beam is further concentrated (by an estimated factor of two) by two optical-quality nested conical surfaces which tend to direct off-axis laser light and the hydrogen propellant toward the laser focal spot. At the focal spot there is a region corresponding to a laser supported "flame" or plasma where the laser beam transfers its energy to the propellant. The hydrogen is forced through this region by the conical concentration surfaces, then has time to mix and recombine in the large holding volume before it exits through the nozzle. The

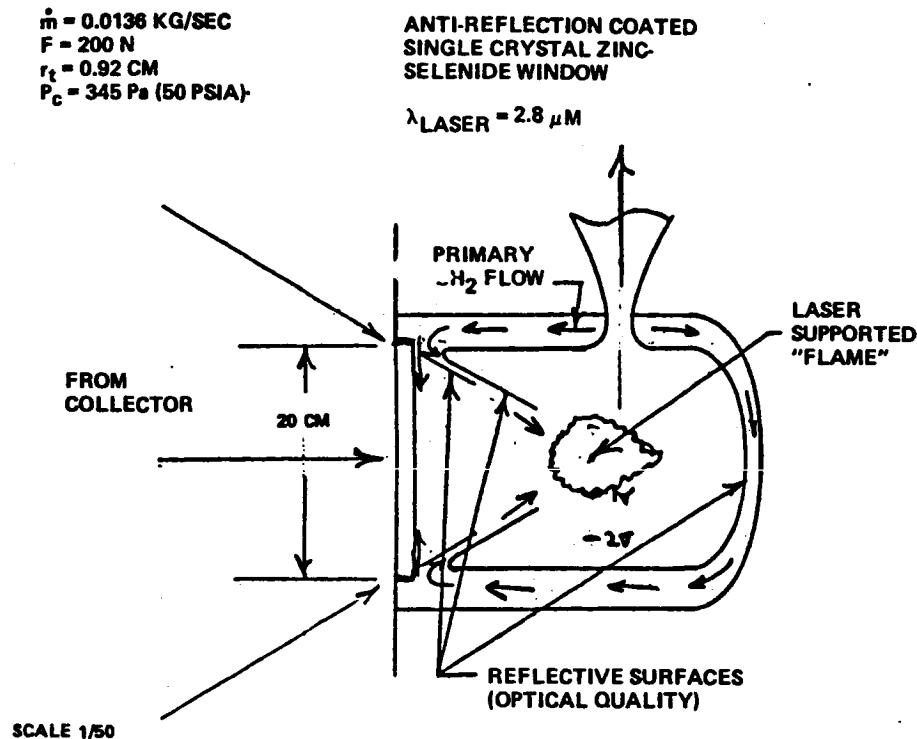


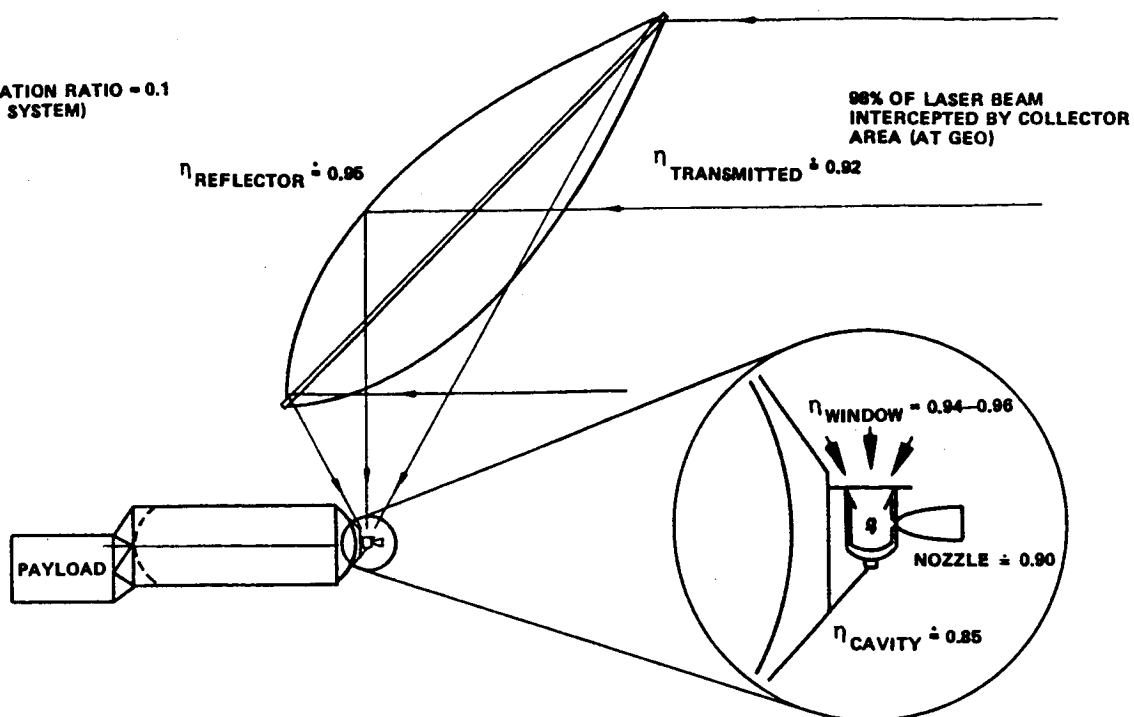
Figure 3.2.2-6: Conceptual 1.5-MW Laser Engine Design

curved aft wall of the combustion chamber is an optical surface which tends to reconcentrate those parts of the incident laser beam which avoided the central flame region and directs them back through that region where they will be absorbed. The one-sigma and two-sigma standard deviation radii assumed are shown to scale in Figure 3.2.2-6. Overall laser engine efficiency is summarized in Figure 3.2.2-7.

Laser Vehicle: The vehicle sized for the 12t delivery mission is shown in Figure 3.2.2-8 with a 200N laser engine shown to scale. The engine and tankage were sized for 24-day spiral ascent and 5-day spiral descent trajectories. The vehicle is shuttle compatible (i.e., it can be launched or returned for servicing inside a standard space shuttle), although its normal operation will be space based. A laser-powered OTV sized for the 60t delivery mission (high mission model) is shown in Figure 3.2.2-9. It is shown inside the proposed shroud outline of a shuttle-derivative vehicle in which it could be launched or returned for ground servicing. In normal operation it would also be space based.

Thus far, with respect to the laser propulsion trade tree (Figure 3.2.2-1), we have estimated an achievable performance level and have selected

OBSCURATION RATIO = 0.1
(ENTIRE SYSTEM)



RESULT: APPROXIMATELY 50% OF BEAM POWER APPEARS IN JET

Figure 3.2.2-7: Laser Engine Efficiency

1/100 SCALE

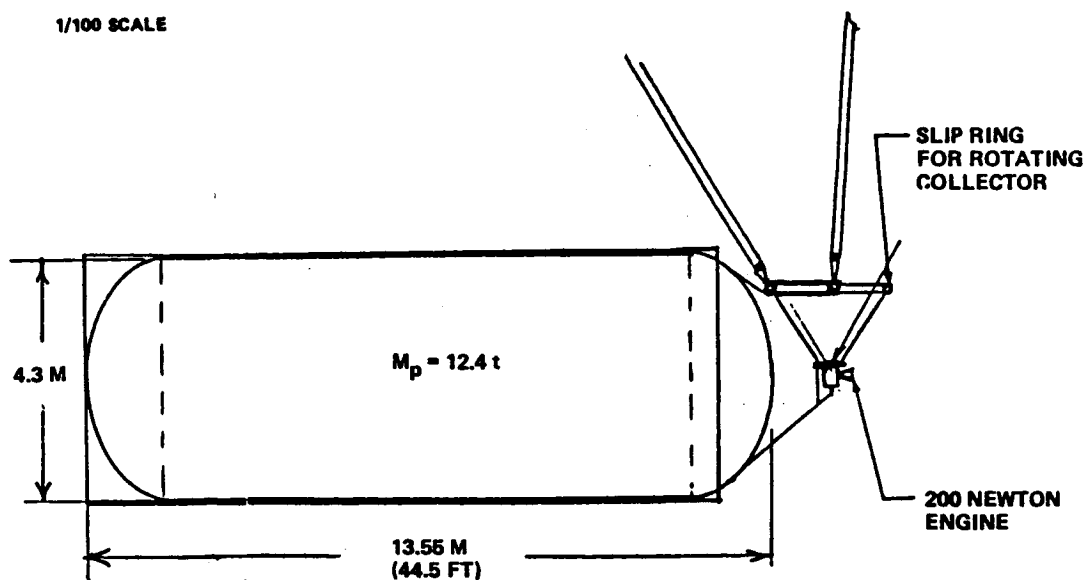


Figure 3.2.2-8: Space-Based Laser Vehicle with 1.5-MW Engine

VEHICLE SIZED FOR 60 t GEO DELIVERY (30 DAY MISSION)

INITIAL $T/V = 0.0007$

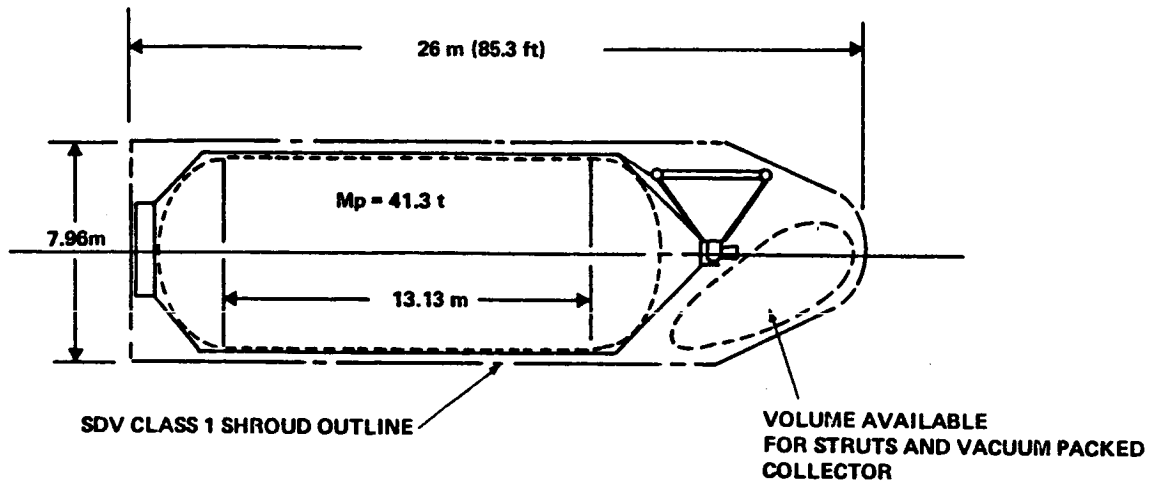


Figure 3.2.2-9: Space-Based Laser Vehicle with 5.63 MW (750N) Engine

a collector type and an engine type. The issues of laser type and laser location will be addressed next.

3.2.2.2 Space-Based Laser System

The space-based laser has certain advantages. For example, in theory, a diffraction-limited beam can be generated in orbit, transmitted distances comparable to LEO to GEO, and concentrated with a collector into a small, relatively efficient, laser engine. Neither the transmitter nor the collector need exceed 30m (100 ft) in diameter and there are no problems with atmospheric distortion or system vibration. In addition, because both the laser and vehicle are in orbit, long burn times are available (in theory) which allows the use of a low-power (approx. 3-MW) laser.

Key assumptions in designing and sizing the space-based laser system were:

1. A single nuclear-powered laser would be placed in 400-km LEO. A low Earth orbit was preferred over a higher orbit to minimize laser launch costs, maximize laser accessibility, and avoid laser safety issues. Nuclear power appeared preferable to multiple solar-powered lasers with relay

optics.

(Note: this issue can be avoided with multiple-impulse trajectories which will be discussed later.)

2. A 30m laser transmitter with $\lambda/20$ diffraction-limited interactive-adaptive optics available by 1995. This assumes straightforward application of present day benchtop (20-cm diameter) optical technology to large space-based systems.
3. A multimewatt-sized, space-based, 25%-efficient CO₂ electron discharge laser (EDL) or 50%-efficient free electron laser would be available by 1995.

The beneficial effect of shorter laser wavelengths on laser power requirements was noted in the previous section. Figure 3.2.2-10 summarizes

	<u>EDL-CO₂ LASER</u>	<u>FEL LASER</u>
ROTATING BED REACTOR POWER PLANT		
THERMAL POWER, MW _T	500	30
ELECTRICAL POWER, MW _E	100	6
POWERPLANT MASS, MT	850	55
LASER TRANSMITTER		
BEAM POWER, MW	25	3
LASER WEIGHT, MT (INCLUDES HEAT REJECT.)	1000	20
30 METER OPTICS, MT + STABILITY AND CONTROL	75	75
TOTAL LAUNCH MASS, MT	1925	150

Figure 3.2.2-10: Space-Based Laser System Sizing

this issue by comparing the laser systems for a $10.6\text{ }\mu\text{m}$ CO_2 EDL and a $2.8\text{ }\mu\text{m}$ FEL (both systems assume a $1/8$ -deg collector surface error). The FEL benefits from the reduced beam power required (3 MW versus 25 MW), the higher laser efficiency (50% versus 25%), and the lower laser specific mass (7 kg/kW versus 40 kg/kW). Hence, the free electron laser was the obvious choice for the space-based laser system. A conceptual design for a 3-MW FEL powered by a 30-MW rotating-bed reactor is shown in Figure 3.2.2-11. Recent advances in direct-pumped solar or nuclear lasers (References 9 and 10) could well preclude this type of installation and result in a smaller, simpler device; but sufficient design data presently are not available to determine relative merit.

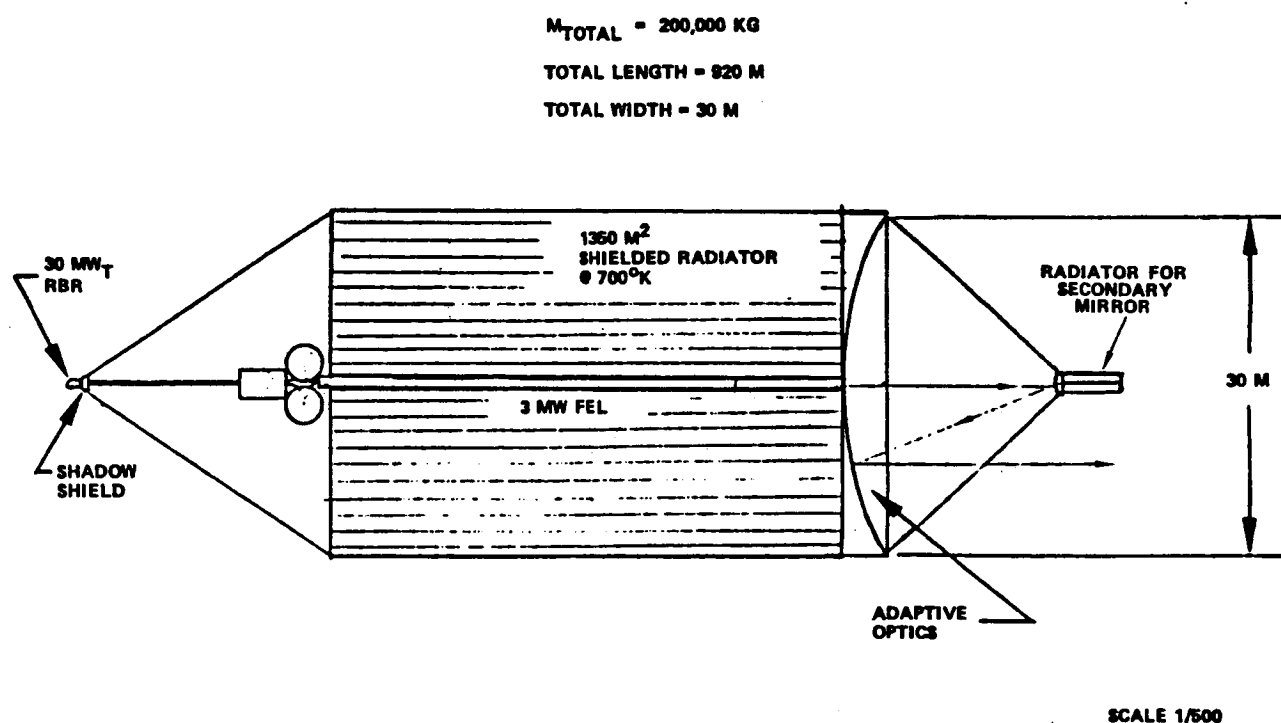


Figure 3.2.2-11: Conceptual Space-Based Laser

Trajectory Optimization: The ΔV required for a LEO-to-GEO transfer is a function of vehicle T/W for continuous burn trajectories and the length of burns allowed for multiple impulse trajectories. If trip time is not severely constrained, relatively low-thrust vehicles can perform multiple short burns at perigee and apogee points and travel from LEO to GEO with little ΔV penalty. The mission model used in the advanced propulsion study required the vehicles to travel from LEO to GEO in 20 to 25 days, which allowed the laser and solar thermodynamic rockets ($T/W \sim 0.001$) to perform

efficient multiple burns. The method for calculation of delta-V losses is discussed in Section 3.2.3, Solar Rocket Trades, and will not be repeated here. The results of trajectory optimization utilizing a space-based laser is illustrated with two examples.

Figure 3.2.2-12 illustrates the spiral trajectory case where the laser and the LEO are in a coplanar 400-km orbit. In this case the laser would trail the LEO base by some 2000 km to maximize the length of the initial burn. The frame of reference in the figure is rotating with the laser satellite so it appears fixed and the numbered dots represent the OTV position at the end of each successive laser orbit. The OTV has a 2000N engine (25-MW laser) and is sized for the 12t delivery mission.

FRAME OF REFERENCE IS ROTATING WITH LASER SATELLITE
 • MISSION IS 12T DELIVERY USING 2000 NEWTON THRUSTER

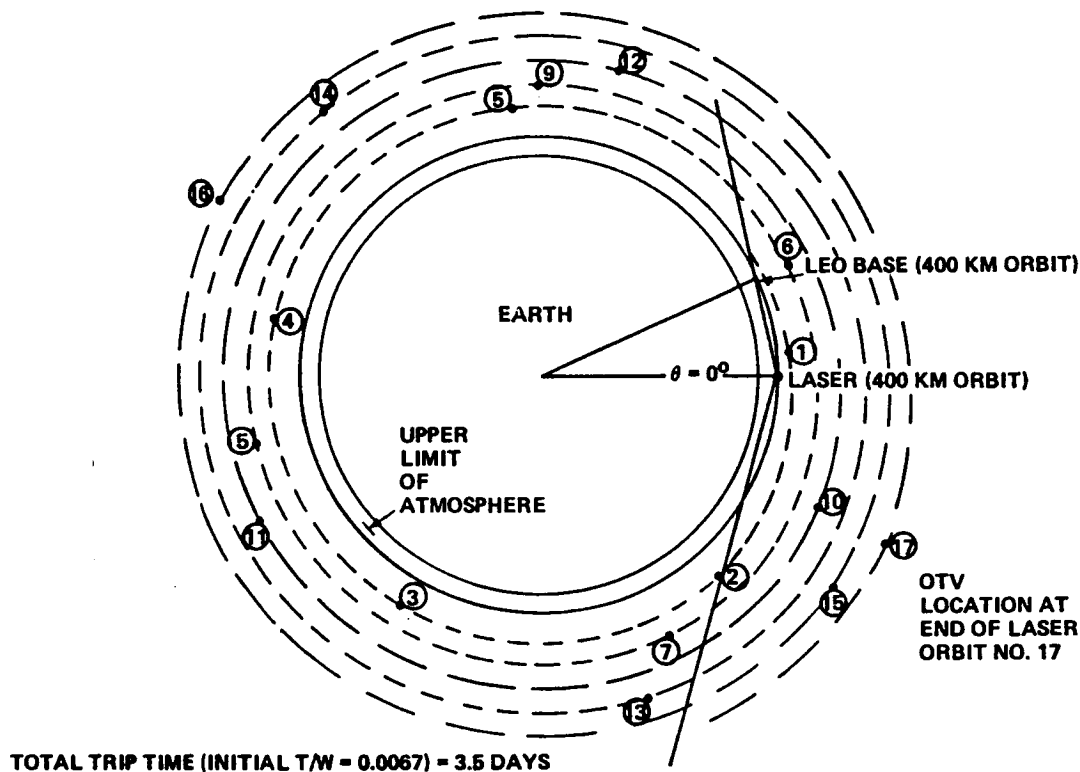


Figure 3.2.2-12: Spiral Trajectory with Space-Based Laser

The initial burn lasts for two laser orbits and then the OTV, which is now in a higher, longer-period orbit, passes beyond line of sight behind the laser. The OTV is behind the Earth for almost three laser orbits, then in view for approximately one orbit, out of sight for 2-1/2 orbits, etc. After about 1 day of intermittent burns, the situation rapidly approaches a state

where the OTV is in view about one-half the time, with consecutive burns 45 min long and 45 min apart. The upleg trip time (LEO to GEO) is 3-1/2 days at an initial T/W of 0.0067 and the upleg delta-V is estimated to be 5910 m/sec.

The alternative multiple impulse trajectory using the same vehicle and laser is characterized in Figure 3.2.2-13. The key in optimizing multiple

BURN NO.	V M/SEC	NO. OF LASER ORBITS UNTIL NEXT BURN	NO. OF OTV ORBITS UNTIL NEXT BURN	OTV ORBIT HOURS	APOGEE RADIUS KM
1	122	24	23	1.609	7168
2	121	12	11	1.682	7587
3	119	8	7	1.762	8040
4	118	5	5	1.850	8530
5	119	24	19	1.947	9063
6	118	4	3	2.056	9644
7	120	24	17	2.177	10282
8	120	3	2	2.313	10986
9	120	8	5	2.467	11767
10	121	12	7	2.643	12640
11	121	24	13	2.846	13624
12	123	2	1	3.083	14743
13	126	24	11	3.364	16029
14	128	12	5	3.700	17526
15	130	8	3	4.111	19295
16	134	3	1	4.625	21425
17	139	24	7	5.286	24052
18	145	4	1	6.167	27391
19	155	24	5	7.400	31808
20	164	6	1	9.250	38001
21	71	LAST PERIGEE BURN		10.581	42163
2623		256 = 16.4 DAYS	150		

**Figure 3.2.2-13: Space-Based Laser Multiple Impulse Trajectory—
12t Payload, 2000 N Thruster**

impulse trajectories is to boost the OTV into interim orbits such that the OTV and the LEO laser both cross the perigee nodal axis simultaneously and in minimum elapsed time. This allows another burn and a new interim OTV orbit. The trajectory scenario that best matched the mission model required an engine thrust of about 2000N and resulted in an upleg trip time of about 21 days. Note that careful selection of the nodal axis would result in the laser always being in sunlight during engine burns, eliminating the need for developing a nuclear powerplant. The delta-V savings with the multiple impulse trajectory were considerable (almost 1600 m/sec) and resulted in significant propellant savings.

Aerobraking: All laser rocket concepts were examined to determine the effect of aerobraking on vehicle performance. However, aerobraking resulted in only a very small propellant savings (approx. 1000 kg) for the laser-powered vehicles. This was due to the high I_{sp} (1500 sec) and low

vehicle masses (7000 kg) available during the return trip. In fact, the mass of the ballute, the ballute coolant, the collector that must be thrown away, and auxiliary propellant that must be added exceeded the mass of the propellant saved. for this reason, aerobraking is not recommended for use on the laser-powered concepts.

3.2.2.3 Ground-Based Laser System

A ground-based laser system has both advantages and disadvantages relative to the space-based system just discussed. First, the key element in the system (the laser) is ground based where it can easily be built and maintained and where it is not perceived as an offensive threat by our political opponents. Second, the very nature of a ground-based laser system requires relatively high thrust which means small gravity and steering losses. The disadvantages stem from the fact that the laser beam must traverse the Earth's atmosphere and that results in unavoidable losses and inefficiencies. In the ground rules it was assumed that the atmosphere-induced aberrations in a ground-based laser beam could be corrected to a beam divergence half-angle of $1 \mu\text{rad}$ using interactive adaptive optics. To achieve this accuracy, a low-power laser beam would be transmitted from the OTV to the ground-based transmitter which would act in this case as a collector and recollimate the beam. As the adaptive optics segments are adjusted to recollimate the incoming low-power beam, which has just traversed the atmosphere, they are automatically being adjusted to correct for the atmospheric-induced aberrations in the more powerful outgoing beam. This process is called interactive adaptive optics.

Even with interactive adaptive optics, a ground-based laser has insufficient beam quality to efficiently power an OTV more than 6000 to 7000 km away. Hence, a decision was made early in the study to add a solar-powered "kick" engine to the ground-based laser-powered OTV which would perform the correction burns above LEO plus the GEO insertion and exit burns. The alternative to the solar kick engine was to add several orbital relay stations which, in theory, have the capability to collect the distorted wavefront emanating from the atmosphere, correct and recollimate it in real time, and then transmit it up to GEO using a 30m adaptive mirror. These relay stations, in the opinion of the authors, require significant breakthroughs in the

technologies of manufacturing and control of large space-based optical systems and for that reason were not seriously considered as part of the ground-based laser system. The solar kick engine would be sized to use the collector required by the ground-based laser (60m diameter) and would allow the ground-based laser system to perform all the planetary missions in the mission model (something which could not be done with relay stations or by the space-based laser).

Trajectory Optimization: A ground-based laser (without relay satellites) obviously would be used to power a series of perigee burns, and the laser-powered OTV would fly a multiple impulse trajectory of the type discussed for the space-based laser. The assumptions used in optimizing the OTV trajectory for the ground-based laser were that (1) a single laser was located on a mountain top near the equator, (2) the ground site was located such that it was obscured by weather no more than 2 days/month, and (3) the laser OTV converts to solar power for maneuvers above 5000 km.

As with the space-based laser, the key to optimizing multiple impulse trajectories is to boost the OTV into interim orbits such that the OTV passes over the laser while at perigee and in minimum elapsed time. This allows another burn and a new interim OTV orbit. Another important consideration with respect to trajectory optimization is the effect of OTV orbit height on a ground-based laser burn time. In the initial 400-km circular orbit, the available burn time is only 258 sec (assuming a minimum laser azimuth angle of 20 deg), and this will decrease as the apogee altitude is raised by each successive burn. To meet the payload and delivery time requirements with this short burn time would require very powerful (1 to 2 GW) lasers which would be exceedingly expensive to develop and operate. The alternative to large lasers is longer burn times which would be made possible by raising the OTV perigee as well as its apogee. The geometry involved in increasing burn time is shown in Figure 3.2.2-14. As noted in the figure, an increase in perigee altitude to 4200 km results in a ninefold increase in burn time and still provides for a reasonably sized collector.

An example scenario of interim OTV orbits is characterized in Figure 3.2.2-15. Note the four apogee burns which raise the perigee radius to 10,600 km (4200-km altitude). The laser power required in this scenario was still excessive, since 88 MW of jet power equals about 350 MW of ground-based laser

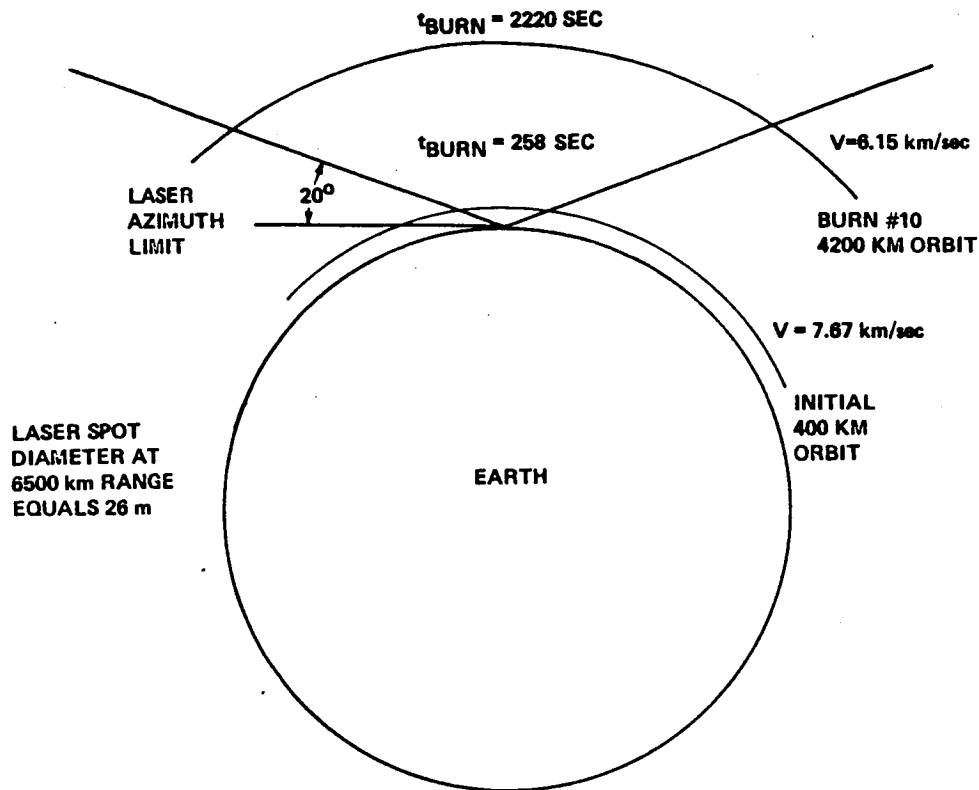


Figure 3.2.2-14: Effect of Vehicle Orbit Height on Ground-Based Laser Burn Time

	ORBITS DAY	T Hours	a km	Rp km	Ra km	Vp km/sec	Va km/sec	ΔV m/sec	M _s kg	Δt sec	P _{JET} MW
INITIAL ORBIT	15.567	1.5417	6775	6775	6775	7.87	7.87	—	30,000	—	—
POST PERIGEE BURN	15	1.600	6939	6775	7103	7.78	7.402	90	29,820	258	78.6
POST APOGEE BURN	14	1.714	7285	7427	7103	7.244	7.574	172	29,470	428	87.2
POST PERIGEE BURN	13	1.846	7633	8163	7103	6.741	7.747	173	29,126	418	88.8
POST APOGEE BURN	12	2.000	8058	8163	7953	6.942	7.125	201	28,730	906	46.9
POST PERIGEE BURN	11	2.182	8532	8163	8901	7.137	6.545	195	28,350	880	46.3
POST APOGEE BURN	10	2.400	9092	9283	8901	6.483	6.762	218	27,930	1308	34.3
POST PERIGEE BURN	9	2.667	9745	10607	8901	5.858	6.978	218	27,520	1268	34.5
POST APOGEE BURN	8	3.000	10559	10607	10511	6.118	6.172	260	27,040	2220	23.3
POST PERIGEE BURN	7	3.429	11542	10607	12477	6.374	5.418	258	26,570	2130	23.7
POST APOGEE BURN	6	4.000	12780	10607	14953	6.631	4.704	257	26,110	2050	24.1
POST PERIGEE BURN	5	4.800	14445	10607	18283	6.897	4.001	266	25,640	1975	25.4
POST APOGEE BURN	4	6.000	18747	10607	22887	7.166	3.321	269	25,175	1895	26.3
POST PERIGEE BURN	3	8.000	20307	10607	30007	7.452	2.634	286	24,690	1825	28.5
FINAL ORBIT	2.026	11.848	26385	10607	42,183	7.749	1.949	297	24,200	1750	30.2
								3158			

Figure 3.2.2-15: Ground-Based Laser Orbital Mechanics

which requires about 1.5 GW of electric power. A further improvement is shown in Figure 3.2.2-16 where the peak jet power is limited to about 50 MW by tailoring the first few pulses and spending more time in LEO. The transfer orbit referred to as burn number 14 is actually a series of burns to circularize into GEO and drift to the correct longitude location.

BURN NO.	ΔV M/SEC	P _{JET} MW	NEW ORBIT REV/DAY	TIME IN ORBIT DAYS
1	50	42.6	15.25	4.0
2	40	34.0	15.0	0.5
3	82	41.6	14.5	2.0
4	80	40.6	14.0	1.0
5	82	42.3	13.5	2.0
6	81	41.6	13.0	0.5
7	201	46.9	12.0	1.0
8	195	46.3	11.0	1.0
9	218	34.3	10.0	1.0
10	216	34.5	9.0	1.0
11	518	47.6	7.0	1.0
12	523	49.9	5.0	1.0
13	556	53.0	3.0	1.0
14	297	29.6	TRANSFER ORBIT	7.0

TOTAL TRANSIT TIME TO GEO = 24 DAYS

Figure 3.2.2-16: Selected Mission for 30-Day GEO Delivery Mission

3.2.2.4 Air-Based Laser System

The air-based laser system operates much like the ground-based system except the laser is divided among a fleet of 747 special performance (SP) airplanes instead of being placed on a mountain top. The advantages of air basing are: elimination of weather problems, elimination of almost all atmospheric absorption, and increased flexibility brought on by highly portable lasers. Key assumptions made in assessing the air-basing option were that (1) the laser beam vibration and tracking inaccuracies generated by the carrier aircraft could be limited to 3 μ rad of half-angle divergence, (2) the

OTV converts to solar power for maneuvers above LEO (same as ground based), (3) each 747 SP carries one 5-MW chemical laser and associated tracking and transmitter gear, and (4) aircraft could fly in close formation (100m apart) at 16-km (50,000 ft) altitude. The process of clustering aircraft, as shown in Figure 3.2.2-17, allows up to 90 MW of laser power (16 airplanes) to be used in a single burn. A 24-day delivery requires 16 aircraft flying 10 hr/day (2 flights per day per aircraft). The extra burns are required because perigee height cannot be raised with the large beam divergence half-angle (3μ rad); hence the need for a large number of short burns.

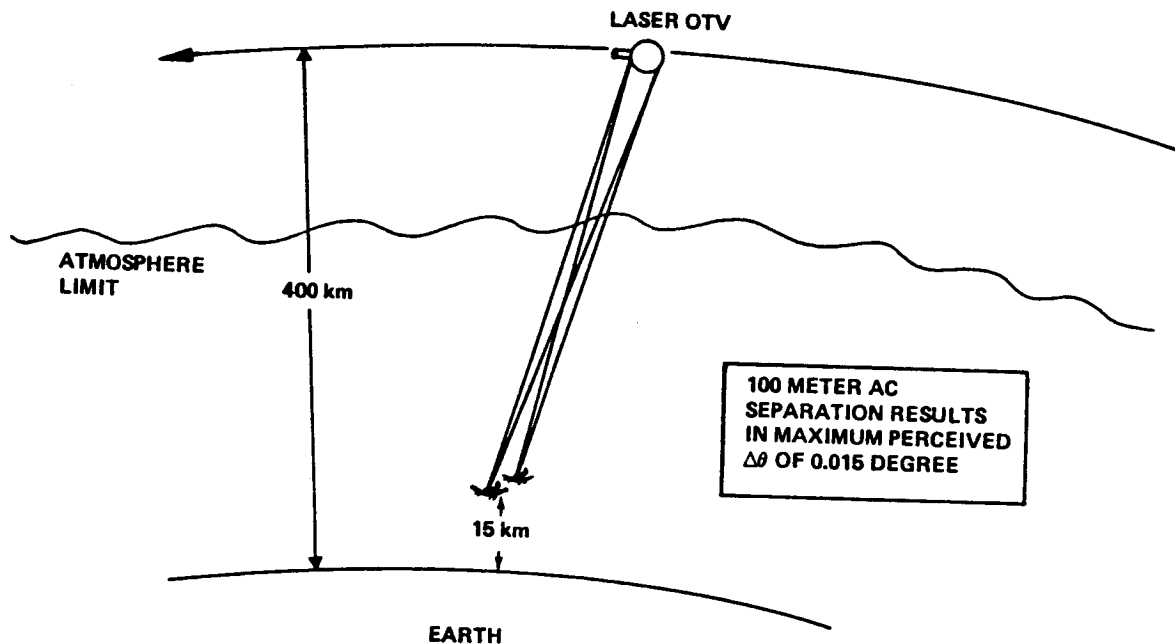


Figure 3.2.2-17: Laser-Carrying Aircraft Clustered To Reduce Trip Time

Preliminary operating costs were estimated for this fleet of aircraft using first-order commercial airline numbers. Assuming a cost per flight (including recharging the laser) of \$50,000 and an aircraft cost (including laser installation) of \$200M with the airplanes depreciated over 200 flights (15 years), then the aircraft operating cost per mission is \$40M (direct operating cost) plus \$16M (depreciation), or \$56M per mission. By any standards, this is highly exorbitant for a support function, so the air-based system was dropped from further consideration.

3.2.3 Solar Rocket Trades

The solar thermodynamic rocket is similar in many ways to the laser thermodynamic rocket discussed in the last section. Both require a large collector/concentrator assembly, and both operate optimally with a windowed engine cavity where the radiant energy is transferred to the propellant/working fluid. But there the similarity ends, because there appear to be no obvious methods for directly coupling the Sun's radiant energy to the hydrogen propellant. Neither inverse Bremsstrahlung nor molecular resonance appear feasible because solar light is not coherent and has its energy spread over such a large bandwidth. This apparent lack of a method for direct coupling means that some form of solid heat exchanger or particulate absorbent is necessary; this presents several unique problems which were not present in the laser rocket engine. Both the solid heat exchanger and particulate absorbent solar engine concepts were assessed during Task 2. A description of both engine configurations follows.

3.2.3.1 Engine Configurations

Solid Heat-Exchanger Solar Rocket: Ordinarily a heat exchanger used in a thermal engine is also a pressure vessel. Its operating temperature is limited not only by the melting of the wall but by the progressive loss of strength at temperatures far less than the melting point. However, when the heat source is highly focused electromagnetic radiation, it becomes possible, and even desirable, to get the energy inside the pressure vessel through a cooled one-way window. Once inside, the radiation falls on a highly absorbent surface which must withstand high temperatures and readily transfer its heat to the hydrogen working fluid but does not have to simultaneously withstand pressure differentials. In fact, if significant pressure and thermal loads are absent, it should be possible to heat the absorber within 100 to 200 deg of its melting point.

The prescription for the heat exchanger would call for a porous structure made of a refractory metal such as tungsten. The essential characteristics would be a high surface area, for the absorption of light and conduction of heat to the working fluid, and a small physical dimension to avoid the buildup of thermal stresses which could destroy the structure during the rapid on-off cycling. A tungsten foil heat exchanger, developed during a nuclear rocket program (Reference 11) and shown in Figure 3.2.3-1, appears ideal for this

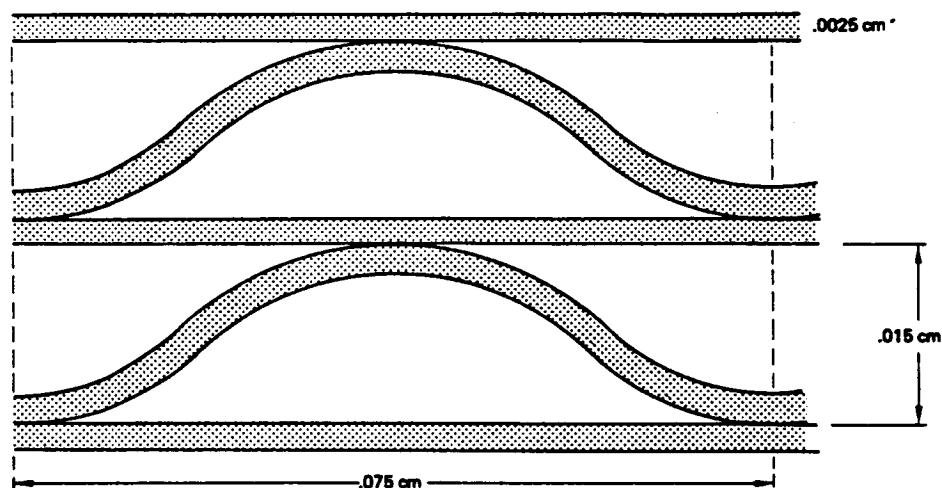


Figure 3.2.3-1: Tungsten Foil Heat Exchanger Element

application. In the original application, the tungsten foil contained a nuclear fuel in the form of uranium dioxide. Such elements did not evaporate or corrode after running for hours at temperatures above 3300°K while hydrogen flowed through them, nor did they break down under extreme and repeated thermal shock conditions. Assuming the tungsten foil absorber is 1 cm thick and arranged such that the focused solar energy falls on one face, this energy would penetrate to the interior in a series of reflections and absorptions with little or no reflection back out the window. If hydrogen was introduced on the back face, it would flow through the heated structure which now acts as a counterflow heat exchanger (i.e., the hydrogen contacts the hottest surfaces as it exits the heat exchanger). A thruster design employing such a heat exchanger/absorber is shown schematically in Figure 3.2.3-2.

The power-handling limitations for such a design are set by the heat transfer rate through the hydrogen boundary layer. For a temperature differential of 100°K between the absorber surface and the bulk gas (conservative,

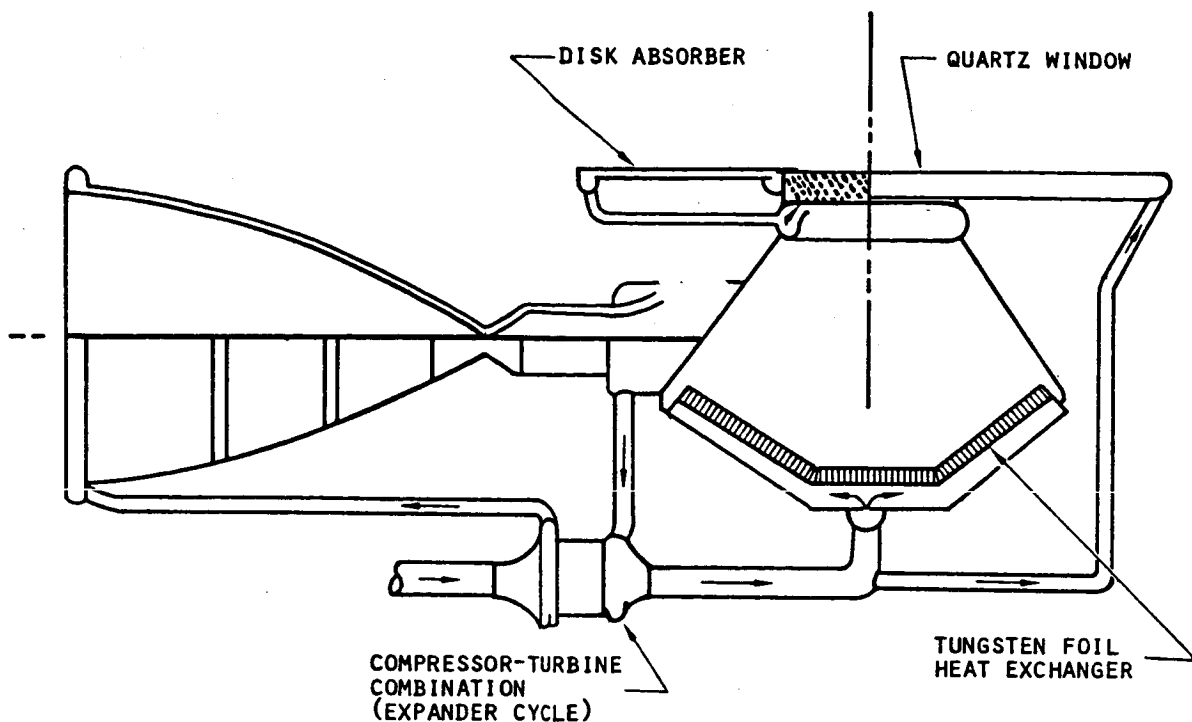


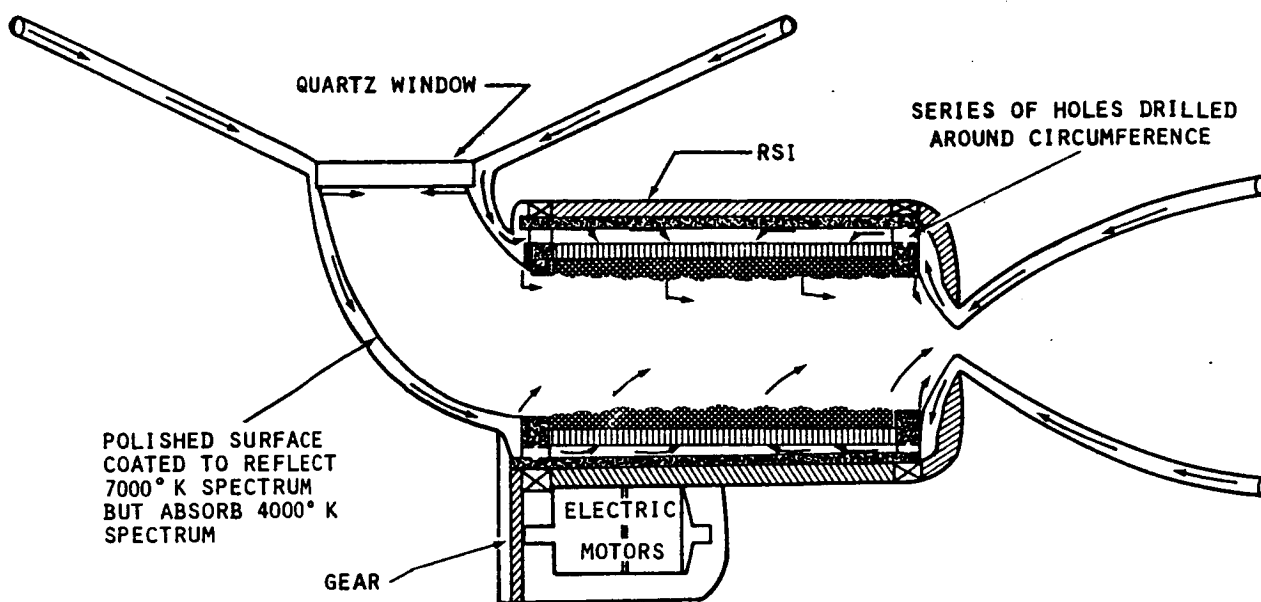
Figure 3.2.3-2: Porous-Wall Solar Rocket Engine

considering the small dimensions) and assuming the solar flux penetrates 20 corrugation widths, or 0.3 cm, the power-handling capability of the foil heat exchanger is about 16 kW/cm^2 of frontal area (Reference 12). The specific impulse for an absorber temperature of 3300°K would approach 1000 sec, providing a compact, highly efficient engine.

Rotating-Bed Solar Rocket: The rotating-bed solar engine operates on the same principles as the porous-wall solar engine discussed in the last section except the tungsten foil heat exchanger is replaced with a rotating fluidized bed of very small ($100 \mu\text{m}$) absorbent particles made of highly refractive material (e.g., tantalum carbide). Use of the very small particles eliminates virtually all material strength requirements and allows unlimited lifetime since particles which break up or evaporate away over time can be replaced periodically. The particle bed absorber also has a very large absorption and heat transfer area available and a 0.5-cm-thick particle bed could handle about 10 kW/cm^2 . This power-handling capability was calculated using a heat transfer rate of $6 \text{ kW/m}^2\text{-}^\circ\text{K}$ from Reference 13, a fluidized bed of $100 \mu\text{m}$ particles, and a temperature differential of 100°K . Because a rotating bed would tend to redistribute the ambient solar flux throughout the bed, it could probably be designed to operate with power levels right up to its thermal

limits. This is its chief advantage over the porous-wall concept, whose design must account for constantly moving hot spots. If tantalum carbide particles with a melting point of 4280°K are used, bulk gas temperatures approaching 4000°K should be possible with a corresponding specific impulse of 1100 sec or more.

The very high operating temperature of a rotating-bed absorber results in a large heating load on the window caused by the infrared reradiation from the absorbent particles. To help alleviate this problem, the proposed rotating-bed engine configuration, shown schematically in Figure 3.2.3-3, contains a cooled corner reflector. The reflector surface is designed to



APPROXIMATELY ONE HALF OF ENERGY IS ABSORBED BY GH_2 PRIOR TO ROTATING BED WHICH ACTS AS SUPERHEATER

Figure 3.2.3-3: Rotating-Bed Absorber Solar Rocket

absorb most of the incident infrared radiation from the particle bed and either transfer the energy to the working fluid or reradiate it at longer wavelengths which are more readily reflected by the window coatings. Use of the cooled corner reflector and spectral coatings on the window should allow cavity efficiencies of 60% or more.

3.2.3.2 Propulsion System Definition

The solar thermodynamic propulsion system selected for initial characterization used a single 60m-diameter inflatable concentrator powering a

single thruster in the configuration shown in Figure 3.2.3-4. The circular concentrator is mounted 42 deg off axis from the mirror axis and so presents a 45m by 60m ellipse to the Sun (2134 m^2 of usable area). The solar concentrator is identical in construction to the laser collector described in Section 3.2.2.1, except the reflector working surface would be silverized, instead of goldized, polished kapton to more effectively reflect the visible light spectrum.

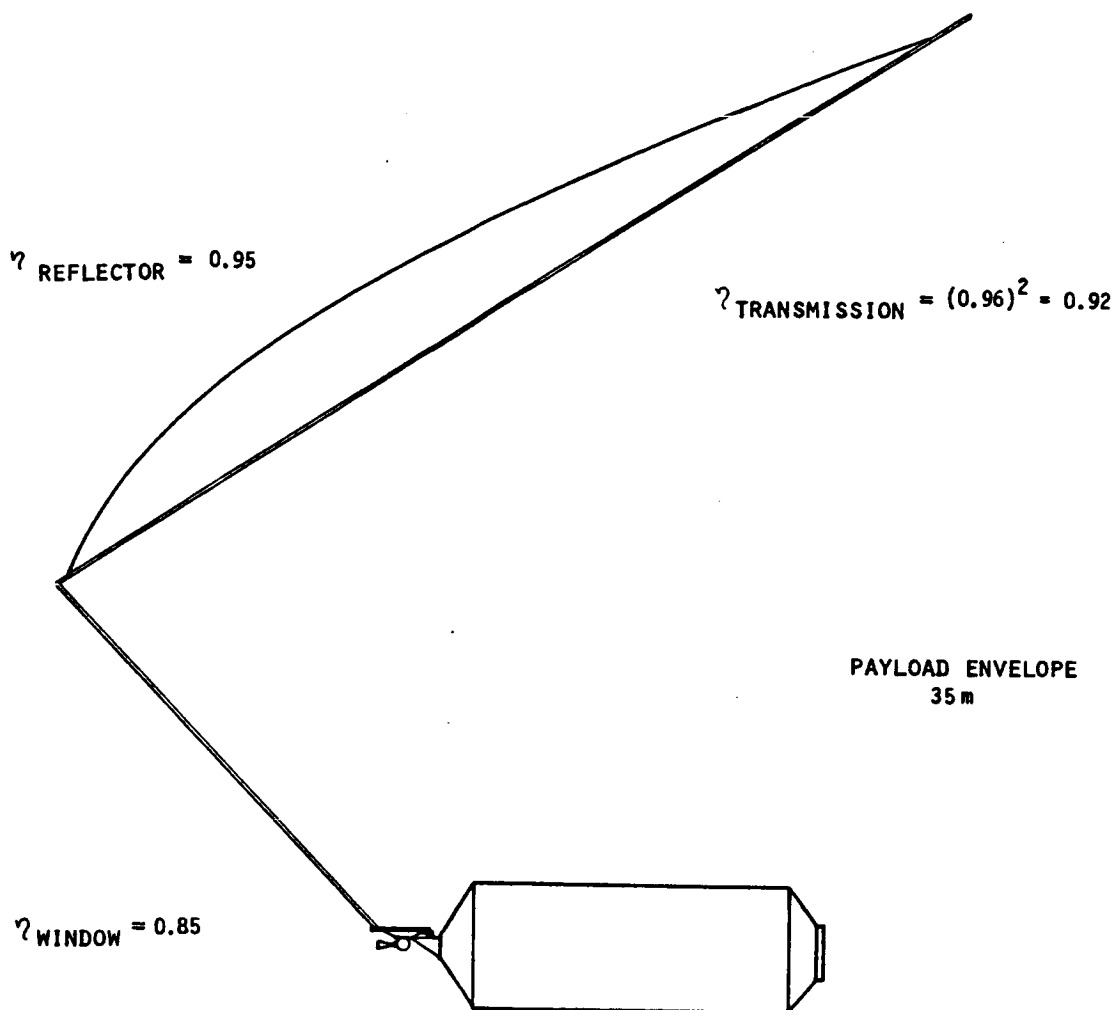


Figure 3.2.3-4: Solar Thermodynamic Rocket Configuration

The mass of the concentrator was estimated by assuming the lens bag was 1 mil thick, giving a specific mass of 0.073 kg/m^2 . This number was then doubled to 0.15 kg/m^2 to account for assembly tapes, rip-stop threads, edge reinforcements, silver, etc. In a similar manner, the astronaut which support the concentrator were estimated to weigh 0.75 kg/m and the toroidal support ring, 140 kg. The total concentrator weight statement is as follows:

Lens assembly (60m)	415 kg
Ring assembly (60m)	140 kg
Support struts	95 kg
Strut actuators (3)	45 kg
Mirror turntable (4m)	90 kg
Gas makeup system	45 kg

830 kg (1829 lb)

Estimated optical properties of the concentrator and absorber window are shown in Figure 3.2.3-4. These indicate that roughly 85% of the solar energy incident on the collector would actually be available to the engine (76% through the window and 9% through disk absorber). It was estimated that the absorber cavity could approach 75% efficiency with proper design (Reference 14) and that the nozzle could approach 90% efficiency. Hence, roughly 60% of the power intercepted by the solar concentrator would be available as thrust power. In near Earth orbit the concentrator would receive 1.345 kW/m^2 , or 2.826 MW of power, which would provide 1.7 MW of thrust power for a thrust of 314N (70 lb_f) at 1100 sec of specific impulse.

The absorber cavity window was sized to be 50 cm (20 in) in diameter, which would result in about 90% of the incident flux striking the window (Figure 3.2.3-5). The other 10% would be absorbed by the disk surrounding the

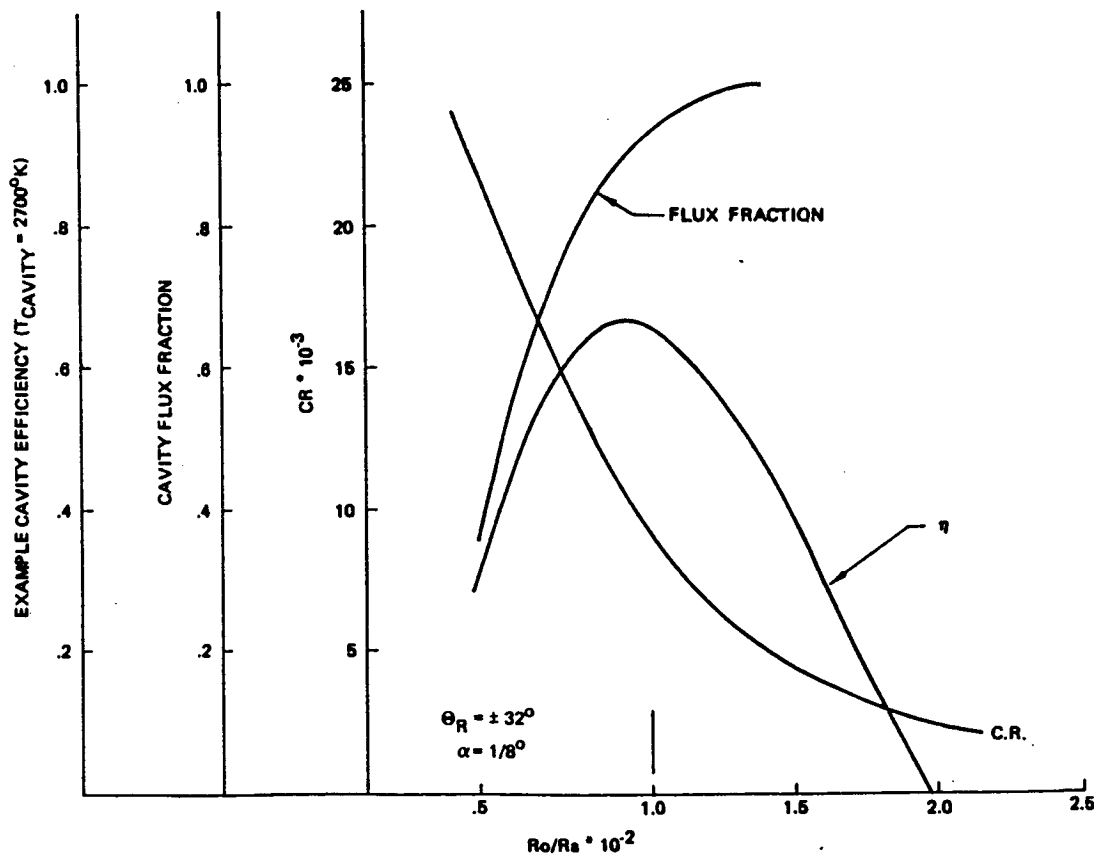


Figure 3.2.3-5: Concentrator Performance (1/8 Deg. Standard Deviation)

window. The estimated mass statement for the absorber cavity and engine shown in Figure 3.2.3-5 follows:

Absorber assembly	136 kg
Window	32 kg
Shell	8 kg
Cover and insulation	5 kg
Mixing chamber	1 kg
Gimbal assembly	6 kg
Pressure vessel	10 kg
Turbopump	2 kg
Ducts and valves	4 kg
Second receiver	32 kg
Feedline	4 kg
Support structure	<u>10 kg</u>
	250 kg

The rotating-bed absorber configuration has the same general geometry and was assumed to have roughly the same mass. A 15% growth margin was added to both the concentrator and the engine during the vehicle sizing trades which follow.

3.2.3.3 Solar Vehicle Sizing

Solar thermal rockets (STR) were sized for 12t and 60t delivery missions as discussed in the ground rules. A mission upleg delta-V of 5030m was assumed, based on Reference 15 ($T/W = 0.007$ initially), for a 24-day multiple-impulse ascent trajectory. Two different tank configurations were studied (see Appendix B) because it was uncertain whether the vehicle could be made shuttle compatible at the fuel volumes required. The vehicle subsystems were designed for a 60-day maximum mission duration, 25-mission lifetime, and each had a solar array capable of supplying 5 kW of electrical power between engine burns. Appendix B contains the detailed mass statement for two baseline vehicle configurations. The first is a shuttle-compatible configuration containing 10.5t of hydrogen propellant and is nominally a laser powered vehicle (mass statements are virtually identical for laser and solar powered vehicles). The second is an SDV-compatible configuration containing 20t of propellant and is nominally a solar powered vehicle.

The initial vehicle sizing was conducted using an engine specific impulse of 900 sec (porous-wall absorber engine) which gave confidence that the engine could be built to last the 1500 to 2000 hr desired (10 missions). This

resulted in a vehicle which required 26.2t of propellant to accomplish the 12t delivery mission. This result was not satisfactory and at the suggestion of NASA, an investigation of the effect of aerobraking, trajectory optimization, and increased cavity temperatures on solar thermal rocket performance was initiated.

Effect of Aerobraking: Implementation of aerobraking resulted in a savings in total mission delta velocity of approximately 2275 m/sec. This resulted in a substantial propellant savings which was only partially offset by the weight of the ballute and transpiration coolant required. In fact, the equivalent specific impulse to accomplish the aerobraking delta-V savings for the mass required was slightly in excess of 5000 sec. Applying aerobraking to the laser and/or solar powered vehicles necessitates jettisoning the inflated collector after the GEO deorbit burn. As with the ballute there appears to be no way to revacuum pack something in a vacuum. Because these vehicles would be space based and need not fit back into the shuttle, there is the possibility that the collector could be mechanically collapsed to a size compatible with aerobraking and then reused; but this option was not assessed during the study. The aerobraked laser/solar vehicle concept examined in this study is shown in Figure 3.2.3-6. This vehicle concept utilizes a small (6000N)

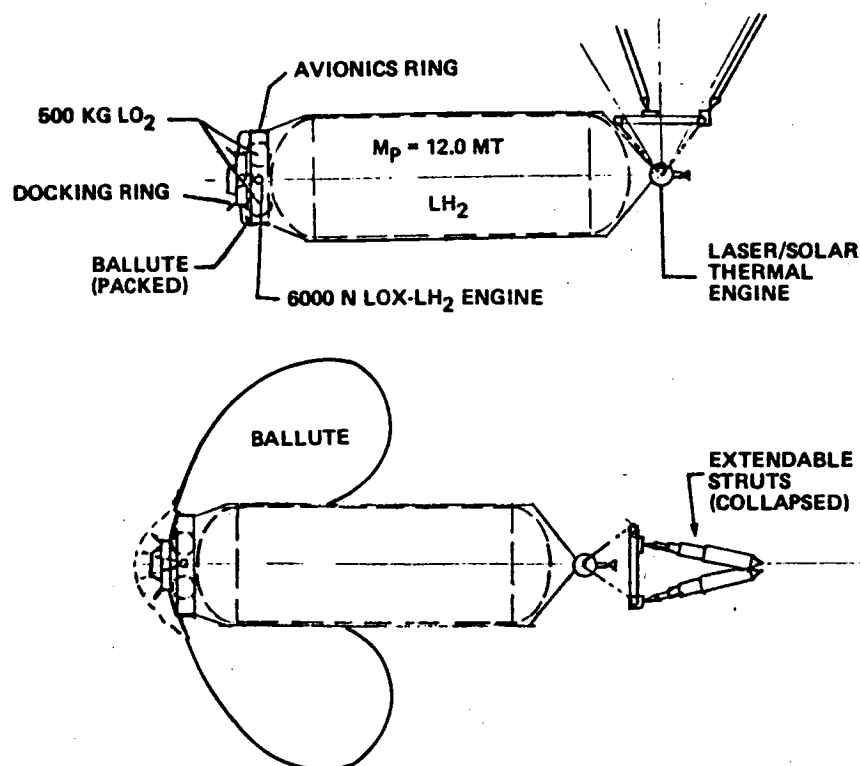


Figure 3.2.3-6: Aerobraked Laser/Solar Vehicle Concept

H₂-O₂ engine mounted at the payload end of the vehicle and a 17.3m (56 ft 9 in) diameter ballute stowed around the payload docking ring.

In operation the engine thrusts through the docking ring and performs the same functions during and after aerobraking as the main propulsion engine in a chemical rocket vehicle. If the docking ring could not stand up to the thermal conditions or reentry when protected only by the engine plume, enhanced protection could be provided by mounting the ballute inside the docking ring and deploying it out around the ring. This would require redesigning the docking ring to modify the external projections to present a circular surface at the ballute front edge.

Effect of Trajectory Optimization: Aerobraking greatly reduces the delta-V required for the return trajectory but has no impact on the upleg. The delta-V required for the LEO-to-GEO transfer is a function of vehicle T/W and the number of burns allowed for multiple impulse trajectories.

For instance, vehicles with very low T/W ratios, such as ion thruster vehicles, must produce up to 5.9 km/sec of delta-V to travel from LEO to GEO while high T/W devices, such as chemical rockets, require only about 4.2 km/sec. The delta-V requirements and one-way travel time from LEO to GEO as a function of vehicle T/W are shown in Figure 3.2.3-7 from Reference 15. The data in this figure are for continuous burn trajectories.

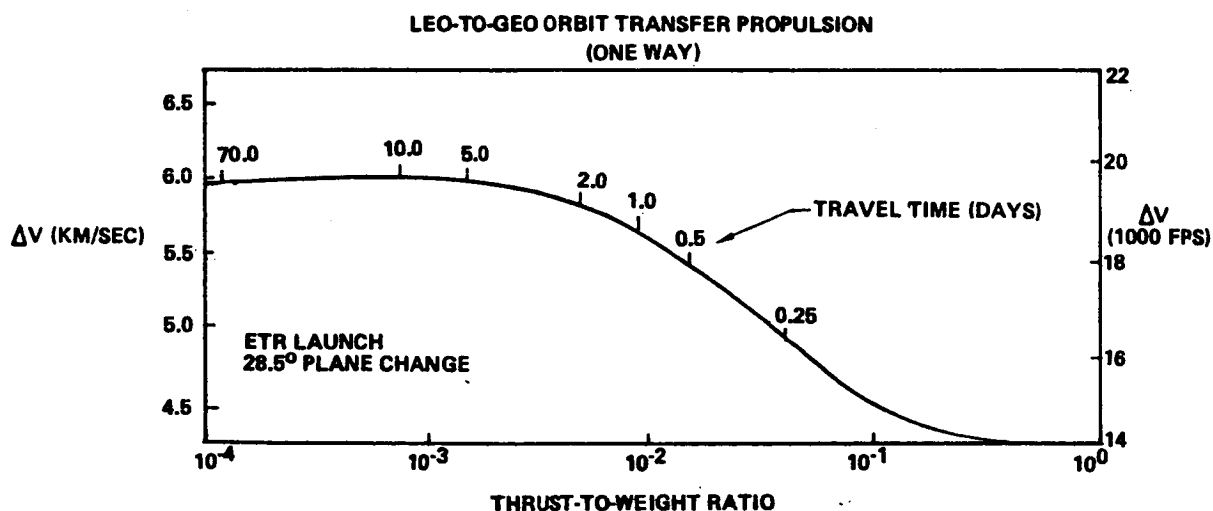


Figure 3.2.3-7: LEO-to-GEO Orbit Transfer Propulsion (One Way)

If trip time is not a constraint, low-thrust vehicles can perform multiple burns at perigee and apogee points and travel from LEO to GEO with little delta-V penalty. The advanced propulsion mission model optimally

requires vehicles to travel from LEO to GEO in 20 to 25 days. Hence laser and solar rocket vehicles with $T/W = 0.001$ will be able to perform multiple burns, while the electrically propelled vehicles with $T/W = 10^{-4}$ to 10^{-5} will perform slow (180 day) continuous burn spirals.

The delta-V requirement for a multiple impulse trajectory depends upon the gravity and steering losses incurred which, in turn, depend upon the variation in the argument of perigee during each burn. The argument of perigee is the angle from the perigee nodal axis to the vehicle location. The larger the argument of perigee at start and stop burn, the greater the delta-V required and the shorter the mission time. These characteristics are shown in Figure 3.2.3-8 which plots LEO-to-GEO transfer delta-V and time versus argument of perigee, θ . As can be seen, significant gravity and steering losses are incurred at the θ 's required to provide 24-day delivery at a T/W of 0.001.

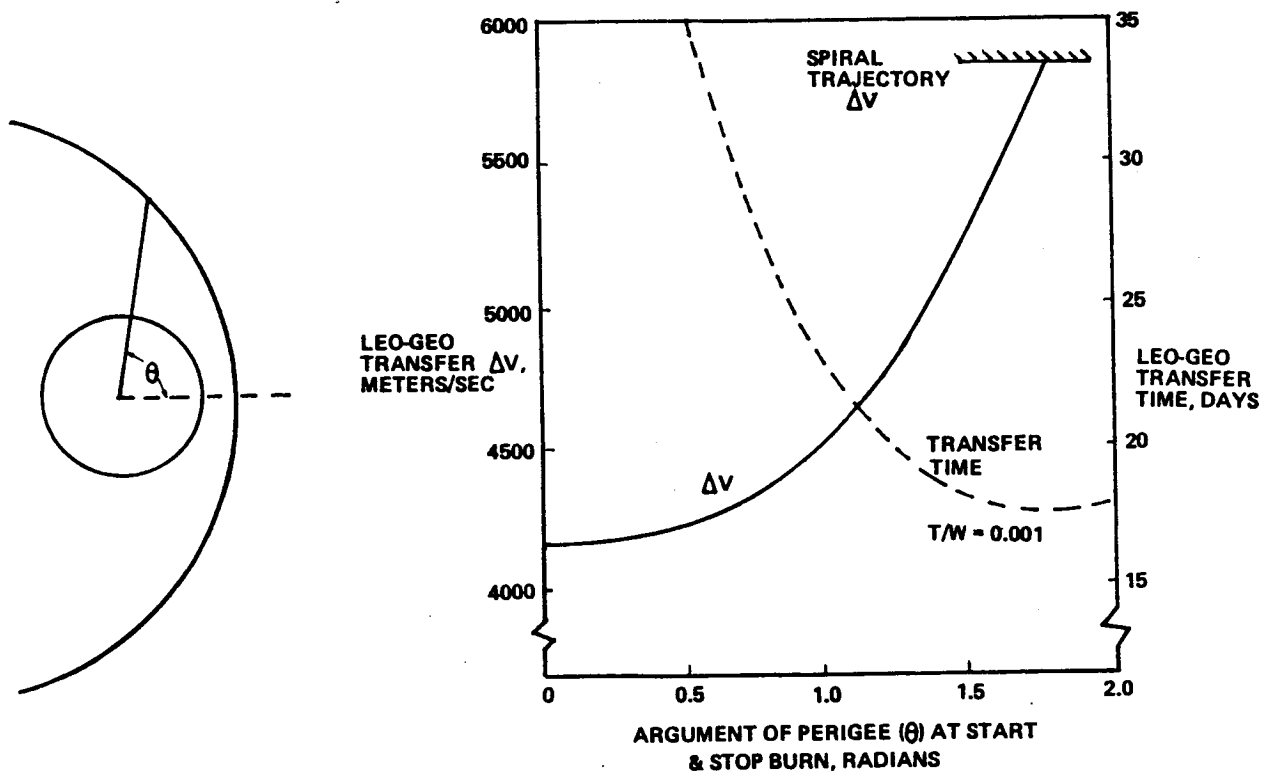
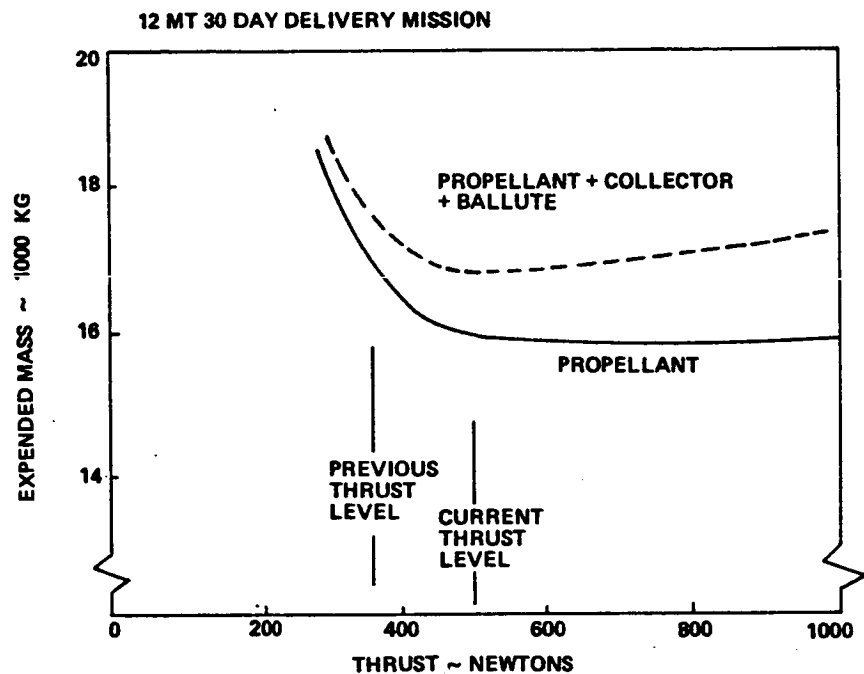


Figure 3.2.3-8: Multiple Impulse Trajectory Characteristics

The initial solar heated rocket had a collector sized to be compatible with the space-based laser which resulted in vehicle T/W of 0.00079. A 24-day transfer at the T/W requires a θ of 1.35 rad (transfer time is inversely proportional to T/W) which results in a delta-V of 5030 m/sec. This delta-V agreed well with data in the previous solar rocket study (Reference 15) and no further trajectory optimization was attempted.

The aerobraked version of the initial solar rocket has a T/W of 0.001, which gave a delta-V of 4460 m/sec and showed marked improvement in performance. This led to the parametric sizing of the aerobraked solar rocket which is summarized in Figure 3.2.3-9. As can be seen from the figure, there



REVISION 3: 3-27-81

Figure 3.2.3-9: Aerobraked Solar Thermal Rocket Sizing

is a definite knee in the propellant consumption curve and the earlier solar rocket configurations had much less than optimal thrust. The optimized aerobraked solar heated rocket has a 70m-diameter collector (inclined at 42 deg) with 500N of thrust at 900 sec of specific impulse ($T/W = 0.0013$). The optimum thrust level was picked to have the minimum expended mass, which is comprised of the vehicle propellant, collector mass, plus ballute and coolant masses. The optimized, aerobraked, solar thermal rocket configuration is shown in Figure 3.2.3-10.

Effect of Increased Operating Temperatures: In a further attempt to assess the potential of solar thermal propulsion, the maximum permissible chamber temperature for long-term operation was increased from 3300 to 4000°K. This is equivalent to switching from the porous-wall engine concept to the rotating-bed concept and results in an increase in specific impulse from 900 to 1100 sec. The 70m-diameter collector which was optimum for the aerobraked

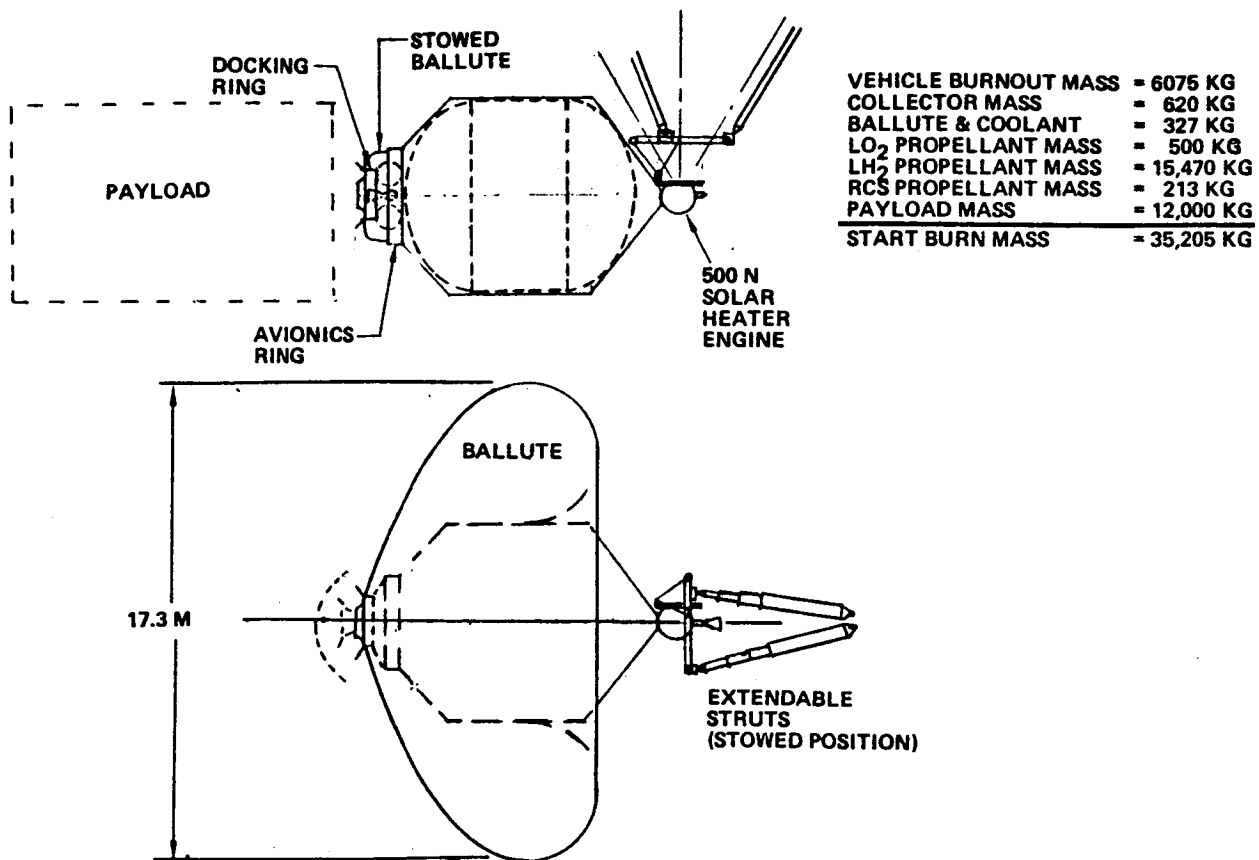


Figure 3.2.3-10: Aerobraked Solar Thermodynamic Rocket Concept

900-sec I_{sp} vehicle now provides only 400N instead of 500N of thrust, but the vehicle $T/W = 0.00134$, which is almost unchanged. This is because the required propellant has decreased from 15,970 kg to 11,655 kg, providing a decrease in burnout mass from 6075 kg to 5380 kg and a decrease in start burn mass from 35,205 kg to 30,305 kg.

Recommendation: The solar thermal rocket in its final configuration appeared to be very competitive with other advanced propulsion concepts and was recommended for systems-level assessment in Task 3.

3.2.4 Electric Propulsion Vehicle Sizing

Electric rockets generally consist of a power source in consort with an electric thruster of some type and its power processing unit, as shown in Figure 3.2.4-1. Contemporary options for electric rockets may be obtained for the matrix of thruster and power source options shown in Figure 3.2.4-2. The approach to evaluation of the various options starts with a well-characterized concept (solar photovoltaic power with argon ion thrusters) and systematically

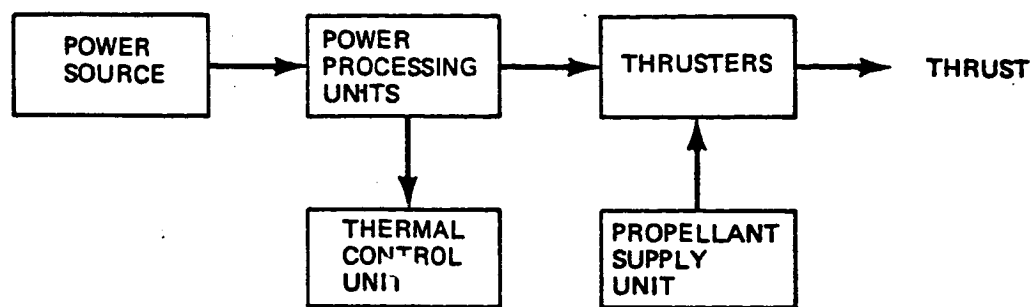


Figure 3.2.4-1: Generalized Electric Propulsion System

THRUSTER	POWER SOURCES									
	SOLAR PHOTOVOLTAIC	ANNEALABLE CELLS	VAPOR DEPOSITED CELLS	NUCLEAR BRAYTON	NUCLEAR THERMIONIC	NUCLEAR THERMOELECTRIC	THERMO PHOTOVOLTAIC	SOLAR THERMOELECTRIC	LASER/ MICROWAVE ELECTRIC	
ION	•	•	•		•		•	•		
MPD					•					
ARC-JET	•									
INDUCTIVE PLASMA										
RESISTOJET										
COLLOID										
RAIL GUN										
MASS DRIVER										

Figure 3.2.4-2: Morphology of Possible Electric Rocket Concepts

evaluates alternative concepts which incorporate either a change of thruster or a change of power source. This procedure establishes the salient features of all possible combinations without actually characterizing each one in detail. Furthermore, this procedure maximizes the applicability of the existing data base for advanced propulsion concepts. Propulsion options to be characterized are:

Solar Photovoltaic Ion Thruster (SPV-Ion): This concept is a second generation of the NASA SEPS-type vehicle which is fully characterizable. All essential technology has been experimentally demonstrated and there is a complete and accurate theory of function relative to experimental behavior

(e.g., a design level of technology has been achieved for ion thrusters, their power processing units (PPU), solar cell arrays, and the required peripheral equipment).

Solar Photovoltaic Arc Jet (SPV-Arc): This evaluation will determine the utility of a low I_{sp} , high-efficiency, high-thrust density arc-jet propulsion concept (in place of ion thrusters) which might result in lower life cycle costs because of reduced solar array, PPU thruster, and transportation costs.

Nuclear Ion Power Source (NPS-Ion): This evaluation will establish the vehicle characteristics of a concept using a nondegradable nuclear electric power source in place of a solar array.

Nuclear MPD (NPS-MPD): This concept will introduce the pulsed magnetoplasmadynamic (MPD) thruster which may have high thrust density, mechanical and electrical simplicity, and which may be uniquely matched to the nuclear power source electrical characteristics.

Thermophotovoltaic Ion (TPV-Ion): Unshielded solar cells may be severely degraded during transits of the proton belt. The TPV-ion concept introduces a power source which allows shielding of the solar cells via high solar concentration.

Solar Thermionic Ion (STI-Ion): This concept uses an inflatable solar concentrator in conjunction with a thermionic or a thermoelectric power converter which rejects heat at high temperature for minimum radiator weight.

The mission by which these low-thrust propulsion concepts will be evaluated is a round trip from a 28.5-deg inclined low Earth orbit to the geosynchronous Earth orbit. Upleg payload is 12,000 kg; downleg payload is zero. This is the generic mission for orbit transfer vehicles. (See the mission capture analysis in Section 2.2.) All low-thrust OTV's will be assumed to operate space based, i.e., servicing and propellant resupply will be at a LEO base.

Electric propulsion rockets comprise a unique class of separately powered space transportation vehicles in that their I_{sp} can generally be specified by the system designer to maximize payload performance or minimize some cost

consideration. Thus, the initial task of characterizing an electric rocket will consist of a parametric synthesis of vehicle characteristics (component and propellant masses, power, levels and number of thrusters) as functions of specific impulse and mission duration. From these data, in conjunction with cost data if desired, the most desirable I_{sp} can be selected.

As an example, the optimum specific impulse as a function of system efficiency and trip time (for an overall specific mass of 20 kg/kW) is shown in Figure 3.2.4-3. The optimization criterion for this example is

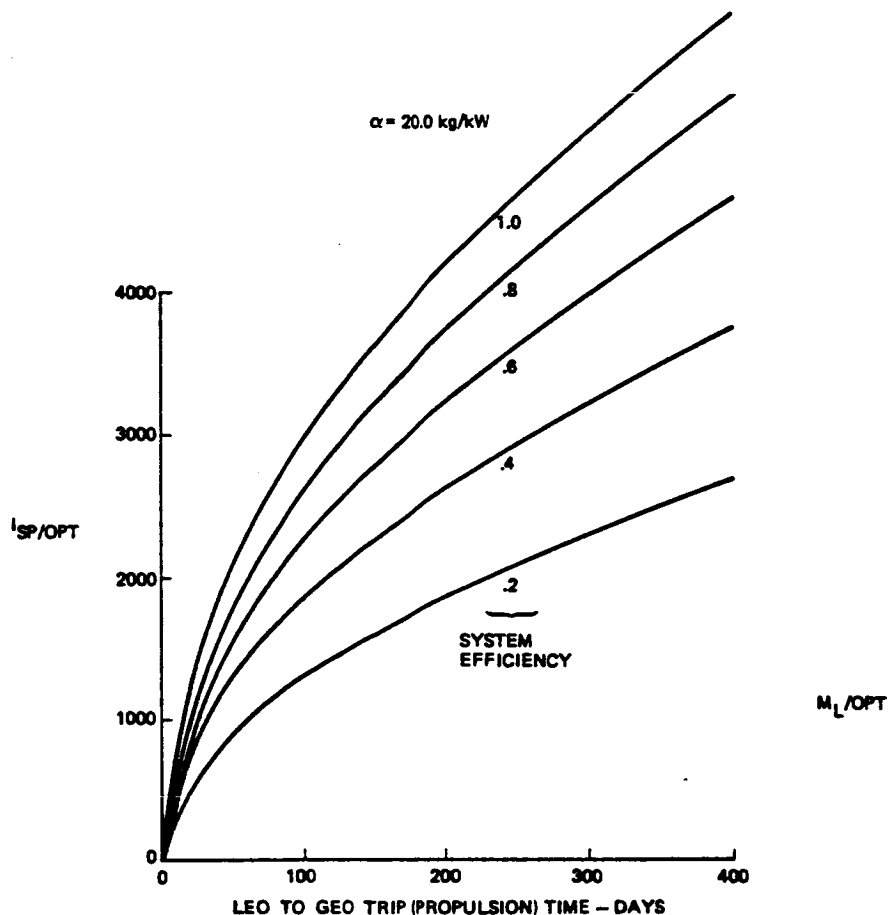
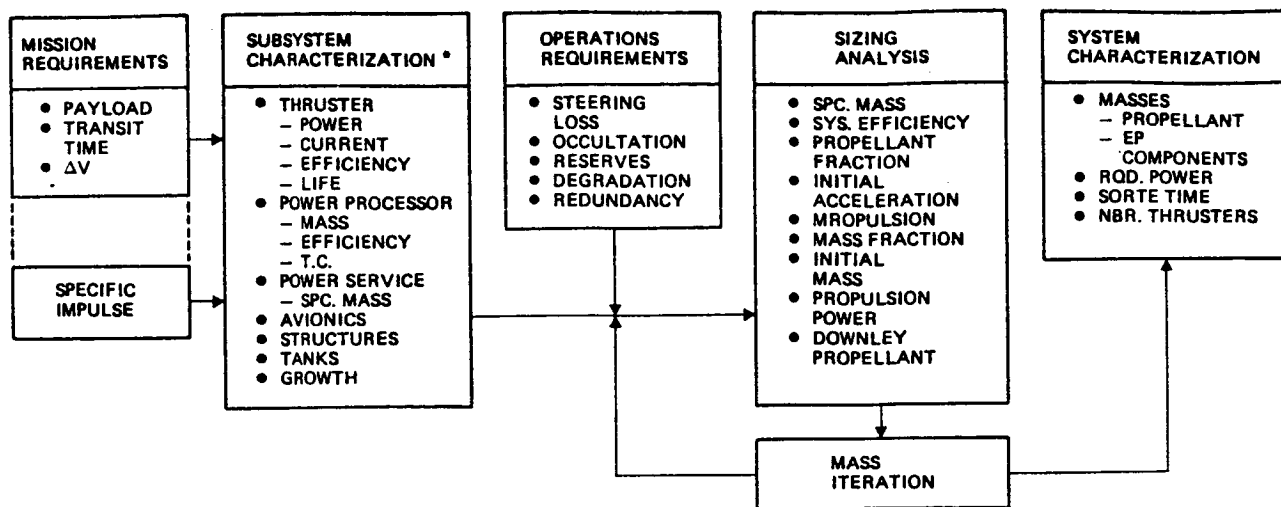


Figure 3.2.4-3: NPS-Ion Optimum Specific Impulse

maximization of the payload fraction (equivalently: minimization of initial mass). Note that low efficiency and/or short propulsion time drive the optimum I_{sp} to low values.

The analytical approach to characterization of electric propulsion OTV's is illustrated in Figure 3.2.4-4. For some assumed mission requirements, the subsystem characteristics (weight, power, efficiency, thrust, life, thermal control, etc.) must be estimated from experimental or theoretical experience.



* THRUSTER AND PPU CHARACTERIZATIONS ARE I_{sp} DEPENDANT

* PULSED SYSTEMS REQUIRE TIME AVERAGED EFFICIENCIES, THRUST, AND SPECIFIC MASS

Figure 3.2.4-4: Electric Propulsion OTV Sizing Procedure

These data should include consideration of mass growth (preliminary design to hardware is 15% for well-characterized technologies) and may reasonably include estimates of technology improvements if a theory which accounts existing experimental technology admits performance extrapolation.

The output of the subsystem characterization is conventionally summarized as overall propulsion system specific mass and efficiency. Subsystems which are not included in this summary (at the discretion of the analyst) can be accounted as part of a pseudopayload. Given overall specific weight and efficiency and estimates of operational penalties, the actual sizing analysis can be made.

A straightforward iteration of the analysis, as suggested in Figure 3.2.4-4, will yield the desired electric propulsion OTV characterization data for the specified mission and I_{sp} requirements. If the propulsion system is designed for steady state operation, the analysis is simple. However, if pulsed electric propulsion systems are being considered, a precursor analysis will be required to obtain time average values for the following:

1. Power source specific mass
2. Power source thermal control system mass
3. Power processing mass
4. Power processing efficiencies
5. Power processing thermal control system mass
6. Thruster efficiency (including mass utilization)

7. Thruster mass
8. Thruster thermal control

Because the power source, power processor, thrusters, and propellant system are dynamically interactive, this precursor analysis may be much more difficult than the vehicle characterization analysis.

Evaluations of the options for advanced propulsion OTV's were based on the following:

1. Published experimental technology demonstration data for key components
2. Theoretical performance prediction methods which correlate experimental data for key components
3. Published analytical data and methodologies for propulsion system characterization
4. Boeing Aerospace Company (BAC) theoretical characterization analyses
5. BAC engineering evaluations of published technology
6. Personal communications with individuals acting in advanced propulsion research

Vehicle concept comparisons included:

1. Assessments of technology status
2. BAC propulsion system characterization data (power requirement, propulsion subsystem mass, propellant mass, trip time effects, and sensitivities to technology uncertainties)
3. STS compatibility
4. Planetary capability
5. Numbers of shuttle derived-(launch) vehicles

Subsequent sections of this document contain detailed propulsion system characterization analyses for each of the vehicle concepts identified above. These analyses will generally be presented with the following syntax:

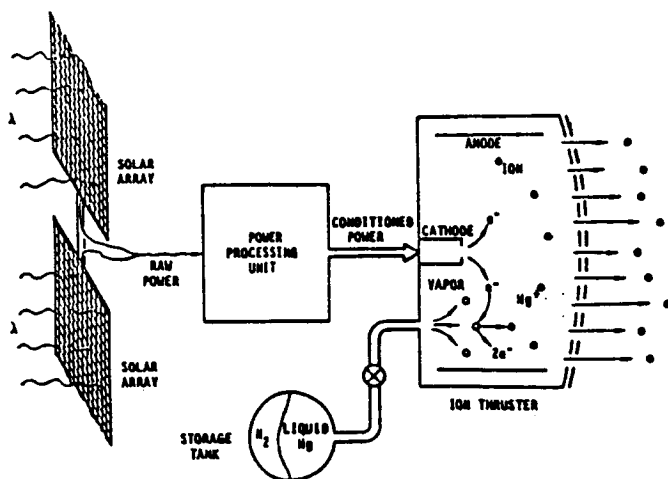
1. Propulsion system description
2. Key features
3. Key assumptions and data sources
4. Functional requirements

5. Key component characterizations
6. Parametric sizing data
7. Recommended characterization
8. Performance and design issues
9. Cost estimates
10. Technology requirements
11. Conclusions
12. Attachments

This narrative of electric propulsion options is concluded with an overview section which contains a variety of comparisons among the propulsion system options.

3.2.4.1 Solar Photovoltaic Ion (SPV-Ion) Rocket

Propulsion System Description: The essential subsystems of this concept are: (1) an array of photovoltaic solar cells sized to provide the required propulsion power, (2) an ion thruster which electrostatically accelerates propellant ions to produce thrust, and (3) a power processing unit (PPU) which converts source power into the power forms required to start and operate the thruster. This source-processor-thruster relationship is generic to electric propulsion and is illustrated in Figure 3.2.4-5.



ADVANTAGES

- FULLY CHARACTERIZED TECHNOLOGY
- HIGH I_{sp} – LOW PROPELLANT REQUIREMENTS

REQUIREMENTS

- MUST ACCEPT OCCULTATION
- MUST ACCEPT SPACE RADIATION

KEY ASSUMPTIONS

- NEW CELL DEGRADATION DATA
- THICK SHIELDING FOR CELLS
- 50-cm ARGON ION THRUSTERS: 20 A.
- END-OF-LIFE SIZING
- PPU SCALED IN MASS AND EFFICIENCY

Figure 3.2.4-5: Solar Electrical Propulsion System Schematic

The contemporary solar electric propulsion (SEP) concept consists of an electron bombardment ion thruster(s) powered by an array of solar cells. Raw solar power must be extensively conditioned (up to 12 power supplies) to operate the thruster. The salient feature of this concept is that the specific impulse can be prescribed by the system designer since it is determined by the design voltage used to accelerate the ions. Hence, the designer can optimize I_{sp} to minimize cost or maximize payload. A single thruster design (the 30-cm mercury thruster) has demonstrated I_{sp} exceeding the range of 1000 sec to 5000 sec.

A typical SEP vehicle consists of a very large solar array which powers a compact propulsion unit (thrusters and PPU's). Figure 3.2.4-6 is an example.

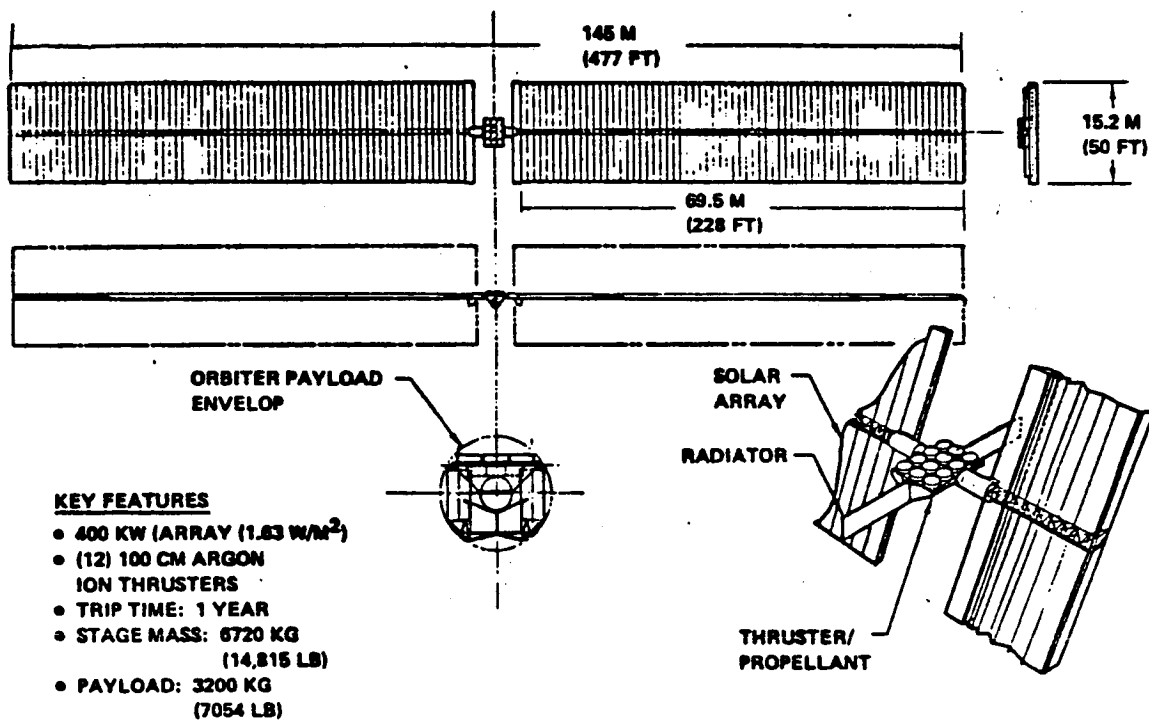


Figure 3.2.4-6: Solar Electric Ion Rocket

High I_{sp} gives high payload performance but acceleration is low (10^{-5} g's) and consequently trip times are long. This vehicle is not suitable for low-altitude (LEO) operation because the mercury thrusters require a 15 to 30 min warmup to vaporize condensed mercury. Thrusters using gaseous propellants (argon, xenon) do not have this problem and more rapid start times will be possible.

The theories of design and performance for each of the main subsystems are mature; i.e., they correlate experimental data and admit straightforward

predictions of performance improvements resulting from design modifications. This situation is called "design level technology," and because of this technological maturity, the SPV-ion concept will be a benchmark for evaluation of all other electric propulsion concepts.

Key Features: The salient feature of the ion propulsion concept is that the specific impulse must be prespecified to optimize some mission parameter such as payload fraction of recurring costs. This is simply accomplished by specifying the acceleration voltage corresponding to the required I_{sp} . (In practice, this is done by designing the PPU to develop the required accelerating voltage.) Since the required propulsion power tends to be a function of the square of I_{sp} , the maximum achievable I_{sp} is almost never selected. Instead, some comparatively low I_{sp} is usually best, generally in the range of 2000 to 6000 sec, depending on the mission, subsystem masses and efficiencies, and the propellant selected.

Key Assumptions:

1. Ion thrusters will have an optical diameter of 50 cm, use argon for propellant, and be rated at 20.0A.
2. The PPU will use combined function power supplies and direct (from the solar array) drive for the screen if system mass is uncompromised.
3. 2.0-mil silicon solar cells at 16% efficiency will be assumed for the baseline solar array. A BAC 0.2-mil vapor-deposited cell was also evaluated.
4. All vehicle sizing analyses will be based on end-of-life (EOL) subsystem performance predictions.

Key Component Characterizations:

Ion Thrusters: Ion thrusters produce thrust by electrostatic acceleration of ions extracted from an electron bombardment ionization chamber. They have been under experimental development for over 20 years; within the last 3, a nearly complete design theory has matured.

The phenomena which characterize an ion thruster are illustrated in Figure 3.2.4-7. The discharge electrons are produced by a hollow cathode.

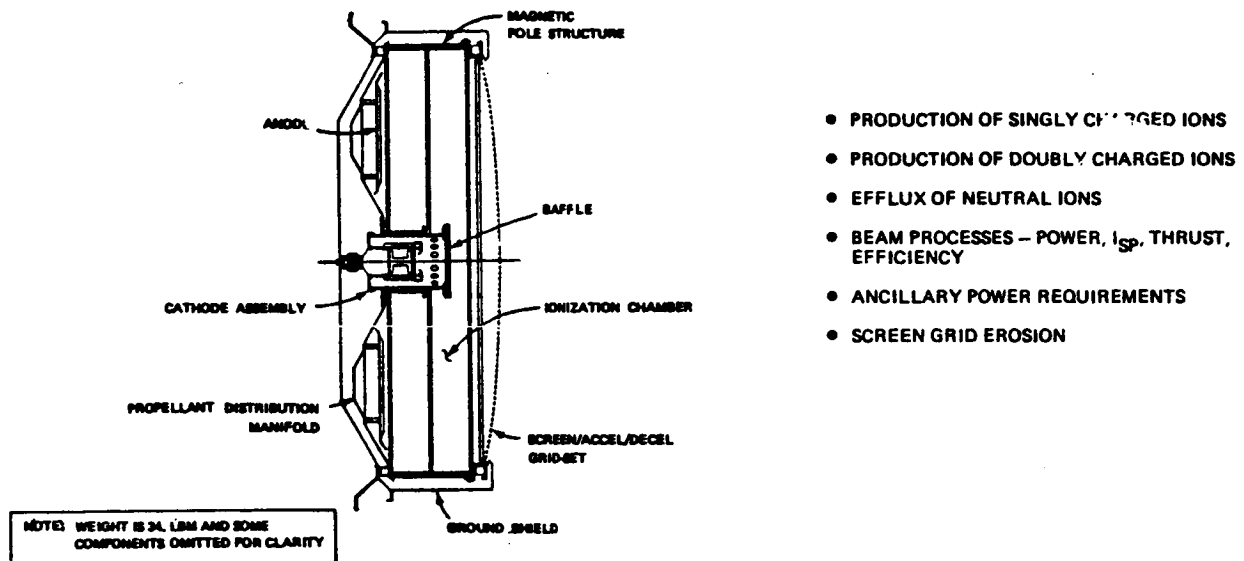


Figure 3.2.4-7: Simulation Requirements

When they enter the ionization (discharge) chamber they produce ions by bombardment of atoms in the dilute propellant gas. Doubly charged ions are also produced. A large fraction of all ions recombine on the chamber walls, causing the major loss of thruster input power. Those ions which enter the holes in the optics (screen grid and accelerator grid) are electrostatically accelerated to produce thrust. Neutral atoms may also pass through these holes but do not produce thrust. Except for a slight divergence, the acceleration of ions is lossless and their velocities are proportional to the square root of the accelerating voltage. Ions which recombine on the screen grid structure have sufficient energy to erode its upstream face. This process generally limits the thruster lifetime.

For the purpose of this study, a characterization of a 50-cm argon ion thruster will be developed to illustrate this maturity of technology and theory. The 50-cm size is arbitrary but has been chosen by the NASA LeRC for technology development by both Hughes Research Labs (HRL) and Xerox Electro-Optical Systems (XEOS). The BAC characterization methodology is independent of the LeRC activity; it applies to any size thruster and was prepared using BAC IR&D program funds.

For thrusters larger than the 30-cm SEPS type (which uses a divergent magnetic field for primary electron confinement), a multipole magnetic con-

tainment field will be required to improve beam uniformity (flatness) and maintain primary electron confinement in the large plasma volume. Both the HRL and XEOS concepts feature multiple magnetic poles. A Boeing multipole concept is shown in Figure 3.2.4-8 (some components have been omitted for clarity). Its design features are:

1. Dished screen and accelerator grids for thermoelastic stability
2. Single cathode - SEPS technology
3. Upstream anode
4. Quick disconnects for easy refurbishment
5. Low-energy recombination surfaces isolated by multiplex magnetic fields (multipoles)

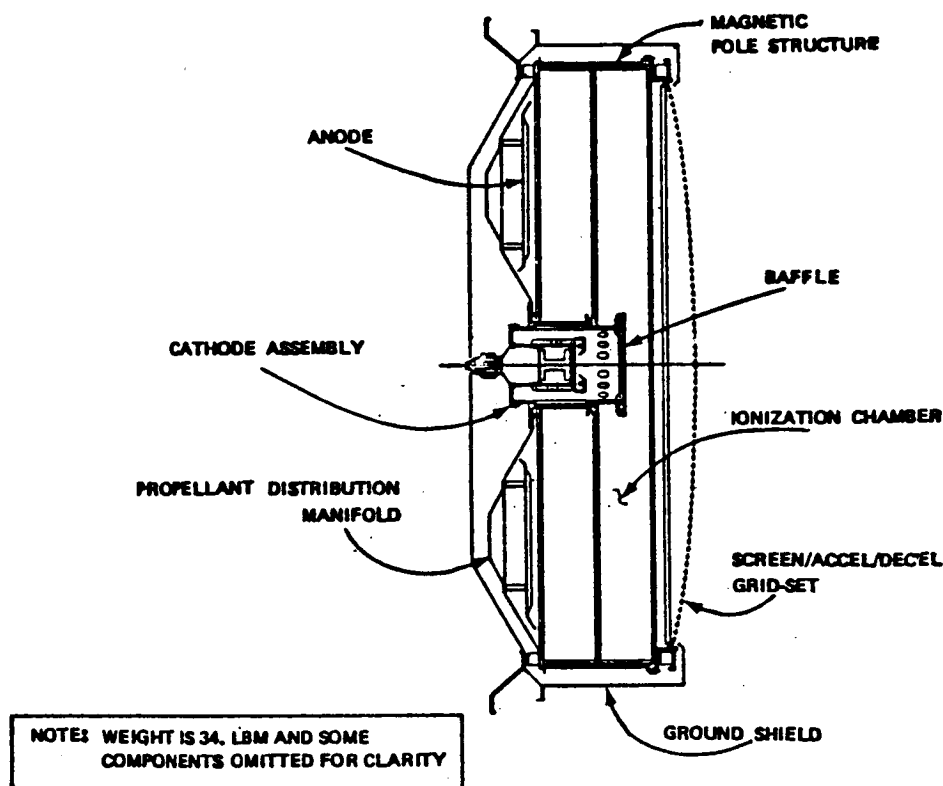


Figure 3.2.4-8: 50-cm Ion Thruster

Thruster characterization requires an analytical description of each of the phenomena which comprise the overall behavior. Collectively, these descriptions (equations) become a mathematical model which can be solved to determine thrust (F), specific impulse (I_{sp}), efficiency (η_t), lifetime (L), and power (P_t). Theoretical models (as opposed to analytical curve-fitting)

are used to enhance the credibility of performance predictions and to illuminate design improvement options and phenomena which might benefit from additional research. This has been accomplished for the following:

1. Production of singly charged ions (discharge process)
2. Production of doubly charged ions
3. Efflux of uncharged propellant atoms
4. Ion extraction including optical transmissivity
5. Ion interception by the screen grid
6. Ion acceleration

Predictions of beam divergence and optical transmissivity depend on empirical data as does the sputtering yield for molybdenum (required for screen grid erosion calculations).

The process of theoretical characterization is shown in Figure 3.2.4-9.

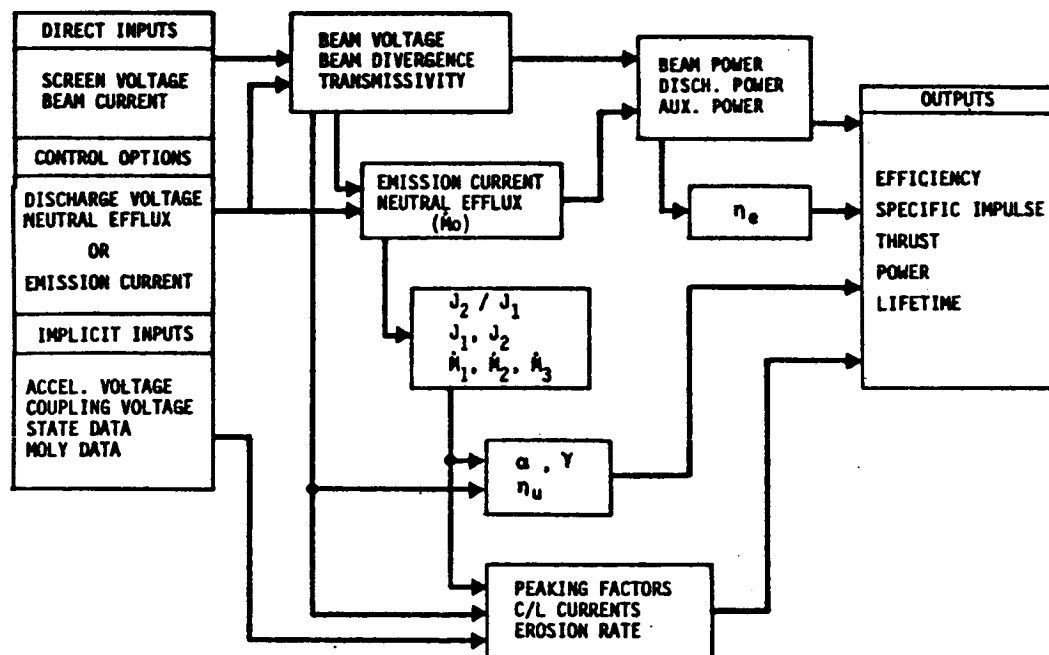


Figure 3.2.4-9: J-Thruster Characterization Program Block Diagram

Its unique features include a first-order theory relating emission current (J_e) with the optical transmissivity (X) of the grids, the discharge voltage (V_d), the neutral mass efflux (M_o), and the beam current (J_b). This relationship is derived in Figure 3.2.4-10. Except for variations in optical transmissivity, the discharge process is independent of ion acceleration, a

ION PRODUCTION: $\dot{N}_I = N_0 * N_p * S_e * \sigma$

BEAM CURRENT: $J_b = \dot{N}_I * V_{01} * X * A_s / A_0 * e$

OPERATING EQUIVALENTS: • $N_p \approx J_e$
• $S_e * \sigma \approx V_i$
• $N_0 \approx \dot{M}_0$

DISCHARGE LAW: • $J_e = (C_1 * (1/X) * (1/V_i) * (1/\dot{M}_0) * J_b$

Figure 3.2.4-10: First Order Discharge Model

circumstance which admits a single characterization model. A derivation of the basic ion thruster efficiency model is included as Appendix C.

Recent research at HRL has resulted in the transmissivity data shown in Figure 3.2.4-11. Since transmissivity theory does not match the experimental data, an empirical correlation (shown) is used. Although the characterization

SEMI-LOG CORRELATION OF EXPERIMENTAL TRANSMISSIVITY

$$X = 0.930 - J_y * (-0.01725 + 100.3/V_s)$$

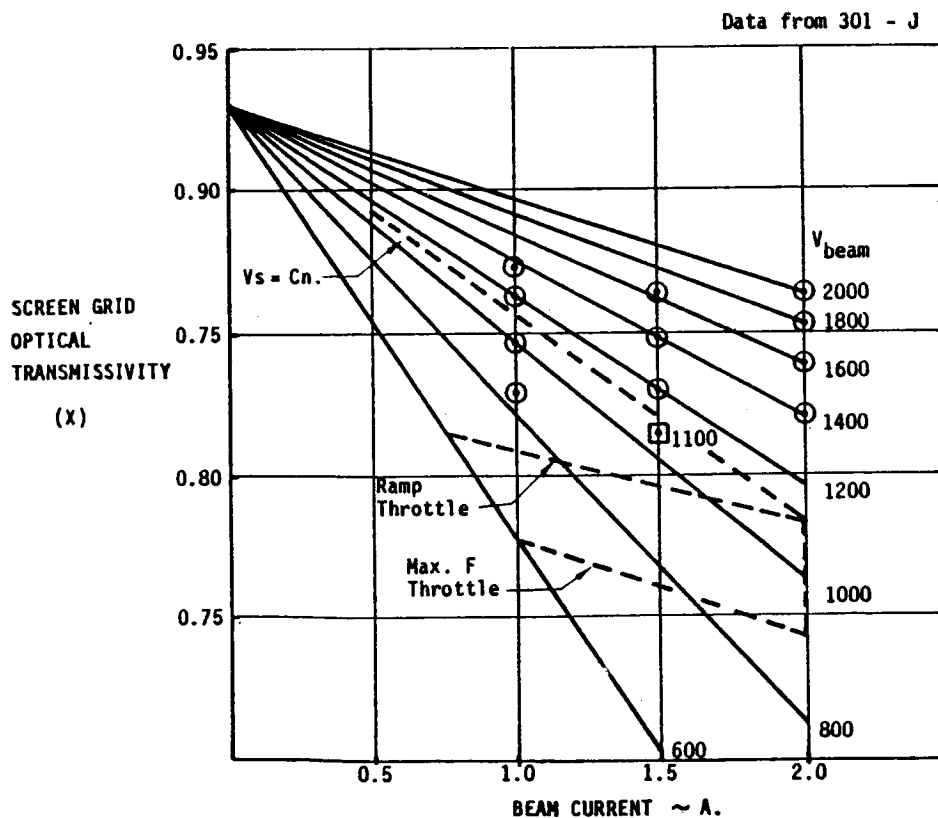


Figure 3.2.4-11: Correlation of J-Thruster Optical Transmissivity Data

model was developed for the NASA SEPS thruster (HRL 30-cm J-type), it can be used for any size thruster provided a reference discharge voltage, discharge current, and double-ion production can be established. There are a variety of approaches to this, including:

1. Scaling from test data from well-developed small thrusters (AIAA 81-0919)
2. Summing energy losses from the plasma balance of energy (BOE) analysis gives only the discharge current for some presumed discharge voltage)
3. Bulk average plasma analysis (a BAC methodology for predicting plasma properties, neutral efflux, and double-ion production (AIAA 78-695))
4. Detailed plasma property prediction (a complex attempt to predict spatially dependent plasma properties for divergent field thrusters developed at Colorado State)

The BAC approach is to use the first three options. For the BAC 50-cm multipole thruster they give the following is given:

Discharge voltage: 37.0V
Discharge current: 67.5A
Neutral efflux: 1.7135A eq.
Transmissivity: 0.706
Double ion fraction: 0.0624 (J2/J1 avg)
Peaking factors: 1/0.8
Beam divergence factor: 0.98

These data satisfy a specification for a screen voltage of 1000V, a beam current of 12A, and an optics design similar to the NASA SEPS thruster.

The first step in thruster characterization is to establish a reasonable discharge control option. This is done by calculating thruster efficiency as a function of neutral efflux (proportional to ionization chamber pressure). These data are shown in Figure 3.2.4-12 and illustrate discharge optimization via trading utilization efficiency against electrical efficiency. The dashed line is the optimum control path but control by constant neutral efflux is simpler and practically as efficient. It is used for subsequent data.

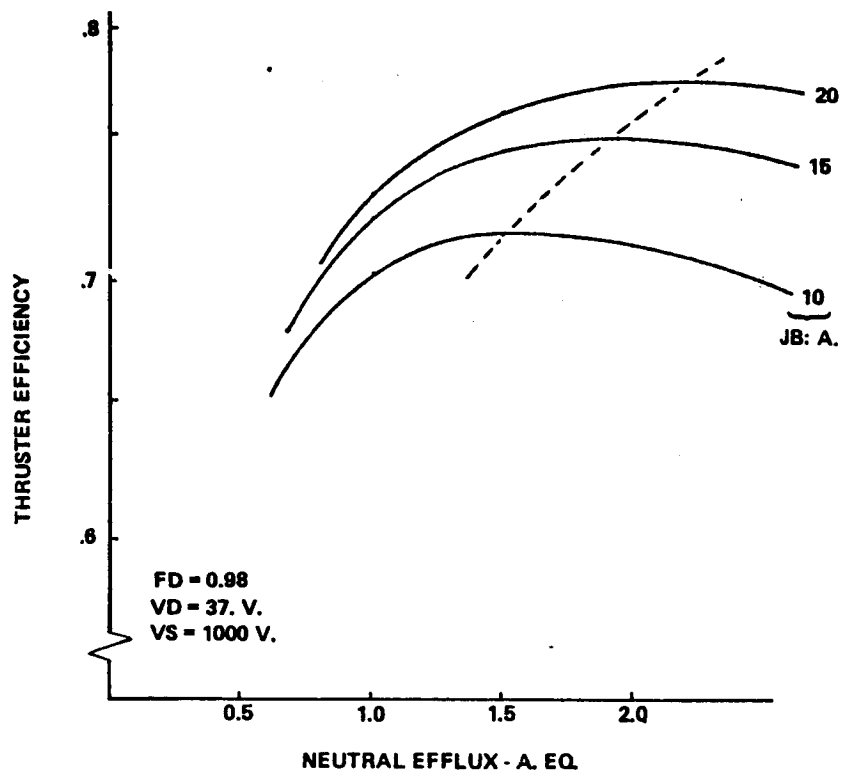


Figure 3.2.4-12: Discharge Control Optimization—50-cm Argon Ion Thruster

Because changing the screen voltage (to change I_{sp}) changes the electrical efficiency, the optimum neutral efflux should also change, as shown in Figure 3.2.4-13. This is not a straightforward option; reducing neutral

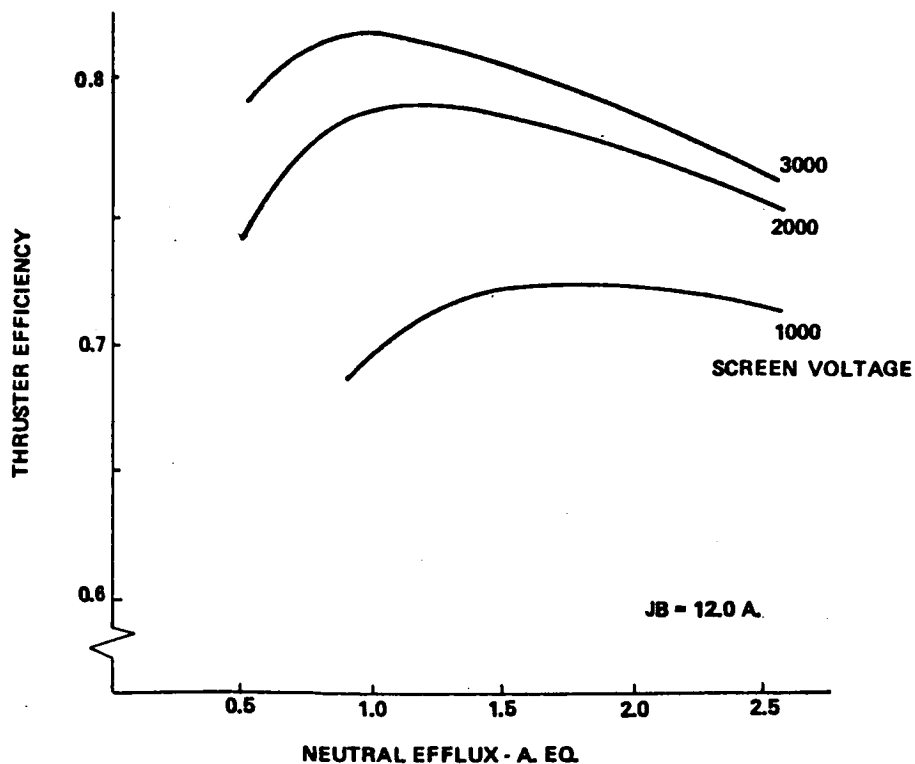


Figure 3.2.4-13: Discharge Optimization, 50-cm Argon Ion Thruster

efflux tends to shorten thruster lifetime as indicated in Figure 3.2.4-14.

Having picked a control scheme, a thruster operating map can be determined as shown in Figure 3.2.4-15. Operation below about 1000V will require

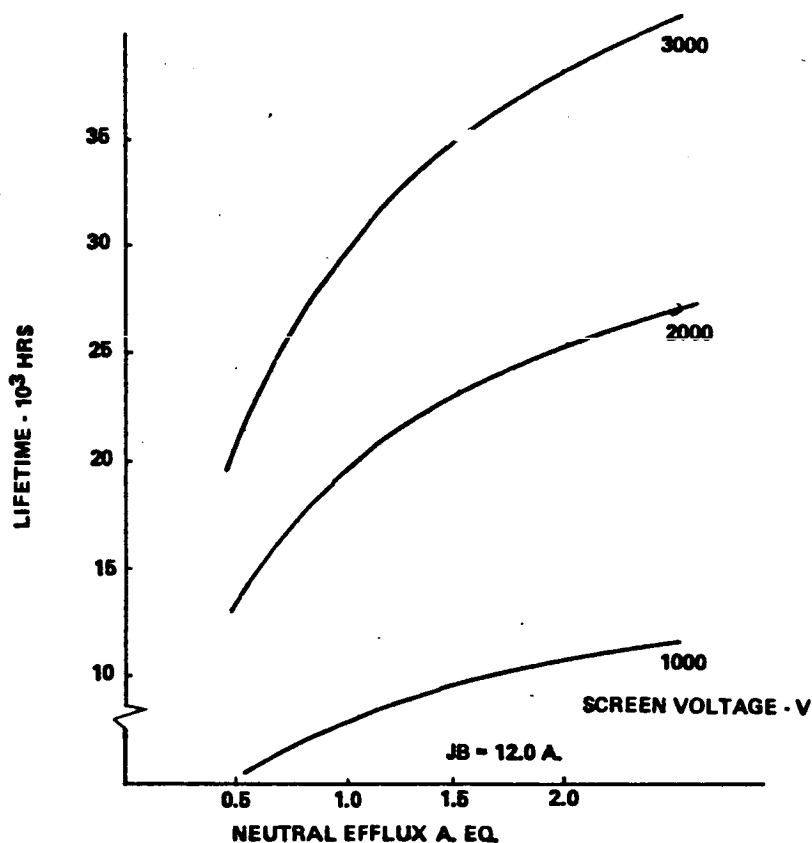


Figure 3.2.4-14: Life Trends for a 50-cm Argon Thruster

triple-grid optics. These data illustrate that a given size ion thruster can operate over a wide range of power and I_{sp} .

Note the above data are based on J-type thruster optics which are non-optimum for argon. Optimized optics for argon should have an increased grid gap (reducing beam divergence and neutral efflux), reduced-size accelerator grid holes (increasing transmissivity and also reducing neutral efflux), or some best combination of these. The operating map data also include efficiency and thrust, shown separately in Figure 3.2.4-16 for clarity.

Because the optical transmissivity is a function of beam current (J_b) and screen voltage (V_s), the interception of ions by the screen grid is also dependent on J_b and V_s , which implies a similar dependence for thruster lifetime. Based on this phenomena, predictions of life trends are shown in Figure 3.2.4-17. These data show that the electric propulsion system designer must consider beam current limitations which are dependent on specific impulse as well as mission duration.

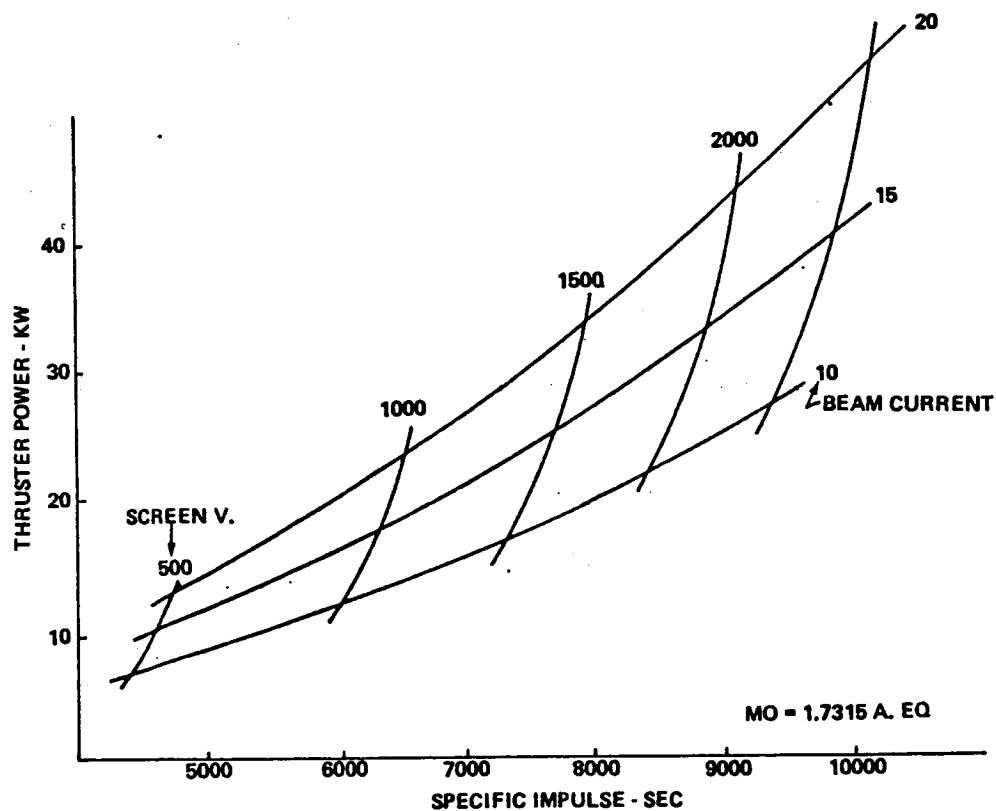


Figure 3.2.4-15: 50-cm Argon Ion Thruster Power Requirement

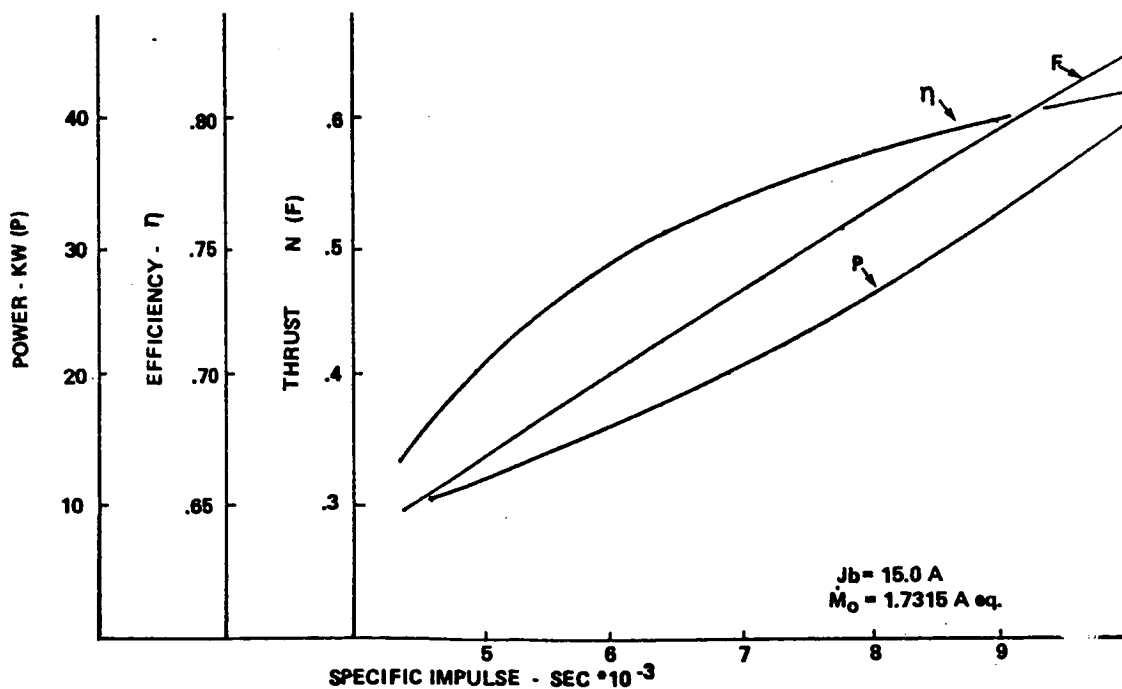


Figure 3.2.4-16: 50-cm Argon Ion Thruster Performance Characteristics

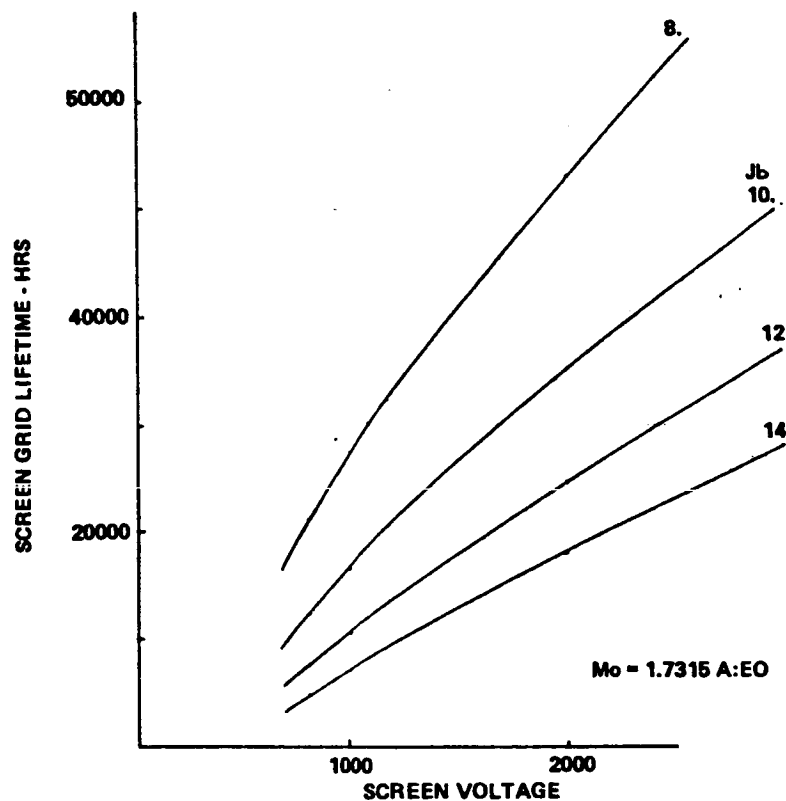


Figure 3.2.4-17: 50-cm Argon Ion Thruster Life Trends

Recommendation: These general data were used in vehicle sizing studies. A thruster beam current of 20.0A was assumed in anticipation of foreseeable technology advances for the 50-cm thruster.

Ion Thruster Power Processing Unit: Contemporary (SEPS technology) power processing units for the 30-cm J-type thruster weigh 70 to 80 lb for a 3-kW, 1100V rating. These PPU's have 10 to 12 separate power supplies (each thruster requirement treated independently), a microprocessor for T/W and control, and input filters and isolation switches for electromagnetic compatibility (EMC). They are intended for scientific payloads sensitive to electromagnetic interference (EMI) and are designed to control I_{sp} in interplanetary space with a naturally varying solar array voltage (100V to 200V). (Actually, controlled I_{sp} is mainly a convenience of the interplanetary mission designer--there is no essential requirement for it.) For Earth orbital missions, there is no requirement whatever for voltage (I_{sp}) regulation, and payloads for mass transit are comparatively insensitive to EMI; therefore, the PPU can be much simpler. Furthermore, combined function



- Figure 3.2.4-18: Power Processing Requirements for 50-cm Argon Thruster**

90

efficiency as functions of I_{sp} and beam current (propellant flow rate). The model developed for this study is based on contemporary power supply and component technology, including the reduced PPU requirements as described above. Figure 3.2.4-19 shows how PPU specific mass and efficiency can be expected to vary with specific impulse for a beam current of 20A.

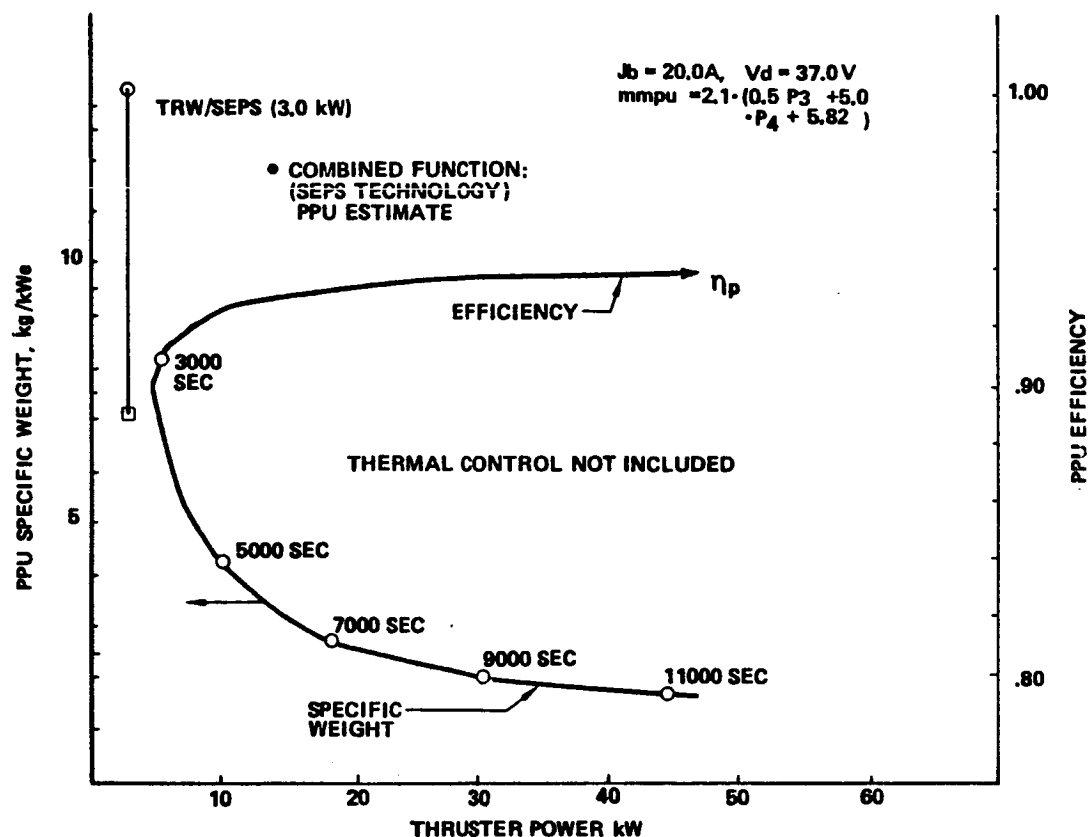


Figure 3.2.4-19: CDVM PPU for 50-cm Argon Ion Thruster

Solar Photovoltaic (SPV) Power Sources: Electrical power is produced by illumination of photovoltaic cells. Power conversion efficiency for solar illumination is low (~16% at 1.0 AU), but the cells can be made thin and lightweight and arrays of them can be made with a lower beginning of life (BOL) specific mass at 1.0 AU than any other demonstrated power conversion technology. (Microwave-electric and laser-electric power transmission schemes may be feasible and lighter than SPV conversion, but these will require multiple transmitter and/or relay stations for effective illumination of the OTV.) Contemporary technology is represented by NASA-inspired flexible solar array blanket designs for their SEPS stage. This design produces 32 kW from 180 m² and will weigh 420 kg (data are approximate) giving a specific mass of 13 kg/kW if all power is used for propulsion. The SEPS technology uses cells

of 8-mil thickness; because cells as thin as 2 mils are being made, significant mass reductions are possible. The technology adopted for this study reflects this general approach to reducing specific mass. The technology for SPV-ion vehicles will baseline the 2-mil cell and the specific mass for these solar arrays (including support structures) will be as shown in Figure 3.2.4-20. These data are based on the BOL power rating. This power

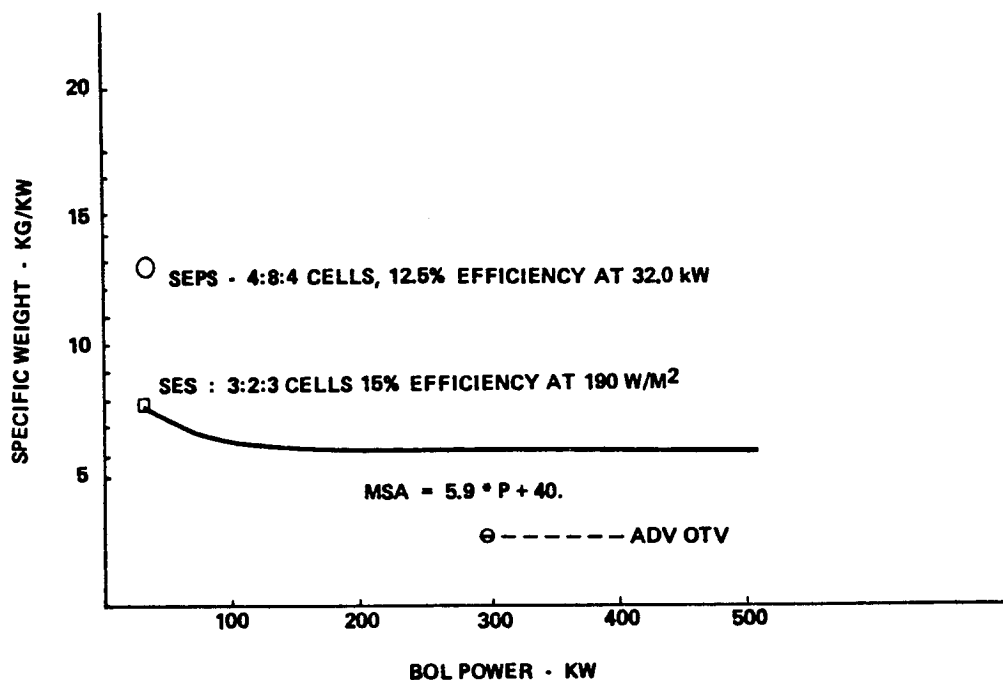


Figure 3.2.4-20: Solar Array Specific Mass

will be degraded during transit of Earth's radiation belts, as shown in Figure 3.2.4-21 for a 3-mil coverslip, 2-mil cell, 2-mil substrate (3-2-2) blanket. Note that a single transit degrades power about 60% and that 10 transits, as assumed for OTV lifetime, leaves only about 20% of the BOL power. Because degradation tends to be logarithmic, i.e., most of it occurs during the first few transits, subsequent vehicle sizing analyses will be based on end of life (EOL) power ratings to avoid payload manifesting issues. The actual data used for silicon cell degradation are presented in Figure 3.2.4-22, which also includes a 12-2-10 blanket. Although this blanket is somewhat heavier (EOL) than the 3-2-2 blanket, the degradation is less and the required BOL power rating will be lower. This suggests lower costs may result from increased shielding. Evidently an optimum shielding design exists and should be established as soon as space test degradation data are available.

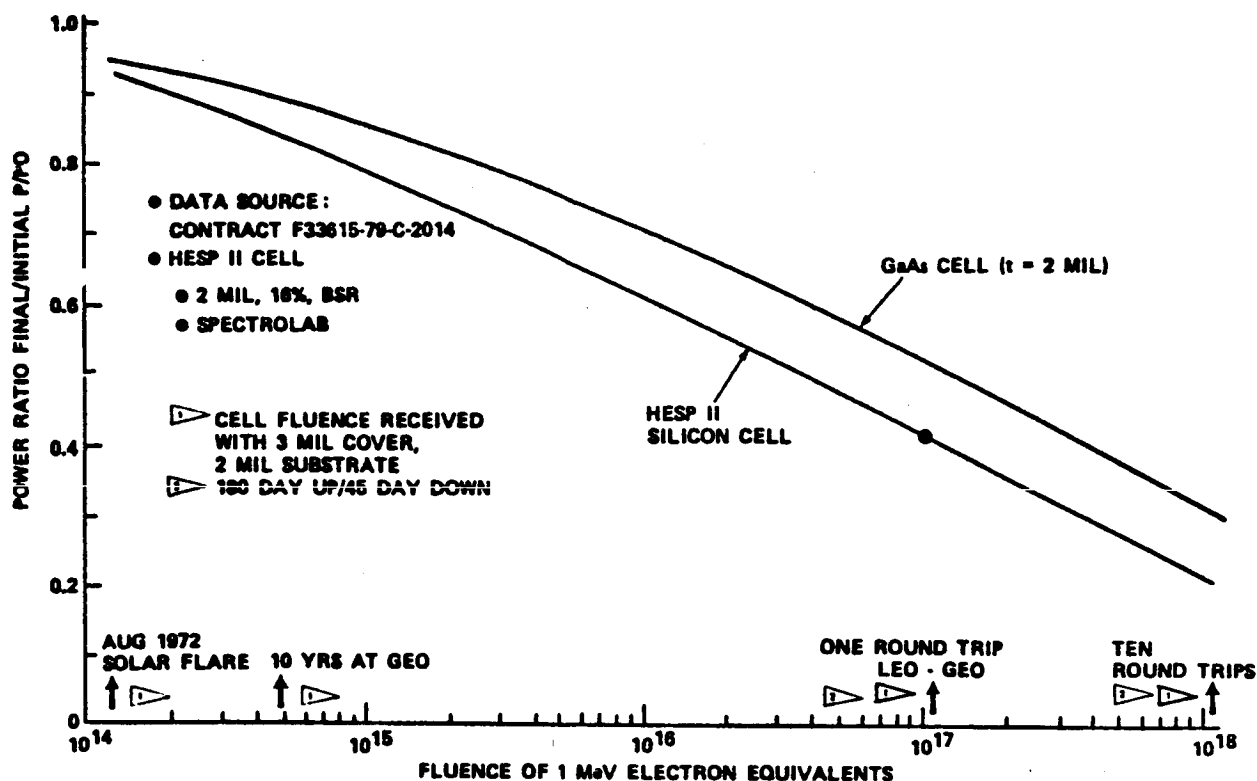


Figure 3.2.4-21: EOTV Design Driver - Van Allen Radiation Impact

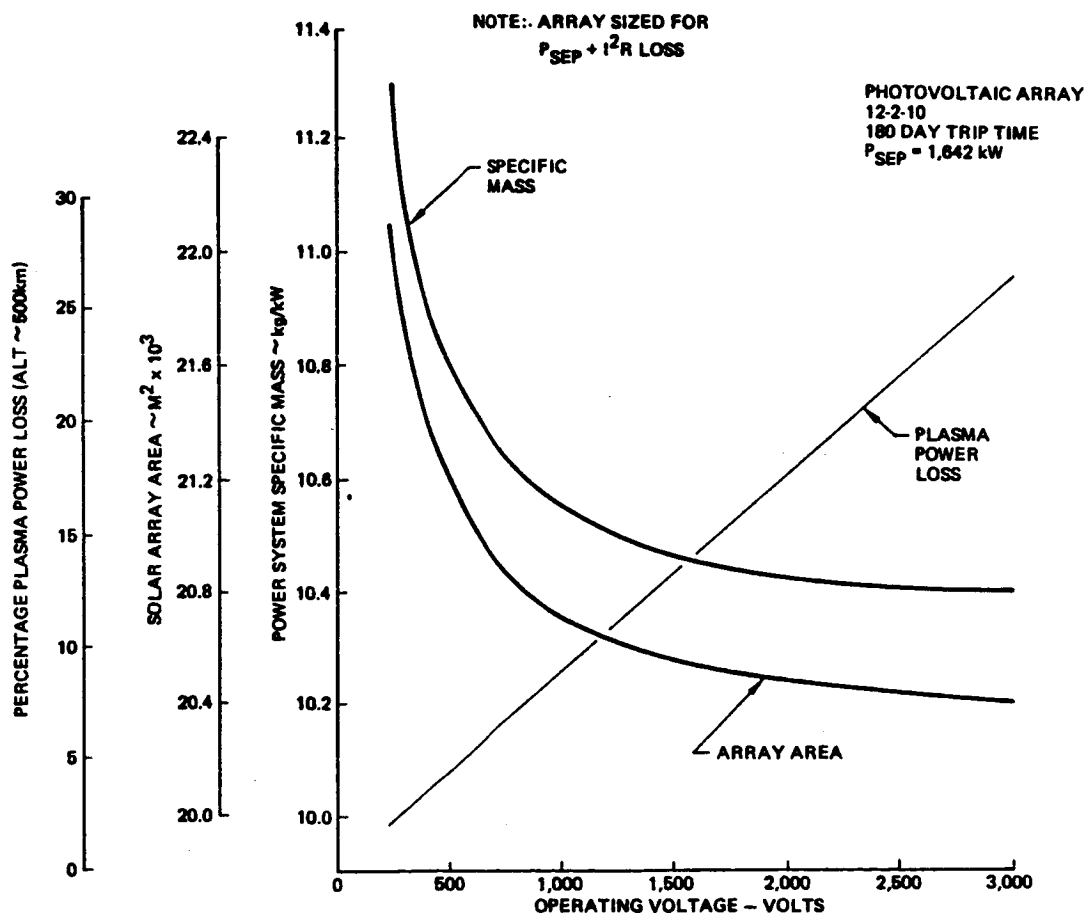


Figure 3.2.4-22: Effect of Thruster Voltage on SPV-Ion Powerplant Characteristics

Parametric Characterization: Parametric sizing data for a 12t payload are shown in Figure 3.2.4-23. These data are for the 12-2-10 blanket design (data for the 3-2-2 blanket are not substantively different). They indicate severe mass penalties for upleg transits of less than 180 days and that the concept is relatively insensitive to I_{sp} variations in the range of 4000 to

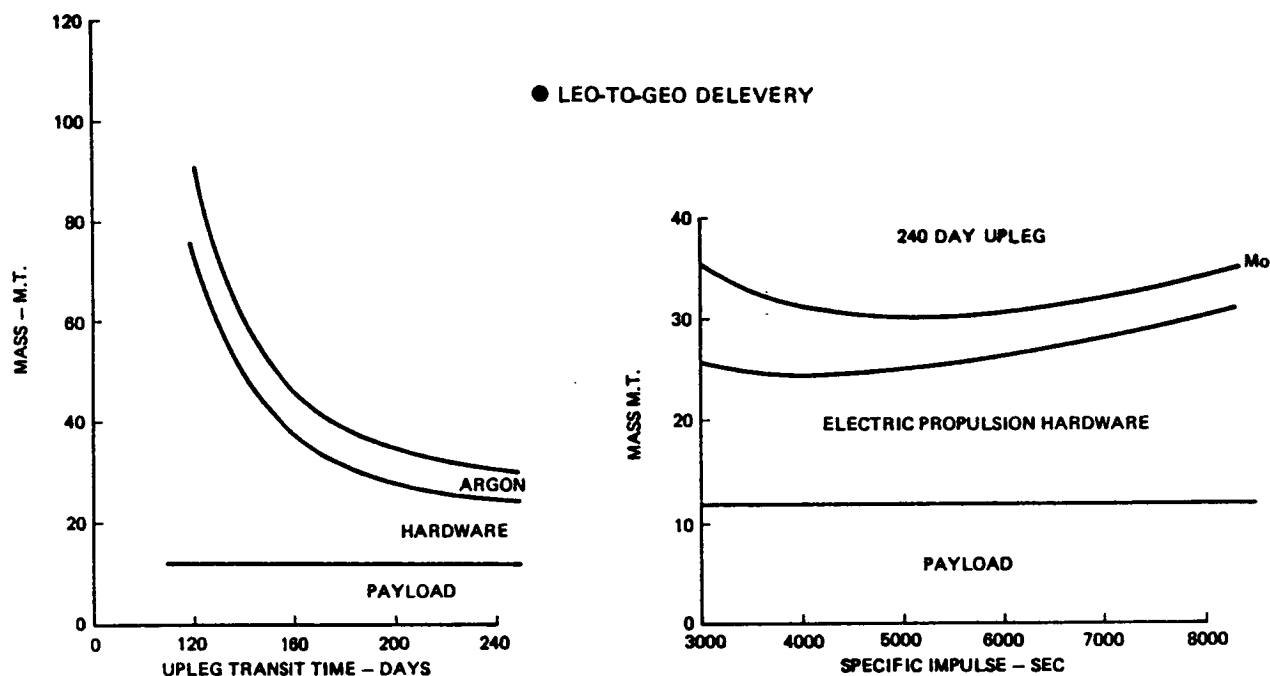


Figure 3.2.4-23: SPV-Ion Parametric Characterization

6000 sec. Note that hardware mass increases below 4000 sec, which indicates that the low efficiency of argon ion thrusters (below 4000 sec) is penalizing the propulsion system. Evidently a propellant with higher molecular weight, for better efficiency at low I_{sp} , would benefit this concept. Figure 3.2.4-24 shows how the BOL power requirement, an indication of hardware costs, varies with transit time and I_{sp} .

One option for reducing the cost of the SPV-ion concept is to use very low-cost solar cells such as those being developed for ground applications. A typical BAC vapor-deposited cell concept is potentially capable of producing complete cell blankets (containing thousands of cells) in one sequence of manufacture. Although efficiency is low (~ 10%), the cells are only about 5 m (0.2 mil) in thickness, giving about the same BOL specific mass as high efficiency blankets of silicon cells. The radiation sensitivity of vapor-deposited polycrystalline cells has not been determined, but preliminary testing indicates degradation might be less than with conventional cells.

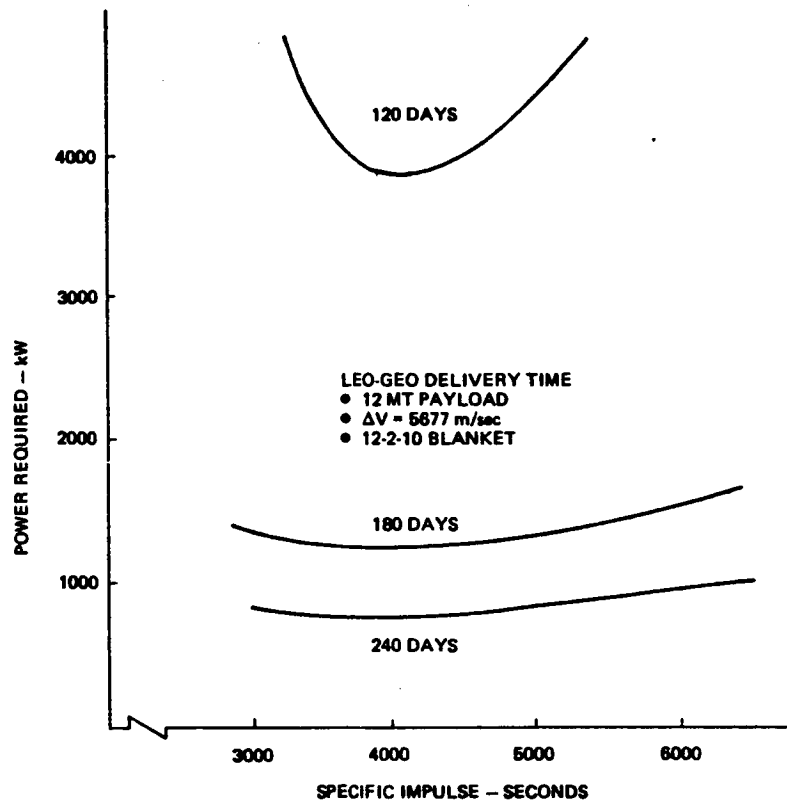


Figure 3.2.4-24: Effect of Specific Impulse and Delivery Time on Solar Array Sizing

Therefore, the sizing analysis for this concept has been done parametrically as indicated in Figure 3.2.4-25. These data generally show that degradation is not critically important below about 40%; above 40%, the degradation must be accurately known to credibly characterize this concept. These data trends also apply to annealable-cell (Si or GaAs) concepts.

Based on the results of Reference 1, the most significant performance improvement for SPV-ion OTV's was related to reducing solar cell radiation degradation effects. In particular, various methods of annealing silicon and GaAs solar cells were examined with the following results:

1. The annealing of GaAs relative to silicon cells was judged to be less effective due to the cell being more complex in its physical makeup.
2. Continuous annealing to minimize proton damage in GaAs is thought to be possible if the array can be run at 125°C . This can be achieved with a concentration ratio (CR) equal to 2. Based on an extremely limited amount of data, it appears less degradation would occur with this method than

for periodic annealing after each trip. In the extreme case, a continuously annealed GaAs array might incur only 1% of the damage normally received in a round trip between LEO and GEO.

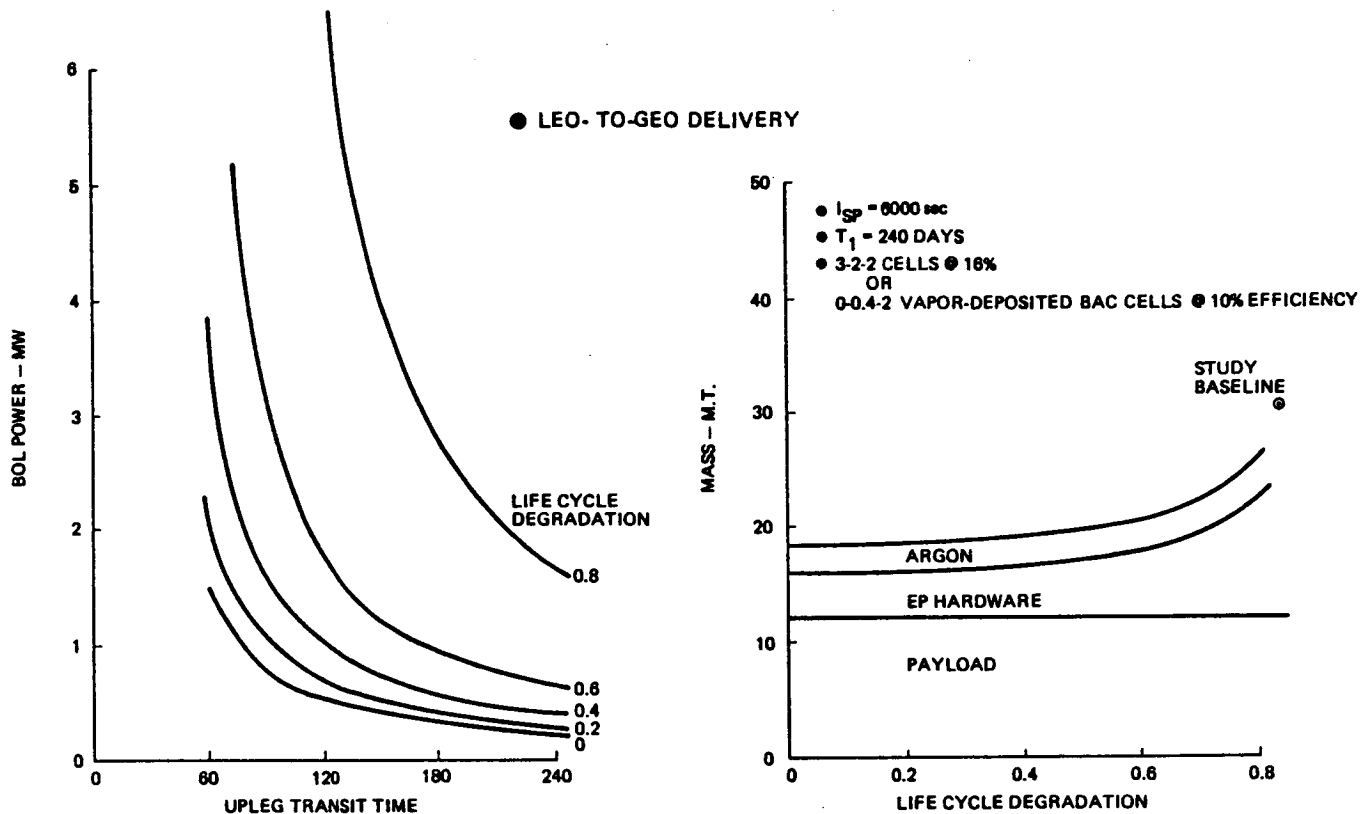


Figure 3.2.4-25: Limit SPV-Ion Performance

Vehicle Characterization: Two SPS-ion vehicles were characterized in Task 2. The first was characterized using technology estimated in Reference 2 to be available by 1995 through a normal growth process. This vehicle had an array consisting of silicon solar cells in a 12-2-10 blanket configuration, with a CR of 1 and no annealing assumed. The second was characterized using technology estimated to be available in 1995 if the normal growth process was accelerated through extra funding of GaAs solar arrays, self-annealing, and direct drive power processors. The effect of accelerating SPV technology is shown in Figure 3.2.4-26. The 4 to 1 reduction in required power (the major driver in system cost) makes accelerated technology appear very attractive; and indeed a direct comparison of these vehicles in Reference 2 showed accelerated technology to be cost effective, consequently it was chosen as the SPV-ion vehicle for system-level assessment in Task 3.

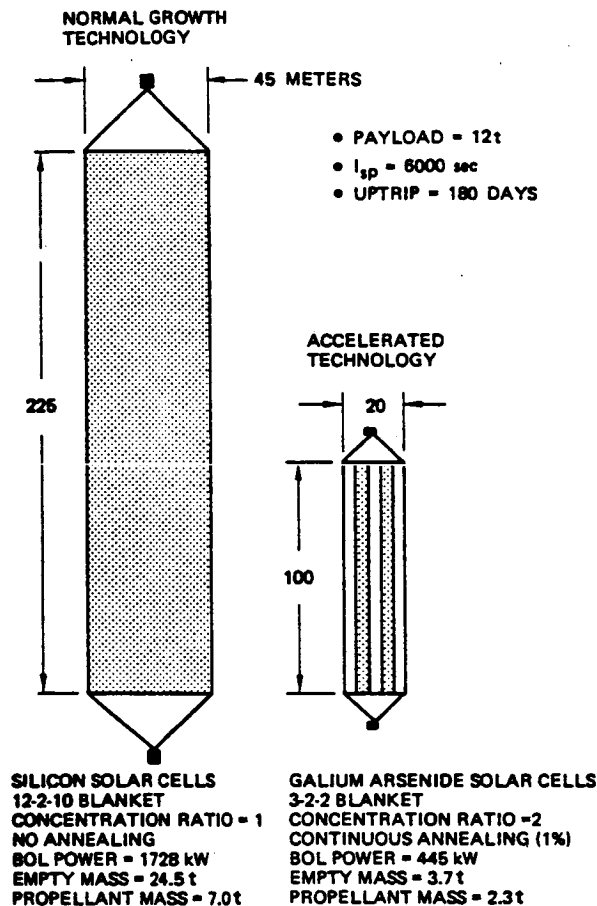


Figure 3.2.4-26: Effect of Accelerated Technology of SPV-Ion Vehicle Configurations

Performance and Design Issues: The only technology issue associated with this concept is the radiation degradation for which the solar array must be sized, including the effectiveness of repeated annealing cycles (if any) or of hardened-cell technology. The radiation issue will also pertain to many potential payloads which may require increased shielding for avionics.

Since long transit times are clearly an operational requirement for this concept, potential users must be prepared to accommodate lost payload revenues (if any), increased avionic packaging masses (for shielding), and any effects on service life due to lengthy LEO-to-GEO transits.

Technology Requirements: All essential technology requirements have been demonstrated, making the recommended SPV-ion concept a low technical risk. A substantial payoff may be obtained, however, via annealable, hardened-cell or thin-film cell technology, or some combination of these. Continued development of the 50-cm thruster and its PPU is desirable to minimize the effects of any requirement for life cycle testing.

3.2.4.2 Solar Photovoltaic Arc-Jet (SPV-Arc)

Propulsion System Description: The SPV-arc concept uses a solar cell array (Section 3.2.4.1) in conjunction with a low I_{sp} , high-efficiency hydrogen arc-jet thruster, and its associated PPU.

Key Features: This thruster/PPU combination is expected to be capable of 90% efficiency at an I_{sp} of 900 sec, thereby (possibly) allowing short transit times or reduced power requirements. In addition, the thruster/PPU combination is capable of high power density and, consequently, low specific mass.

Key Assumptions: The key assumptions used for this evaluation are the thruster I_{sp} and efficiency (900 sec and 90%). Although these are believed to be reasonably achievable for this thruster concept, they are undemonstrated and experimental verification will be required if the SPV-arc vehicle concept has merit.

Functional Requirements: The propulsion system must accept the thermal transients associated with solar occultation, and hydrogen must be the propellant.

Key Component Characterization: The key component for this vehicle concept is the arc-jet thruster illustrated in Figure 3.2.4-27. This thruster heats hydrogen with an electric arc and expands the hydrogen in a conventional nozzle to produce thrust. An essential feature is the mixing chamber between the arc chamber and the nozzle. This chamber must be long enough to allow relaxation of dissociated and ionized propellant constituents so that frozen expansion losses are minimized. The structure is insulated to minimize heat losses. The maximum achievable structural temperature will determine specific impulse.

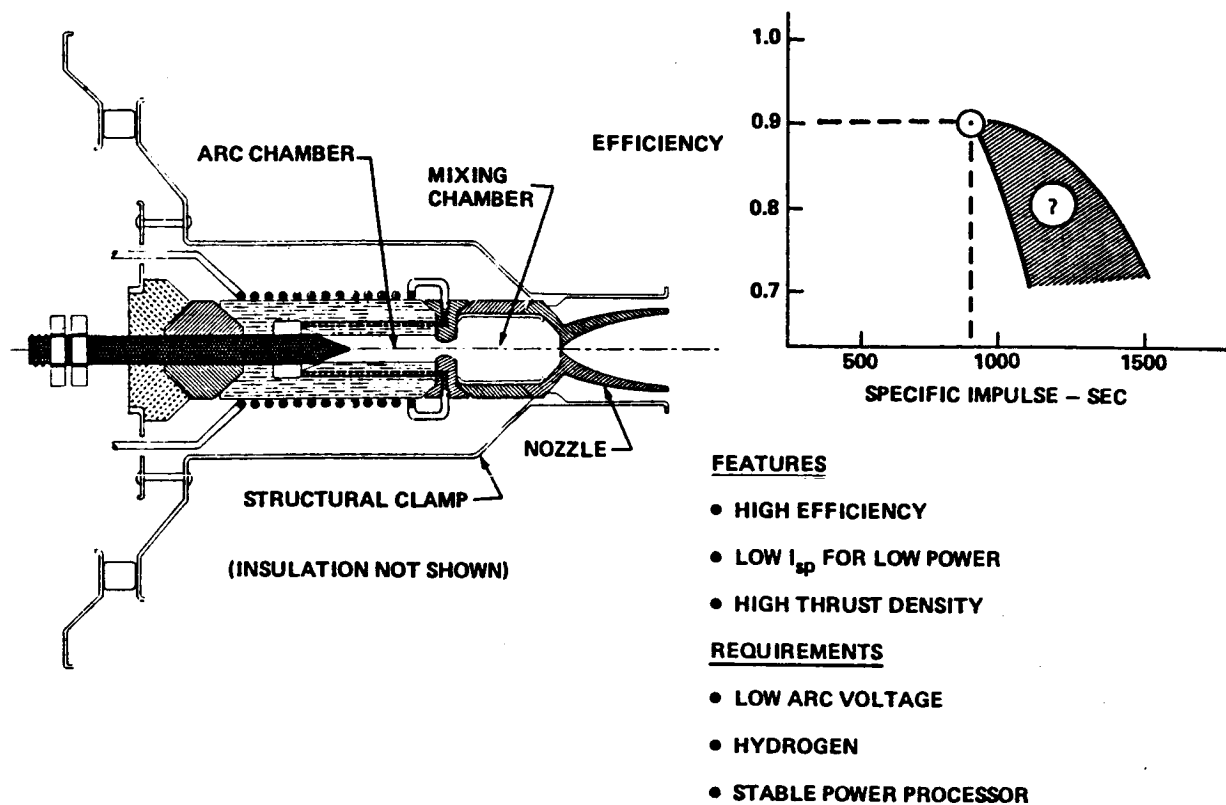


Figure 3.2.4-27: 25-kW Thermal Arc-Jet Concept

Because the mass of the solar array is significantly reduced if the bus voltage is designed to about 1000V, a PPU will be required to reduce this voltage to operate the thruster. This PPU can be comparatively simple (with respect to an ion thruster PPU) and can have a specific mass of less than 2.0 kg/kW. Sizing analyses for this study will assume 2.0 kg/kW at 90% efficiency.

Solar array characterization will assume the 12-2-10 blanket design described in Section 3.2.4.1.

Since long-term (~ 1 year) storage of the hydrogen propellant is required, meteoroid shielding, multilayer insulation, and meticulous thermal insulation will be required for the storage subsystem. Estimated mass for this type of subsystem is shown in Appendix B.

Parametric Sizing Data: The effects of trip time on subsystem masses are shown in Figure 3.2.4-28. These data show that the required propellant mass is very high and that short transit times are not practical. Increasing I_{sp} (Figure 3.2.4-29) enhances performance significantly but does not make SPV-arc competitive with other electric vehicle concepts.

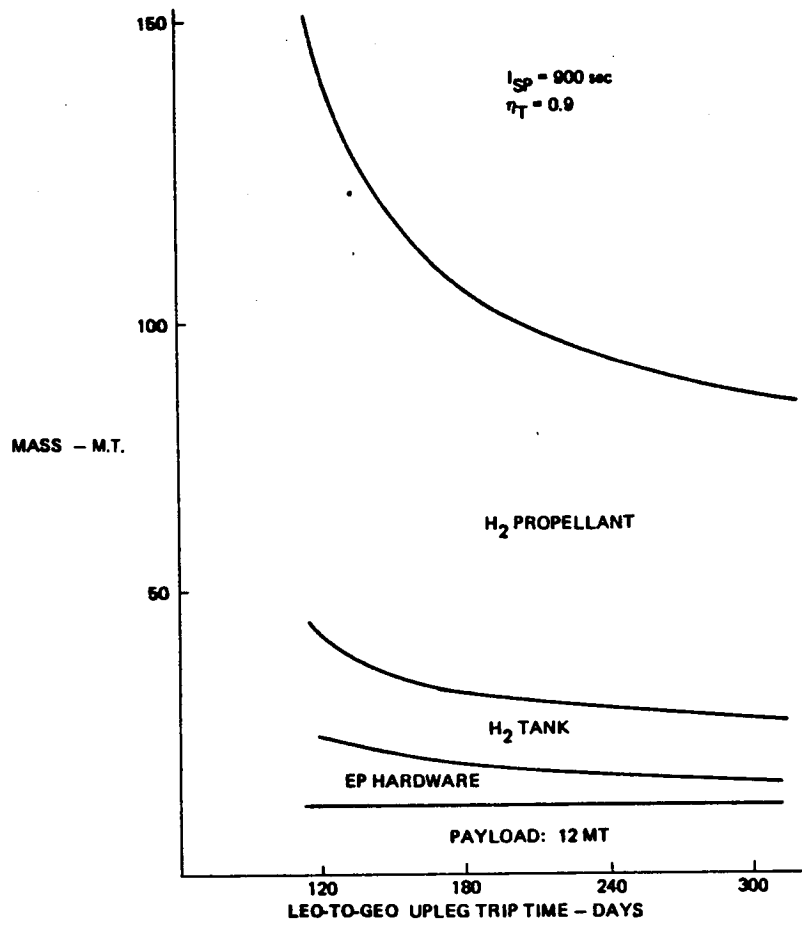


Figure 3.2.4-28: Effect of Trip Time for SPV-Arc Concept

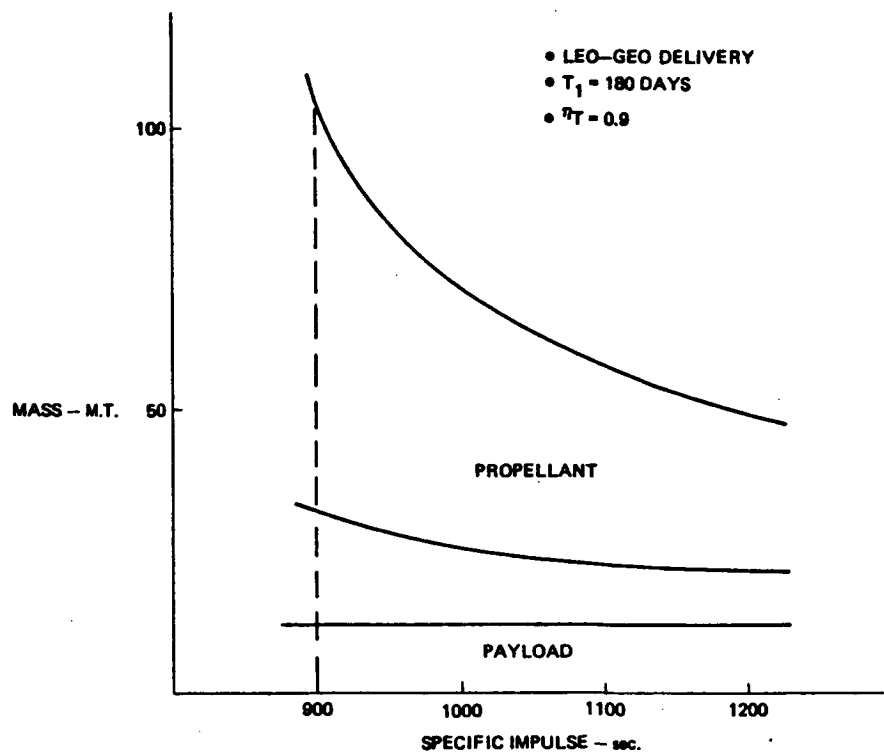


Figure 3.2.4-29: Effect on I_{sp} on SPV-Arc OTV Performance

Recommended Characterization: None. The SPV-arc vehicle concept is not competitive with high I_{sp} electric propulsion options.

3.2.4.3 Solar Thermophotovoltaic Ion (TPV-Ion) Thruster

Propulsion System Description: The TPV power concept is based on the fact that silicon solar cells have a much higher efficiency if the light spectrum is at a much lower temperature (2000°K to 2400°K) than the Sun ($\sim 6000^{\circ}\text{K}$). In practice, this phenomena can be used as indicated in Figure 3.2.4-30. A high CR reflector is used to heat a tungsten reradiator which illuminates the solar cells. The cells must be cooled to prevent them from overheating. The power developed is used, in this concept, to operate argon ion thrusters.

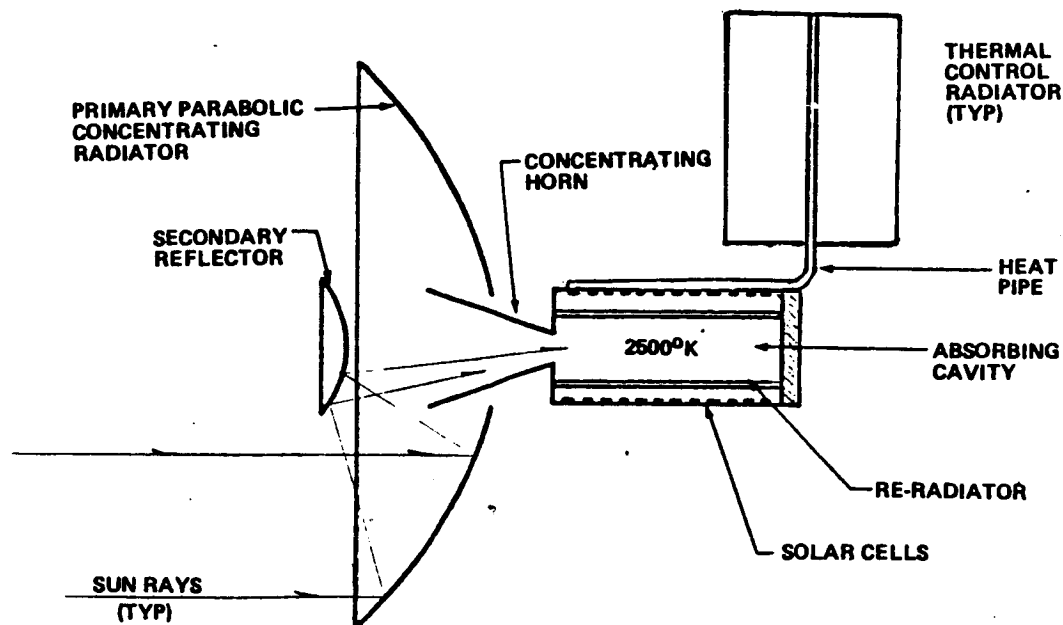


Figure 3.2-4-30: Key Elements of the Thermophotovoltaic Concentrator

Key Features: Because of the possibility of high conversion efficiency, this concept is expected to have low specific mass. In addition, the cell area is small and the cells are naturally shielded from space radiation by their thermal control structure. Thus, lower cost and good radiation hardness are expected.

Key Assumptions: The following assumptions have been used for vehicle characterization:

1. No cell degradation
2. No optical system degradation
3. Thermal control radiator specific mass is 8.0 kg/kW (radiated) at 60°C
4. 50-cm argon ion thrusters

Functional Requirements: Being solar powered, the TPV components must accept thermal transients associated with occultations.

Key Component Characterization: The key component for this vehicle concept is the TPV power converter. It conceptually consists of a lightweight, inflatable, parabolic concentrating reflector, a cavity which receives the concentrated sunlight and reradiates it to a solar cell assembly (including the heat pipes), and radiators required to control the cell temperature.

An inflatable concentrator 45 ft in diameter was built for the USAF in 1965 (AFAPL-TR-64-156). Its reflecting surface (1-mil aluminized mylar) was formed on a parabolic tool, inflated to the desired final curvature (to minimize tool discontinuities), and rigidized with foam on its back surface. A peak CR of approximately 3000 resulted, but the rigidizing process notably reduced surface quality because of nonuniform curing rates. A natural conclusion resulting from this experiment was that simple inflation would have resulted in a superior concentrator. Rigidized concentrators have shown about 3/8-deg surface deviation, while nonrigidized concentrators are estimated to have 1/8-deg, which will be assumed for subsequent characterization studies.

The overall performance for the 1/8-deg concentrator and its cavity is shown in Figure 3.2.4-31. It obtains peak efficiency (cavity reradiation power divided by actual reflected power) at aperture ratio of 0.016. These data establish the concentrator/cavity performance for scaling purposes.

The area specific mass of the inflatable concentrator is estimated to be 0.261 kg/m² for 1-mil surfaces including extensible support structures.

TPV cell characteristics are shown in Figure 3.2.4-32. These are based on BAC predictions for cell efficiency at 340°K and generalized measurements of the effect of temperature on the efficiency of a variety of silicon cells.

Since the illumination intensity seen by the TPV cells will be hundreds of suns, artificial thermal control will be required. If conventional aluminum heat pipes and radiators are used, with radiation from both surfaces

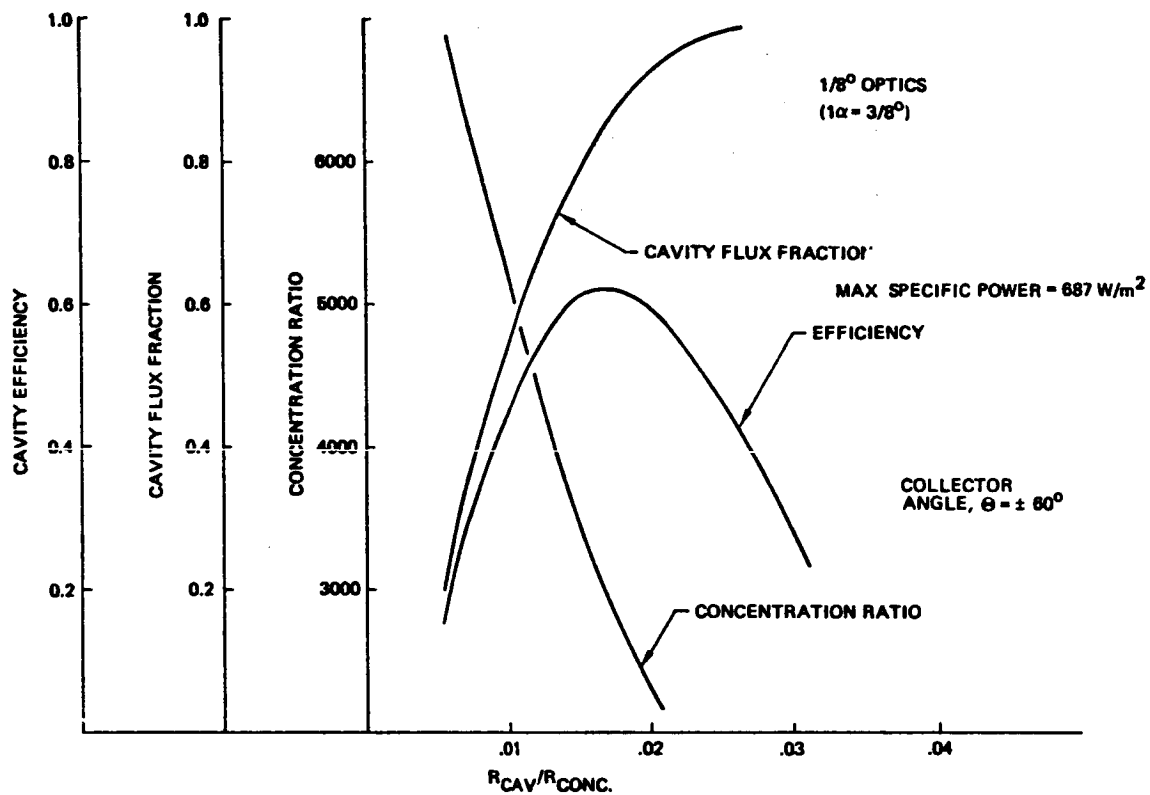


Figure 3.2.4-31: Optical Response of Lightweight Inflatable Solar Concentrator

and a high view factor, a specific mass of 8.0 kg/kW (at 60°C) should be realizable.

The above data admit power source optimization as shown in Figure 3.2.4-33. These data should be regarded as preliminary in nature because they are based on technology rules of thumb and not experimentally optimized components or detailed design analysis. Nonetheless, the minimum specific mass of 13.0 kg/kW is believed to be conservative and therefore suitable for vehicle characterization. The ion thrusters and their PPU's are as described in Section 3.2.4.1.

Parametric Characterization Data: Parametric data on TPV-ion OTV characteristics are shown in Figure 3.2.4-34. These data show that the nondegrading TPV vehicle is capable of two sorties per year at a power rating of 1100 kW or one per year at 311 kW.

Recommended Characterization: Recommended vehicle characteristics are illustrated in Figure 3.2.4-35.

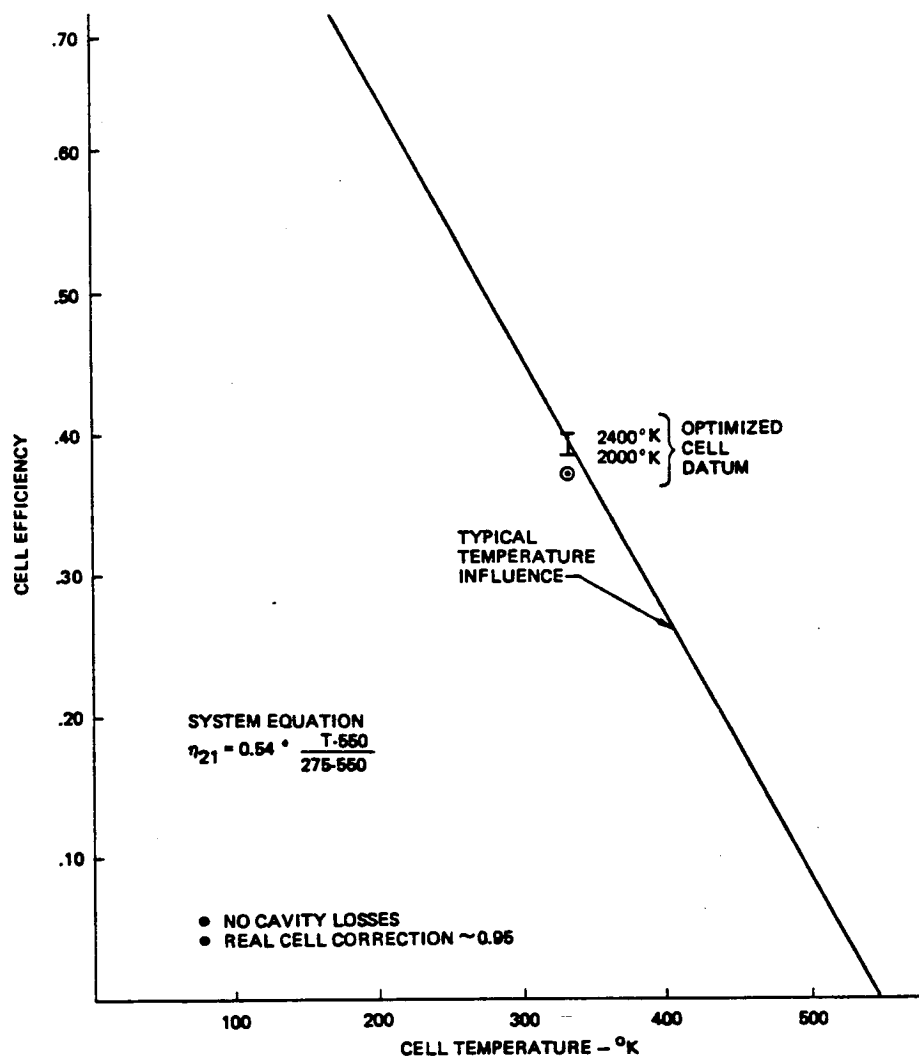


Figure 3.2.4-32: Estimated Cell Performance for TPV System

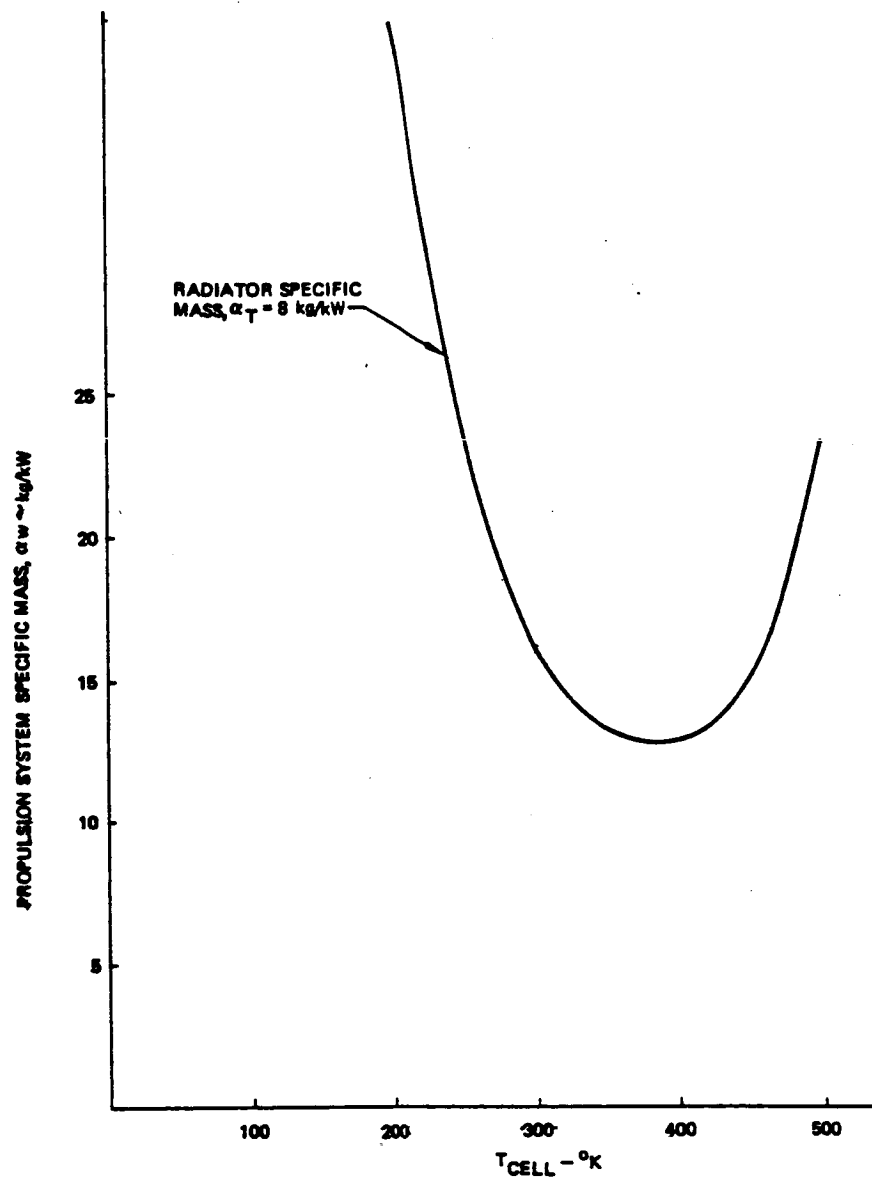


Figure 3.2.4-33: Optimization of TPV Cell Temperature

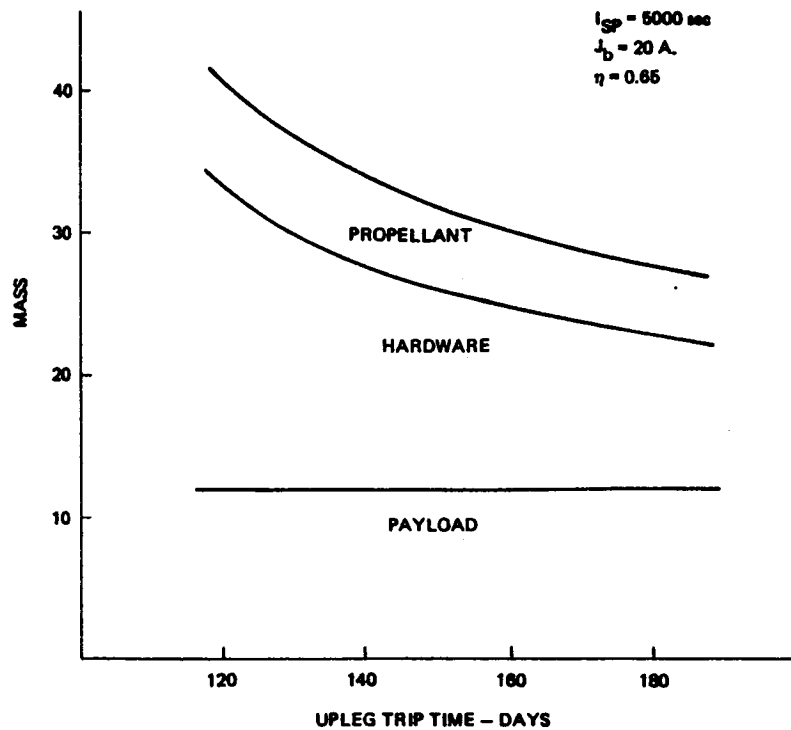


Figure 3.2.4-34: TPV-Ion OTV Parametric Performance

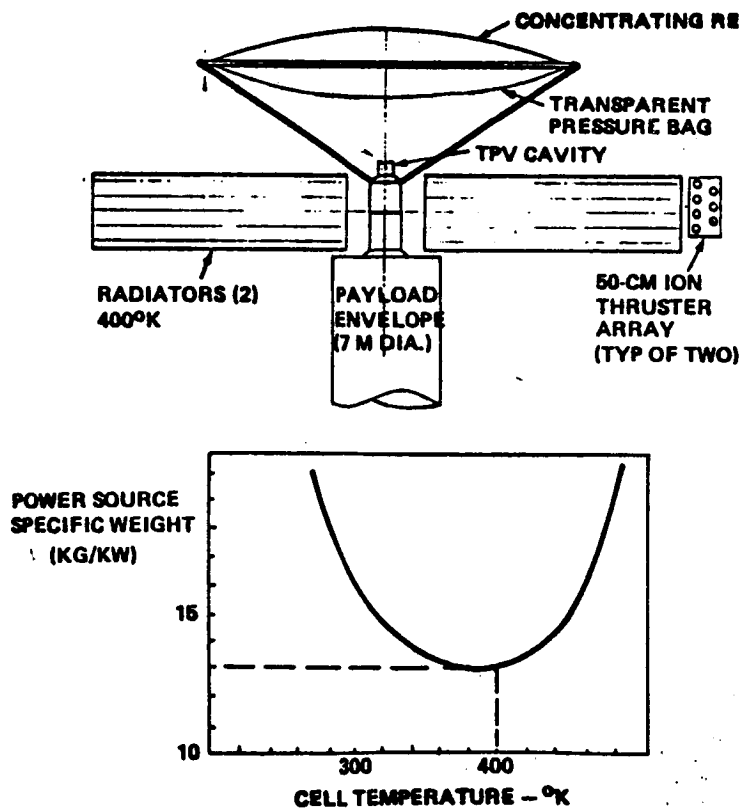


Figure 3.2.4-35: TPV-Ion OTV Characteristics--240-Day Uplink Transits

Performance and Design Issues: The following issues require resolution to assure TPV-ion concept credibility:

1. Optical quality after packaging for launch
2. Pointing accuracy
3. Optical degradation due to space radiation
4. Cell thermal control system design
5. Cell contamination effects due to tungsten vapor
6. Cavity design
7. Optimized cell performance
8. Overall design optimization including STS packaging

A preliminary design study is warranted and should be complemented with a scale model demonstration test.

Technology Requirements: The key technological requirement is the demonstration of a cell optimized for the TPV application. This demonstration has begun at BAC.

3.2.4.4 Solar Thermoelectric Ion (STE-Ion)

Propulsion System Description: An examination of the TPV concept (Section 3.2.4.3) shows it to be characterized by the very large radiator required for thermal control of the silicon conversion cells. Thus the available high-conversion efficiency is compromised by system optimization which leads to higher temperature for the cells to reduce radiator mass. An alternate concept which shows promise is a high-temperature converter such as the JPL thermionic or thermoelectric diodes designed for use with a nuclear power source (Section 3.2.4.5). These conceptual devices are believed capable of 15% efficiency—low compared to silicon solar cells—but at high temperature; about 1650°K on the hot side and 950°K on the heat rejection side. Using JPL mass estimates leads to an STE specific mass of only about 6 kg/kW. This concept may be one of the best available if the JPL technology matures as expected and should be reevaluated in light of their progress.

3.2.4.5 Nuclear (Fission) Power Source Ion (NPS-Ion) Thruster

Propulsion System Description: The NPS-ion concept consists of a nuclear electric power source in combination with ion thrusters and their PPU's (described in Section 3.2.4.1). A contemporary JPL configuration concept is shown in Figure 3.2.4-36.

FEATURES

- DEEP SPACE CAPABLE
- CHARACTERIZABLE THRUSTERS
- STS COMPATIBLE
- HIGH PROPULSION EFFICIENCY

REQUIREMENTS

- SHIELDED SPACE OPERATIONS
- CRYOGENIC ARGON STORAGE
- POWER PROCESSING FOR THRUSTERS

KEY ASSUMPTIONS

- JPL NTI POWER SOURCE
- NO DEGRADATION
- 50-cm ARGON ION THRUSTERS-20 A.

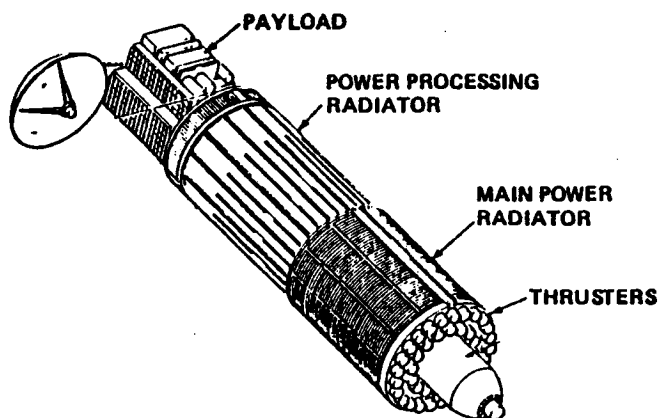


Figure 3.2.4-36: Nuclear Thermionic-Ion Thruster OTV (NTI-Ion)

Key Features: The NPS is considered to be a nondegradable substitute for a photovoltaic power source and, having no solar dependence, it may be uniquely capable of many deep-space missions which are beyond the capability of solar powered propulsion systems. The JPL configuration is intended to be compatible with the STS and the use of credibly characterizable ion thrusters ensures high propulsion system efficiency.

Key Assumptions and Data Sources: For this study the NPS will be assumed to operate without degradation for the mission cycle at a rating of 20 kg/kW (baseline). The ion thrusters will be the 50-cm argon thrusters (and PPU) described in Section 3.2.4.1. Data sources for the NPS are the JPL/Los Alamos Scientific Laboratory (LASL) progress reports on reactor technology development.

Functional Requirements: Because the power source is nuclear, flight units will not be pretested on the ground, and they should be capable of very long service with little or no reactor system maintenance. Also, NPS OTV

operations must be planned so that payloads and manned facilities are protected from nuclear radiations.

Key Component Characterization: For the NPS-ion concept, the unique component is the power source. The preferred characterization datum for the NPS is specific mass. Contemporary data for specific mass are shown in Figure 3.2.4-37. These analytical data are based on advanced technology estimates of thermal-to-electric power conversion efficiency, regardless of the conversion

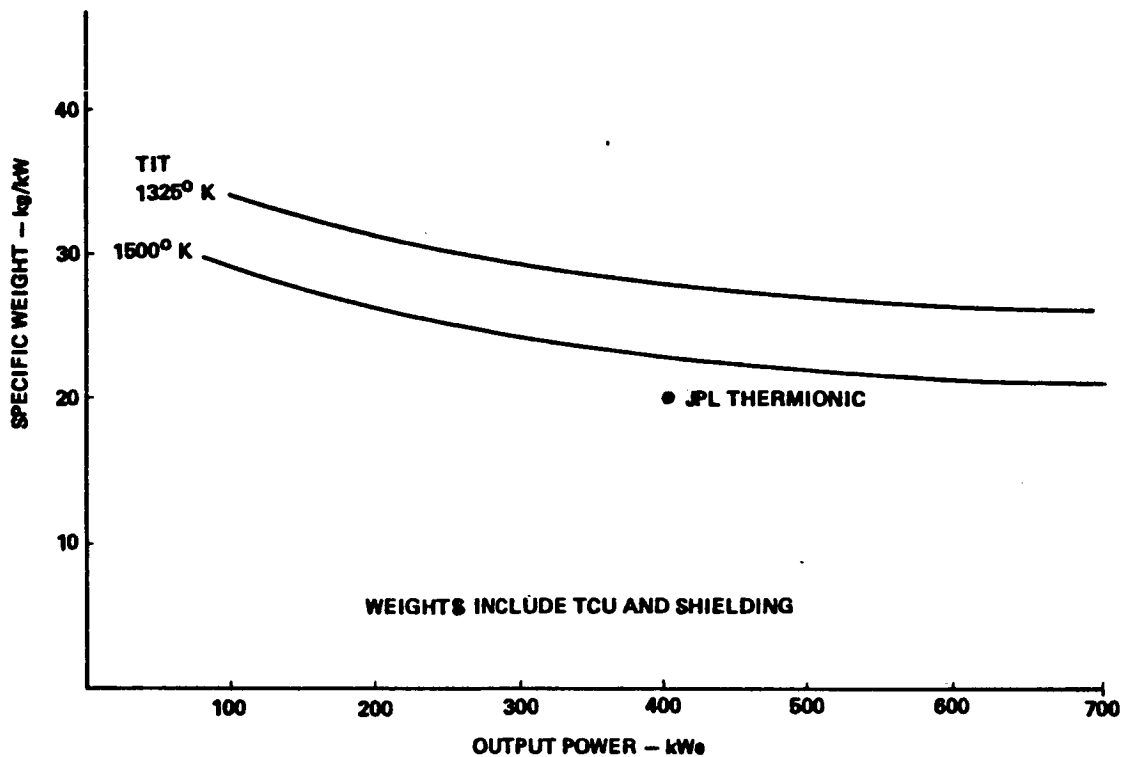


Figure 3.2.4-37: Predicted Specific Weight for Nuclear Brayton Cycle Power Systems

method. As might be expected, achievable specific mass is dependent on efficiency as indicated in Figure 3.2.4-38. A demonstration of conversion efficiency, including life cycle degradation (if any), will be required to credibly characterize the NPS options and vehicle concepts based on them.

For this study, a specific mass of 20.0 kg/kW will be baselined but the effects of uncertainties in conversion efficiency will be assessed by treating specific mass as a parameter to illustrate development risks and payoffs. Considerations of the type of thermal-to-electric power conversion (Brayton, thermoelectric, Rankine, or thermionic) are not germane to this study except as a risk element for design, development, test, and evaluation (DDT&E) costing.

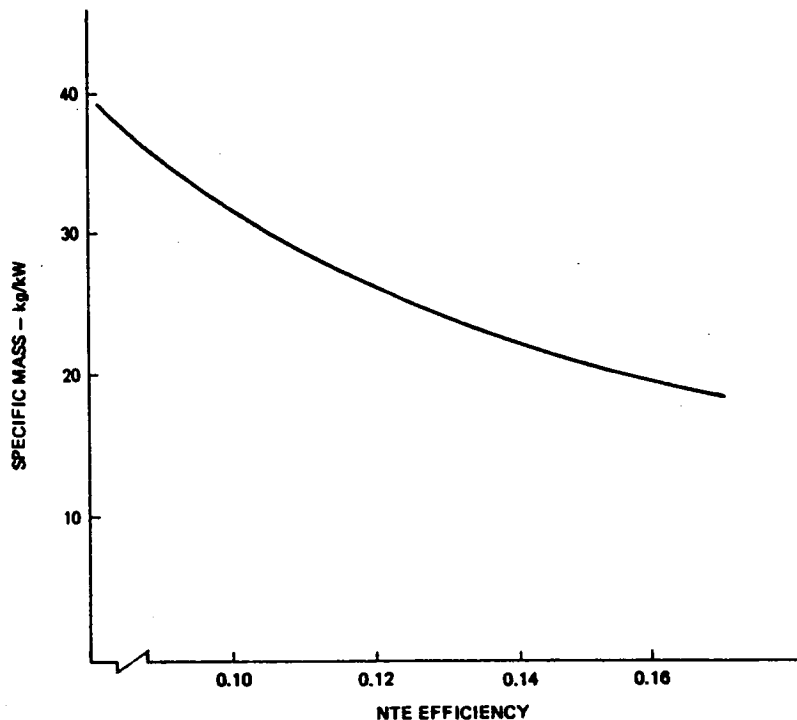


Figure 3.2.4-38: Sensitivity of NPS-Ion Specific Mass to Energy Conversion Efficiency

Parametric Vehicle Characterization: The influence of upleg transit time and NPS specific mass are indicated by Figure 3.2.4-39. These data are based on ion thruster performance at an I_{sp} of 6000 sec and a beam current of 20.0A.

They indicate that transits of less than 240 days will significantly increase propulsion power and hardware mass, and that even vehicles sized for long transits are sensitive to achievable lifetime averaged values of power conversion efficiency. The NPS-ion concept is sensitive to specific mass but appears to be reasonably competitive with the SPV-ion concept if the NPS specific mass can be held to less than 30 kg/kW.

Recommended Characterization: The recommended characterization for the NPS-ion OTV concept is given in Figure 3.2.4-40.

Performance and Design Issues:

1. Achievable power conversion efficiency and life cycle NPS specific mass
2. Selection of power conversion concept: direct (thermionic or thermo-electric) or dynamic (Brayton or Rankine cycle)

3. Total NPS system design including ancillary subsystems (instrumentation, control, isolation switches, etc.) and their thermal control components

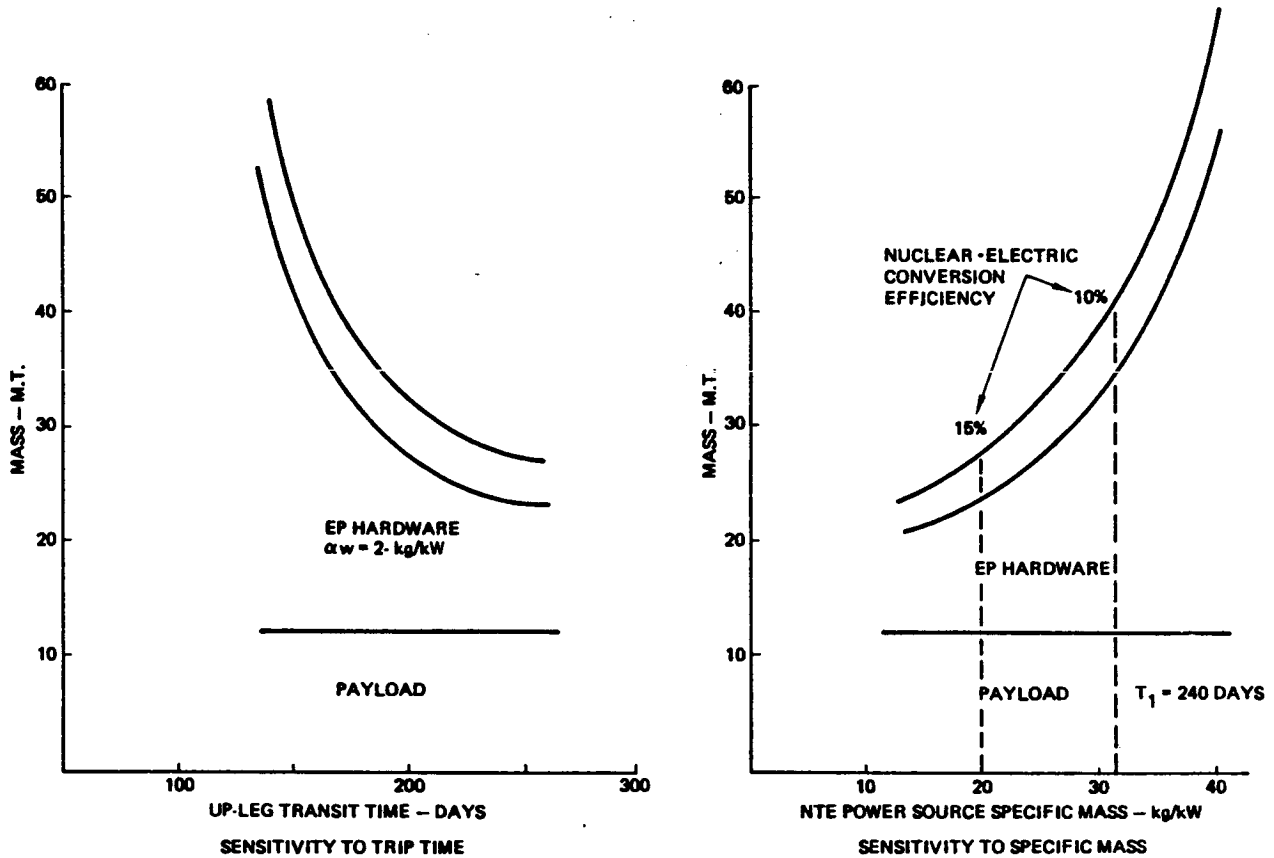


Figure 3.2.4-39: NEP-Ion OTV Sizing Data

• UP-LEG TRANSIT TIME	240 DAYS
• SORTIE PROPULSION TIME	353 DAYS
• RATED POWER	374 kW
• POWER SOURCE SPECIFIC MASS	20 kg/kW
• SPECIFIC IMPULSE	6000 sec
• SYSTEM EFFICIENCY	0.704
• NUMBER OF THRUSTERS	16.5 (18)
• START-BURN MASS SUMMARY (kg)	
- POWER SOURCE	7490
- THRUSTERS AND PPU's	1450
- MISCELLANEOUS	2850
EPS	11 790
- PROPELLANT	3990
- PAYLOAD	12 000
INITIAL MASS	27 780

Figure 3.2.4-40: NPS-Ion OTV Nominal Characteristics

4. Nuclear radiation backscattering from propellant plume
5. Auxiliary propulsion requirements of payload and servicing operations
6. Life cycle performance and reliability testing

Technology Requirements:

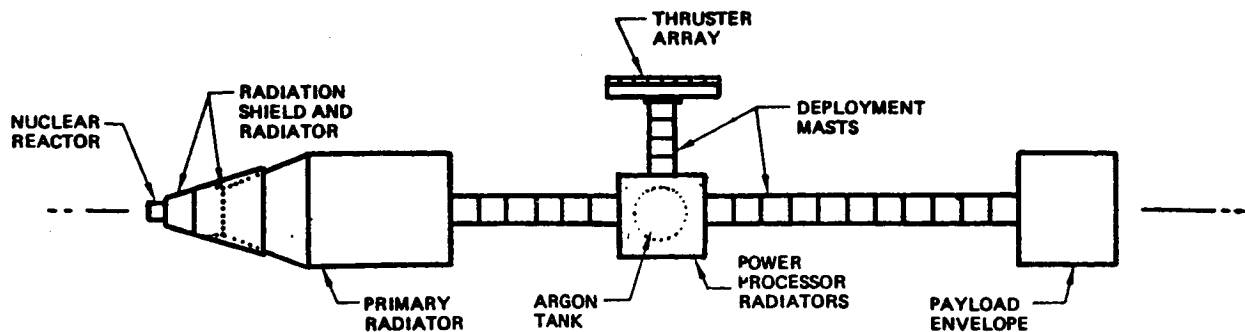
1. A viable, efficient power conversion concept
2. An NPS prototype demonstration
3. Life cycle degradation data

Conclusions: If the anticipated NPS specific mass of about 20 kg/kW can be achieved, the NPS-ion concept can be useful for both the OTV mission and for deep-space missions. However, the costs for technology verification are such as to preclude development unless they can be shared with other NPS users.

3.2.4.6 Nuclear Power Source MPD (NPS-MPD) Propulsion Systems

Propulsion System Description: This concept uses a nuclear electric power source (as described in Section 3.2.4.5) in conjunction with an MPD thruster of the type being studied at Princeton University and JPL. Since this thruster requires very high arc currents for effective operation, the system concept requires operation in a pulsed mode; and an electrical energy storage system is required for efficient utilization of the power source. The recommended configuration is shown in Figure 3.2.4-41 which also calls out the system elements and subelements. The side thrusting layout is desirable because it locates the thrusters, thrust vector control (TVC), and propellant system in a benign radiation environment and minimizes radiation backscattering from the propellant plume.

System elements for steady state propulsion concepts are completely characterizable by their static characteristics. This is not true of pulsed systems because their elements must be dynamically matched, first by analysis to optimize the duty cycle, arc current, and pulse duration (to give a best combination of system specific mass and efficiency), and then by experiment to confirm assumptions used in the analysis. No such analysis describing all



SYSTEM ELEMENTS

PRIMARY

- NUCLEAR REACTOR
- PRIMARY SHIELD
- POWER CONVERTER ASSEMBLY
- THRUSTER ARRAY
- POWER PROCESSING

ANCILLARY

- CONTROL-ACTUATORS, SENSORS, THERMAL CONTROL
- SHIELD THERMAL CONTROL
- PRIMARY RADIATORS, INSTRUMENTATION AND THERMAL CONTROL, WARM-UP HEATERS
- TVS, ISOLATION SWITCHING, THERMAL CONTROL
- REDUNDANCY SWITCHING, THERMAL CONTROL

Figure 3.2.4-41: Candidate Nuclear-Electric OTV Configuration

system elements has been made and, therefore, the practicality of the pulsed MPD propulsion concept is undetermined. Nonetheless, contemporary research activities directed to it warrant a parametric evaluation.

Key Features: The NPS-MPD propulsion system offers several attractive features:

1. There is a substantial technology for reactor design and this power system could have many other applications.
2. Thermoelectric or thermionic converter arrays lend to low-voltage/high-current power conversion, which seems to match the thruster requirements.
3. The nuclear power source will not be degraded by space radiation.
4. The MPD thruster has high thrust density and the propulsion system may only require one or two thrusters, exclusive of redundancy.

5. Because there is no solar dependence, the NPS-MPD concept has deep-space capability.
6. Contemporary configuration studies from JPL indicate straightforward STS compatibility for the fully configured power source; therefore, no large-scale space deployment is required.
7. The MPD thruster, as currently being researched at Princeton, is a simpler physical concept relative to contemporary ion thrusters.
8. The combination of a simple thruster, a simple nondynamic electrical power converter, and a heat-pipe-cooled nuclear reactor suggests fundamental design simplicity and ruggedness.

Key Assumptions and Data Sources: Data for the specific mass of the nuclear power source are adopted from the "Nuclear Reactor Technology Development Program" progress reports published by JPL. These data are summarized in Section 3.2.4.5. For this MPD evaluation, a specific mass of 20.0 kg/kW will be baselined for parametric sensitivity evaluations.

Data on the efficiency of MPD thrusters are adopted from Princeton publications (AIAA) and from a theoretical, one-dimensional analysis provided by D. Q. King of JPL. The best recent description of experimental efficiency data is contained in: "Effect of Thrust Chamber Configuration on MPD Arcjet Performance," D. Q. King, W. W. Smith, R. G. Jahn, and K. E. Clark, AIAA 79-2051.

Functional Requirements: The principal functional requirements are:

1. 1-year sortie duration (without servicing) for the OTV mission
2. Automated or remote servicing of radioactive components
3. A remote, shielded, or unmanned servicing facility in LEO, separate from the manned LEO base
4. 10-year (+) lifetime without servicing for deep-space missions (redundant components may be added)

Anticipated functional requirements for the propulsion subsystems are approximately as follows:

1. 1 ms arc current and propellant pulses
2. 20,000A to 40,000A peak arc current, determined by the optimum average I_{sp}
3. 100 to 300 cycles per second determined by optimized use of the power source, thermal control of the thrusters, and optimized arc pulse duration
4. 10^9 to 10^{11} cycles on the propellant control valves and any power switch used in the energy storage units

Key Component Characterization: Components requiring parametric characterization for vehicle synthesis (sizing) are identified in Figure 3.2.4-41 (ancillary components are accommodated in a mass contingency allowance). The following data have been adopted for this study:

1. Nuclear Power System: Data on specific mass are presented in Section 3.2.4.5. For the MPD thruster propulsion system, a specific mass of 20 kg/kW will be baseline. However, the specific mass of thermionic or thermoelectric power systems is sensitive to achievable efficiency, which is a function of both static, full-power efficiency and the dynamic use of power with the pulsed mode of operation. The baseline datum is for steady-state performance assuming an undemonstrated 15% lifetime average efficiency. If this efficiency is only 10%, the power subsystem specific mass will nearly double. Furthermore, if the design of the energy storage system should require periodic variations in output power, the nuclear power source would have to be designed for the maximum instantaneous power and operated at some reduced average power and efficiency, which will also increase the effective specific mass. Whereas the magnitude of this penalty may be conceptually small, it is in fact unknowable without a design analysis of the system as a whole. Existing analyses do not address this aspect of the system definition problem.

2. The MPD Thruster: This thruster, illustrated in Figure 3.2.4-42, has been under study as a propulsion device since about 1970 at Princeton University and, more recently, has been adopted for study and experimental development at JPL.

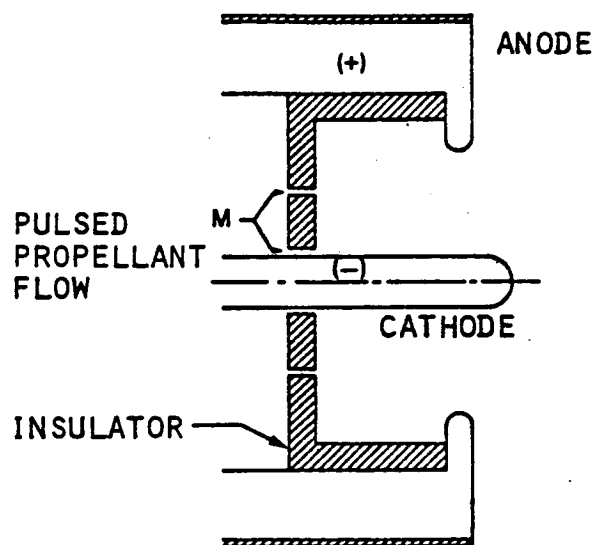


Figure 3.2.4-42: Princeton Pulsed Self-Field Thruster

Magnetoplasmadynamic thrusters produce thrust by body-force acceleration of a continuum plasma in a $\mathbf{J} \times \mathbf{B}$ field. This conceptually simple thrust device consists of an axial cathode with a circumferential anode. A very strong radial current ($\sim 10^4 \text{ A}$) is used to induce a toroidal magnetic field (self-field) and the two combine to accelerate a plasma which forms during the arc process. The instantaneous power required for this device is so large ($\sim 10 \text{ MW}$) that only pulsed operation is practical for vehicles in the 12t payload class.

The physical simplicity of the MPD thruster belies its theoretical complexity. The process of simultaneous plasma formation and acceleration is so complex that no encompassing theory has been sufficiently developed to allow design by analysis. All existing technology is experimentally based. A summary of calculated efficiencies for the Princeton MPD thruster is shown in Figure 3.2.4-43. The cathode length may be varied (within limits) to maximize efficiency for some desired specific impulse, but there is no evidence from currently available data that an efficiency much greater than 0.3 to 0.4 is realizable.

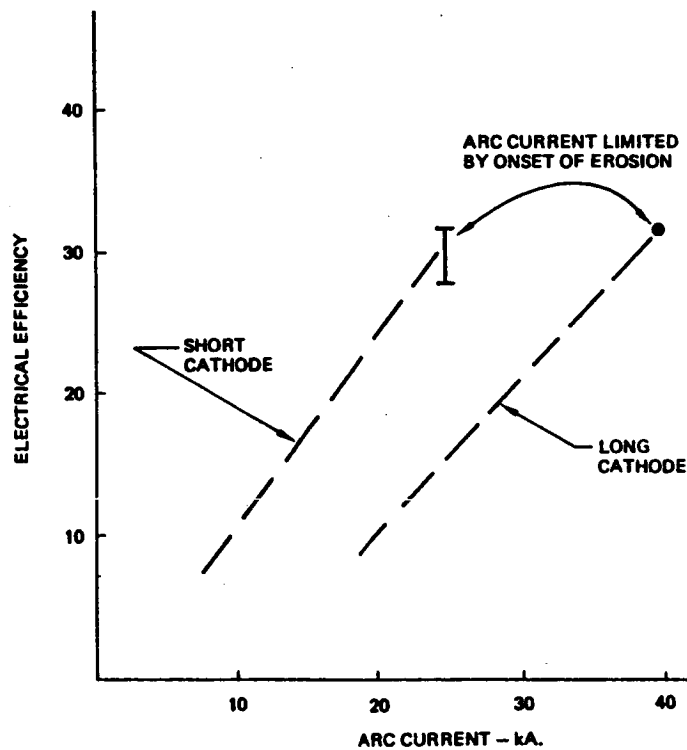


Figure 3.2.4-43: Summary of Princeton MPD Thruster Inferred Efficiency Data

Princeton data are based on a thrust calculated by integrating plasma acceleration through a $J \times B$ field and their absolute accuracy has not been tested. All estimates assume 100% mass utilization efficiency and are based on instantaneous mass flow rate within the arc while, in fact, utilization efficiency may be appreciably less than 100%. Because reported efficiencies are based on instantaneous flow, the system efficiency must reflect the square of utilization efficiency. An efficiency convention for MPD is derived in Appendix D.

Figures of merit for MPD thrusters are lifetime, achievable I_{sp} , efficiency, average thrust (including duty cycle), and thruster mass including TVC and power cabling. Thruster mass is generally negligible with respect to the remainder of the propulsion components (provided natural radiation cooling is adequate). Contemporary MPD thrusters have an I_{sp} limit of about 3000 sec with argon, which meets or exceeds the optimum I_{sp} for the OTV mission.

The above efficiency data are for quasi-steady-state operation. If pulsed operation requires thruster operation over some range of arc current, the efficiency will vary as indicated in Figure 3.2.4-43. In this circumstance, the average efficiency required for system characteri-

zation must be obtained by time averaging. This penalty may be small if the average current can be kept near the onset current but no system analyses are yet available to quantify the penalty.

Contemporary efficiency estimates (steady state) are compared in Figure 3.2.4-44, which includes a recent theoretical, one-dimensional calculation by D. Q. King of JPL. Efficiencies estimated from plasma

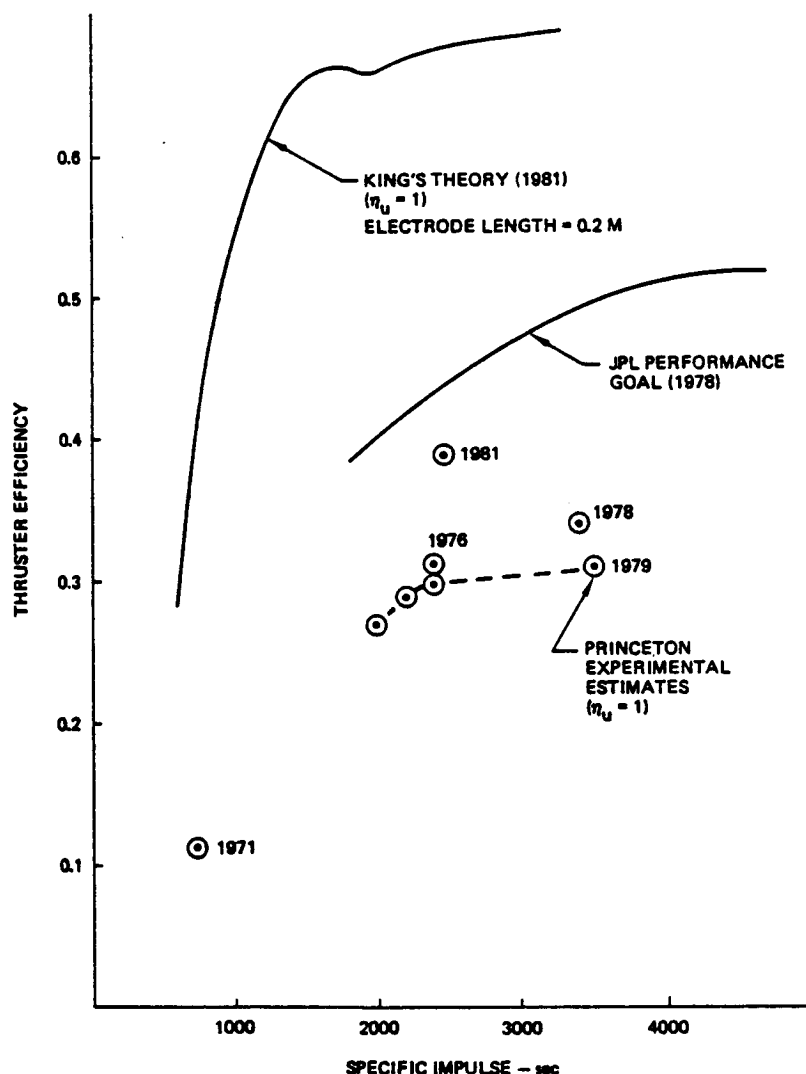


Figure 3.2.4-44: Efficiency Comparison for Princeton MPD Thruster

measurements at Princeton are shown as data points. A JPL judgment prognosis (circa 1978) is also shown, but no design modification process which will increase efficiency beyond the current experimental values is known. In fact, the experimental data suggest an efficiency limit of roughly 30% to 40% independent of I_{sp} . King's calculations represent a substantial advance in analytical theory but, as far as is known, they do

not correlate with experimental evidence. In this circumstance, the utility of this theory remains to be determined.

In summary, the MPD thruster efficiency is poorly understood with a wide disparity between theory and experiment. More research is required and a system-level characterization study is necessary to quantify the effects of pulsed operation.

A final concern is thruster lifetime. According to Princeton data, operation at an arc current at the limit of erosion (higher currents causing measurable erosion) is required to maximize efficiency. Thus the system designer is compelled to specify operation very near the erosion limit because efficiency is degraded in proportion to any reduction in maximum current.

Considering the electrically noisy characteristics of arcs in general, offmaximum operation will be advisable and some additional efficiency penalty may have to be accepted.

For the purposes of this analysis, thruster electric efficiency will be treated as a parameter ranging from 0.3 to 0.7. A propellant utilization efficiency of 0.9 will be assumed.

3. Power Processing: The key to pulsed operation is power storage during off intervals. The device to be used for this will be called a PPU to be consistent with other electric propulsion concepts. The published data on MPD PPU's emphasize inductive storage, which calls for switching an inductor alternately to the power source for charging and then to the thruster to produce thrust. Switching must be done at high current levels (~ 20,000A) to obtain high utilization of the power source (~ 90%). Unfortunately, no switching device is known which will both survive the MPD duty cycle requirements and also have acceptable thermal control characteristics. Therefore, some form of capacitance storage appears to be desirable since switching with capacitance storage can be done at zero current, possibly using the thruster itself as a plasma switch. This may be accomplished by using a separately powered high-voltage, low-power spark to initiate the thruster discharge (arc), which discharges the PPU through the conducting plasma until it is switched off at some low current. Unfortunately, a deep discharge of the capacitor is required, which will result in large cyclic variations in

the power source output and the thruster current (increasing specific mass) and in reduced average thruster efficiency. Also, it is unlikely that the current pulse from this simple system could closely match the propellant pulse, leading to poor propellant utilization efficiency.

Because of this utilization problem, JPL experts now propose to use pulse-forming networks within the PPU which will enable matching the current pulse with the propellant pulse. A very high utilization (greater than 0.9) is expected for this approach; however, no data (either experimental or analytical) are available to support this expectation. In fact, no overall system characterization analysis at any level of sophistication is available. Without this analysis, performance claims can only be speculative judgments and related vehicle sizing analyses are without basic credibility. The required system analysis must include the following: a circuitry concept for the PPU, dynamic characteristics of all interactive elements, and a dynamic solution of the describing equations. The required solution data must include time-averaged specific mass for the power source, overall efficiency (including utilization), and provisions for thermal control (system stability should also be a consideration). The objectives of this analysis are to: (1) establish the optimum duty cycle, pulse duration, and maximum arc current so that average specific mass and efficiency are enjoined to maximize OTV performance; and (2) treat the thermal control of the power source, PPU, and thruster (if any) since radiator mass will be a function of the averaged operating state of the system. The required propulsion system power is a constraint which will influence duty cycle options.

BAC: A BAC design study of a suitable PPU is described in Section 3.4.2 of Volume I. This analysis is only one part of the problem as a whole and no attempt at optimization was made. Nonetheless, it is clear that PPU mass and thermal control requirements may be significant.

NPS-MPD Vehicle Characterization: Although the component characterization data for this concept are as yet indefinite, sample sizing data have been developed to illustrate possible technology development payoffs for this vehicle concept. This analysis will assume the following baseline data:

System efficiency: 0.3 to 0.7 (1500 to 3500 sec)

Power source specific mass: 20.0 kg/kW

PPU mass: 200 kg

PPU radiator: 8.0 kg/kW (radiated)

Thruster mass: 100 kg

Thruster radiat .. None

These assumptions will be used as if they were time-averaged values for one duty cycle at the EOL of the OTV. Since achievable specific mass and system efficiency (product of average thruster efficiency, including utilization and PPU efficiency) are in dispute, these data will be parametrically varied to establish a measure of concept risk or payoff.

The effects of varying I_{sp} on major vehicle start-burn weights is shown in Figure 3.2.4-45 for an OTV sortie upleg transit time of 240 days. Note

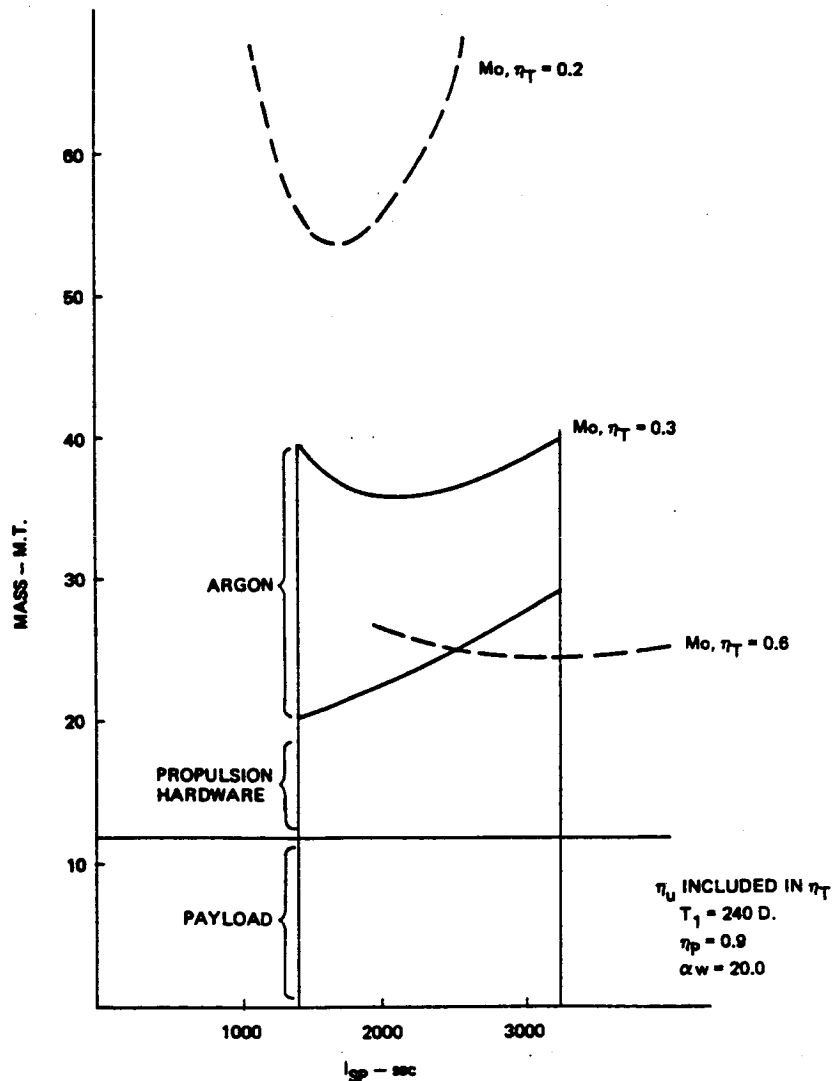


Figure 3.2.4-45: Effect of Thrust Efficiency and I_{sp} Variation on NPS-MPD OTV Performance

that the optimum I_{sp} for minimum start-burn mass varies between 1500 and 3000 sec. Also shown in this figure are initial weights for limit efficiencies based on contemporary data and theory. These were estimated by assuming a PPU efficiency of 0.9 and a utilization efficiency of 0.9, with thruster efficiencies of 0.3 (experimental datum) and 0.7 (King's theory). Resulting system efficiencies are 0.22 and 0.51.

Figure 3.2.4-46 shows the power dependence for this mission. Because

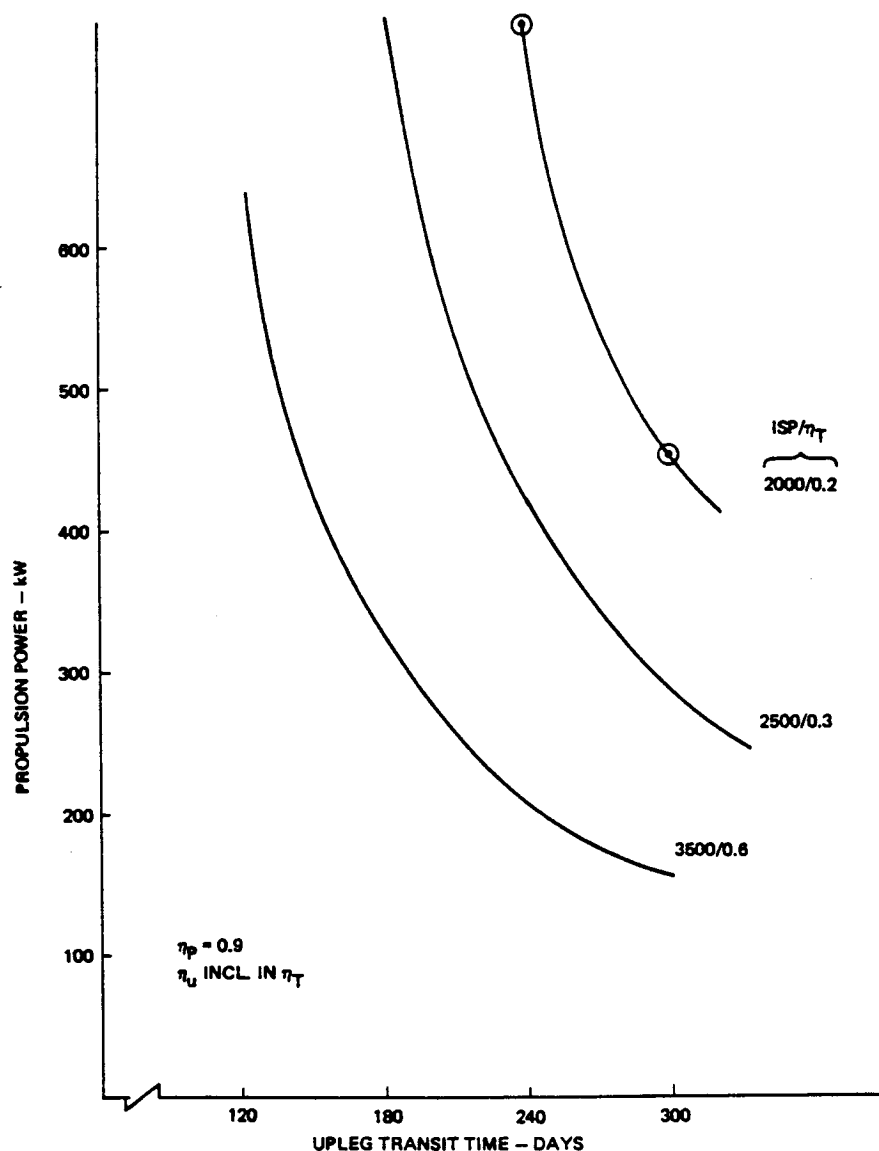


Figure 3.2.4-46: Effect of Thrust Efficiency on Powerplant Size for NPS-MPD OTV

power is an indication of hardware costs, it is evident that high thruster efficiency is desirable, especially if component costs are high, as they may be for nuclear power sources. The effects of uncertainties in power source specific mass and system efficiency on OTV inert mass were shown in Figure 3.2.4-39. Since the specific mass contribution of the thruster, PPU, and the

PPU thermal control unit may be less than 10% of the specific mass of the power source (a positive feature of this concept), these data are insensitive to small uncertainties in these masses.

Sizing uncertainties for the pulsed MPD OTV concept are very large. A measure of this risk is suggested in Figure 3.2.4-47. If JPL levels of

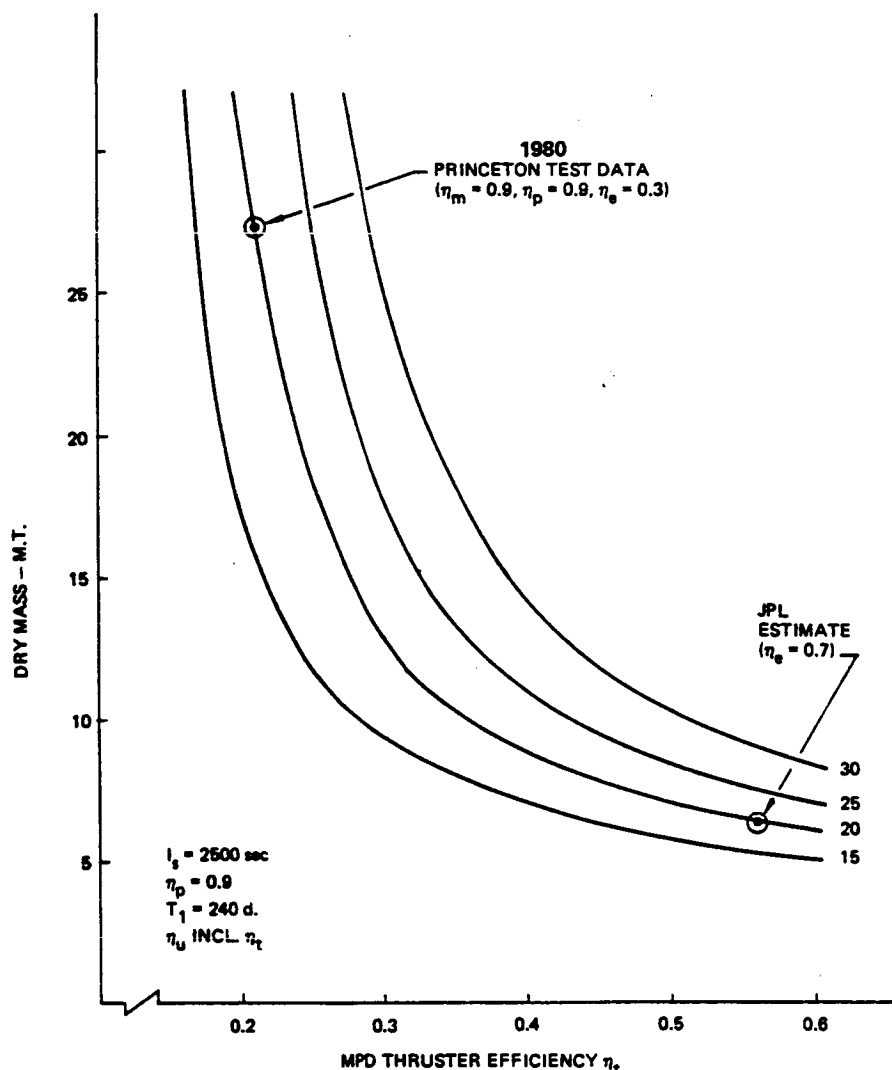


Figure 3.2.4-47: Effective Efficiencies on MPD Vehicle Characteristics

technology can be achieved, the concept is very attractive. However, if thruster efficiency remains at the currently demonstrated level or if pulsed system penalties accrue, the concept may be impractical for this mission. Clearly, a credible pulsed MPD propulsion system analysis is required and thruster technology (including theory) must be improved.

Performance and Design Issues: The following list indicates issues which require resolution to make the nuclear MPD a viable contender for the OTV mission:

1. No MPD thruster theory currently exists which correlates experimental data and provides design improvement insights.
2. No data exist on thruster lifetimes. We need to know how close to the maximum efficiency point the thruster can be operated and still be within acceptable erosion limits.
3. The technology for power conversion thermoelectric diodes needs experimental demonstration so that the specific mass of nuclear electric power sources can be credibly established.
4. The lifetime degradation characteristics of thermoelectric diodes needs to be determined.
5. The optimized characteristics of the energy-storage/pulse-forming systems are needed so that overall propulsion system efficiency and mass can be determined.
6. The dynamic performance (specific mass and efficiency) of the pulsed MPD propulsion system is undetermined.

Conclusions: The pulsed MPD propulsion system requires considerably more technology development before it can be considered a competitive concept. This conclusion does not apply to steady-state MPD propulsion concepts which do not have utilization or PPU uncertainties. In fact, if adequate cathode cooling is available, the MPD thruster could perform quite well in the high mission model where the power levels are high enough to operate steady state.

3.3 Task 3 - Competitive Transportation System Definition and Cost Evaluation

The objectives of this task were to (1) develop alternative space transportation system scenarios using the advanced propulsion vehicle configurations defined in the previous task and (2) estimate the relative life cycle costs of each scenario for the low and high mission models. The first step was to determine the types and numbers of vehicles required in each scenario to satisfy the requirements of the low mission model. This part of the task is discussed in Section 3.3.1. Next, the DDT&E costs and production

costs of the vehicles involved were estimated. These cost estimates are summarized in Section 3.3.2 and covered in depth in Volume III. Operational costs were then assessed and relative total life cycle costs estimated. These results are presented in Sections 3.3.3 and 3.3.4. The high mission model was treated separately; all results are summarized in Section 3.3.5.

3.3.1 Space Transportation System Scenarios

A number of vehicle configurations were defined in Task 2 (Section 3.2) and those recommended for system-level assessment are characterized in Figure 3.3.1-1. Note that all vehicles were sized for the low mission model. The

	LOW MODEL-12MT PAYLOAD							
	CHEMICAL ABOTV	NUCLEAR RBR	SPACE-BASED LASER OTV	GROUND-BASED LASER OTV	SOLAR THERMAL ABOTV	SPV ION	TPV ION	NPS ION
INPUT POWER, MW	—	500	25	100	3.85	0.445	0.311	0.374
JET POWER, MW	—	460	15	50	2.3	0.313	0.219	0.263
ENGINE ISP, SEC	485	1050	1500	1500	1100	6000	6000	6000
VEHICLE THRUST, N	132,000	89,000	2000	6700	400	10.6	7.4	8.9
STARTBURN MASS, KG	46,840	39,720	25,300	31,200	30,300	17,800	21,640	26,340
PROPELLANT MASS, KG	30,500	18,860	8320	12,220	11,650	2310	2790	3640
BURNOUT MASS, KG	4340	8550	4740	6570	5380	3700	6850	10700
POWER SOURCE, KG/KW SPECIFIC MASS	—	0.004	—	—	0.75	3.7	13	20
UPLUG TRIPTIME, DAYS	0.5	0.5	18	24	24	180	213	227

Figure 3.3.1-1: Characteristics of Vehicles Selected for Costing – Low Model

vehicles sized for the high model will be discussed separately in Section 3.3.5. Each vehicle in Figure 3.3.1-1 was capable of performing the 12t LEO-to-GEO delivery mission, the chemical aerobraked OTV (ABOTV) and the nuclear rocket are capable of the manned mission, and all but the space-based laser OTV are capable of the planetary exploration missions. The two solar electric vehicles performed the Neptune orbiter mission by accelerating an

aerocapture bus into a Jupiter swingby trajectory similar to those used by the thermodynamic rockets. Only the NPS-ion vehicle actually thrust itself into Neptune orbit.

The low mission model was simplified for cost analysis by assuming that every mission required the entire vehicle capability, thereby eliminating any partial payload manifesting. The simplified low model, shown in Figure 3.3.1-2, consists of 146 12t delivery mission equivalents, 8 planetary mission

LOW MISSION MODEL HAS 297 MISSIONS OF WHICH 63 ARE LESS THAN 6 MT AND WILL ASSUMED TO BE DONE WITH 1ST GENERATION CHEMICAL OTV'S. MISSIONS REMAINING FOR ADVANCED CONCEPTS ARE:

- LARGE ASSEMBLED SATELLITES WHICH REQUIRE (37) 12 MT LAUNCHES
- CARGO TO GEO BASE WHICH REQUIRES (6) 12 MT LAUNCHES
- MANNED GEO SORTIES WHICH REQUIRE (68) MANNED LAUNCHES
- UNMANNED SERVICING WHICH REQUIRES (103) 12 MT LAUNCH EQUIVALENTS
- PLANETARY EXPLORATION WHICH REQUIRES (8) 12 MT LAUNCH EQUIVALENTS

TOTAL 12 MT LAUNCHES OR EQUIVALENTS = 154 TOTAL MANNED LAUNCHES = 68

Figure 3.3.1-2: Low Mission Model

equivalents, and 68 manned launches over 16 years. The numbers and types of vehicles and engines required to meet this simplified model are shown in Figures 3.3.1-3 and 3.3.1-4. It was assumed that the chemical AB OTV's and nuclear rockets had a lifetime of 40 missions, the laser and solar thermal rockets had a lifetime of 20 missions, and the electric vehicles had a lifetime of 10 missions. The decrease in vehicle lifetimes was attributed to the number of fuel tank pressurization cycles for the laser and solar rockets and the length of missions (9 months) for the electric vehicles.

Note that for all vehicles except the space-based laser OTV, the planetary missions offer an opportunity to dispose of a vehicle near the end of its useful life. It was assumed that two vehicles of each type should be available at all times, in case a backup or rescue mission was required, and that spare engines should be produced in case some were lost in an accident.

The transportation system scenarios involved not only OTV's but the launch vehicles (SDV's) and tankers required to place the equipment and propellants

	CHEMICAL ABOTV	NUCLEAR RBR	SPACE-BASED LASER	GROUND BASED LASER	SOLAR ABOTV
• STAGES					
• ADVANCED OTV's					
FLEET SIZE	2	2	2	2	2
PLANETARY FLIGHTS	8	8	—	8	8
WEAROUT	—	—	6	—	—
• CHEMICAL OTV's					
MANNED OTV's	—	—	2	2	2
PLANETARY FLIGHTS	—	—	8		
• ENGINES					
• ADVANCED PROPULSION (10 FLIGHTS/ENGINE)	—	22 + 2*	8 + 2*	15 + 2*	15 + 2*
• CHEMICAL (20 FLIGHTS/ENGINE)	22 + 2*	—	22 + 2*	6 + 2*	6 + 2*

*SPARES

Figure 3.3.1-3: Production Quantities for High-Thrust Concepts

	SPV-ION	TPV-ION	NPS-ION
• STAGES			
• ELECTRIC OTV's (10 MISSION LIFETIME)			
FLEET SIZE	5	5	5
PLANETARY FLIGHTS	8	8	8
WEAROUT	2	2	2
• CHEMICAL OTV's (40 MISSION LIFETIME)			
MANNED OTV's	2	2	2
• PLANETARY FLIGHTS	—	—	—
• ENGINES			
ION (10 FLIGHTS/ENGINE)	240+32*	210 + 28*	270 + 36*
CHEMICAL (20 FLIGHTS/ENGINE)	8 + 2*	8 + 2*	8 + 2*

*SPARES

Figure 3.3.1-4: Production Quantities for Low-Thrust Concepts

into LEO. Figures 3.3.1-5 and 3.3.1-6 show the number of SDV launches required to service the various scenarios. Note in Figure 3.3.1-5, that both

	AEROBRAKED CHEMICAL OTV	ROTATING BED ROCKET PLUS ABMOTV	SPACE BASED LASER	GROUND BASED LASER	AEROBRAKED SOLAR THERMAL ROCKET
OTV FLEET SIZE REQUIRED	10	10	8+10 CHEM	10+2 CHEM	10 + 2 CHEM
SDV LAUNCHES REQUIRED TO MAINTAIN FLEET	6	13	8	8	8
SDV LAUNCHES REQUIRED TO INTRODUCE UNIQUE SUPT EQUIPMENT	—	1	3/14 (3 MW/25 MW) LASER	—	—
SDV LAUNCHES REQUIRED TO PROVIDE EXPENDABLES	134 (6900 MT)	84 (4375)	35/24 (1810/1170)	37 (1920 MT)	35 (1825 MT)
SDV LAUNCHES REQUIRED TO SUPPORT SUPP. CHEM OTV's	—	—	48	43	43
TOTAL SDV LAUNCHES	140	98	94	88	86

REVISED 3-16-81: ADD 52.5 MT SDV LH₂ TANKER & AEROBRAKED SOLAR THERMAL ROCKET

REVISED 3-26-81: INCLUDES ALL CONSUMABLE & 1100 SEC SOLAR ROCKET

*Figure 3.3.1-5: Comparison of SDV Launch Requirements —
Low Model High-Thrust Concepts*

	SPV-ION	TPV-ION	NPS-ION
<u>ADVANCED VEHICLES</u>			
OTV FLEET SIZE	(15)	(15)	(15)
SDV OTV LAUNCHES	3	3	3
SDV PROPELLANT LAUNCHES	6	8	10
TOTAL FOR ADV. OTV's	9	11	13
<u>SUPPLEMENTARY CHEM OTV's</u>			
SDV CHEM OTV LAUNCHES	1	1	1
SDV CHEM PROPELLANT LAUNCHES	43	43	43
TOTAL SDV LAUNCHES	53	55	57

*Figure 3.3.1-6: Comparison of SDV Launch Requirements—
Low Model Low-Thrust Concepts*

the 3-MW and 25-MW space-based laser options were investigated and that the savings in fuel launches produced by going to the higher power laser were exactly cancelled by the increased launch mass of the laser itself. The tanker vehicles used in estimating the number of SDV launches required for propellants are shown in Figures 3.3.1-7 and 3.3.1-8. By coincidence, both had delivered a fuel capacity around 52.5t and a lifetime of 50 missions. The argon propellant for the electric vehicles was assumed to be launched space available in disposable tanks with other payloads, so individual tankers were not designed or costed.

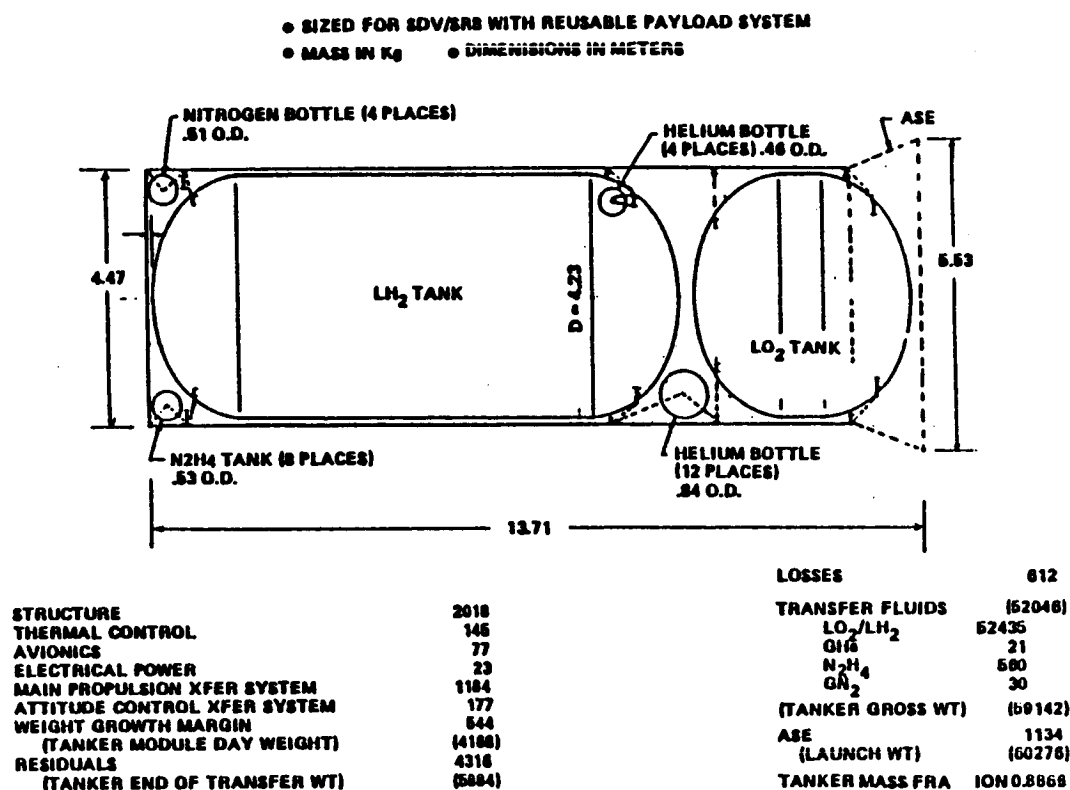
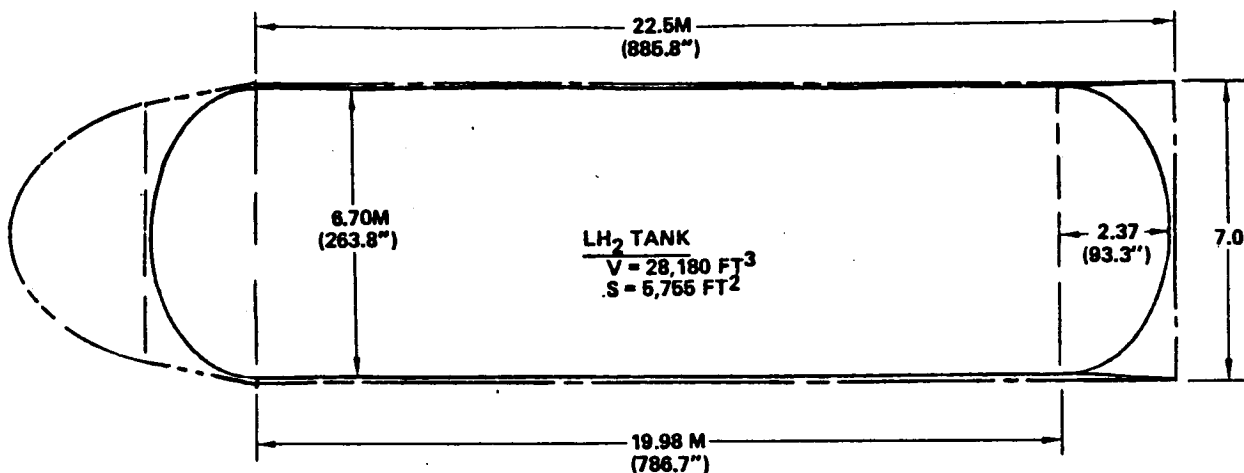


Figure 3.3.1-7: Propellant Tanker

TOTAL LH₂ MASS (4% ULLAGE & LOADING ON GROUND) ~ 54.35 MT



- NOTE: (1) TANK REMAINS INSIDE SDV SHROUD
(2) TANK TRANSFERS FUEL DIRECTLY TO USING SPACECRAFT

Figure 3.3.1-8: Maximum Size LH₂ Tank Compatible with SDV-1 Launch—Ground-Based Tank Module

3.3.2 System Acquisition Costs

System acquisition costs are the DDT&E and production costs for each vehicle type involved in a particular scenario. For scenarios examined here, the vehicles usually required were (1) the chemical AB OTV used for the manned portion of the mission model, (2) the advanced propulsion vehicle used for delivery and planetary missions, (3) the reusable shuttle-derivative vehicles used to launch vehicles, equipment, and propellant tankers into LEO, and (4) the tanker vehicles used to carry the propellants into LEO.

Ground rules used for determining the DDT&E and production costs are shown in Figure 3.3.2-1. The primary tool used for estimating DDT&E and production costs was the Boeing-developed parametric cost model (PCM). PCM develops costs from physical hardware descriptions and program schedules and allows the integration of any known costs (or outside-generated costs such as subcontractor or vendor estimates) into the total estimate. In this way, we can assemble a program cost from the best available source data. Engine and powerplant costs came from the advocate data base. Costs of the other subsystems are based on costs generated in Reference 1.

- BOEING PCM USED TO ESTIMATE DDT&E AND PRODUCTION COSTS FOR FLIGHT VEHICLES AND GSE
- AIRBORNE SUPPORT EQUIPMENT ASE COSTS DERIVED FROM PHASE A COSTS
- 2.75 EQUIVALANT UNITS OF TEST HARDWARE (FLT. VEHICLES AND ASE)
- 2 SETS OF GSE INCLUDED IN DDT&E
- ONE TEST FLIGHT INCLUDED IN DDT&E
- FLIGHT TEST UNITS REFURBISHED FOR OPERATIONAL FLEET
- 10% INITIAL SPARES
- 90% PRODUCTION LEARNING CURVE ON STAGES
- 95% PRODUCTION LEARNING CURVE ON ENGINES
- ENGINES/ POWERPLANT COSTS FROM ADVOCATE DATA BASE

Figure 3.3.2-1: System Acquisition Costing Groundrules


DDT&E and theoretical first unit (TFU) costs for each OTV type are presented as Figures 3.3.2-2 through 3.3.2-9. The methodology and assumptions to calculate these estimates are found in Volume III. Only the results of cost


DDT&E	(\$95.0)	TFU	(30.8)
• FLIGHT HARDWARE DESIGN	(369.5)		
STRUCTURE	15.3	STRUCTURE	4.5
THERMAL CONTROL	10.2	THERM. CON	0.6
AVIONICS	32.2	AVIONICS	11.1
POWER	10.6	POWER	3.8
PROPULSION	275.0 (1)	PROPULSION	5.5
ATTITUDE CONTROL	1.2	ATT. CON.	0.9
BALLUTE	25.0	ASSY. & C/O	4.4
• SYSTEMS ENGRG. & INTEGRATION	(15.2)		
• INITIAL TOOLING	(10.3)		
• SYSTEMS TEST	(202.9)		
TEST HARDWARE	128.5		
TEST OPERATIONS	74.4		
• ASE	(11.4)		
• GSE	(18.9)		
• SOFTWARE	(19.3)		
• LIAISON/DATA	(8.2)		
• PROGRAM MANAGEMENT	(39.3)		

MILLIONS OF 1980 DOLLARS

(1) INCLUDES ADVANCED SPACE ENGINE AT \$271 M DDT&E, \$1.86 M TFU

Figure 3.3.2-2: H₂O₂ OTV DDT&E and TFU Cost Estimate

<u>DDT & E</u>	(1048.8)
• FLIGHT HARDWARE DESIGN	(609.2)
STRUCTURE	25.6
THERMAL CONTROL	14.6
AVIONICS	32.2
POWER	10.6
PROPULSION 	500
ATTITUDE CONTROL	1.2
BALLUTE	25.0
• SYSTEMS ENGRG. & INTEGRATION	33.5
• INITIAL TOOLING	18.0
• SYSTEMS TEST	
TEST HARDWARE	127.6
TEST OPERATIONS	129.8
• ASE	12.0
• GSE	31.4
• SOFTWARE	32.1
• LIAISON DATA	10.8
• PROGRAM MANAGEMENT	44.4


<u>TFU</u>	(48.4)
STRUCTURE	9.3
THERMAL CONTROL	1.0
AVIONICS	11.1
POWER	3.8
PROPULSION 	15
ATTITUDE CONTROL	0.9
ASSEMBLY & C/O	5.3


MILLIONS OF 1980 DOLLARS

 COST FROM LA-5044-MS VOL. III (1972) UPDATED TO 1980

 ENGINE COST \$9M

Figure 3.3.2-3: Rotating-Bed Rocket DDT&E and TFU Cost Estimate

<u>DDT & E</u>	(\$612.9M)
• FLIGHT HARDWARE DESIGN	(311.8)
STRUCTURE	14.8
THERMAL CONTROL	11.8
AVIONICS	32.2
POWER	12.8
PROPULSION 	239
ATTITUDE CONTROL	1.2
• SYSTEMS ENGRG. & INTEGRATION	16.8
• INITIAL TOOLING	13.3
• SYSTEMS TEST	
TEST HARDWARE	93.5
TEST OPERATIONS	80.4
• ASE	12
• GSE	21.2
• SOFTWARE	22.4
• LIAISON DATA	8.1
• PROGRAM MANAGMENT	33.4

<u>TFU</u>	\$34 M
STRUCTURE	4.3
THERMAL CONTROL	0.7
AVIONICS	11.1
POWER	6.0
PROPUSION 	7.0
ATTITUDE CONTROL	0.9
ASSEMBLY & C.O	4.0

MILLIONS OF 1980 DOLLARS

 INCLUDES \$25 M FOR DEVELOPMENT OF LIGHTWEIGHT RECIEVER, \$10M FOR POINTER TRACKER, AND \$200 M FOR LASER ENGINE

 INCLUDES \$0.5 M FOR RECIEVER, \$2.0 M FOR POINTER/TRACKER & \$2.5 M FOR LASER ENGINE

Figure 3.3.2-4: Space-Based Laser OTV DDT&E and TFU Cost Estimate

<u>DDT & E</u>	(853.6)	<u>TFU</u>	(401)
• FLIGHT HARDWARE DESIGN	(520.4)		
STRUCTURE	20.0	STRUCTURE	6.5
THERMAL CONTROL	14.2	THERMAL CONTROL	1.0
AVIONICS	32.2	AVIONICS	11.1
POWER	12.8	POWER	6.0
PROPULSION ¹	440	PROPULSION ²	10.0
ATTITUDE CONTROL	1.2	ATTITUDE CONTROL	0.9
• SYSTEMS ENGRG. & INTEGRATION	18.0	ASSEMBLY & C.O.	4.6
• INITIAL TOOLING	16.0		
• SYSTEMS TEST			
TEST HARDWARE	110.3		
TEST OPERATIONS	84.4		
• ASE	12.0		
• GSE	22.9		
• SOFTWARE	24.0		
• LIAISON DATA	8.9		
• PROGRAM MANAGMENT	36.7		

MILLIONS OF 1980 DOLLARS

¹ INCLUDES \$10 M TRACKER, \$25 M RECIEVER, \$250 M LASER THRUSTER & \$150 M SOLAR THRUSTER

² INCLUDES \$2 M TRACKER, \$1.0 M RECIEVER, \$2.5 M LASER THRUSTER & \$2 M SOLAR THRUSTER

Figure 3.3.2-5: Ground-Based Laser DDT&E and TFU Cost Estimate

<u>DDT & E</u>	(777.8)	<u>TFU</u>	(33.8)
• FLIGHT HARDWARE DESIGN	(448.6)		
STRUCTURE	19.0	STRUCTURE	6.1
THERMAL CONTROL	13.4	THERMAL CONTROL	0.9
AVIONICS	32.2	AVIONICS	11.1
POWER	12.8	POWER	6.0
PROPULSION ¹	345	PROPULSION ²	4.8
ATTITUDE CONTROL	1.2	ATTITUDE CONTROL	0.9
BALLUTE	25.0	ASSEMBLY & C.O.	4.0
• SYSTEMS ENGRG. & INTEGRATION	20.2		
• INITIAL TOOLING			
• SYSTEMS TEST	14.7		
TEST HARDWARE	93.0		
TEST OPERATIONS	90.0		
• ASE	11.2		
• GSE	25.6		
• SOFTWARE	26.9		
• LIAISON DATA	9.1		
• PROGRAM MANAGMENT	37.5		

MILLIONS OF 1980 DOLLARS

¹ INCLUDES 1500 lb_f LOX-LH₂ ENGINE AT \$164M AND SOLAR COLLECTOR AT \$27 M

² INCLUDES 1500 lb_f LOX-LH₂ ENGINE AT \$0.8 M AND SOLAR COLLECTOR AT \$0.8 M

Figure 3.3.2-6: Solar Thermal Rocket DDT&E and TFU Cost Estimate

DDT & E	(520)	TFU	(107)
• FLIGHT HARDWARE	(162)		
POWER GENERATION	100	POWER GENERATION	58.4
THRUSTERS	1.4	THRUSTERS	6.3
PPU	4.8	PPU	9.6
STR,TANK & TCU	11.8	STR,TANK & TCU	0.7
AVIONICS	32	AVIONICS	12
OTHER (RCS & EPS)	12	OTHER	6
• SYSTEM ENGRG. & INTEG.	14	ASSEMBLY & C/O	14.0
• TOOLING	6		
• SYSTEMS TEST			
TEST HARDWARE	194		
TEST OPERATIONS	58		
• ASE	12		
• GSE	12		
• SOFTWARE	19		
• LIAISON/DATA MANAG.	8		
• PROGRAM MANAGEMENT	35		

MILLIONS OF 1980 DOLLARS

Figure 3.3.2-7: 445-kw SPV-Ion DDT&E and TFU Cost Estimates

DDT & E	(480)	TFU	(70)
• FLIGHT HARDWARE	(119)		
POWER GENERATION	48	POWER GENERATION	20.6
THRUSTERS	1.4	THRUSTERS	5.6
PPU	7.1	PPU	16.4
STR,TANK & TCU	18.5	STR,TANK & TCU	1.4
AVIONICS	35	AVIONICS	12
OTHER (RCS & EPS)	12	OTHER	5
• SYSTEM ENGRG. & INTEG.	18	ASSEMBLY & C/O	9.0
• TOOLING	19		
• SYSTEMS TEST			
TEST HARDWARE	133		
TEST OPERATIONS	84		
• ASE	12		
• GSE	23		
• SOFTWARE	24		
• LIAISON	10		
• PROGRAM MANAGMENT	38		

Figure 3.3.2-8: 311-kw TPV-Ion DDT&E and TFU Cost Estimates

DDT & E	(946)	TFU	(120)
• FLIGHT HARDWARE	(473)		
POWER GENERATION	400	POWER GENERATION	45
THRUSTERS	1.4	THRUSTERS	7.3
PPU	7.1	PPU	21.1
STR,TANK & TCU	17.5	STR,TANK & TCU	2.8
AVIONICS	36	AVIONICS	12
OTHER (RCS&EPS)	12	OTHER	5
• SYSTEM ENGRG. & INTEG.	22	ASSEMBLY & C/O	26.8
• TOOLING	30		
• SYSTEMS TEST			
TEST HARDWARE	216		
TEST OPERATIONS	96		
• ASE	12		
• GSE	21		
• SOFTWARE	22		
• LIAISON	11		
• PROGRAM MANAGMENT	43		

Figure 3.3.2-9: 374-kw NPS-Ion DDT&E and TFU Cost Estimates

estimating procedures will be included here. Note that the test hardware for the electric vehicle was equivalent to only one unit and not 2.75 units as assumed for the thermodynamic rockets (because of the modular test approach with electric vehicles).

Production costs were estimated using production quantities described in Section 3.3.1 and the learning curves shown in Figure 3.3.2-1. The resultant acquisition costs for the various OTV's and their individual support systems are shown in Figures 3.3.2-10 and 3.3.2-11. This does not include the DDT&E and production costs of the SDV launch vehicles or the tankers. These numbers were calculated separately using data obtained from Reference 1 and are found in Volume III.

<u>DDT& E COSTS</u>	<u>CHEMICAL ABOTV</u>	<u>NUCLEAR RBR</u>	<u>SPACE-BASED LASER</u>	<u>GROUND-BASED LASER</u>	<u>SOLAR ABOTV</u>
ADVANCED OTV's	-	1050	615	855	780
CHEMICAL SUPPORT OTV's	695	-	695	695	695
SUPPORT SYSTEMS	-	100	2465 (25 MW FEL)	530 (200 MW EDL)	-
<u>PRODUCTION COSTS</u>					
ADVANCED OTV's	375	1000	355	570	445
CHEMICAL SUPPORT OTV's	-	-	375	90	90
PECULIAR SUPPORT SYSTEMS	-	30	955	-	-
TOTAL	1070	2180	5460	2740	2010

COSTS IN MILLIONS OF 1980 DOLLARS

Figure 3.3.2-10: High-Thrust System Acquisition Costs

	SPV-ION	TPV-ION	NPS-ION
<u>DDT & E COSTS</u>			
ADVANCED OTV's	520	480	946
CHEM SUPPORT OTV's	695	695	695
SUPPORT SYSTEMS	-	-	100
<u>PRODUCTION COSTS</u>			
ADVANCED OTV's (15)	1755	1125	1875
SUPPLEMENTARY CHEM OTV's (2)	90	90	90
SUPPORT SYSTEMS	-	-	30
TOTAL ACQUISITION COST	3060	2390	3736

COST IN MILLIONS OF 1980 DOLLARS

Figure 3.3.2-11: Low-Thrust System Acquisition Costs

3.3.3 Operations Costs

OTV operations costs were developed from several sources, with the Phase A OTV study (Reference 2) providing most of the ground rules. For flight-related costs, the largest item is the \$2.5M charge per flight for mission-peculiar software and data, which comes directly from the Phase A cost analysis. Other flight-related operations costs are 1.3% of TFU per flight for operational spares and \$100,000 per flight to purchase propellant. The yearly costs are principally for facilities and manpower and these were assumed to be \$36M per year for the thermodynamic rockets and \$38M per year for the electric vehicles. These costs include the charges for space-based operations, ground operations, and sustaining engineering. There is a fixed \$30M per year charge for space-based operations (maintenance, fueling, payload manifesting, etc.). This charge is the same for all concepts because all are space based, all will require turnaround in about the same length of time, and all, except the chemical AB OTV, have unique handling problems which will cause them to be remotely serviced from the LEO base.

Because no discriminators could be found between propulsion concepts with respect to LEO base manpower and because the cost of LEO base operations is still very tentative, a fixed yearly charge was assessed for operations and sustaining engineering. The difference between the yearly cost of the high-thrust rockets and the electrics is because the electrics have multiple missions flying most of the time and need extra ground support. OTV operation cost estimates are summarized in Figure 3.3.3-1. The basic flight-related cost was \$2.75M per flight. This was the cost of mission software, data, spares, and propellant for the chemical AB OTV. There was an additive cost for equipment expended, which for the chemical AB OTV amounted to \$0.5M for the ballute and related hardware. For the other advanced propulsion concepts, the basic flight-related cost is multiplied by a complexity factor which denotes the estimated increase in mission complexity and spares cost. The solar AB OTV is the only other concept with expendable equipment and the \$1.3M per flight additive charge reflects the cost of the solar collector plus the ballute.

	CHEMICAL ABOTV	NUCLEAR RBR	SPACE-BASED LASER OTV	GROUND-BASED LASER OTV	SOLAR ABOTV	SPV ION	TPV ION	NPS ION
<u>YEARLY COSTS</u>								
\$30 M/YR SPACE-BASED OPERATIONS	480	480	480	480	480	480	480	480
\$6-8 M/YR GROUND SUPPORT	95	95	95	95	95	130	130	130
<u>FLIGHT RELATED COSTS</u>								
\$2.75 M/YR FLIGHT OPS + EXPENDABLES	720 (1x+0.5)	1220 (2.0x)	850 (1.5x)	855 (1.5x)	930 (1.2x +1.3)	855 (1.5x)	815 (1.4x)	1070 (2.0x)
TOTAL OTV OPS COSTS	1295	1795	1425	1430	1505	1465	1425	1680

COST IN MILLIONS OF 1980 DOLLARS

Figure 3.3.3-1: OTV Operations Costs—Low Model

SDV operations costs were estimated to be \$22M per launch using data from Reference 1. Later data concerning the increased cost of solid propellant indicate that \$33M per launch might be a better number. Both launch costs were used to determine the impact. Tanker operations costs were estimated to be \$1.5M per mission. STS operations costs are dependent upon the payloads launched, which are the same for each system. A constant STS operations cost of \$1860M was estimated assuming 64 shuttle launches would be required to support OTV operations.

3.3.4 Life Cycle Costs

The life cycle costs are the combined total of the DDT&E, production, and operations costs over the 16 years of the mission model. Summaries of the life cycle cost estimates divided by hardware element are shown in Figures 3.3.4-1 and 3.3.4-2. Note that these cost estimates include the costs of developing and producing the shuttle-derivative vehicles and the propellant tankers as well as the OTV's.

An interesting conclusion from the life cycle costing was that the operational cost savings accrued by using the advanced propulsion vehicles would be completely cancelled by the increased system acquisition costs of having developed two separate vehicle types to service the low mission model. The nuclear rotating-bed rocket scenario does not require development of the

<u>QTV SYSTEMS</u>	<u>SPACE BASED CHEMICAL ABOTV</u>	<u>NUCLEAR ROTATING BED ROCKET</u>	<u>SPACE BASED LASER + COTV</u>	<u>GROUND BASED LASER + COTV</u>	<u>SOLAR THERMAL ROCKET + COTV</u>
DDT&E	695	1150	3775	2080	1475
PRODUCTION	365	1030	1685	660	535
OPERATIONS	<u>1295</u>	<u>1795</u>	<u>1425</u>	<u>1430</u>	<u>1505</u>
	2355	3975	6885	4170	3515
<u>TANKER</u>					
DDT&E	215	310	410	410	410
PRODUCTION	100	80	130	130	130
OPERATIONS	<u>200</u>	<u>125</u>	<u>35</u>	<u>55</u>	<u>55</u>
	515	515	575	595	595
<u>SDV/RPS</u>					
DDT&E	1100	1100	1100	1100	1100
PRODUCTION	450	450	450	450	450
OPERATIONS	<u>3080</u>	<u>2155</u>	<u>2070</u>	<u>1935</u>	<u>1890</u>
	4630	3705	3620	3485	3440
<u>STS</u>					
DDT&E	-	-	-	-	-
PRODUCTION	-	-	-	-	-
OPERATIONS	<u>1860</u>	<u>1860</u>	<u>1860</u>	<u>1860</u>	<u>1860</u>
TOTAL LCC	9360	10055	12940	10110	9410

COST IN MILLIONS OF 1980 DOLLARS

Figure 3.3.4-1: Life Cycle Cost Summary by Hardware Element—High-Thrust Concepts

<u>QTV SYSTEMS</u>	<u>SPV-10N + COTV</u>	<u>TPV-10N + COTV</u>	<u>NPS-10N + COTV</u>
DDT&E	1215	1175	1740
PRODUCTION	1845	1215	1995
OPERATIONS	<u>1465</u>	<u>1425</u>	<u>1680</u>
	4525	3815	5415
<u>SDV/RPS</u>			
DDT&E	1100	1100	1100
PRODUCTION	450	450	450
OPERATIONS	<u>1165</u>	<u>1210</u>	<u>1255</u>
	2715	2760	2805
<u>COTV TANKER</u>			
DDT&E	215	215	215
PRODUCTION	70	70	70
OPERATIONS	<u>65</u>	<u>65</u>	<u>65</u>
	350	350	350
<u>STS</u>			
DDT&E	-	-	-
PRODUCTION	-	-	-
OPERATIONS	<u>1860</u>	<u>1860</u>	<u>1860</u>
TOTAL LCC	9450	8785	10430

COST IN MILLIONS OF 1980 DOLLARS

Figure 3.3.4-2: Life Cycle Cost Summary by Hardware Element, Low-Thrust Concepts

chemical rocket because it would be capable of performing the manned missions, but its high development and production costs would negate its operational cost savings also. The one possible exception would be the TPV-ion scenario, which showed a cost advantage over the chemical OTV scenario before interest costs during delivery were added.

The life cycle costs for the low model are summarized in Figure 3.3.4-3. Costs are those shown in the previous figures except interest charges during delivery have been added. Interest charges were calculated by adding the cost

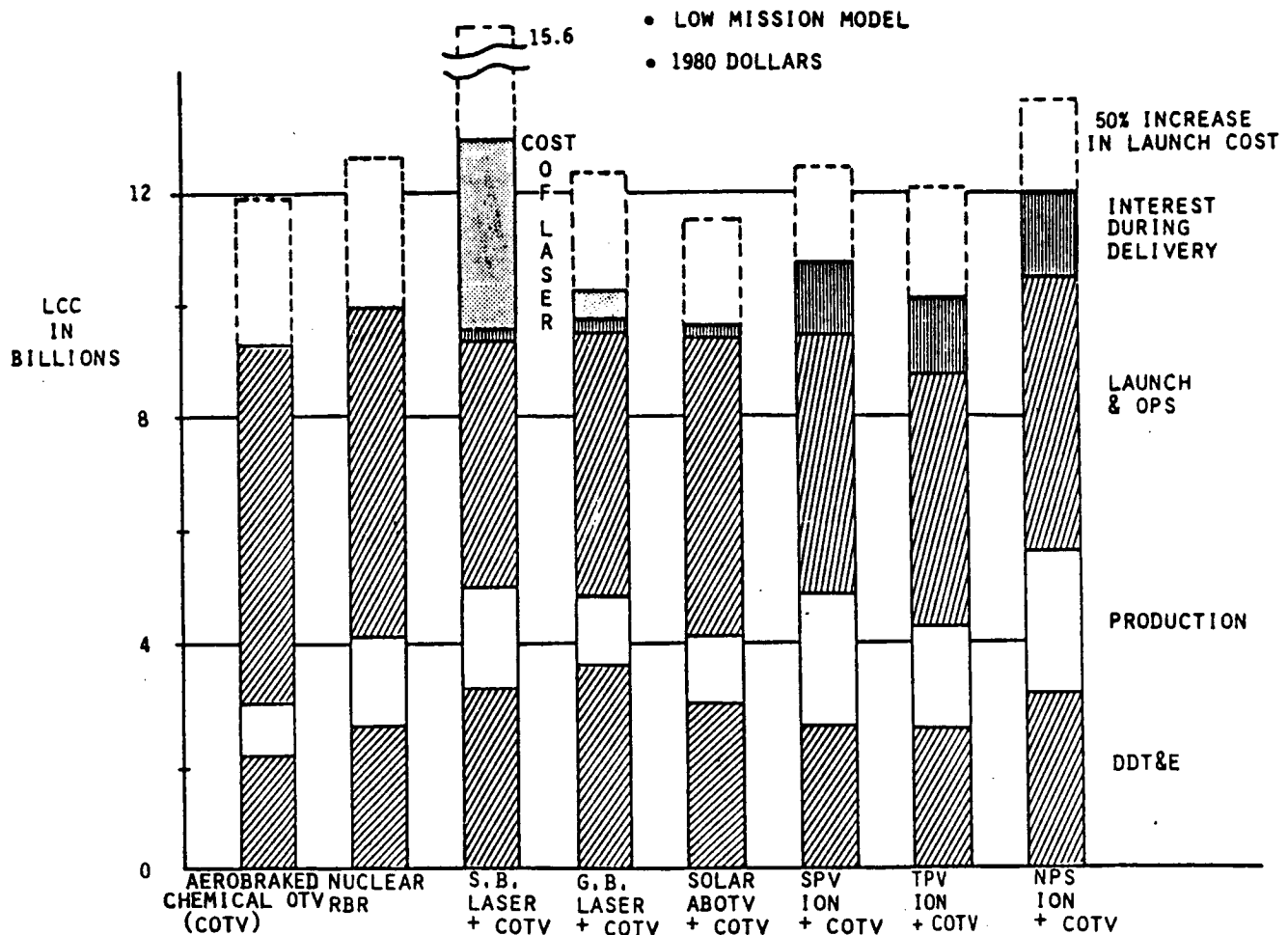


Figure 3.3.4-3: Life Cycle Cost Summary Chart

of the spacecraft (assumed to average \$100M) to the launch costs of the spacecraft and propellants and to the cost of the propellants themselves, and then determining the interest accrued (at 15% annual interest) on this amount during the LEO-to-GEO delivery time. This interest cost is equivalent to the interest paid by a user on the money invested at the time of launch until the time the spacecraft is deployed and begins earning revenue. The interest

costs vary from negligible for the high-thrust concepts, which deliver in 1/2 day, to \$1.5B for the NPS-ion vehicle, which requires 220 days. Also shown in Figure 3.3.4-3 is the increase in LCC if launch costs increase 50% as expected.

The most surprising result from the LCC estimates is that the chemical AB OTV would do so well. Based on these results, two conclusions can be drawn. First, it appears unlikely that any of the advanced options would ever be developed for cost-saving reasons within the low mission model. Second, because most advanced options do not increase LCC's either, there is a possibility one or more could be developed for a specific mission (as yet unspecified) and be used in a mixed fleet for little or no cost penalty.

3.3.5 High Mission Model Life Cycle Costs

LCC's for the high model were calculated in the same manner and using the same rules as LCC's for the low model. In fact, the high model contains the low model as a subset and can be incremented from it by adding the large vehicles and extra missions required. The new large OTV's were assumed to be delivered in 2005, some 10 years after the smaller vehicles associated with the low model. The vehicles selected for life cycle costing in the high model are characterized in Figure 3.3.5-1.

HIGH MODEL-60MT PAYLOAD					
	CHEMICAL ABOTV	NUCLEAR RBR	SOLAR ABOTV	SPV ION	TPV ION
INPUT POWER, MW	—	500	16.4	2.230	2.060
JET POWER, MW	—	460	10.4	1.565	1.450
ENGINE ION, SEC	485	1050	1100	6000	6000
VEHICLE THRUST, N	198,000 (each stage)	89,000	1825	56.0	49.3
STARTBURN MASS, KG	185,400	122,500	117,750	90,200	114,600
PROPELLANT MASS, KG	113,400	50,100	42,700	11,550	15,420
BURNOUT MASS, KG	5,120 (each stage)	11,760	11,250	18,890	39,320
POWER SOURCE, KG/KW	—	0.004	0.23	3.7	13
UPLEG TRIPTIME, DAYS	0.5	1.0	24	180	180

Figure 3.3.5-1: Characteristics of Vehicles Selected for Costing — High Model

The two laser powered vehicles and the NPS-ion vehicle were not costed in the high model for the following reasons. A comparison of SDV launch requirements for the thermodynamic (high thrust) systems is shown in Figure 3.3.5-2. The ground-based laser OTV requires seven more SDV launches than the

	HIGH MISSION MODEL—HIGH THRUST SYSTEMS				
	AEROBRAKED CHEMICAL OTV	ROTATING BED ROCKET	SPACE BASED LASER	GROUND BASED LASER	AEROBRAKED SOLAR ROCKET
FLEET SIZE REQUIRED	10 S + 20L	10 S + 20L	10 S + 20L	10 S + 20L	10 S + 20L
SDV LAUNCHES REQUIRED TO MAINTAIN FLEET	16	23	26	26	30
SDV LAUNCHES REQUIRED TO INTRODUCE UNIQUE SUPPORT EQUIP.	—	1	54	—	—
SDV LAUNCHES REQUIRED TO PROVIDE CONSUMABLES	977	465	227	363	352
SDV LAUNCHES REQUIRED TO SUPPORT SUPPLEMENTARY CHEM OTV's	—	—	73	58	58
TOTAL SDV LAUNCHES	1004	499	380	447	440

Figure 3.3.5-2: Comparison of SDV Launch Requirements

solar thermal AB OTV plus it has the cost of the laser. Therefore, the ground-based laser was dropped in favor of the solar thermal rocket. Likewise, the space-based laser OTV saves 60 SDV launches (between \$1320M and \$1980M) relative to the solar thermal rocket but requires the development and operation of a 100-MW laser in LEO. Even the most optimistic analyses place the cost of such a laser at \$5B (Reference 16); therefore, the space-based laser also was dropped in favor of the solar thermal rocket. The NPS-ion rocket was not competitive with other electric concepts for the low model and all indications were that scaling up the nuclear thermoelectric power system would not improve its specific power, so it was dropped in favor of the two solar electric concepts. The SDV launch requirements for the five remaining system concepts are shown in Figure 3.3.5-3, and the production quantities required to complete each scenario are shown in Figure 3.3.5-4.

	AEROBRAKED CHEMICAL OTV	NUCLEAR RBR	SOLAR ABOTV	SPV ION	TPV ION
FLEET SIZE REQUIRED	10S + 20L	10S+20L	10S+20L	15S+3M+40L	15S+3M+40L
SDV OTV LAUNCHES	27	33	30	16	32
SDV LAUNCHES OF UNIQUE SUPPORT EQUIP.	—	1	—	—	—
SDV LAUNCHES TO PROVIDE CONSUMABLES FOR UNMANNED MISSIONS	919	430	352	94	125
SDV LAUNCHES TO PROVIDE CONSUMABLES FOR MANNED MISSIONS	58	35	58	58	58
TOTAL SDV LAUNCHES	1004	499	440	168	215

Figure 3.3.5-3: Comparison of SDV Launch Requirements — High Mission Model

	CHEMICAL ABOTV	NUCLEAR RBR	SOLAR ABOTV	SPV ION	TPV ION
STAGES					
ADVANCED OTV'S					
FLEET SIZE	4	2	2	5	5
WEAR OUT	16	18	18	35	35
CHEMICAL OTV'S FOR ADDITIONAL MANNED MISSIONS	1	—	1	1	1
ENGINES					
ADVANCED PROPULSION (10 FLIGHTS/ENGINE)	—	38 + 2*	38 + 2*	3040	3600
CHEMICAL (20 FLIGHTS/ENGINE)	114	2	2	2	2

*SPARES

Figure 3.3.5-4: Production Quantities for Vehicles Unique to High Model

The DDT&E and TFU costs for the high model are shown in Figures 3.3.5-5 through 3.3.5-9. Costing rules were identical to those used for the low model except the avionics and propulsion DDT&E portions were costed at 10% of the values used for the low model. This savings was due to the assumption that the same technology would be used on the later high model vehicles as had been developed for the low model vehicles. OTV system acquisition costs for the high model are summarized in Figure 3.3.5-10.

<u>DDT& E</u> (527.7)		<u>TFU</u> (48.0)	
● FLIGHT HARDWARE DESIGN	(175)		
PROPULSION	100	PROPULSION	11.9
AVIONICS	3	AVIONICS	12
OTHER	72	OTHER	18.6
● SYSTEM ENGR. & INTEGRATION	11.3	ASSEMBLY & c/o	5.5
● INITIAL TOOLING	30.7		
● TEST HARDWARE	162.9		
● TEST OPERATIONS	63.5		
● ASE	12		
● GSE	14.3		
● SOFTWARE	15		
● LIAISON/DATA	8.4		
● PROGRAM MANAGEMENT	34.6		

Figure 3.3.5-5: Large Solar ABOTV DDT&E and TFU Cost Estimate

<u>DDT& E</u> (478.7)		<u>TFU</u> (51.)	
● FLIGHT HARDWARE DESIGN	(113)		
PROPULSION	50	PROPULSION	15
AVIONICS	3	AVIONICS	12
OTHER	60	OTHER	18
● SYSTEM ENGR. & INTEGRATION	19	ASSEMBLY & c/o	6
● INITIAL TOOLING	24.8		
● TEST HARDWARE	171.8		
● TEST OPERATIONS	58		
● ASE	12		
● GSE	18		
● SOFTWARE	19		
● LIAISON/DATA	8.4		
● PROGRAM MANAGEMENT	34.7		

Figure 3.3.5-6: Large Nuclear RBR DDT&E and TFU Cost Estimate

<u>DDT& E</u> (342.4)		<u>TFU</u> (34.5)	
● FLIGHT HARDWARE DESIGN	(83)		
PROPULSION	30	PROPULSION	7.5
AVIONICS	3	AVIONICS	12
OTH.	50	OTHER	11
● SYSTEM ENGR. & INTEGRATION	8	ASSY&C/O	4
● INITIAL TOOLING	12.1		
● TEST HARDWARE	121.9		
● TEST OPERATIONS	53.4		
● ASE	12		
● GSE	10		
● SOFTWARE	10.6		
● LIAISON/DATA	6.1		
● PROGRAM MANAGEMENT	25.3		

Figure 3.3.5-7: Large Chemical ABOTV DDT&E and TFU Cost Estimate

<u>DDT& E</u> (493.3)		<u>TFU</u> (228)	
● FLIGHT HARDWARE DESIGN	(64)		
PROPULSION	22	PROPULSION	180
AVIONICS	3	AVIONICS	12
OTHER	39	OTHER	8
● SYSTEM ENGR. & INTEGRATION	6.3	ASSEMBLY & C/O	26
● INITIAL TOOLING	30.6		
● TEST HARDWARE	268.3		
● TEST OPERATIONS	48.3		
● ASE	12		
● GSE	8		
● SOFTWARE	8.4		
● LIAISON/DATA	9.2		
● PROGRAM MANAGEMENT	38.2		

▷ \$45/WATT SOLAR ARRAY
 (85/YEAR PRODUCTION RATE)
 \$1M TFU THRUSTER + PPU

Figure 3.3.5-8: Large SDV-Ion DDT&E and TFU Cost Estimate

<u>DDT& E</u> (460)		<u>TFU</u> (148)	
● FLIGHT HARDWARE DESIGN	(91)		
PROPULSION	32	PROPULSION	109
AVIONICS	3	AVIONICS	12
OTHER	56	OTHER	10
● SYSTEM ENGR. & INTEGRATION	8.9	ASSEMBLY & c/o	17
● INITIAL TOOLING	45.5		
● TEST HARDWARE	180.3		
● TEST OPERATIONS	56.1		
● ASE	12		
● GSE	11.2		
● SOFTWARE	11.8		
● LIAISON/DATA	8.4		
● PROGRAM MANAGEMENT	34.6		

MILLIONS OF 1980 DOLLARS	
● PROPULSION	109
● AVIONICS	12
● OTHER	10
● ASSEMBLY & c/o	17

MILLIONS OF 1980 DOLLARS	
● PROPULSION	109
● AVIONICS	12
● OTHER	10
● ASSEMBLY & c/o	17

Figure 3.3.5-9: Large TPV-Ion DDT&E and TFU Cost Estimate

<u>DDT& E COSTS</u>	<u>CHEMICAL ABOTV</u>	<u>NUCLEAR RBR</u>	<u>SOLAR ABOTV</u>	<u>SPV ION</u>	<u>TPV ION</u>
LOW MODEL OTVS (ADV. & COTVS)	695	1150	1475	1215	1175
NEW HIGH MODEL OTVS	<u>340</u> 1035	<u>480</u> 1630	<u>530</u> 2005	<u>495</u> 1710	<u>460</u> 1635
<u>PRODUCTION COSTS</u>					
LOW MODEL ADVANCED OTVS	375	1000	445	1755	1125
HIGH MODEL ADVANCED OTVS	860	1890	1335	6680	5360
CHEMICAL SUPPORT OTVS	<u>-</u> 1235	<u>-</u> 2890	<u>135</u> 1915	<u>135</u> 8570	<u>135</u> 6620

MILLIONS OF 1980 DOLLARS

Figure 3.3.5-10: High Model Systems Acquisition Costs

OTV operations costs for the high model were calculated using the same ground rules as before. The yearly costs were calculated in two periods: the first, 1995-2004, is identical with the low model; the second, 2005-2010, has extensive flight operations leading up to the first SPS and is costed separately (see Figure 3.3.5-11 for the operations cost breakdown).

	CHEMICAL ABOTV	NUCLEAR RBR OTV	SOLAR ABOTV +COTV	SPV-ION + COTV	TPV-ION + COTV
YEARLY COSTS (1995-2004)					
\$30 M/YR SPACE-BASED OPS	300	300	300	300	300
\$6-8 M/YR GROUND SUPPORT	60	60	60	80	80
YEARLY COSTS (2005-2010)					
\$150 M/YR SPACE-BASED OPS	750	750	750	750	750
\$30-40 M/YR GROUND SUPPORT	180	180	180	240	240
FLIGHT RELATED COSTS					
LOW MODEL VEHICLES	720	1220	1020	1050	1050
\$2.75 M/FLIGHT + EXPENDABLES	(1x+0.5)	(2.0x)	(1.2x+1.3)	(1.5x)	(1.5x)
HIGH MODEL VEHICLES	2850	2470	2850	2140	2140
\$3.25 M/FLIGHT + EXPENDABLES	(2x+1.0)	(2.0x)	(1.2x+3.6)	(1.5)	(1.5)
TOTAL OTV OPS COSTS	4860	4980	5160	4560	4560

COSTS IN MILLIONS OF 1980 DOLLARS

Figure 3.3.5-11: OTV Operations Costs, High Model

Interest charges for the high model are shown in Figure 3.3.5-12. The interest was charged for bulk cargo deliveries (i.e., nuclear waste disposal (NWD) and SPS demo) because they are not revenue-generating payloads.

	CHEM ABOTV	NUC RBR	SOLAR ABOTV	SPV ION	TPV ION
CAPITAL COST, \$M	205	165	160	140	145
ΔT , DAYS	0.5	1.0	24	180	180
INTEREST COST, \$M PER FLIGHT	.039	0.063	1.477	9.990	10.346
<hr/>					
HIGH MODEL, \$M INTEREST COST	-	3.5	167	1242	1466

Figure 3.3.5-12: Interest Costs—High Model

LCC's for the high model are summarized in Figures 3.3.5-13 and 3.3.5-14. For the high model, there appear to be significant differences in LCC's between propulsion concepts. This is because launch costs for this large mission model begin to predominate, and the number of launches is largely a function of upper-stage specific impulse. The high model LCC's are shown in

	SPACE-BASED CHEMICAL ABOTV	NUCLEAR ROTATING BED ROCKET	SOLAR THERMAL ABOTV +COTV	SPV ION +COTV	TPV ION +COTV
OTV SYSTEMS					
DDT& E	1035	1630	2005	1710	1635
PRODUCTION	1235	2890	1915	8570	6620
OPERATIONS	4860	4980	5160	4560	4560
	<u>7130</u>	<u>9500</u>	<u>9080</u>	<u>14840</u>	<u>12815</u>
TANKER					
DDT& E	215	310	410	350	350
PRODUCTION	275 (20)	260 (10)	240 (8+2)	85 (2+2)	100 (3+2)
OPERATIONS	495	315	295	205	220
	<u>985</u>	<u>885</u>	<u>945</u>	<u>640</u>	<u>670</u>
SDV/RPS					
DDT& E	1100	1100	1100	1100	1100
PRODUCTION	2250 (10)	1125 (5)	1125 (5)	450 (2)	450 (2)
OPERATIONS	33130	16465	14520	5545	7095
	<u>36,480</u>	<u>18,690</u>	<u>16,745</u>	<u>7095</u>	<u>8645</u>
INTEREST DURING DELIVERY	15	3.5	167	1242	1466
TOTAL LCC	44610	29080	26940	23815	23495

COSTS IN MILLIONS OF 1980 DOLLARS

Figure 3.3.5-13: Life Cycle Costs Summary by Hardware Element for High Model

	CHEM ABOTV	NUC RBR	SOLAR ABOTV +COTV	SPV ION +COTV	TPV ION +COTV
DDT& E	2350	3040	3515	3160	3085
PRODUCTION	3760	4275	3280	9105	7170
OPERATIONS	38,485	21,760	19,975	10,310	11,875
INTEREST	-	3.5	167	1242	1466
TOTAL LCC	44,610	29,080	26,940	23,815	23,495

Figure 3.3.5-14: High Model LCC by Category

chart form in Figure 3.3.5-15. Observing the very large operation costs (mostly launch costs) of the chemical ABOTV, it appears that an investment in a heavy lift launch vehicle (HLLV) at the beginning of the high model would be a wise move. In this manner, an expenditure of \$5B to develop an HLLV by 2000 could save roughly half of the \$30B spent on fuel launches between 2000 and 2010. Development of an HLLV also appears to be cost effective for the

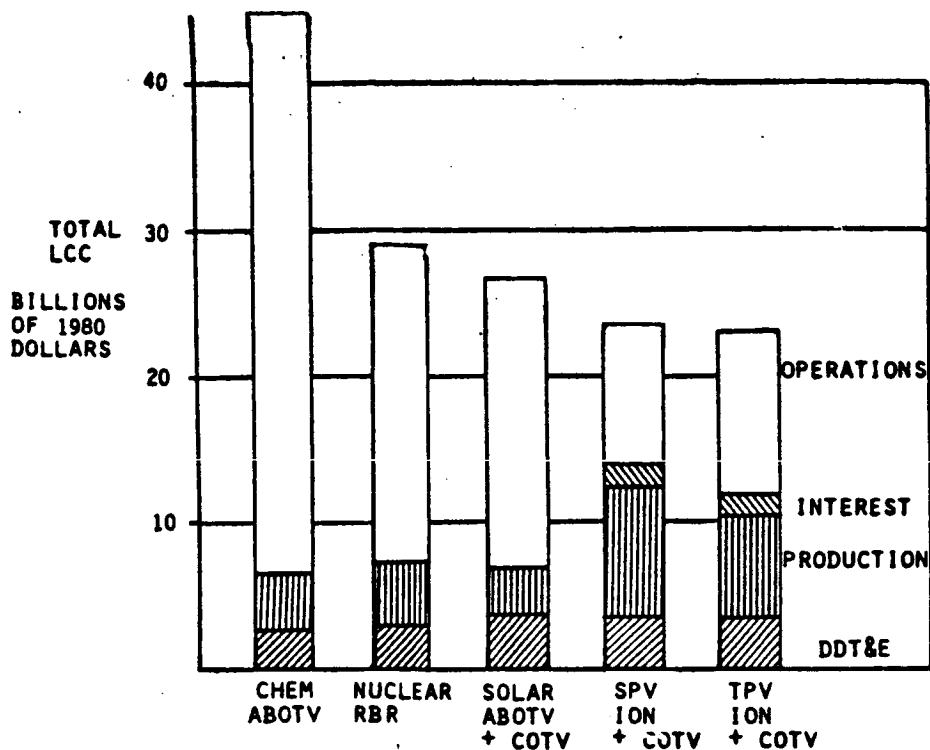


Figure 3.3.5-15: Life Cycle Cost Summary Chart—High Mission Model

nuclear rotating-bed reactor (RBR) and solar thermal AB OTV scenarios. Possible development of a new generation of launch vehicles was not part of this study and was not pursued any further; however, it appears that with the high model we have reached the point where development of an HLLV is economically justifiable.

3.4 Task 4 - Definition of Key Technology Development Requirements

This final task was to define key technology development requirements for each advanced propulsion option recommended for 1995 IOC. Unfortunately, the results of this study showed that no advanced propulsion options capable of early development would significantly improve space transportation in the early era (low mission model). Hence, the vehicle recommended for 1995 IOC is the advanced H_2-O_2 rocket with aeroassist, a vehicle whose development requirements are already well documented (References 1 and 2).

This does not mean that development of all other advanced propulsion technologies should be abandoned. Propulsion requirements in the future, as in the past, are highly dependent upon mission scenarios, and mission scenarios appear to change every 4 to 5 years. Hence, it is recommended that each propulsion option carried in Task 3 be subjected to periodic study and review. Then, if there is a technological breakthrough which could significantly enhance performance or costs or if mission requirements should change, a logical development sequence could be established. The above statements apply to the low mission model scenario. How about the long-term view of space transportation?

The high mission model assumes that humankind will embark upon a significant (and expensive) space industrialization scenario shortly after the year 2000. There is certainly nothing in the present political or economic climate to suggest this is possible, but 20 years is a long time and much can change. If a large-scale space industrialization or energy initiative should develop, a mixed fleet of upper-stage vehicles could be attractive. In this case, an H_2-O_2 aeroassisted OTV would be required for manned missions and priority cargo, with a solar thermodynamic or solar electric rocket for bulk cargo delivery. If a large laser should be developed, deployed, and operated by some other agency and be made available on demand for a nominal user fee, a laser thermodynamic rocket would also be very competitive as a bulk cargo carrier. If an additional mission scenario should occur from factors unforeseen at this time, the preferred vehicle mix could easily change. For instance, if manned exploration of the solar system should become a priority

mission, a nuclear thermodynamic rocket should be included; should unmanned deep-space exploration become a high priority mission, a nuclear electric vehicle should be added.

At the time of this writing (1981), two key technologies exist which appear worthy of enhanced development. One is the low-cost, vapor-deposited solar array which appears to offer not only an order of magnitude reduction in power supply costs but also the possibility of radiation hardening as well. Second is the lightweight inflatable collector which appears to be the key technology item for solar thermal, laser, and TPV-ion rockets. These two items should be pursued with technology development studies leading up to hardware demonstration.

Propulsion technology development for possible applications in the high model should be directed toward the general goals of increasing efficiency and reducing costs. Examples of such technology are: efficient coupling of radiant energy (solar or laser) with propellant/working fluid; high-efficiency direct nuclear-to-electric power conversion; or a low-cost, high-power, direct-pumped nuclear laser. Such items constitute technological breakthroughs which cannot be scheduled, but high leverage items such as these are worthy of a continued level of support.

One definite improvement in space transportation economics in the high model era would be improved launch vehicle economics from a second-generation shuttle or HLLV. This is beyond the scope of the current study, but any future effort to improve upper-stage transportation economics should include improved launch vehicles.

Looking further into the future, one sees a definite need for high-energy nuclear propulsion from fusion or pulsed fission rockets. They are the only propulsion systems capable of manned deep-space operations. They will undoubtedly require a long development cycle and the required design data should begin to be available in 1 to 2 years. Small study efforts to determine the design requirements for these vehicle types would be in order at that time.

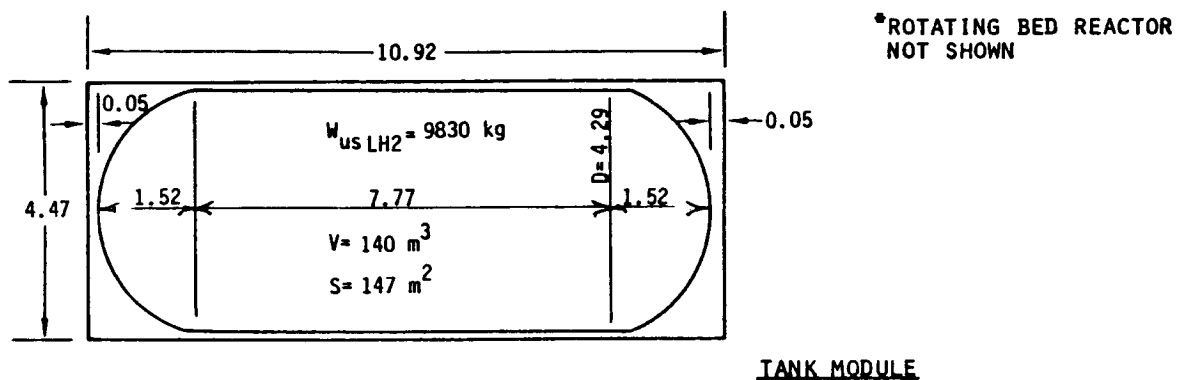
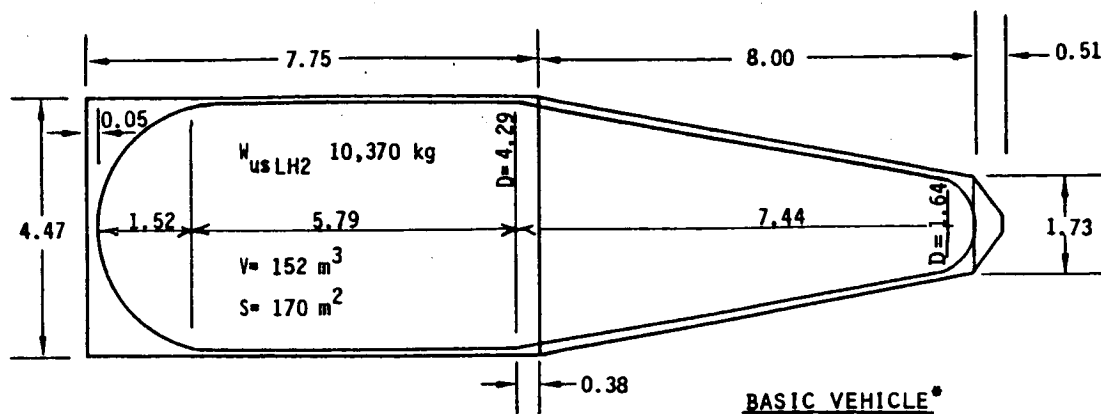
4.0 REFERENCES

1. Davis E. E., "Future Orbital Transfer Vehicle Technology Study," Final Report, Contract NAS1-16088, Boeing Aerospace Company, September 1981.
2. Caluori, V. A. et al, "Orbital Transfer Vehicle Concept Definition Study," Final Report, Contract NAS8-33532, Boeing Aerospace Company, D180-26090, vol. 1-6, 1980.
3. Cruz, M. I., "The Aerocapture Vehicle Mission Design Concept," AIAA paper No. 79-0893, JPL, July 1979.
4. Cruz, M. I., "Technology Requirements for a Generic Aerocapture System," AIAA paper No. 80-1493, JPL, July 1980.
5. Project Daedalus Study Group, "Project Daedalus: The Final Report on the BIS Starship Study," JBIS, vol. 31 supplement, 1978.
6. Warman, E. A., "Proceedings of the National Symposium on Natural and Manmade Radiation in Space," NASA TMX-2440, pp 40-64, January 1972.
7. Jones, W. S., Forsyth, J. B., and Skratt, J. P., "Laser Rocket System Analysis," NASA CR-159521, Lockheed Missiles & Space Company, September 1978.
8. Etheridge, F. G. et al, "Solar Rocket System Concept Analysis," Final Technical Report, AFRPL-TR-79-79, Space System Group, Rockwell International, November 1979.
9. Rodgers, R. J., "Initial Conceptual Design Study of Self-Critical Nuclear Pumped Laser Systems," NASA CR-3128, Final Report, Contract NAS1-14329, United Technology Laboratories, April 1979.
10. Boody, F. P. et al, "Progress in Nuclear-Pumped Lasers," Proceedings of the Third Conference on Radiation Energy Conversion in Space, Astic 202749, Ames Research Center, January 1978.
11. Kingsbury, D., "Atomic Rockets," Science Fact Department, Analog Science Fiction, Dec. 1975.
12. Selph, C. and Horning, W., "Laser Propulsion," IAF Paper 76-166, 27th IAF Congress, Anaheim, Calif., 1976.
13. Lindauer, G. C., Tichler, P., and Hatch, L. P., "Experimental Studies on High-Gravity Rotating Fluidized Beds," Brookhaven National Laboratory, BNL-50013 (T-435), Sept. 1966.

14. Shoji, J., "Solar Rocket Component Study," Phase 1 - Concept Assessment Review, AFRPL Contract F04611-80-C-0039, Rocketdyne Division of Rockwell International, April 1981.
15. Etheridge, F. G. et al, "Solar Rocket Concept Analysis," AFRPL-TR-79-79, Final Technical Report, Rockwell International, November 1979.
16. Holloway, P. F. and Garrett, L. B., "Utility of and Technology for a Space Central Power Station," Presented at 2nd AIAA Conference on Large Space Platforms, San Diego, California, 1981.

APPENDIX A

SUMMARY WEIGHT STATEMENT
SINGLE-STAGE NUCLEAR OTV



*Preliminary Configurations Single-Stage Nuclear OTV**
(Dimensions in Meters)

SUMMARY WEIGHT STATEMENT*
SINGLE-STAGE NUCLEAR OTV

	BASIC VEHICLE $W_p = 10.37t$	TANK MODULE $W_p = 9.83t$
STRUCTURE	2,145	1,918
THERMAL CONTROL	154	100
AVIONICS	285	27
ELECTRICAL POWER SYSTEM (EPS)	261	9
MAIN PROPULSION SYSTEM (MPS)	3,043	50
ATTITUDE CONTROL SYSTEM (ACS)	132	--
SPACE MAINTENANCE PROVISIONS	179	--
WEIGHT GROWTH MARGIN—EXCLUDE MAIN ENGINE INSTALLATION	503	315
(OTV DRY WEIGHT)	(6,702 kg)	(2,419 kg)
MPS RESIDUAL FLUIDS & GASES	229	209
ACS RESIDUAL FLUIDS & GASES	19	--
EPS RESIDUAL FLUIDS & GASES	9	--
ACS RESERVE PROPELLANT	36	--
EPS RESERVE PROPELLANT	27	--
MPS INFLIGHT LOSSES	258	227
MPS PROPELLANT—INCL RESERVE	10,370	9,830
ACS NOMINAL PROPELLANT	363	--
EPS NOMINAL REACTANT	136	--
(OTV GROSS WEIGHT)	(18,150 kg)	(12,685 kg)
OTV MASS FRACTION = $\frac{\text{MPS PROP, NOM + RESERVE}}{\text{GROSS WEIGHT}}$ =	0.571	0.775

*CONFIGURATION SKETCHES AND GROUP WEIGHT STATEMENTS ON FOLLOWING PAGES.

GROUP WEIGHT STATEMENT
SINGLE-STAGE NUCLEAR OTV

	BASIC VEHICLE $W_p = 10.37t$	TANK MODULE $W_p = 9.83t$
STRUCTURE	(2,145)	(1,918)
LH ₂ TANK-INCL SUPPORT STRUTS	726	689
BODY STRUCTURES	767	540
SANDWICH PANELS (10-MIL FACE SHTS)	508	412
FORWARD RING (LATCHING INTERFACE)	23	23
LH ₂ TANK SUPPORT RINGS	27	32
AFT RING (LATCHING INTERFACE)	--	32
AVIONICS RING SECTION	95	--
MISC. MOUNTING/SUPPORT STRUCTURES	9	9
RMS GRAPPLE FITTING	5	5
THRUST STRUCTURE	54	--
BERTHING PROBES-EXTENDABLE	14	--
UMBILICAL INTERFACE, OTV-TO-ASE	9	9
ASSEMBLY & INSTALLATION HARDWARE	23	18
LATCHING MECHANISM-FWD INTERFACE	45	45
UNIVERSAL DOCKING ADAPTER	113	227
METEOROID PROTECTION*	494	417
THERMAL CONTROL	(154)	(100)
ACTIVE THERMAL CONTROL	54	--
AVIONICS COOLING	36	--
FUEL CELL COOLING	18	--
INSULATION		
MLI INSULATION-LH ₂ TANK { 25 LAYERS OF	91	100
0.15-MIL KAPTON		100
MLI INSULATION-EPS TANKS	9	--

* SUPPORTING DATA ATTACHED

GROUP WEIGHT STATEMENT
SINGLE-STAGE NUCLEAR OTV

	BASIC VEHICLE $W_p = 10.37t$		TANK MODULE $W_p = 9.83t$	
AVIONICS		(285)		(27)
GUIDANCE & NAVIGATION		59		--
BASIC G&N	41		--	
GPS	18		--	
COMMUNICATIONS		35		--
DATA MANAGEMENT		77		--
RENDEZVOUS & DOCKING		46		--
INSTRUMENTATION		68		27
PROPELLANT LOADING/MEASUREMENT	27		23	
OTV MEASURING SYSTEM	41		4	
ELECTRICAL POWER SYSTEM (EPS)		(261)		(9)
POWER SOURCE		113		--
FUEL CELLS (2 @ 2.0 kW NOM/3.5 kW PEAK, EACH)	45		--	
BATTERY (25 AMP-HR)	11		--	
O ₂ TANK ASSY	20		--	
H ₂ TANK ASSY	10		--	
PLUMBING SYSTEMS	27		--	
CONVERSION & DISTRIBUTION		148		9
ELECTRONICS	57		--	
WIRE HARNESS	91		9	
MAIN PROPULSION SYSTEM (MPS)		(3,043)		(50)
MAIN ENGINE INSTALLATION*		2,830		--
PROPELLANT SYSTEM		68		18
LH ₂ FEED	45		9	
LH ₂ FILL, DRAIN, DUMP	23		9	
THRUST VECTOR CONTROL		91		--
PRESSURIZATION & VENT		36		27
LH ₂ TANK AUTOGENOUS PRESS SUPPLY	23		14	
LH ₂ TANK VENT/RELIEF - SPACE	13		13	
PNEUMATICS		18		5
PLUMBING SYSTEM	13		5	
HELIUM BOTTLE	5		--	

* CONSISTS OF ROTATING BED REACTION (1383 kg), 15% GROWTH MARGIN ON REACTOR (209 kg), INTERNAL SHIELDING (240 kg), AND EXTERNAL DISC SHIELD (998 kg). NO GROWTH REQUIRED ON SHIELDING.

GROUP WEIGHT STATEMENT
SINGLE-STAGE NUCLEAR OTV

	BASIC VEHICLE $W_p = 10.37t$	TANK MODULE $W_p = 9.83t$
ATTITUDE CONTROL SYSTEM (ACS)	(132)	(--)
THRUSTER MODULES (4)—INCL 24 THRUSTERS	30	--
TANKAGE/PROPELLANT SYSTEM	102	--
N ₂ H ₄ TANK ASSEMBLIES (5)	67	--
N ₂ H ₄ FEED	17	--
N ₂ H ₄ FILL, DRAIN, DUMP—SPACE BASING	5	--
N ₂ BOTTLES	9	--
N ₂ PRESS PLUMBING	4	--
SPACE MAINTENANCE PROVISIONS	(179)	(--)
CRITICAL AVIONICS ASSEMBLIES REMOVAL	25	--
FUEL CELL REMOVAL	12	--
MAIN ENGINE REMOVAL	68	--
THRUSTER MODULE REMOVAL	11	--
ADDITIONAL INSTRUMENTATION	41	--
BUILT-IN TEST EQUIPMENT	22	--
WEIGHT GROWTH MARGIN—EXCLUDE MAIN ENGINE INSTALLATION	(503)	(315)
OTV DRY WEIGHT	6,702 kg	2,419 kg
MPS RESIDUAL FLUIDS & GASES	(229)	(209)
TRAPPED LH ₂	14	14
GH ₂ IN EMPTY LH ₂ TANK	213	195
GHe FOR PNEUMATICS—TOTAL	2	--
ACS RESIDUAL FLUIDS & GASES	(19)	(--)
TRAPPED N ₂ H ₄	7	--
GN ₂	12	--
EPS RESIDUAL FLUIDS & GASES	(9)	(--)
TRAPPED O ₂	5	--
TRAPPED H ₂	1	--
TRAPPED PRODUCT WATER	3	--

GROUP WEIGHT STATEMENT
SINGLE-STAGE NUCLEAR OTV

	BASIC VEHICLE $w_p = 10.37t$	TANK MODULE $w_p = 9.83t$
ACS RESERVE PROPELLANT	(36)	(--)
EPS RESERVE REACTANT	(27)	(--)
MPS INFLIGHT LOSSES	(258)	(227)
LH ₂ FOR CHILLDOWN/START/STOP	22	--
LH ₂ BOILOFF/VENT LOSS-20 DAY	236	227
MPS PROPELLANT-INCL RESERVE	(10,370)	(9,830)
ACS NOMINAL PROPELLANT	(363)	(--)
EPS NOMINAL REACTANT-20 DAY	(136)	(--)
OTV GROSS WEIGHT	18,150 kg	12,685 kg

ADDED METEOROID PROTECTION ASSESSMENT

$$\text{TANK SIDE PROTECTED AREA} = \left\{ \begin{array}{l} 53 \text{ m}^2 \text{ BASIC VEHICLE} \\ 43 \text{ m}^2 \text{ TANK MODULE} \end{array} \right. \\ 96 \text{ m}^2$$

$$\text{TRIP TIME} = 20 \text{ DAYS} = 0.055 \text{ YR}$$

$$\text{AREA TIME PRODUCT} = 5.3 \text{ m}^2/\text{YR} \text{ (ASSUMES LEO STORAGE BETWEEN FLIGHTS)}$$

$$t_{\text{SHIELD,REQ'D}} = 0.112 \text{ cm AL} \left\{ \begin{array}{l} \text{ASSUMES } P_0 = 0.995, 1/3 \text{ BUMPER} \\ 2/3 \text{ BLACKWALL, 7.6 cm SPACING MIN.} \end{array} \right.$$

$$t_{\text{G/E SANDWICH FACE SHEET}} \times 2 = 0.050 \text{ cm G/E}$$

$$t_{\text{AL EQUIV, G/E SANDWICH FACE SHTS}} = 0.030 \text{ cm AL}$$

$$t_{\text{AL EQUIV OF MLI BLANKET}} = 0.005 \text{ cm AL*}$$

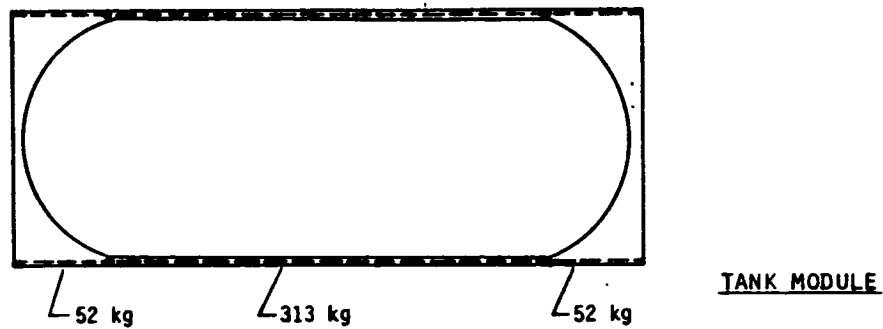
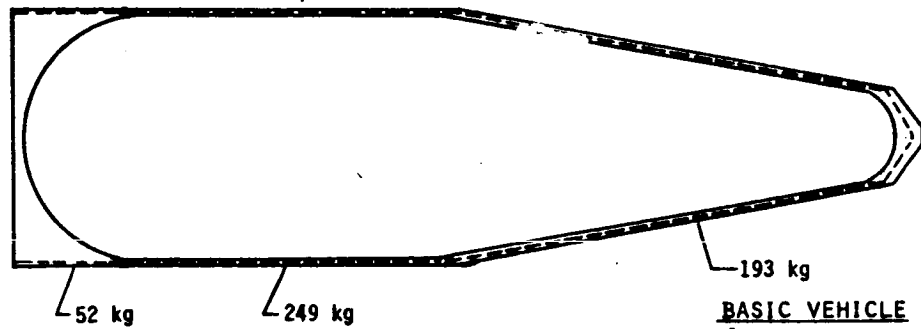
$$t_{\text{REQ'D, AL BACKWALL}} = \left\{ \begin{array}{l} 0.077 \text{ cm AL; 7.6 cm SPACING} \\ 0.095 \text{ cm AL; 6.4 cm SPACING} \end{array} \right.$$

$$\text{BACKWALL INSTALLATION FACTOR} = 10\%$$

$$\text{BACKWALL INSTALLED WEIGHT} = \left\{ \begin{array}{l} 2.34 \text{ kg/m}^2; 7.6 \text{ cm SPACING} \\ 2.88 \text{ kg/m}^2; 6.4 \text{ cm SPACING} \end{array} \right.$$

$$* \text{ 25-LAYER BLANKET} \left\{ \begin{array}{l} 2 \text{ LAYERS OF 0.5 MIL} \\ 23 \text{ LAYERS OF 0.15 MIL} \end{array} \right.$$

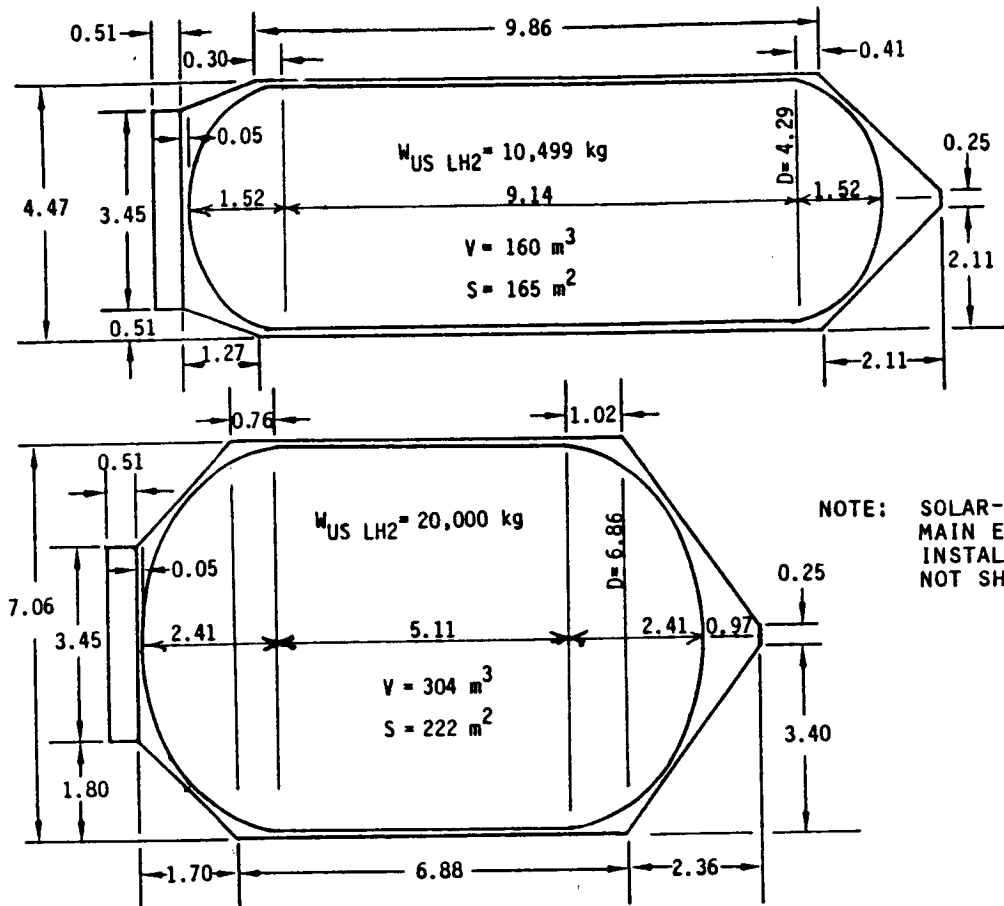
ADDED METEORIOD PROTECTION { --- 0.077 AL cm + 10% INSTL (2.34 kg/m²)
 = 0.095 AL cm + 10% INSTL (2.88 kg/m²)



Nuclear OTV

APPENDIX B

SUMMARY WEIGHT STATEMENT
SINGLE-STAGE SPACE-BASED SOLAR-POWERED OTV



NOTE: SOLAR-POWERED MAIN
MAIN ENGINE
INSTALLATION
NOT SHOWN

*Preliminary Configurations Solar/Laser OTV'S
(Dimensions in Meters)*

SUMMARY WEIGHT STATEMENT*
SINGLE-STAGE SPACE-BASED SOLAR-POWERED OTV

	<u>W_p = 10.5t</u>	<u>W_p = 20.0t</u>
STRUCTURE	2,082	3,156
THERMAL CONTROL	204	254
AVIONICS	285	285
ELECTRICAL POWER SYSTEM (EPS)	494	494
MAIN PROPULSION SYSTEM (MPS)	1,333	1,333
ATTITUDE CONTROL SYSTEM (ACS)	102	132
SPACE MAINTENANCE PROVISIONS	145	145
WEIGHT GROWTH MARGIN—EXCLUDE MAIN ENGINE INSTALLATION	508	683
(OTV DRY WEIGHT)	(5,153 kg)	(6,482 kg)
MPS RESIDUAL FLUIDS & GASES	227	421
ACS RESIDUAL FLUIDS & GASES	19	19
EPS RESIDUAL FLUIDS & GASES	6	6
ACS RESERVE PROPELLANT	23	36
EPS RESERVE PROPELLANT	--	--
MPS INFLIGHT LOSSES	408	635
MPS PROPELLANT—INCL RESERVE	10,499	20,000
ACS NOMINAL PROPELLANT	227	363
EPS NOMINAL REACTANT	9	9
(OTV GROSS WEIGHT)	(16,571 kg)	(27,972 kg)
OTV MASS FRACTION = $\frac{\text{MPS PROP. NOM + RESERVE}}{\text{GROSS WEIGHT}}$ =	0.634	0.715

*CONFIGURATION SKETCHES AND GROUP WEIGHT STATEMENTS ON FOLLOWING PAGES.

SUMMARY WEIGHT STATEMENT
SINGLE-STAGE SPACE-BASED SOLAR-POWERED OTV

	<u>W_p = 10.5t</u>	<u>W_p = 20.0t</u>
STRUCTURE	(2,082)	(3,156)
LH ₂ TANK—INCL SUPPORT STRUTS	734	1,397
BODY STRUCTURES	671	880
SANDWICH PANELS (10-MIL FACE SHTS)	421	521
FORWARD RING (LATCHING INTERFACE)	23	23
LH ₂ TANK SUPPORT RING (2)	27	45
AVIONICS RING SECTION	59	59
MISC. MOUNTING/SUPPORT STRUCTURES	14	14
RMS GRAPPLE FITTING	4	4
THRUST STRUCTURE/AFT BODY COVER	77	154
BERTHING PROBES—EXTENDABLE	14	14
UMBILICAL INTERFACE, OTV-TO-ASE	9	14
ASSEMBLY & INSTALLATION HARDWARE	23	32
LATCHING MECHANISM—FWD INTERFACE	45	45
UNIVERSAL DOCKING ADAPTER	113	113
METEOROID PROTECTION*	517	721
THERMAL CONTROL	(204)	(254)
ACTIVE THERMAL CONTROL	36	36
AVIONICS COOLING	36	36
INSULATION	168	218
MLI INSULATION—LH ₂ TANK { 50 LAYERS OF 0.15-MIL KAPTON	168	218

* SUPPORTING DATA ATTACHED

GROUP WEIGHT STATEMENT
SINGLE-STAGE SPACE-BASED SOLAR-POWERED OTV

	<u>W_p = 10.5t</u>	<u>W_p = 20.0t</u>
AVIONICS		(285)
GUIDANCE & NAVIGATION		59
BASIC G&N	41	
GPS	18	
COMMUNICATIONS		35
DATA MANAGEMENT		77
RENDEZVOUS & DOCKING		46
INSTRUMENTATION		68
PROPELLANT LOADING/MEASUREMENT	27	
OTV MEASURING SYSTEM	41	
ELECTRICAL POWER SYSTEM (EPS)		(494)
POWER SOURCE		335
SOLAR ARRAY (56 m ²)*	200	
FUEL CELLS (4 @ 2.0 kW NOM/3.5 kW	91	
PEAK, EACH)		
BATTERY (25 AMP-HR)	11	
O ₂ TANK ASSY	1	
H ₂ TANK ASSY	1	
PLUMBING SYSTEMS	31	
CONVERSION & DISTRIBUTION		159
ELECTRONICS	68	
WIRE HARNESS	91	
MAIN PROPULSION SYSTEM (MPS)		(1,333)
MAIN ENGINE INSTALLATION -		
INCL GROWTH**		1,238
PROPELLANT SYSTEM		50
LH ₂ FEED	27	
LH ₂ FILL, DRAIN, DUMP	23	
THRUST VECTOR CONTROL	(incl in eng.)	
PRESSURIZATION & VENT		27
LH ₂ TANK AUTOGENOUS PRESS SUPPLY	14	
LH ₂ TANK VENT/RELIEF-SPACE	13	
PNEUMATICS		18
PLUMBING SYSTEM	13	
HELIUM BOTTLE	5	

* PROVIDES 10 kW PEAK @ START OF FIRST FLIGHT; 5 kW PEAK @ END OF 25TH FLIGHT.
INITIAL SPECIFICS ARE: 20 kg/kW 0.180 kW/m² 3.6 kg/m²

** CONSISTS OF 60m-DIAMETER SOLAR COLLECTOR ASSY (830 kg), 15% GROWTH ON COLLECTOR (122 kg), LASER ENGINE INCL PUMPS AND TVC ACTUATORS (249 kg), 15% GROWTH ON ENGINE PACKAGE (36 kg).

GROUP WEIGHT STATEMENT
SINGLE-STAGE SPACE-BASED SOLAR-POWERED OTV

	<u>W_p = 10.5t</u>	<u>W_p = 20.0t</u>
ATTITUDE CONTROL SYSTEM (ACS)	(102)	(132)
THRUSTER MODULES (4)—INCL 24 THRUSTERS	30	30
TANKAGE/PROPELLANT SYSTEM	72	102
N ₂ H ₄ TANK ASSEMBLIES	42	67
N ₂ H ₄ FEED	16	17
N ₂ H ₄ FILL, DRAIN, DUMP—SPACE BASING	5	5
N ₂ BOTTLES	5	8
N ₂ PRESS PLUMBING	5	5
SPACE MAINTENANCE PROVISIONS	(145)	(145)
CRITICAL AVIONICS ASSEMBLIES REMOVAL	25	
FUEL CELL REMOVAL	23	
MAIN ENGINE REMOVAL	22	
THRUSTER MODULE REMOVAL	11	
ADDITIONAL INSTRUMENTATION	41	
BUILT-IN TEST INSTRUMENTATION	23	
WEIGHT GROWTH MARGIN—EXCLUDE MAIN ENGINE INSTALLATION	(508)	(1,683)
OTV DRY WEIGHT	5,153 kg	6,482 kg
MPS RESIDUAL FLUIDS & GASES	(227)	(421)
TRAPPED LH ₂	9	9
GH ₂ IN EMPTY LH ₂ TANK	216	410
GHe FOR PNEUMATICS—TOTAL	2	2
ACS RESIDUAL FLUIDS & GASES	(19)	(19)
TRAPPED N ₂ H ₄	7	
GN ₂	12	
EPS RESIDUAL FLUIDS & GASES	(6)	(6)
TRAPPED O ₂	2	
TRAPPED H ₂	negl.	
TRAPPED PRODUCT WATER	4	

GROUP WEIGHT STATEMENT
SINGLE-STAGE SPACE-BASED SOLAR-POWERED OTV

	<u>W_p = 10.5t</u>	<u>W_p = 20.0t</u>
ACS RESERVE PROPELLANT	(23)	(36)
EPS RESERVE REACTANT	(--)	(--)
MPS INFLIGHT LOSSES	(408)	(635)
LH ₂ BOILOFF/VENT LOSS-60 DAY	408	635
MPS PROPELLANT-INCL RESERVE	(10,499)	(20,000)
ACS NOMINAL PROPELLANT	(227)	(363)
EPS NOMINAL REACTANT-10-HR CAPACITY*	(9)	(9)
OTV GROSS WEIGHT	16,571 kg	27,972 kg

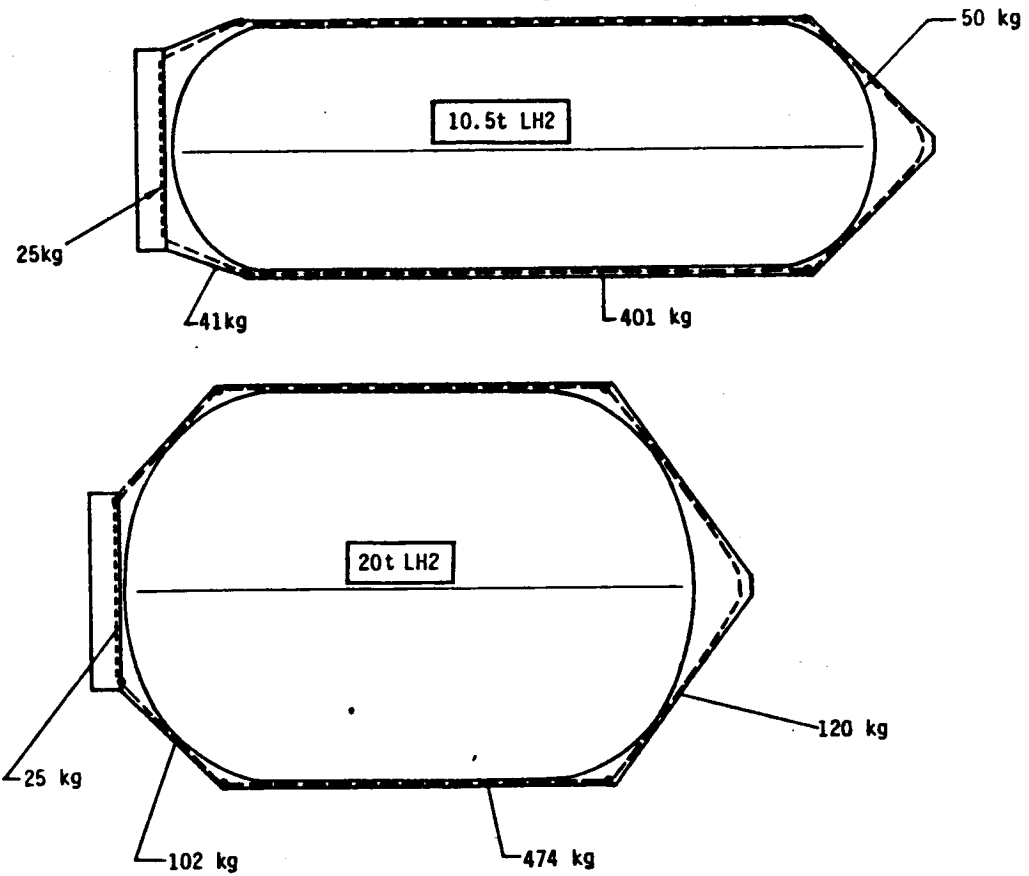
* REGENERATIVE FUEL CELL SYSTEM

ADDED METEOROID PROTECTION ASSESSMENT

	<u>$W_p = 10.5t$</u>	<u>$W_p = 20.0t$</u>
TANK SIDE AREA	50 m ²	61 m ²
TRIP TIME	60 DAYS (0.164 YR)	60 DAYS (0.164 YR)
AREA TIME PRODUCT (ASSUMING LEO STORAGE BETWEEN FLTS)	8.2 m ² /YR	10.0 m ² /YR
\bar{t}_{SHIELD} , REQ'D (ASSUMES 1/3 BUMPER, 2/3 BACKWALL, 7.6 cm SPACING MIN)	0.117 cm AL	0.122 cm AL
$t_{G/E}$ SANDWICH FACE SHEET x 2	0.051 cm G/E	0.051 cm G/E
t_{AL} EQUIV, G/E SANDWICH FACE SHEETS	0.030 cm AL	0.030 cm AL
t_{AL} EQUIV OF MLI BLANKET	0.010 cm AL*	0.010 cm AL*
$t_{REQ'D}$, AL BACKWALL { 7.6 cm SPACING 6.4 cm SPACING	0.076 cm AL 0.095 cm AL	0.081 cm AL 0.102 cm AL
BACKWALL INSTALLATION FACTOR	10%	10%
BACKWALL INSTALLED WEIGHT { 7.6 cm SPACING 6.4 cm SPACING	2.32 kg/m ² 2.90 kg/m ²	2.47 kg/m ² 3.09 kg/m ²

* 50-LAYER BLANKET { 2 LAYERS OF 0.5 MIL
48 LAYERS of 0.15 MIL

SINGLE-STAGE SPACE-BASED OTV
10.5t AND 20t LH₂



Solar/Laser OTV Added Meteoroid Protection

APPENDIX C

BASICS OF ION THRUSTER EFFICIENCY

Basics of Ion Thruster Efficiency

The efficiency of an ion thruster is a function of the loss of neutral atoms (mass utilization efficiency: η_m), discharge power loss (\mathcal{L}), the beam divergence (Fd), the expellant (beam) velocity (Sb), and the molecular weight (M) of the propellant. For a thruster that produces only singly charged ions, the dependence of thruster efficiency on these variables can be simply derived from the laws of physics as follows:

1. Conservation of energy: $(1/2) M * Sb^2 = e * Vb$
 $e \sim$ electron charge
 $Vb \sim$ net voltage impressed on acceleration system
2. Conservation of species: $\dot{M}b = Jb * M/e$
 $\dot{M}b \sim$ mass flow rate of ions in the beam
3. Conservation of momentum: $s = Sb * \eta_m * Fd$
 $S \sim$ effective expellant velocity (e.g., $Isp * go$)
 $\eta_m = \dot{M}b / \dot{M}$
 $\dot{M} =$ total mass flow rate: beam + neutrals

Combining the above:

$$(1/2) * \dot{M} * S^2 / (\eta_m * Fd^2) = Jb * Vb = Pb$$

where: Pb is the beam power.

Define: $\eta_e = Pb/Pt$, then:

$$P_T = (1/2) * \dot{M} S^2 / (\eta_e * \eta_m * Fd^2)$$

Since: $\eta_e = Pb / (Pb + PL)$ and the power loss: $PL = \mathcal{L} * Jb$

where: $\mathcal{L} \sim$ discharge loss (W/beam-Amp.)

$Jb \sim$ beam current

then: $\eta_e = 1 / (1 + \frac{2}{V_b})$

The conservation equations can be combined to give:

$$V_b = (1/2) * (M/e) * S^2 / (\eta_m^2 * Fd^2)$$

giving:

$$\eta_e = \frac{1}{\frac{1 + 2 * \frac{\eta_m^2}{m} * Fd^2}{(M/e) * S^2}}$$

Note that heavy atoms (M) and high expellant velocity (Isp) enhance electrical efficiency.

Finally, the thruster efficiency is given by:

$$\eta_t = \eta_e * \eta_m * Fd^2$$

and the propulsion system efficiency by:

$$\eta = \eta_t * \eta_p$$

where: η_p is the power processing efficiency.

If doubly charged ions must be accounted (and they must for real thrusters), then the mass utilization efficiency (η_m) is conventionally modified to become an overall utilization efficiency in accordance with a formalism derived by Hughes Research Laboratory.